Technische Universiteit Delft

Modelling subsidence in the Dutch Holocene coastal-plain

Investigating subsidence components and their relevance for different situations

S. E. ten Bosch

TU Delft

Modelling subsidence in the Dutch Holocene coastal-plain

Investigating subsidence components and their relevance for different situations

by

S. E. ten Bosch

to obtain the degree of Master of Science
at the Delft University of Technology,
to be defended publicly on wednesday 16 december at 14:30

Student number:	4381971	
Project duration:	February 2, 2020 – December 16, 2020	
Thesis committee:	Prof. dr. ir. C. Jommi	TU Delft
	Dr. J. Gebert	TU Delft
	Dr. ir. F. J. López Dekker	TU Delft
	Dr. ir. F. Bisschop	Arcadis
	S. van Laarhoven, MSc.	Arcadis

ARCADIS TU Delft

Summary

Land subsidence is a complicated phenomenon, relevant in the Holocene coastal-plain of the Netherlands, that can be triggered by many different mechanisms and components. To cope with the effects of land subsidence, detailed information on which mechanisms are causing subsidence and its variation over time and space are needed. Subsidence studies predominantly focus on grass and agricultural areas with organic soils above the groundwater level. In this study, subsidence is also evaluated for dikes and the urban environment. It is attempted to model subsidence behaviour of four different projects, grass plots within the Krimpenerwaard polder, locations along the N3 Dordrecht, an embankment constructed for the A5 Badhoevedorp and locations along the Markermeerdikes, and to verify these model results with subsidence measurements available. Existing one-dimensional models for different subsidence components are used in the evaluations.

For grass and agricultural areas it is found that subsidence behaviour could be modelled and the results lie within the range of uncertainty of the subsidence measurements used. However, the equations used are often empirical and do not include all relevant influencing factors and couplings. Compression by degradation of organic material as a response to drainage of organic soil is the main subsidence component in these areas. Anaerobic degradation of organic material is also included in the modelling approach, a component that is often neglected in other subsidence studies. Two infrastructure related projects provided insight to subsidence components in the urban environment. Compression by loading is the main subsidence component relevant in this area type, and thus settlement models are suitable to approximate the subsidence behaviour. However, a slight underestimation of creep shows that the existence of a small additional subsidence component for a situation with soft soil layers pushed below the water table could not be excluded. Unravelling subsidence behaviour from dikes showed to be more complicated, where an interplay between different components is relevant. Based on the evaluation in this study compression by loading and compression by an oxidation or shrinkage component are indicated the main subsidence components. Many uncertainties and assumptions used in this evaluation influenced the results.

For all area types disentangling subsidence into contributions of separate components based on a total measured subsidence signal causes large uncertainties, as modelled subsidence contributions for individual components could not be verified.

Preface

This report describes land subsidence in the Netherlands for different areas. With great pleasure I have looked at this trending topic which I found to be very broad with many different disciplines involved. Finding subsidence related articles in the newspapers during the time I have worked on my project has greatly encouraged me. The topic is getting more attention and I believe there is still much more to discover about the working, interaction and modelling of different subsidence processes around the world.

This project is the final part of my master programme geotechnical engineering at the TU Delft. The study program has felt challenging in the best way possible. I have seen different sides of the geotechnical field, ranging from environmental geotechnics to georisk management. During this thesis work I often looked back at material from different courses. I would like to thank my supervisors from the TU Delft, Cristina Jommi, Julia Gebert and Paco López-Dekker for their input and feedback during this project.

Furthermore I would like to thank Rik Bisschop and Simon van Laarhoven, who have supervised me on a weekly basis. I am very grateful that after everyone's life had changed completely because of the Covid-19 epidemic, both of them made time for a weekly meeting with me. In these coffee breaks I could ask every question I had and discuss all my ideas. From Arcadis I also wish to thank Muriël for making this project possible and Swaen for her tips and support.

During my project I have discovered that many people throughout the Netherlands are always willing to tell about their knowledge related to this topic. I have had the opportunity to meet with many professionals. I would like to thank Henk Kooi, Erik Kwast and Mariet Hefting for sharing their visions on this complicated topic with me, Joost van der Meer, Jan-Willem Oudhof and Erik Vossenaar for providing needed information about different projects, and many others for answering specific questions throughout my project.

Last, I would like to say that I am extremely grateful to my friends and family that have supported me in this journey. My work would not have been possible without the support from my parents, who have put up with me working from home for several months.

Sofie ten Bosch
Delft, December 2020

Contents

List of Figures

List of Tables

List of Definitions

Subsidence the vertical downwards movement of points at surface level or below surface level, compared to a defined datum

Land subsidence the downwards movement of a point at surface level, which can be caused by different processes

Settlement subsidence caused by the weight of a loading component, that induces compression of the subsoil. It should be noted that settlement refers to the vertical movement of the original ground surface level, also when the loading component is a soil structure which raises the land.

Klink the compression of soil by its own weight. The geotechnical definition of 'klink' is used in this study, in contrast to the definition from the soil science perspective where it is used to define compression of peat as a result of lowering the groundwater level, due to shrinkage and oxidation and a loss in buoyancy which causes an additional load (Zuur, 1958).

Compression the reduction of the soil volume, which can be caused by different processes, like external loading, oxidation and shrinkage.

Compaction the (often mechanical) densification of soil by the expulsion of air or water from the soil pores.

Organic Soil a soil with an organic matter content higher than 20 m%, following the geotechnical engineering definition

Peat a soil with an organic matter content higher than 75 m%, following the geotechnical engineering definition

1

Introduction

The west and northern area of the Netherlands can be characterised as a coastal-deltaic plain, where soft soil conditions are encountered. These coastal-deltaic plain deposits are found at approximately 50% of the surface area of the Netherlands (Koster et al., 2018a), where the thickness is generally increasing from east to west (TNO-GSN, 2016). Soft soil layers have been deposited during the latest period on the geological timescale, the Holocene, and find their foundation on sandy Pleistocene depositions.

Two problems faced in this area, but also in many other coastal-deltaic areas around the world, are sea-level rise and land subsidence. Where the combination of these two processes imposes an even larger relative sea-level rise to these coastal areas, compared to sea-level rise itself. The first problem, sea-level rise, requires a global response where humanity needs to act as one. In contrast, the second one is a local problem where local governments and entities focus on.

Different mechanisms cause and have caused land subsidence in the Netherlands. A division can be made between deeper and shallower mechanism. This is illustrated in figure 1.1, which is based on a Dutch figure from STOWA (2019). Deeper processes causing subsidence are isostacy and tectonics, and shallower processes are compression by loading (which includes initial compression, primary and secondary consolidation), compression by aerobic and anaerobic decomposition of organic material and compression by shrinkage. This study focuses on shallow subsidence processes. Relevant anthropogenic and natural drivers are shown in figure 1.1 as well, these drivers can trigger mechanisms that cause subsidence.

Coastal-deltaic plains throughout the world support a large proportion of the population and this will only increase, as the ongoing trend of coastal migration is expected to continue (Neumann et al., 2015). Land subsidence in coastal-deltaic areas has different consequences. Some of the most important consequences are (Van den Born et al., 2016):

- Increased vulnerability to flooding
- Damages to infrastructure, pipelines and buildings because of differential subsidence
- Increase in upward seepage of brackish groundwater
- Local hotspots of water accumulation caused by a high precipitation event
- Threat to archeological preservation
- Negative adhesion of pile foundations (when soft soil layers subside faster than the foundation pile itself, this poses an additional load on the pile foundation)
- Possible problems with wooden foundations that end up above the groundwater level

Together these problems cause an increase in maintenance costs, for both the flood defence system and the maintenance of housing and infrastructure. Gilles Erkens mentioned in an interview with Boersma (2015) that the extra costs per resident in the Netherlands are approximately €250 only for the maintenance of housing and infrastructure due to subsidence. Van den Born et al. (2016) showed that land

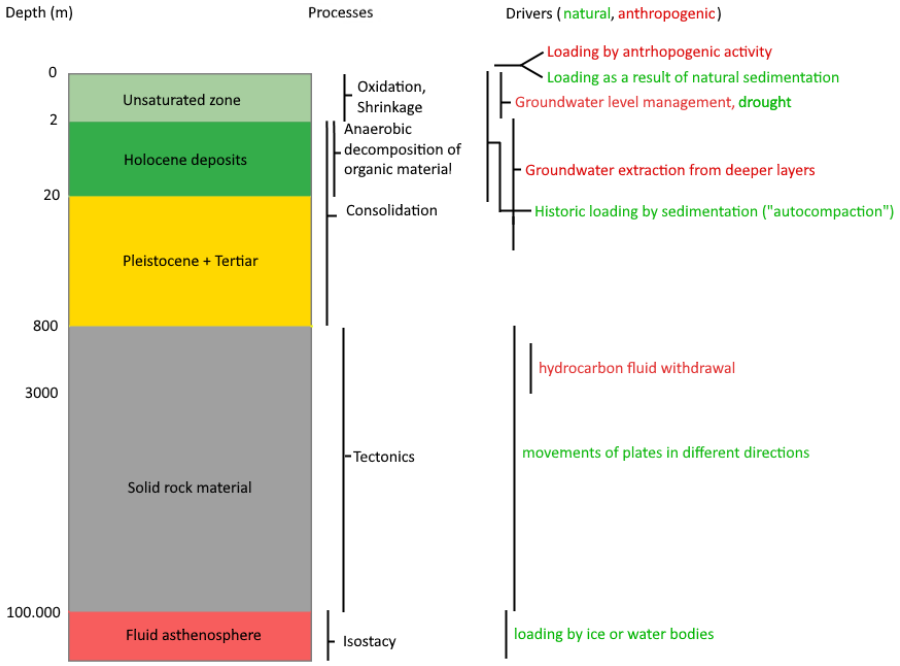

Figure 1.1: Main mechanisms and drivers of land subsidence, based on STOWA (2019)

subsidence in the Netherlands will lead to high costs (approximately €21 miljard between 2010 and 2050) and a change in policy might be needed to lower these costs.

To cope with the effects of land subsidence, detailed information on which mechanisms are causing subsidence and its variation over time and space are needed. Different coping mechanisms can be applied, based on which mechanisms are acting. Two examples are the use of lightweight construction materials when compression by loading is the main mechanism and raising the water table when compression by oxidation is the main mechanism.

1.1. Scope

Most land subsidence studies in the Netherlands focus on grass- and agricultural areas, and often urban areas are avoided because of surface sealing and problems with restricted areas (Van Asselen et al., 2018). Surface sealing (by pavements and roads for example) and restricted areas (not accessible) limit the availability of the soil for taking samples. Two studies that both did differentiate in these land use types are that of Koster et al. (2018b), who considered both grass- and agricultural lands and the cities Amsterdam and Rotterdam in their study and Van Asselen et al. (2018) who even differentiated between six study areas, varying in subsurface and loading components. These six types are no loading sites, agricultural loading sites, natural heavy-loading sites, modest urban loading, heavy urban loading and dike embankment loading. In this research it is proposed to separate three different types of areas present in the coastal-deltaic plane of the Netherlands to further study the mechanisms of land subsidence. These are:

- Dikes
- Grass and agricultural lands
- Residential areas and infrastructure

The characteristics, expected relevant mechanisms, drivers and consequences of land subsidence are explained below for each distinguished area type.

Area 1: dikes

The first study area are dikes, where soft soil areas loaded by these embankments are considered. Different mechanisms are working here. Considering the subsoil of the embankment, compression by external loading (the embankment) is relevant. Van Asselen et al. (2018) showed that peat under embankments can already be compressed up to 75%, which means a height reduction of 75% relative to the initial decompressed height, but this depends on the time since loading, the overburden weight and the organic matter content of the peat. Compression by shrinkage and oxidation of the layers in the natural subsoil is not expected to contribute much to subsidence of the embankment, because this material is often pushed below the groundwater table level. Compression by anaerobic decomposition is also not expected to contribute much, due to the absence of the usage of fertilizers. Oxidation, shrinkage and anaerobic decomposition can be relevant for land subsidence of the hinterland of the dike.

For the embankment body itself, compression by shrinkage and loading through the construction material itself is important. Oxidation might also be relevant, but to a lower extent, as only a certain degree of organic material in clay is accepted for the construction of an embankment. Potential stabilization/destabilization of this organic matter should be considered. The compression of the soil in the embankment body itself is called klink. An important consequence of subsidence of these constructions is the increase in flooding risk, but also differential settlements can be harmful to the functionality of dikes.

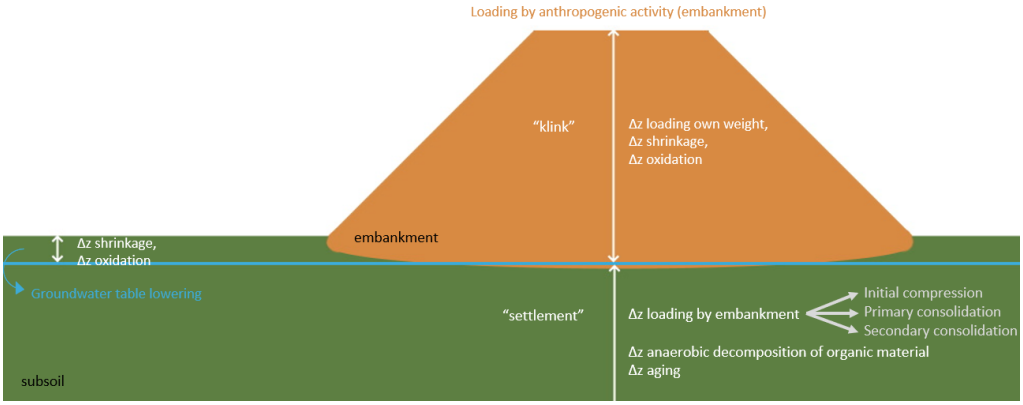

Figure 1.2: Schematic representation of relevant subsidence mechanisms for dikes

Area 2: grass and agricultural lands

The second area type is areas that have experienced continued loading by lowering of the groundwater level for agricultural purposes. These areas are mostly peat lands or clay covered peat lands. The main subsidence mechanisms that are relevant for this area are expected to be compression by loading, shrinkage and oxidation. Schothorst (1977) quantified the contribution of different mechanisms to the total subsidence for low moor peat soils in this area type, and found that approximately 65% of total subsidence can be attributed to compression by shrinkage and peat oxidation above the groundwater table and only 35% was attributed to compression of layers below the groundwater table caused by loading through the peat above the water table that lost its buoyancy. Many other studies agree that peat oxidation and shrinkage are the main contributing mechanisms to land subsidence in grass- and agricultural areas (Beuving and van den Akker, 1996, Erkens et al., 2016, Fokker et al., 2019, Stouthamer et al., 2008, Van Asselen et al., 2018). Compression by anaerobic decomposition of organic material can also be relevant here (Smolders et al., 2013), because of oxidation and the use of fertilizers, which enhance the presence of nitrate in the saturated soil layers.

To reduce subsidence from compression by oxidation and shrinkage, maintaining current water levels or even raising them can work (Kooi and Erkens, 2020, Querner et al., 2012, Van Hardeveld et al., 2017). However, higher groundwater levels have negative consequences for the agricultural sector. The potential loss of biodiversity in the ecosystems can be a consequence of subsidence in this area type

(Parish et al., 2008). Another important factor in the relevance of land subsidence for this area type are the emissions of carbon dioxide (CO_2) caused by oxidation.

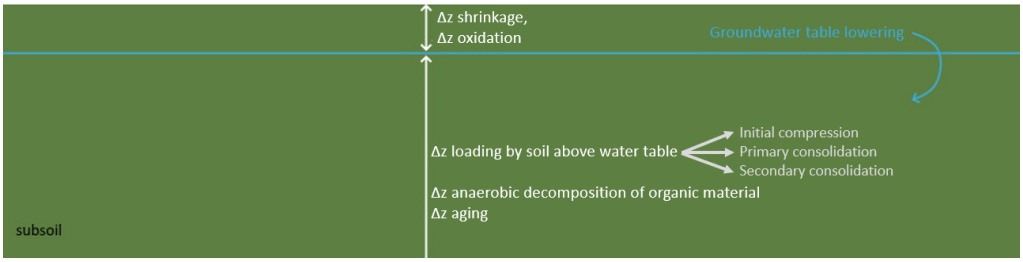

Figure 1.3: Schematic representation of relevant subsidence mechanisms for grass- and agricultural lands

Area 3: residential areas and infrastructure

This area type is mostly characterised by buildings and infrastructure. The main mechanisms that are relevant for this area are compression by loading and (to a lesser extent) oxidation and shrinkage. Van Laarhoven (2017) showed that compression by oxidation no longer contributes to subsidence in parts of the city Gouda, but the mechanism responsible for the main part of observed subsidence here is compression caused by urban loading. Koster et al. (2018b) showed that contributions of loading and oxidation differ from between grass- and agricultural areas and the two cities considered, differences in contributions of shrinkage were not mentioned in the study.

The main driver of land subsidence in this area is loading by anthropogenic activity, as a result of construction of civil projects, but also groundwater table lowering can contribute. Consequences of land subsidence in this area type are an increased flooding risk, negative adhesion on foundation piles, damage of wooden foundation piles, flooded cellars, differential settlements that cause damages to infrastructure and buildings and local hotspots of water accumulation. An important characteristic of this area is the type of soil which has been used for raising the land, that can be found here. This layer has a varying thickness for different locations. In case of infrastructure, this layer consists mainly of sand, while in case of residential areas both clay and sand are used to raise the natural areas.

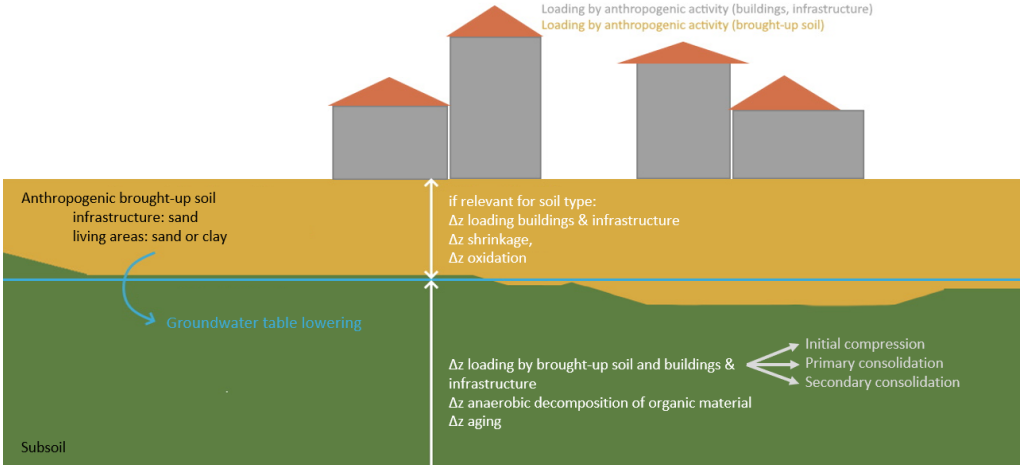

Figure 1.4: Schematic representation of relevant subsidence mechanisms for living areas and infrastructure

1.2. Land subsidence calculation models

Different models exist to predict land subsidence in the Netherlands. The most important ones are described in table 1.1, which is based on the Dutch version from STOWA (2019).

Software Package	**Processes included**	**Application**	**Most Important Limitation**
Atlantis	- Peat oxidation - Compression because of changes in groundwater level (Isotache & Koppejan)	Regional / national maps; long timeframes; focus on Holocene deposits	No Darcy (only Terzaghi); no shrinkage (or partly implemented through oxidation)
SUB-CR	- Compression because of changes in groundwater level and hydraulic head (Isotache)	Regional, relatively deep groundwater systems; influence of withdrawal	Not suitable for large phreatic lowerings; no oxidation/shrinkage
D-Settlement	- Compression caused by loading at the surface (Isotache & Koppejan)	Local area; settlements by loading (often embankments); vertical drainage	Not suitable for time dependent phreatic level; no oxidation/shrinkage
FlexPDE	- Compression by loading at the surface and by changes in phreatic or hydraulic head (Isotache)	Local area; settlements because of increment and subsidence because of variation of phreatic level and/or hydraulic head	Not suitable for large phreatic level lowerings; no oxidation/shrinkage
Plaxis	- Compression/deformation by general external/interal loadings (2D soft soil creep)	Local area; 2D geotechnical; situations with deformations in multiple dimensions	No oxidation/shrinkage

Table 1.1: Overview of some relevant software packages used in the Netherlands to predict shallow land subsidence, (STOWA, 2019)

1.3. Problem description

The often negative consequences of land subsidence were described before and these show the problem of this topic in itself. To better mitigate these negative effects, or even prevent them from occurring, a good understanding and predicting of the mechanisms causing these problems is necessary. Large differences between the relevant mechanisms and drivers are found considering different coastal-deltaic regions, but even within one coastal-deltaic region these differences exist. In the Netherlands this complexity has two main causes: 1. the high heterogeneity of the subsurface and 2. the high spatial variability in loading by different components (lowering water table, structures and buildings).

The previous section on already existing subsidence models shows the large variety in modelling approaches and also their main limitations. Models to predict land subsidence often do not include all mechanisms (oxidation and/or shrinkage and potential anaerobic decomposition) and some of them are only applicable on a regional or national scale. There is a need for a more local model that does include all relevant processes and can be used to predict land subsidence on a project scale, by combining the effects from all the relevant processes. Project scale is meant here on a spatial scale, since the temporal effect should not be limited to a project only. The main problem here is the step from theory to application which is essential for developing such a tool. A smaller step in this process is the identification of the contributions of different mechanisms to total subsidence for different projects, which is not fully understood yet.

For the three types of study areas defined before, different components that can contribute to land subsidence were identified. However, as mentioned before, there is still a debate on the contributions from these different mechanisms and their coupled behaviour. Zain (2019) showed that there are effects of oxidation on the compression behaviour, the swelling behaviour and the water retention capacity of a peat soil. Improving knowledge on disentangling total subsidence into its separate components is the first step in the process from theory to application which can help with the design of projects on the coastal-deltaic plane.

Considering dike embankments a division can be made between subsidence mechanisms of the subsoil and subsidence mechanisms of the embankment body. In current design practices, often only settlements of the subsoil due to compression of by loading are evaluated in calculations. In some

design cases an average subsidence rate for grass-and agricultural areas is added to consider subsidence in general for the design but also values from the "bodemdalingskaart" (land subsidence map of the Netherlands) are used for incorporating subsidence in design practices. Klink of the embankment body itself is sometimes considered by the contractor, who uses a percentage of the design height, based on experience, to identify additional height needed. A better understanding of the contributions of different processes and their interaction can help with the design practices of these soil structures.

For the grass and agricultural lands the contribution of anaerobic decomposition of organic material is often not included in land subsidence studies (as it is assumed not to be relevant), and its potential contribution has not been quantified. This topic is currently getting more attention, as potential anaerobic degradation is also relevant for rewetting/renaturing peatlands.

Looking at the third area type, it can be seen that more residential areas are constructed due to both the growth in population and the trend of urbanisation. These residential areas are constructed on soft-soil deposits where the impact of these constructions on the existing subsidence rates is relevant.

Another factor that complicates land subsidence studies is that the existing studies to modelling of separate land subsidence components often do not define clearly all relevant limitations, definitions and boundary conditions, which makes it hard to identify what can actually be concluded from these researches. Land subsidence is an interdisciplinary problem and terminology can differ amongst disciplines.

1.4. Objective and research questions

This research aims to gain insight into contributions of different shallow subsidence sources to total land subsidence on a project scale, considering areas with different land uses in the Netherlands using current land subsidence modelling techniques and verification with project data. It is important to mention that only one-dimensional modelling techniques are used. The main research question and subquestions used to gain insight into land subsidence are:
How do different shallow land subsidence processes contribute to total land subsidence for areas with different land uses over time, measured on a project scale and can these be modelled accurately on this project scale using existing modelling techniques?

- What is the result of the comparison of project data for grass and agricultural areas (area type 2) and residential areas and infrastructure (area type 3) to the land subsidence model result (sum of all individual components over time)
- What is the result of the comparison of project data for dikes (area type 1) to the land subsidence model result (sum of all individual components over time)?
- How sensitive are model results to potential variation of input and model parameters, due to heterogeneity of soil?
- Can it be assumed that there are no other effects contributing to subsidence than primary and secondary consolidation when soft soil layers (soft clays and peat) are pushed below the groundwater level?
- What happens with the subsidence rate in grass and agricultural areas when shallow groundwater table lowering stops and the water table is not lowered any further from the current level?
- How does a shift from grass and agricultural areas to residential areas, infrastructure or dikes influence the already existing land subsidence rate?

I

Background

2

Soft soil

To understand the relevance of land subsidence in the Netherlands, the Holocene subsoil deposits, sections 2.2 and 2.3, and their formation, section 2.1, are evaluated in this chapter. The last section, 2.4, goes into soil water interaction.

2.1. Formation of the Holocene coastal-deltaic plain in the Netherlands

In the Netherlands, formation of peat began as a result of rapid sea-level rise that caused drowning of the area around 9500 cal year BP (Van de Plassche, 1982). This peat that was formed on top of the Pleistocene deposits is referred to as basal peat, since it forms the base of the Holocene sequence. From 8500 cal year BP onwards the setting changed, the sea-level rise decreased, and the coastal and delta plain diversified, where marine transgression succeeded the formation of peat (Hijma et al., 2009). Basal peat formation continued to form in distal flood basins. In the fluvial part of the coastal-deltaic plain meandering rivers occurred. During this period, up to around 5500 cal year BP, sequences of intercalated peat and overbank clastic layers formed due to a shift in sediment supply to the flood basins over time. These shifts were caused by repeated avulsion of tidal and river channels (van Asselen et al., 2017). As the relative sea-level rise further decreased around 5500 cal yr BP (Van de Plassche, 1982), a coastal beach barrier-complex began to form, which disconnected tidal basins from the sea. Because of this disconnection, the water became less saline and less clastic sediments reached the lower coastal plain. This facilitated the widespread peat formation in the back-barrier area (Vos, 2015), where thick and extensive peat beds developed. An overview of three of the landscapes during this described time frame is shown in figure 2.1, these are paleogeographical maps constructed by Vos (2015).

Around 1000 CE anthropogenic activities began to cause deterioration of the peatlands, ditches created to drain the peatland by gravity resulted in land subsidence of the area. In the fluvial dominated parts, deforestation and increased erosion in the catchment area caused increased loads of sediments in clay and silt (Erkens et al., 2006), which then influenced the avulsion behaviour of the rivers in the period 500 BCE to 1000 CE.

When drainage of the peatlands by gravity was restricted by equaling water levels of the rivers and tidal inlets, changes occurred in the water management for mainly agricultural practices. Over a longer timeframe 'polders' were created to manage groundwater levels. Currently, each polder has its own water regime and therefore the groundwater levels are spatially variable.

Koster et al. (2018a) stated that at present there are three types of landscapes in the coastal-deltaic plain of the Netherlands. The first type is the central coastal plain, distal to sea ingressions and overloaded river branches. Original thick peat beds here were spared from sedimentation and peat can be exposed at the surface. The last 1000 years, these areas have been mainly in agricultural use. The second area type is where the peat beds have been clay covered. These can be found along major rivers, marine ingressions and estuaries. Last, there are the areas which are covered by anthropogenic brought-up soil, due to urbanisation, and these form the third type of area.

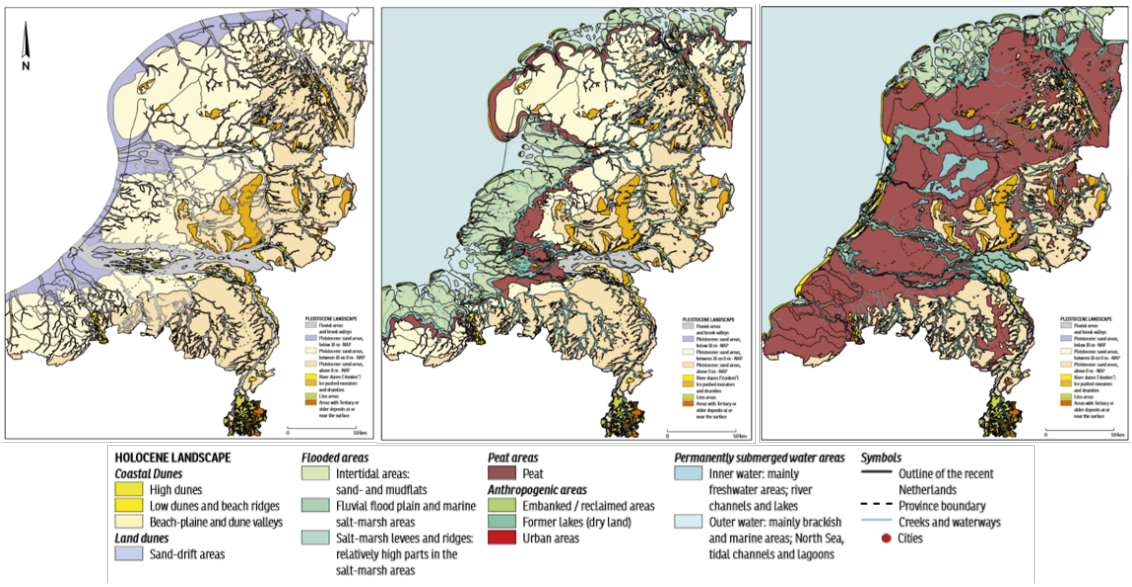

Figure 2.1: Paleogeographical reconstructions of the Netherlands during the Holocene, from Vos (2015). From left to rigth: 9000 BC, 5500 BC and 1500 BC

2.2. Clay soil

Soft clay layers are common in the coastal-deltaic plane of the Netherlands. These can be problematic because of its natural states with high compressibility. Clay is a mineral soil type. Its particles are generally identified by their grain size, which is smaller than 0.002 mm. The size of pores in clay is small, which limits air and water movement in the soil. The type of clay mineralogy and the amount of clay minerals in the soil influences its properties, like its plasticity, its swelling potential and the ability to adsorb ions and molecules.

2.3. Organic Soil and Peat

Organic soil is a general term for a soil with a high content of organic matter. Some of its characteristics (low bulk density, swelling and shrinkage behaviour and high porosity) make it difficult to describe the soil behaviour with concepts and methods for mineral soil (Dettmann et al., 2014). The distinction of peat and organic soil is a difficult matter, geotechnical definitions are used in this report (see the List of definitions).

Peat soil is formed by accumulation of partially decomposed and undecomposed biomass, where the accumulation rate is higher than the degradation rate. It is heterogeneous and can have an anisotropic character, caused by a potential preferred pore orientation during the peat-forming process and layering of root and plant material within the soil matrix (Kruse et al., 2008). These effects strongly influence water movement in peat soils (Beckwith et al., 2003a). Though, this anisotropic character can be lost upon degradation of the material, caused by for example artificial drainage (Beckwith et al., 2003b). General characteristics of peat soils are a low unit weight, as the solid matter only contributes little to the total weight of the soil, and a high water content. Peat soil has a sponge type of structure, this can be seen in figure 2.3, which can retain a lot of water.

The structure of peat influences its engineering behaviour. Peat holds a double level structure, consisting of a microstructure and a macrostructure, this can be seen in figure 2.2 which illustrates general composition of peat. The macrostructure refers to features that can be observed with the naked eye, while the microstructure refers to features at the particle or fibre level.

The total porosity of peat is very high, it often exceeds 80% (Boelter, 1968), and pores are highly irregular. The structure and arrangement of pores in peat soil are largely controlled by the degree of decomposition of the organic material and the peatland vegetation. In general peat contains three

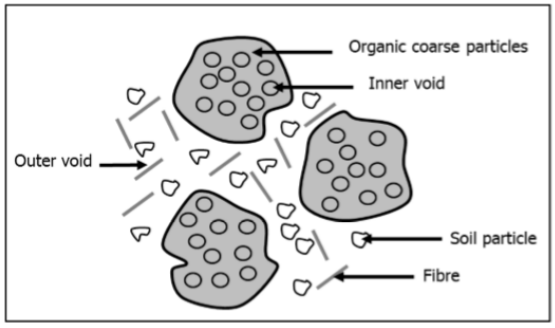

Figure 2.2: Schematic representation of the composition of peat (Huang et al., 2009)

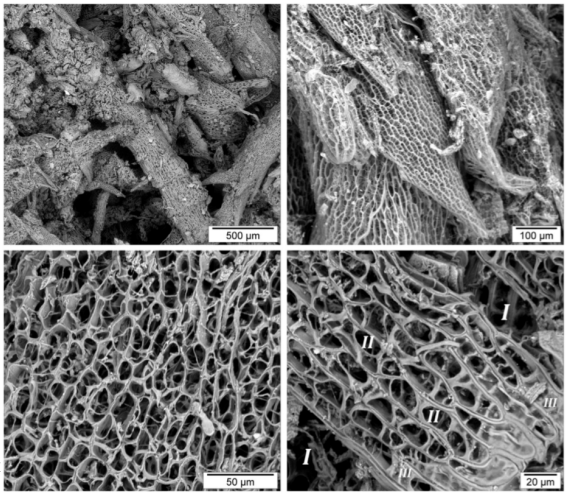

Figure 2.3: Back-scattered electron (BSE) images of a sphagnum peat soil in Canada, with pore types indicated at the 20µm picture. (Rezanezhad et al., 2016)

different types of pores, (Rezanezhad et al., 2016): (I) open and connected macropores, (II) closed or partially closed cells and (III) dead-end or isolated pore spaces. These three zones are indicated in figure 2.3. Pores from type I form the 'active porosity' of the soil that allows water movement, while pores type II and III together represent the 'inactive porosity' where the water fraction is immobile.

Upon further decomposition of the organic material, the proportion of large pores becomes smaller as the material is broken down into smaller fragments, which reduces the interparticle space. Moreover the degree of decomposition is also linked to the water retention capacity of peat soil. Peat soil that is undecomposed and has a large active porosity can releases more of its saturated water content to drainage than decomposed peat.

Organic soils are commonly described by their organic matter content, but there are also other factors that can be used to classify organic soils or peat. Examples are the state of decomposition, the vegetation type of the origin material and the appearance of the soil. Different systems used for the classification of peat soils are explained in appendix A.1.

2.4. Soil water

Soil contains water under natural conditions. The gravimetric water content of the soil w and the volumetric water content θ are defined as

$$w = \frac{M_w}{M_s} \qquad \theta = \frac{V_w}{V_s} = w \cdot \frac{\rho_s}{\rho_w}, \tag{2.1}$$

where M_w is the mass of water [kg], M_s is the mass of the solid particles [kg], V_w is the volume of water [m^3], V_s is the soil volume [m^3], ρ_s is the density of the soil [g/cm^3], ρ_w is the density of water [g/cm^3]. Water in soil can be divided in different categories, by the type of binding. Water that is not bound to the soil and can be drained by gravity is called percolating water. Adhesive water is the water that surrounds solid particles due to the attraction of water to the mineral surface, the amount of adhesive water in the soil is linked to the surface area of the soil particles. Capillary water is retained by capillary forces in soil pores. This is shown in figure 2.4.

Capillary forces strongly influence the amount of water that can be retained in the soil, for soil water often its potential is considered. Potential (ψ) is defined as *"the work required to lift a unit quantity (volume, mass or weight) from a free water surface to a specific height in a pore (capillary) or to remove it from the soil matrix"* (Blume et al. (2016), p.232). The total potential is a sum of different components:

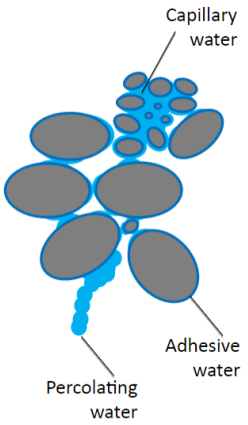

Figure 2.4: Retention of soil water, (Gebert, 2018/2019)

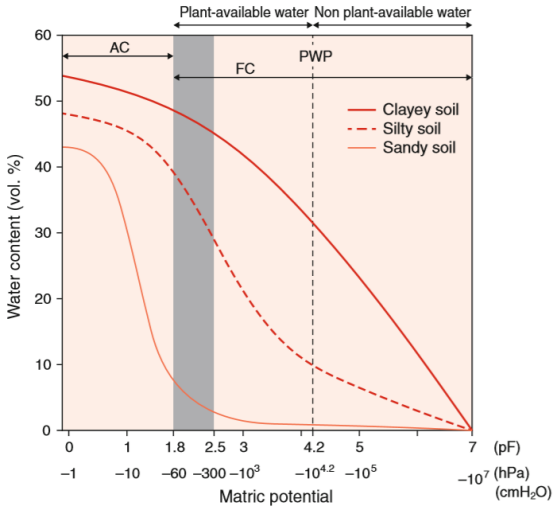

Figure 2.5: Soil water retention curves, (Blume et al., 2016). AC is the air capacity, FC is field capacity and PWP is the permanent wilting point.

$$\psi = \psi_z + \psi_m + \psi_o + \psi_g. \tag{2.2}$$

In this equation ψ is the total potential [kPa], ψ_z is the gravitational potential [kPa], ψ_m is the matric potential [kPa], ψ_o is the osmotic potential and ψ_g is the gas potential [kPa]. The gravitational potential represents the work that is needed to lift a unit of water from a reference level to a new level. The matric potential is the work that is needed to extract a unit of water from the soil. Its value has a negative sign because it counteracts the gravitation. The osmotic potential is the work that is needed to extract a unit of pure water from the soil solution, and it is related to the amount of dissolved salts in the free pore water. This value also has a negative sign. The gas potential is considered when the soil air pressure does not correspond with the pressure at a selected reference level, often this term is not needed.

Water content (gravimetric or volumetric or degree of saturation) and matric potential are correlated and this is defined through a soil water retention curve (SWRC). A decrease in water content results in a higher matric potential. These curves vary for different soil horizons and layers, as the curve is mainly determined by the particle size distribution and pore volume. These curves also vary for drainage compared to wetting and this phenomenon is called hysteresis. Examples of SWRCs are shown in figure 2.5.

3

Compression by loading

As a result of the ongoing growth of population and the increase in urbanisation, construction is now dealing with areas with more problematic soft soil conditions. Settlements related to the load from constructions on these soft soils can be evaluated using consolidation models and settlement models. Different loading steps and phases are often included.

Another situation where consolidation and settlement models can be used is when the groundwater level is lowered. The soil layer that ends up above the groundwater level faces a loss of buoyancy where it then exerts an additional load to the layers below. Compared to other loading by construction components, this will only be a small component, though very relevant for subsidence problems in the agricultural and grasslands.

Changes in the stress state of the soil causes deformations of soil, where time-dependent behaviour is relevant. Considering Terzaghi's effective stress principle a change in effective stress can be caused by either a change in the total stress component or the pore pressure:

$$\sigma'_v = \sigma_v - u, \tag{3.1}$$

where σ'_v is vertical effective stress [kN/m^2], σ_v is total vertical stress [kN/m^2] and u is pore water pressure [kN/m^2]. For this research, an increase in the total stress (loading by an external component) and a decrease in pore water pressure (lowering of the water table level) are most relevant. In general, a loading component causes settlement. This total settlement component can be seen as the sum of three components

$$S_t = S_i + S_{co} + S_{cr}, \tag{3.2}$$

where S_t is the total settlement [m], S_i is the immediate settlement [m], S_{co} is the consolidation settlement [m] and S_{cr} is the creep settlement [m]. Figure 3.1 shows a general curve of settlement over time, including the three components of total settlement. In this figure the so-called 'hypothesis B' is adapted, where part of the creep settlement is considered to occur already during consolidation (Degago et al., 2011). Sometimes a fourth component is mentioned, which is called tertiary compression. More information on this component and its relevance is provided in section 3.4. This component is generally not included in settlement calculations.

3.1. Settlement components

Initial compression

For one-dimensional settlement considerations the immediate settlement component follows from the initial compression of the soil, caused by the elasticity of soil structure and by compression and expulsion of gas in the soil pores. This settlement component is often small compared to the total settlement.

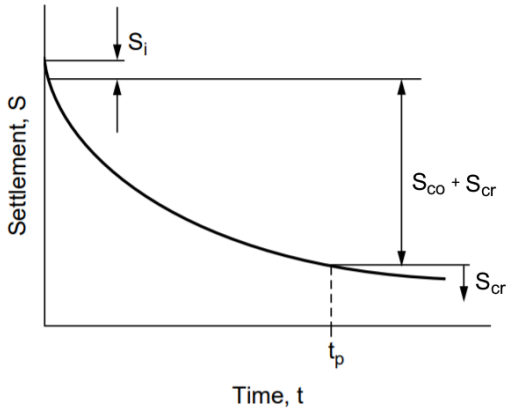

Figure 3.1: General settlement over time curve

Consolidation

When there is a change in the pressure state of a saturated soil with a low hydraulic conductivity, initially pore water reacts in absence of drainage. This creates a situation with excess pore water pressure. Over time this excess pore water pressure dissipates, as water drains from the soil, and the vertical effective stress increases, the soil approaches its final steady state pore water pressure distribution. This process is called consolidation. Rearrangement of soil grains and drainage of pore water cause a volume change of the soil.

Different factors influence the consolidation process. The generation of excess pore water pressures is governed by the rate of loading compared to the rate at which the soil can drain. The permeability of the soil is an important parameter here, where a higher permeability allows for faster consolidation, if all other factors remain unchanged. Due to the presence of fine grained soils with generally low permeability's, like clay and peat, in the coastal-deltaic plain, this consolidation process is relevant in for the study areas in this project. The layer thickness and boundary conditions also affect the consolidation process. A thicker layer will need more time to complete consolidation and the boundary conditions define the maximum length of the drainage path. The duration of consolidation is called the hydrodynamic period.

Creep

After the hydrodynamic period has ended, and no change of effective stress can be measured anymore, still some settlements may occur. This effect is often called creep and can be described using visco-plasticity. It is a mechanical process which has different explanations. Le et al. (2012) identified five main groups of explanations for soft soil creep deformations, which are (1) creep due to breakdown of interparticle bonds (2) creep due to jumping of molecule bonds (3) creep due to sliding among particles (4) creep due to water flows in a double pore system and (5) creep due to structural viscosity. As mentioned by both Le et al. (2012) and Kaczmarek and Dobak (2017), depending on the explanation, some of these processes overlap at some points.

In soils with clay particles, different types of bonding occur, for example the primary valence bonds, van der Waals forces, hydrogen bonds, etc. Due to the consolidation process these interparticle bonds may be disconnected. It is proposed that the breakdown of these interparticle bonds may lead to further rearrangement of grains over time, causing creep settlement. This mechanism was proposed by Terzaghi (1941) and accepted by others (Crooks et al., 1984, Mesri, 2003, Mesri and Godlewski, 1977). The second mechanisms of creep is linked to the theory of rate process. It mentions that for the movement of molecules and atoms causing creep, sufficient activation energy is needed. Related to this activation energy, Mitchell et al. (1968) concluded creep is a thermally activated process. Mesri (1973) however mentioned that the effect of temperature is insignificant compared to the influence of other factors. The third principle is creep due to sliding among particles. As consolidation is explained as

the drainage of water without slipping between soil grains, creep can be explained as a volume reduction due to slippage of soil grains. Bonds between particles increase friction and cause resistance to sliding, which explains the slow occurrence of creep settlement. A generally accepted theory for peat and other organic soils is creep due to water flow in a double porosity system (De Jong, 1968, Zhang and O'kelly, 2013). It is stated that creep results from the pore water movement from micropores to macropores, while consolidation is the result of drainage from the macropores. Some studies also mention the degradation of organic material as a component of creep settlements for organic soils. Last, structural viscosity is mentioned as a cause of creep. It means a structural resistance to compression within a clay structure, caused by the absorbed water layer surrounding clay particles.

3.2. Consolidation models

One dimensional consolidation can be considered for land subsidence. Terzaghi's one dimensional consolidation, equation (3.3), can be derived from the general three-dimensional consolidation equation using the following assumptions:

- Loading is one dimensional
- There is saturated flow
- Fluid is incompressible
- Soil grains are undeformable
- Soil is uniform
- Stiffness in the soil is constant
- Hydraulic conductivity of the soil is constant
- Flow is controlled by Darcy's law
- Small strain hypothesis

$$\frac{\delta u}{\delta t} = c_v \frac{\delta^2 u}{\delta z^2}, \tag{3.3}$$

where u is the excess pore water pressure [kN/m^2], c_v is the consolidation coefficient [m^2/s], z is the vertical direction [m] and t is time [s]. The consolidation coefficient is defined as

$$c_v = \frac{k}{\gamma_w \cdot m_v} = \frac{k \cdot E_{oed}}{\gamma_w}, \tag{3.4}$$

with c_v the consolidation coefficient [m^2/s], k is the vertical permeability [m/s], γ_w is the unit weight of water [kN/m^3] and m_v (= $1/E_{oed}$) is the compressibility coefficient [m^2/kN].

Terzaghi's one dimensional consolidation equation can be solved either analytically or numerically. The analytical solution uses an overall degree of consolidation factor, which relates to the time factor of the problem. The numerical approach uses a step-wise numerical solution of the problem, where the degree of consolidation, effective stress and pore pressures are calculated at different points in space and time. The analytical solution is further discussed in section 3.2.1 and the numerical approach in section 3.2.2. The implementation of the degree of consolidation factor in settlement models is shown for different constitutive models (Deltares, 2016):

$$\Delta h(t) = \begin{cases} U(t)\Delta h_{cons}(\sigma') + \Delta h_{creep}(\sigma', t) & \text{for Koppejan} \\ U(t)\Delta h_{drained}(\sigma', t) & \text{for a/b/c isotache and NEN-Bjerrum.} \end{cases} \tag{3.5}$$

In this equation σ' is the vertical effective stress [kN/m^2], Δh_{cons} is the consolidation contribution to settlement from Koppejan [m], Δh_{creep} is the creep contribution to settlement from Koppejan [m], $\Delta h_{drained}$ is the theoretical layer deformation under drained conditions according to a/b/c isotache or NEN-Bjerrum [m] and $\Delta h(t)$ is the total settlement over time [m].

3.2.1. Analytical solution (Terzaghi model)

The analytical solution of the one dimensional consolidation equation works with a degree of consolidation, that symbolizes the progress of consolidation over time. This can be calculated with

$$U(t) = 1 - \frac{8}{\pi^2} \sum_{i=1}^{\infty} \frac{1}{(2i-1)^2} \exp\left[-(2i-1)^2 \frac{\pi^2}{4} \frac{c_v t}{h^2} \right], \tag{3.6}$$

where $U(t)$ is the degree of consolidation [-], c_v is the coefficient of consolidation [m^2/s], h is length of the drainage path [m] and t is the time [s]. Some approximation formulas for this complicated equation have been developed, and these are evaluated in appendix A.2.

When multiple consolidating layers are present between drainage boundaries, the analytical solution works with a fictitious homogeneous soil layer that has an equivalent coefficient of consolidation. This is a simplification of reality. Soil layers that are considered drained are often assumed to have a 100% degree of consolidation from the beginning in the calculation approach.

3.2.2. Numerical (Darcy model)

The other option for solving the one-dimensional consolidation equation is using a numerical solution where pore pressures and effective stress are calculated at different points in space and time. The pore pressure distribution over time can be solved using an integrated spatial Fourier interpolation along sections of the vertical profile. Settlements at the interfaces of different sections are solved through iterations within each time step. The value of this time step should be determined in such a way that a stable solution can be ensured. It is an approach where the general storage equation, equation (3.7), is used to determine the influence of excess pore pressure on soil settlements of different layers. This method derives the deformation during consolidation from the development of the effective stress. To do this, excess pore pressures are calculated at different points in time and space, according to

$$\frac{k}{\gamma_w}\frac{d^2u}{d^2z}+\frac{d\varepsilon}{dt}+L=0, \tag{3.7}$$

where u is the excess pore water pressure [kN/m^2], k is the Darcy vertical permeability [m/day], $\frac{d\epsilon}{dt}$ is the strain rate and L is a leakage term in case of the application of vertical drains. Equation 3.7 is based on excess pore pressure and full saturation is assumed below the water level. Therefore, changes in phreatic storage and permeability caused by a variation in saturation are neglected. The permeability of a soil is actually a function of its void ratio. The numerical solution approach allows to use a strain dependent permeability, calculated by

$$k=k_0\cdot 10^{-\frac{1+e_0}{C_k}\varepsilon}, \tag{3.8}$$

where k_0 is the initial permeability [m/s], $\frac{C_k}{1+e_0}$ is the permeability strain modulus [-], ϵ is the strain [-], C_k is the permeability strain factor [-] and e_0 is the initial void ratio [-]. Situations with multiple consolidating layers between drainage boundaries can accurately be represented using this modelling approach, as the degree of consolidation is calculated at different depths and no average coefficient of consolidation needs to be determined.

3.2.3. Discussion consolidation models

The numerical solution approach is often recommended, this is due to several reasons. Most important is a higher accuracy compared to the analytical solution (Deltares, 2016). Other differences are shown in table A.2 in appendix A.2.

3.3. Constitutive models

Three different constitutive models to calculate settlements over time exist. These are the Koppejan, NEN-Bjerrum and the abc isotache model. The NEN-Bjerrum and the abc isotache model share the same isotache formulation theory, but the NEN-Bjerrum uses linear strain, ε^C and the abc isotache model uses natural strain, ε^H. A graphical representation of this difference is shown in figure 3.2. The strains are defined as:

$$\varepsilon^C=\frac{h_0-h}{h_0} \qquad \varepsilon^H=-\ln\left(\frac{h}{h_0}\right)=-\ln\left(1-\varepsilon^C\right). \tag{3.9}$$

It can be seen through the definition of linear strain that values of strain higher than one can occur, which mean a settlement larger than the thickness of the layer. This problem is not there when natural strain is used, its value tends to infinite when the height tends to zero. Considering small strains, the two definitions become nearly equivalent.

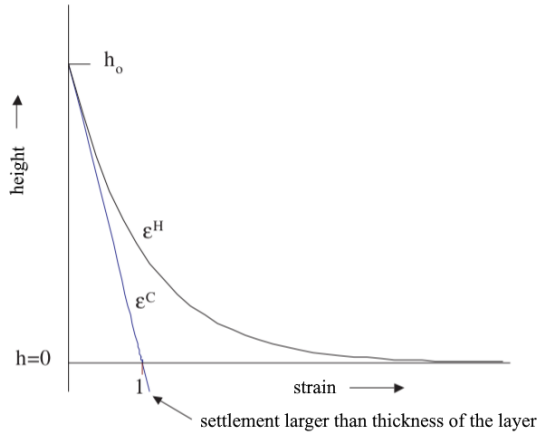

Figure 3.2: Difference natural and linear strain (Den Haan, 2003)

3.3.1. Koppejan model

The Koppejan model is a traditional choice to model settlements in the Netherlands. The model was developed by Koppejan who combined theories from Terzaghi and Keverling-Buisman to describe overall settlement behaviour (Koppejan, 1948). The model distinguishes between contributions to total settlements based on vertical effective stresses lower or higher than the preconsolidation pressure. In total, four different contributions can be distinguished in this model:

- Consolidation settlement for $\sigma' < \sigma_p$, governed by the consolidation compression coefficient C_p
- Consolidation settlement for $\sigma' > \sigma_p$, governed by the consolidation compression coefficient C'_p
- Creep settlement for $\sigma' < \sigma_p$, governed by the consolidation compression coefficient C_s
- Creep settlement for $\sigma' > \sigma_p$, governed by the consolidation compression coefficient C'_s

Combining the consolidation and creep contributions gives two equations for the total settlements, one for a situation with a stress below preconsolidation pressure, equation (3.10) and one for the situation with stress higher than the preconsolidation pressure, equation (3.11):

$$\frac{\Delta h}{h_0} = \frac{\Delta h_{cons} + \Delta h_{creep}}{h_0} = \left[\frac{U(t)}{C_p} + \frac{1}{C_s} \log\left(1 + \frac{t}{\tau_0}\right)\right] \ln\left(\frac{\sigma'}{\sigma_0}\right), \ \sigma_0 < \sigma' < \sigma_p, \tag{3.10}$$

$$\begin{aligned} \frac{\Delta h}{h_0} = \frac{\Delta h_{cons} + \Delta h_{creep}}{h_0} = &\left[\frac{U(t)}{C_p} + \frac{1}{C_s} \log\left(1 + \frac{t}{\tau_0}\right)\right] \ln\left(\frac{\sigma_p}{\sigma_0}\right) + \\ &\left[\frac{U(t)}{C'_p} + \frac{1}{C'_s} \log\left(1 + \frac{t}{\tau_0}\right)\right] \ln\left(\frac{\sigma'}{\sigma_p}\right), \ \sigma_0 < \sigma_p < \sigma'. \end{aligned} \tag{3.11}$$

In these equations Δh is total change in height [m] which consists of a consolidation Δh_{cons} and a creep Δh_{sec} contribution, h_0 is the initial height [m], $U(t)$ is the degree of consolidation [-], t is time [days], τ_0 is the reference time [days], σ' is the vertical effective stress [kN/m^2], σ_0 is the initial vertical effective stress [kN/m^2] and σ_p is the preconsolidation pressure [kN/m^2]. If the preconsolidation pressure is equal to the initial vertical stress for the calculation ($\sigma_p = \sigma_0$) equation (3.11) simplifies to

$$\frac{\Delta h}{h_0} = \left[\frac{U(t)}{C'_p} + \frac{1}{C'_s} \log\left(1 + \frac{t}{\tau_0}\right)\right] \ln\left(\frac{\sigma'}{\sigma_p}\right), \ \sigma_0 = \sigma_p < \sigma'. \tag{3.12}$$

The degree of consolidation factor ($U(t)$) is implemented in a way that it corresponds with equation (3.5) and this factor only influences the consolidation settlements over time. Figure 3.3 shows the settlement behaviour as a function of the natural logarithm of stress, together with the parameters mentioned above.

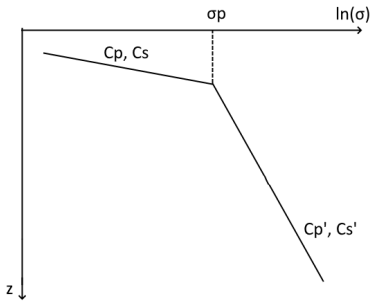

Figure 3.3: Koppejan settlement graph with parameters

3.3.2. NEN-Bjerrum model

Both the NEN-Bjerrum and the abc isotache model are based on the same isotache formulation. This isotache formulation is a theoretical basis for the creep rate. In the isotache formulation it is implied that all compression which is not elastic results from visco-plastic creep, where it should be noted that this visco-plastic part includes both consolidation and creep components as defined in this study. This model works with the assumption that creep strain is described by both a stress dependent and stress independent part. Creep rate reduces with a higher overconsolidation, which is influenced through ageing and unloading situations. This principle was noticed first by Bjerrum (1967), but Den Haan (1994) developed the mathematical formulation. It is shown using the NEN-Bjerrum parameters in figure 3.4 and with the abc parameters in figure 3.5. The NEN-Bjerrum isotache lines are parallel with a slope of $CR-RR$. Parameter RR is coupled to the direct (elastic) strain, and parameters CR and C_α are related to the secular visco-plastic component. Parameter CR is coupled to the stress dependent part of the formulation and C_α is coupled to the stress independent part.

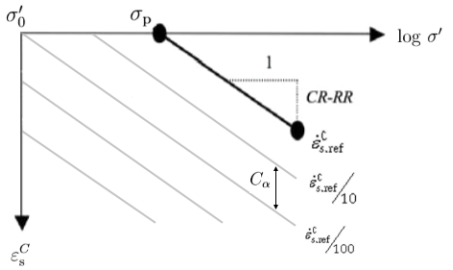

Figure 3.4: Isotache principle with NEN-Bjerrum parameters, based on Deltares (2016)

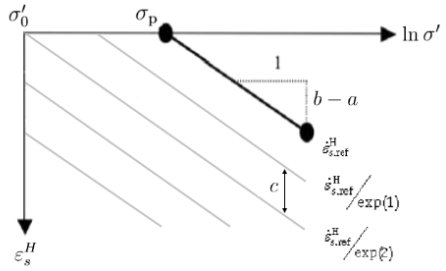

Figure 3.5: Isotache principle with abc parameters, based on Deltares (2016)

This model supports the current international standards for settlement predictions. Linear strain soil parameters are used under the assumption that strains are small. Its parameters can be easily determined based on oedometer tests. Considering idealized drained NEN-Bjerrum behaviour, there are three contributions to total settlement, the direct (elastic) settlement, consolidation settlement and creep settlement,

$$\frac{\Delta h}{h_0} = RR\log\left(\frac{\sigma_p}{\sigma_0}\right) + CR\log\left(\frac{\sigma'}{\sigma_p}\right) + C_\alpha \log\left(\frac{t}{\tau_0}\right), \tag{3.13}$$

using

$$CR = \frac{C_c}{1+e_0} \qquad RR = \frac{C_r}{1+e_0},$$

where C_r is the reloading/swelling index [-], C_c is the compression index above preconsolidation pressure [-], C_α is the coefficient of secondary compression [-], and e_0 is initial void ratio [-]. Figure 3.6 shows the parameters used in this model and how they are related to settlements. It should be noted that these graphs are based on idealized drained behaviour.

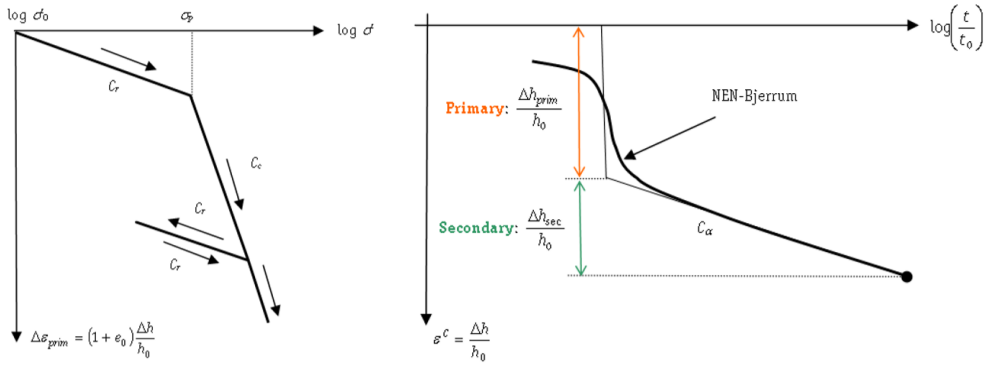

(a) Primary settlement during loading

(b) Primary and secondary settlement over time

Figure 3.6: Idealized NEN-Bjerrum settlements graphs for drained conditions with relevant parameters (Deltares, 2016)

The full mathematical formulation of the solution for the NEN-Bjerrum model, including the time effect through the degree of consolidation and considering several loading, reloading and unloading steps is given in the equations below:

$$\varepsilon^C(t) = U(t) \cdot \left(RR \log\left(\frac{\sigma_p}{\sigma'_0}\right) + CR \log\left(\frac{\sigma'_n}{\sigma_p}\right) + C_\alpha \log\left(\frac{t - t_n + \theta_n}{\tau_0}\right)\right), \tag{3.14}$$

where

$$\theta_n = \left(\frac{\sigma'_{n-1}}{\sigma'_n}\right)^{\frac{CR-RR}{C_\alpha}} \cdot (\theta_{n-1} + t_n + t_{n-1}),$$
$$\text{with } \theta_0 = \tau_0 \times \left(\frac{\sigma_p}{\sigma'_1}\right)^{\frac{CR-RR}{C_\alpha}}, \tag{3.15}$$

$$\sigma_p = \begin{cases} \sigma'_0 + \text{POP} & \text{for POP compression} \\ \sigma'_0 \times \text{OCR} & \text{for OCR compression} \\ \sigma'_0 \times \left(\frac{t_{age}}{\tau_0}\right)^{\frac{C_\alpha}{CR-RR}} & \text{for equivalent age compression.} \end{cases} \tag{3.16}$$

In this equation θ_n is the equivalent age [days], t_n is the begin time of step n [days] and n is the number of the load step [-], POP is the pre-overburden pressure [kPa] and OCR is the overconsolidation ratio [-].

3.3.3. Abc isotache model

As mentioned before, the abc isotache model is similar to the NEN-Bjerrum model, only this model uses natural strain and natural strain parameters. In case of large strains it is expected that this model gives more realistic settlement curves.

The isotache principle is shown in figure 3.5 using abc isotache parameters. Parameter a is coupled to the direct strain, and parameters b and c are related to the so-called 'secular component' (which includes both consolidation and creep). Parameter b is coupled to the stress dependent part of the secular strain formulation and c is coupled to the stress independent part. Isotache lines are parallel with a slope of $b - a$. Den Haan (1994) avoided the use of the terminology elastic compression for the

direct component, as he expressed some doubts regarding the full reversibility of this component upon unloading. Similar to the NEN-Bjerrum model, there is a full mathematical formulation of the drained solution for the abc isotache model, considering several loading, reloading and unloading steps,

$$\varepsilon^H(t) = U(t) \cdot \left(a \ln\left(\frac{\sigma_p}{\sigma'_0}\right) + b \ln\left(\frac{\sigma'_n}{\sigma_p}\right) + c \ln\left(\frac{t - t_n + \theta_n}{\tau_0}\right)\right), \tag{3.17}$$

where

$$\begin{aligned} \theta_n &= \left(\frac{\sigma'_{n-1}}{\sigma'_n}\right)^{\frac{b-a}{c}} \times (\theta_{n-1} + t_n + t_{n-1}), \\ &\text{with} \quad \theta_0 = \tau_0 \times \left(\frac{\sigma_p}{\sigma'_1}\right)^{\frac{b-a}{c}}, \end{aligned} \tag{3.18}$$

$$\sigma_p = \begin{cases} \sigma'_0 + \text{POP} & \text{for POP compression} \\ \sigma'_0 \times \text{OCR} & \text{for OCR compression} \\ \sigma'_0 \times \left(\frac{t_{age}}{\tau_0}\right)^{\frac{c}{b-a}} & \text{for equivalent age compression,} \end{cases} \tag{3.19}$$

where ε^C is the linear strain [-], θ_n is the equivalent age [days], t_n is the begin time of step n [days] and n is the number of the load step, POP is the pre-overburden pressure [kPa] and OCR is the overconsolidation ratio [-].

3.3.4. Discussion constitutive models

In this section the previously presented constitutive models are evaluated. Houkes (2016) reviewed multiple settlement prediction models and validated then on the basis of some case studies in the Netherlands. All three constituve models presented above were included in this review, and two (NEN-Bjerrum and abc isotache) were included in the validation part. Amongst others, this study provided input for this discussion.

Koppejan:
Limitations:

- The superposition principle used in the Koppejan model is proved to be incorrect (De Rijk, 1978). Using the Koppejan method together with the analytical (Terzaghi) consolidation approach leads to problems when a new loading phase is applied while consolidation following the previous loading phase is not 'fully' finished yet, due to this superposition principle. This is because the time for the second creep function starts from the moment the next loading is applied, while the effective stress used in this equation does not exist yet because the previous loading step has not completely consolidated yet. This then leads to an overestimation of the creep settlement Van Baars (2003).

- The model has not been designed to model unloading and reloading behaviour (Deltares, 2016). Unloading and reloading behaviour is relevant for projects where, for example, temporary surcharges are used. This is a common method in the Netherlands to limit residual settlements for construction purposes.

- The model works with the linear strain concept: when the loading component is large with respect to the initial effective stress, unrealistic large strains are modelled. Natural strain concept is introduced for the Koppejan model, but this requires the model parameters to be determined based on natural strain as well, which is often neglected in practice.

- This model assumes that creep is stress-dependent, also below the preconsolidation pressure. This is different from the other two constitutive models.

- The parameter U(t) is only implemented for the consolidation settlement. Consequently, the largest creep settlement already occur after the first day, even when the hydrodynamic period is larger than one day. To limit this effect, sometimes the U(t) factor is also applied to the creep term

(DWW, 1991), but this is theoretically incorrect as it is conflicting with the assumptions used to derive the 1D consolidation theory of Terzaghi.

Positive aspects:

- The Koppejan model is and has been a standard settlement model in the Netherlands, because of its simplicity. Consequently, many geotechnical engineers have experience working with this model.
- Duffy et al. (2020) showed potential for the parametrization of NEN-Koppejan settlement prediction using CPT (cone penetration testing). These and similar methods could reduce the influence of human error on settlement prediction.
- An incremental Koppejan method has been developed by Van Baars (2003). This method was reported to work well for staged loading. However, the incremental method is commonly not implemented in settlement prediction software.

NEN-Bjerrum
Limitations:

- The model works with the linear strain concept: when the loading component is large with respect to the initial effective stress, unrealistic large strains are modelled.
- No clarity on implementation of the degree of consolidation in the equation was found. At the moment the implementation of the parameter $U(t)$ in equation (3.14) is based on test scenarios with D-Settlement software. For the Koppejan settlement model it is clearly stated in literature that the degree of consolidation should be used for the consolidation settlements only (C_p and C'_p). The same clarity was not found for the NEN-Bjerrum model. Test scenarios with only the direct component (RR) or only creep settlement (C_α) showed that the degree of consolidation is also used in the calculation of these components over time.

Positive aspects:

- Isotache principle: does not use superposition principle anymore, and is therefore more suitable to model unloading/reloading situations

Abc-isotache
Limitations:

- No clarity on implementation of the degree of consolidation in the equation was found. At the moment the implementation of the parameter $U(t)$ in equation (3.17) is based on test scenarios with D-Settlement software. Same as for the NEN-Bjerrum model.
- Generally there is less experience on working with the abc isotache model compared to working with the Koppejan model.

Positive aspects:

- This model provides the most complete theoretical description as:
  - Natural strain is introduced in settlement predictions
  - Intrinsic time is used
  - Parameters b and c are independent of stress and time

Generally
All three models are evaluated in literature, with geotechnical engineers having different opinions on which model is most suitable in what situation. Generally, an uncertainty margin of 30% is given for settlement predictions with these constitutive models (CROW, 2004).

Houkes (2016) compared multiple different settlement prediction methods for soft soils in the Netherlands. Many limitations of settlement models and the use of their parameters were evaluated in this work. For the results obtained during that research the NEN-Bjerrum model yielded the best results in practice, though it was mentioned that *"theoretically, the abc model provides the most sound and versatile description of soil behaviour upon compression as well as unloading, as a function of time and stress, in a natural strain formulation*" (Houkes (2016), p.105).

Parameter determination is an important factor for the use of all consitutive models. Compression coefficients for the Koppejan and the NEN-Bjerrum models can be converted to each other. For converting these parameters to abc-isotache compression parameters more caution is needed, because these are natural strain parameters and the others are linear strain parameters. Some formulas for this conversion are given in Den Haan et al. (2004). When it is known what model is intended to be used, the parameter determination should be targeted at this constitutive model as directly as possible.

All constitutive models described here are limited to one dimensional problems. This should be considered when facing problems were two dimensional effects could have their influence. In commonly used software, like D-Settlement, an option for two dimensional settlement predictions is provided. This should be used with caution as still one dimensional vertical settlement prediction models are used. In this project, when possible, multiple constitutive models are used to evaluate their different results. This mostly depends on the availability of soil parameters.

3.4. Discussion

Two aspects that have not been considered, but do have an influence on the modelling of compression behavior from loading are discussed below. These are the tertiary compression phase, as found in literature, and characteristics of compression behaviour for organic and peat soils.

Tertiary compression

Research indicated that sometimes the rate of creep is not constant with logarithmic time, as observed by Edil and Dhowian (1979) in peat soils and by Bishop and Lovenbury (1969) in clay soils. This lead to the term 'tertiary compression', introduced by Edil and Dhowian (1979), which indicates a change in the strain rate during creep. The component is shown in figure 3.7.

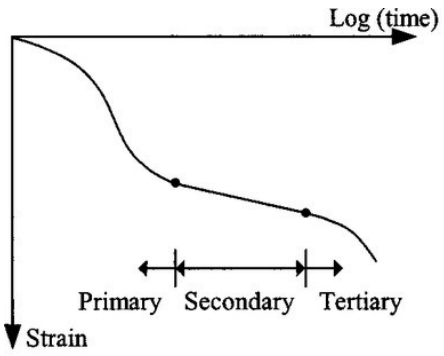

Figure 3.7: Tertiary compression included on time versus strain figures (Liingaard et al., 2002)

Edil and Dhowian (1979) suggested that this behavior is related to a major structural change, that occurs at some value of strain for a particular load increment. It was indicated that for peat this tertiary compression occurred at all stress levels, but that a higher stress level caused it to occur more quickly and to have a lower intensity.

This phase is not included in current modelling techniques. Den Haan and Edil (1994) mentioned that caution needs to be taken for modelling practical problems of peat compression with the abc isotache model over large periods of time, in relation to the tertiary compression findings. Related to compression for peat soils, Den Haan (1994) introduced the possibility of using an additional parameter d in the abc isotache model to include tertiary compression behavior. The drained formulation of the abc isotache model is then

$$\begin{aligned}\varepsilon^H(t) &= a\ln\left(\frac{\sigma_p}{\sigma'_0}\right) + b\ln\left(\frac{\sigma'_n}{\sigma_p}\right) + \left(c + d\ln\left(\frac{\sigma'_n}{\sigma_p}\right)\right)\ln\left(\frac{t-t_n+\theta_n}{\tau_0}\right) \\ &= a\ln\left(\frac{\sigma_p}{\sigma'_0}\right) + \left(b + d\ln\left(\frac{t-t_n+\theta_n}{\tau_0}\right)\right)\ln\left(\frac{\sigma'_n}{\sigma_p}\right) + c\ln\left(\frac{t-t_n+\theta_n}{\tau_0}\right).\end{aligned} \tag{3.20}$$

The determination of the parameter d is difficult and the tertiary effect is known to be small relative to the overall final strain. Equation (3.20) has not been used and the tertiary component is often neglected in practice. Though Malinowska (2016) mentioned that tertiary compression in should be included in consolidation settlement models .

Organic soils / peat

Describing behaviour of organic soil with models on the basis of mineral soil can be problematic. Fibres in organic soil strongly influence the compression behavior of the soil, especially in peat soils. With a higher fibre content, the behavior of these soils will differ more from the behavior of inorganic soils. Johari et al. (2016) and Duraisamy et al. (2007) showed that a higher fibre content will result in a higher compression index and a larger settlement.

Fibres in the soil also cause an anisotropic factor in the material, where for instance differences in horizontal and vertical hydraulic conductivity are relevant (Beckwith et al., 2003a). Considering a one-dimensional consolidation problem, the vertical hydraulic conductivity is used. The hydrodynamic period for peat soil is relatively short because of its commonly high initial hydraulic conductivity. However, during loading the hydraulic conductivity of peat decreases strongly.

Robinson (2003) indicated that the use of Terzaghi's one dimensional consolidation theory might be inappropriate, as organic particles in peat soils can be compressible. This is a violation of one of the assumptions that was used in the derivation of the equation (see the list in section 3.2). Yang and Liu (2016) mentioned part of the initial settlement might come from organic matter compression but no detailed studies to this component had been found. Moreover, in their study it is indicated that the compression of gas bubbles in the peat soil can complicate the situation further. These gasses are the result of degradation processes and can be trapped within the peat soil voids. The deformation of peat soil is then defined as a coupled process of three components: drainage of pore water, volume change of gas bubbles in the soil and compression of organic particles. Yang and Liu (2016) derived a new consolidation model for peat soils, where both gas bubbles and possible compression of organic matter grains were included:

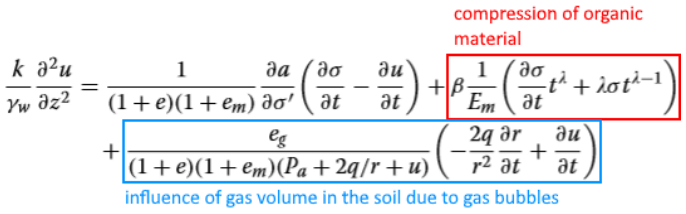

Figure 3.8: Consolidation equation for peat, including effects of compressible organic matter and gas bubbles, from Yang and Liu (2016)

It was concluded based on comparison of test data with the model results that this model equation could be used to analyze the consolidation behavior of peat soil. A drawback of this method is the many parameters that are used, like the time factor λ, the initial constrained modulus E_m and the gas bubble radius r. It is expected that the compressibility of organic material in peat soil itself is often not a relevant contribution compared to other subsidence processes, as the actual organic material in peat soil is only about 5 to 10% of its total soil volume.

4

Compression by degradation of organic material

An important component of subsidence in the Netherlands is compression by degradation of organic matter. In this section this process will be evaluated. The current knowledge on this process is summarized, including factors that influence the subsidence or subsidence rate caused by this component, section 4.1. After that, existing modeling techniques that were found in literature are evaluated and discussed, section 4.2.

4.1. Degradation process

Organic matter is a complex material that consists of many different organic compounds and can be found in aquatic and terrestrial environments. Organic compounds are a class of chemical compounds, they consist of carbon atoms bonded to hydrogen and often bonded to other elements as well. Soil organic matter (SOM) describes the organic matter component in mineral soil. It consists of all plant and animal residues and their organic transformation residues. Living components, soil flora and fauna, are not included in the SOM. When constant environmental conditions are maintained, there is an equilibrium between the supply and degradation of organic matter in the soil. This equilibrium results in a characteristic organic matter content.

Degradation or decomposition of SOM is the conversion from complex chemical compounds to smaller and more simplified compounds through different processes in the soil. These are physical-mechanical, chemical and biological processes. The biological processes, decomposition by micro-organisms in soil, are most important for the degradation. Different processes are relevant during degradation, which can happen simultaneously or sequentially. Definitions of some important processes are given below:

- *Mineralization*: Complete decomposition by micro-organisms that convert organic matter to inorganic compounds. The carbon of the organic compounds is released as CO_2 or methane (CH_4), though it should be noted that CH_4 is not an inorganic compound. Plant nutrients are released as well.
  - *Assimilation*: Micro-organisms use organic components as building material for their cell material.
  - *Dissimilation*: Micro-organisms oxidize organic components to obtain energy for their life functions.
- *Immobilization*: Conversion of inorganic compounds to organic compounds
- *Humification*: Formation of humus, which is derived from microbial decomposition of organic residues. Under natural conditions, soil humus is decomposed very slow. Humus can persist

for large time frames (several hundred years) in combination with soil minerals, as interaction between these components can limit availability for microbial degradation.

Decomposition of organic material can be aerobic or anaerobic, based on the availability of oxygen. When SOM decomposition under aerobic conditions is considered, for example due to the increase extent of aeration following the drainage of peatlands, often the term 'oxidation' is used. Under aerobic conditions oxygen functions as electron acceptor. The endproduct of this process is CO_2. Under anaerobic conditions other components function as electron acceptor, as oxygen is not available. The use of other components proceeds in a sequential order, based on redox potential. This results in an order of processes, which is denitrification, fermentation, sulfate reduction and last methanogenesis. These are important pathways for SOM degradation considering situations with organic soils and high groundwater levels in the Netherlands. End products of this decomposition process can be CO_2 and CH_4, together with many others.

Through the emission of these greenhouse gasses, degradation of organic matter has an influence on enhanced global warming. CO_2 emissions from aerobic degradation of SOM in peat soils in the Netherlands are about 4.2 million ton CO_2 per year (Van den Akker et al., 2012), which is approximately 3% of the total yearly emission of greenhouse gasses in the Netherlands. Emissions of CH_4 are often evaluated with respect to rewetted peatlands, where anaerobic circumstances might cause an increase of CH_4 emissions. Compared to CO_2, CH_4 has a lower atmospheric lifetime but a larger radiative efficiency (Myhre et al., 2013).

Organic compounds each have an own decomposition rate, some compounds are more easily degradable than others. SOM consists of organic material at different stages of their decomposition process. Examples of different chemical compounds of organic matter are cellulose, hemicellulose, soluble sugars and lignin. Reaching further in the decomposition process, the material often becomes more resistant against further decomposition, due to a decrease in both hydroxyl and methoxyl groups and an increase in the carboxyl groups (Alexander et al., 1961).

The decomposition rate for aerobic situations is higher than for anaerobic situations, considering a peat soil. Freeman et al. (2001) stated that this anaerobic decomposition rate for peat soils is low because of the chemical composition of peat soil. It contains a high amount of phenolic compounds, which are not easy degradable without oxygen as the enzyme phenol oxidase is nearly inactive in anaerobic conditions. Moreover, these phenolic compounds act as inhibitors by preventing hydrolase enzymes from carrying out normal decomposition processes (Freeman et al., 2001). Fenner and Freeman (2011) showed that when oxygen is introduced to the system, there is a double effect where the phenolic compounds itself start to be decomposed and normal decay process for other compounds can be resumed as well by hydrolase enzymes. However, Brouns et al. (2016) concluded that this emzymic latch theory was not supported by their research for drained peat soils in the Netherlands.

Peat and organic soils are soil types where possible degradation of organic material is relevant. Drainage of peatlands creates a loss of water that is retained in the 'sponge' like material. When oxygen then is introduced to the system, through for example intensive drainage and agriculture, SOM can be degraded. This degradation and humification leads to the degradation of the structure of the soil, which causes a reduction in the water retention, water storage and water transmission capacity of the soil (Kechavarzi et al., 2010). Through this process a subsidence component is introduced, which consists mostly of the loss of water that is retained, as the volume of the organic particles themselves is small compared to the total soil volume. This process is shown in figure 4.1.

An important factor to consider is that not all SOM is available for decomposition. Part of the organic matter is stabilized through interaction with the soil matrix, isolation in soil pores, physical occlusion within aggregates and absence of the required microbial decomposers (Bailey et al., 2019, Smernik and Skjemstad, 2009). Kleber et al. (2011) showed that chemical recalcitrance of older organic matter may not be as relevant for stabilization as was previously considered.

Next to this stabilization/destabilization effect, some other factors also have influence on the decomposition rate of organic material. Influences of temperature, water content, oxygen supply, pH, soil properties and composition of the organic material are evaluated.

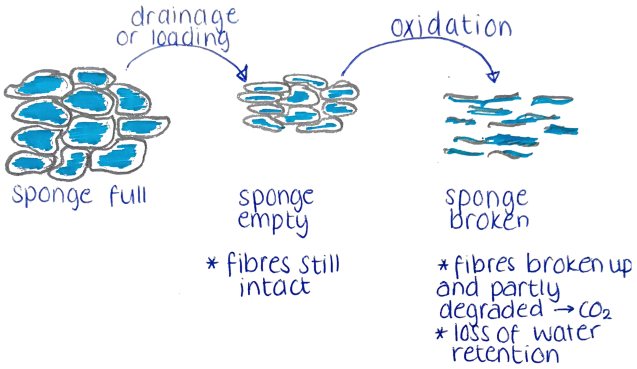

Figure 4.1: Schematic representation of processes upon drainage of peat soil, based on sketch from Julia

Temperature

The rate of decomposition for any microbiological process increases with an increase in temperature, until a certain optimal temperature is reached. This effect was described by Arrhenius (1889) using

$$k = A * e^{-E_a/RT}, \tag{4.1}$$

where k is the reaction rate constant [time^{-1}], A is a pre-exponential factor, E_a is the activation energy [J mol^{-1}], R is the universal gas constant [J mol^{-1} K^{-1}] and T is the temperature [K].

This effect is often characterized by a Q10 temperature coefficient (Tate et al., 1987). The Q10 value is a value that describes the effect of an increase of 10°C on the degradation rate. It depends on the microbial reaction, the composition of the organic matter, and the temperature range. Many different studies have been conducted to find this value for decomposition of organic material in the temperature range from 15-35°C. It is commonly stated that generally this value lies between 2 and 3 (Addiscott, 1983, Campbell et al., 1981, von Lützow and Kögel-Knabner, 2009), considering SOM as one homogeneous pool. Bunnell et al. (1977) stated that this Q10 value increases with depth in the soil. Vermeulen and Hendriks (1996) concludes this as well and states that this shows micro-organisms in the top soil are better adapted to a situation with temperature fluctuations. Most micro-organisms are mesophilic, which means there optimal temperature lies between 20-40°C, with an optimum of 35°C. Micro-organisms that prefer much higher temperatures (> 45°C) are called thermophilic and the ones that have a low optimal temperature (< 20°C) are psychrophilic. Micro-organisms that are best adapted to the prevailing environmental conditions will proliferate. As they each have different degradation qualities and rates, this can indirectly influence the degradation rate as well.

The temperature effect considering degradation of SOM is relevant considering climate change scenarios. Querner et al. (2008) stated that an increase of temperature of 2°C together with a change in air circulation in the future increases the rate of subsidence and CO_2 emissions, caused by aerobic degradation, by 68%.

Water content

With a low amount of water in the soil, soil dries and its matric potential increases. This exerts an osmotic force on micro-organisms which restricts them. Different micro-organisms have different tolerances towards decreasing water potentials. At a very low matric potential, the remaining water in the soil is located in the smallest pores and in a thin water film around the soil particles. This can also limit micro-organisms in the degradation process when nutrients cannot move by diffusion through these thin water layers, and micro-organisms become substrate-limited.

In contrast, when the water content gets too high a lack of oxygen caused by a slow diffusion rate of oxygen in water limits aerobic decomposition of organic material. Water content and oxygen content in pores are linked, since pores filled with water cannot contain gas and the other way around.

Statements on an optimal water content for microbiological processes should be treated with care,

as this effect of water always depends on the pore size distribution, which is determined by soil texture and compaction. In general it can be said that the water content should be high enough not to have the osmotic force, but not too high where it limits the water-free porosity of the soil.

A variation in water content of soil has an accelerating effect on decomposition of stabilized organic material (Denef et al., 2001). Due to alternation swelling and shrinkage conditions some organic material gets physically mechanically decomposed. This previously stabilized organic mass then becomes available for further decomposition by micro-organisms. This is relevant in peatlands, where varying groundwater levels can cause these alternating situations.

Considering aerobic decomposition of organic material, quality of the pore water is can also be an influencing factor. Brouns et al. (2014) showed that salinization could reduce aerobic decomposition with 50%, and this response does not depend on land use and peat origin. Salinization showed no effect on the anaerobic decomposition rate.

Oxygen supply

Oxygen supply in the soil is determined by diffusion laws. The main important parameter governing this behaviour is the gas diffusion coefficient of soil, which depends on many variables. It is mostly determined by the texture and compaction of soil, which drive soil parameters like porosity, air-filled porosity (AFP), aggregation, connectivity and tortuosity of pores (Moldrup et al., 2001). More irregular shapes of pores cause the diffusion coefficient to be lower and reduce oxygen transportation (Hendriks, 1991). As mentioned before, oxygen supply can limit degradation, and this is connected with water content as well because oxygen has a low diffusion coefficient in water (a factor of about 10^4 lower than in air).

Even with a low water content and a high water-free porosity, oxygen deficiency can occur, due to a high concentration of other gases produced in the soil. In soil aggregates porosity is commonly lower than the overall porosity. This slows down transportation of oxygen and influences possible occurrence of anaerobic conditions.

Whether aerobic conditions or anaerobic conditions occur can vary over time, because of variations in groundwater level and, in agricultural context, possible tillage operations. Moreover, shrinkage processes have a positive influence on the oxygen supply in the soil, through shrinkage cracks.The possible variation of effective diffusion coefficient over time is also important. Increasing compression of soil will decrease the effective diffusion coefficient, and thus decrease the depth that oxygen can diffuse into the soil.

pH value

Microorganism activity in the soil is greatest near neutral pH, though the optimal pH value varies for different types of microorganisms (McCauley et al., 2009). Most bacteria function optimal in an environment with a neutral pH value. In acidic conditions fungi will be more represented, as they are better resistant to these conditions. Bacteria commonly grow faster and decompose more material to CO_2 than fungi, and therefore neutral conditions generally have a positive influence on the decomposition rate. Though this should be treated with care as some organic compounds are more easily decomposed by fungi than by bacteria.

Soil properties

The influence of the soil properties can be connected to its water retention properties, its pore size distribution and therefore its water and gas transport properties. When a soil is too coarse grained, not enough water can be retained, but when a soil is too fine grained, the oxygen supply is limited.

Chemical properties of the soil have its influence through the nutritional elements that are or are not present in the soil, and also govern soil pH and salinity, of which the influence was discussed before. Many studies tried to relate total organic carbon (TOC)/total nitrogen (C/N) ratios to decomposition rates (Dijk, 1980, Hassink, 1995, Liu et al., 2007, Murayama and Zahari, 1991), but it is shown that variation in environmental conditions and different types of organic matter have influences on such a relation. In general organic matter with low C/N ratios are better degradable than organic matter with high C/N ratios, considering the same environmental conditions. Brouns et al. (2016) identified phosphorus enrichment as a potential driver of an increase in decomposition rate in drained peat soils in

the Netherlands.

Composition of organic matter
Another important chemical influence on the decomposition rate is the composition of the organic matter. Different organic constituents have different decomposition rates, as mentioned before. Below organic constituents are mentioned from easy to decompose to very difficult to decompose.

$$sugars \rightarrow proteins \rightarrow hemicellulose \rightarrow cellulose \rightarrow fats,\ waxes\ and\ resins \rightarrow lignin$$

In the Netherlands, old organic and peat soils are present, with a generally high degree of humification. Therefore, the composition of humus material itself is relevant. Humus exists of humic substances. These substances can be subdivided in three groups, based on their solubility in water for different levels of acidity, these are: humins, humic acids and fulvic acids.

- *Humins*: The fraction of humic substances that is not soluble in water at any acidity level. This fraction has functions related to the soil water retention capacity, the soil structure and stability and the cation exchange system. This component is the most resistant against decomposition.
- *Humic acids*: The fraction of humic substances that is soluble in water at an acidity level of pH > 2 (acid-insoluble materials)
- *Fulvic acids*: The fraction of humic substances that is always soluble in water, independent of acidity level. Results from Qualls (2004) supported the hypothesis that fulvic acid is more rapidly degraded than humic acid, and thus the least stable of the three.

4.2. Existing modelling techniques

The currently available modelling techniques for subsidence following degradation of organic material are described here. These modelling techniques are developed for compression by oxidation, not for anaerobic decomposition of organic material.

Stephens et al., 1984

Stephens et al. (1984) developed a modelling equation which links soil temperature and drainage depth to soil subsidence in low-moor peat soils, called the "Stephens-Stewart-Chew" basic subsidence equation. This equation is based on Arrhenius's law. The Stephens-Stewart-Chew subsidence equation is

$$S(T,h) = (a + bh)e^{k(T-T_0)} \tag{4.2}$$

where $S(T,h)$ is the biochemical subsidence rate [cm year^{-1}], h is the depth of the water table [cm], k is the reaction rate constant [-], T is the soil temperature [°C], T_0 is a threshold soil temperature below which the biochemical reaction is not active [°C], and a [cm year^{-1}] and b [year^{-1}] are fitting parameters.

The values for k and T_0 were determined based on laboratory data for peat soils in Everglades, Florida. The parameters a and b could then be found using measured yearly subsidence rate. The following equation was then constructed, where T_x is the annual average soil temperature at 10 cm depth:

$$S(T,h) = (-0.1035 + 0.0169h)(2)^{(T_x-5)/10}. \tag{4.3}$$

A positive aspect from this model is that it includes the effect of temperature on the decomposition rate and thus on the subsidence rate from oxidation. Drawbacks are that the model parameters are found for Everglades peat soils and not for Dutch peat soils. Laboratory and field data is necessary to determine model parameters for other soils. Influences of water content, pH, soil properties and the composition of organic matter are not included through the formula, but embedded in the a and b parameters itself. Influence of temperature differences over depth are not considered. Moreover, it is questionable whether this models only subsidence from oxidation, as its parameters are determined by comparing total subsidence with measurements.

Van der Meulen et al., 2007

Van der Meulen et al. (2007) estimated the sediment deficiency in the Netherlands. To estimate the volume loss due to peat oxidation they used

$$\Delta h_t = h_{dry} \cdot (1 - e^{-V_{ox} \cdot \Delta t}), \tag{4.4}$$

in which Δh_t is the height reduction of the peat layer above the phreatic water level at time t [m], V_{ox} is the rate of peat oxidation [m m^{-1} year^{-1}], Δt is the increase in time [year] and h_{dry} is the total thickness of the peat organic matter thickness above phreatic water level [m]. Other studies were this equation was used as well are Fokker et al. (2015), Muntendam-Bos et al. (2009) and Koster et al. (2018b).

This equation uses the parameter V_{ox}, which is determined for a typical Holocene peat in the Netherlands. The value that is commonly used is 0.015 m m^{-1} year^{-1}, found by Van der Meulen et al. (2007), who stated that this value was empirically obtained. It is not clear how this value of 0.015 m m^{-1} year^{-1} was empirically obtained, therefore it cannot be concluded for what conditions this is valid. Influences of temperature, pH, water content, soil properties and the composition of organic matter are not included directly, but can be included through a variation of this parameter.

Van den Akker et al., 2008

Van den Akker et al. (2007) determined empirical relations between land subsidence and drainage of peatland for situations with and without a clay layer on top. These empirical relations are based on subsidence measurements at the Zegveld polder. Linear relations were proposed between the ditch water level (DWL) or the average deepest groundwater level (ADG, dutch: GLG) and land subsidence rates. This is shown in figure 4.2. All subsidence mechanisms following shallow groundwater lowering are all indirectly represented in these equations, which is the largest limitation of this modelling approach.

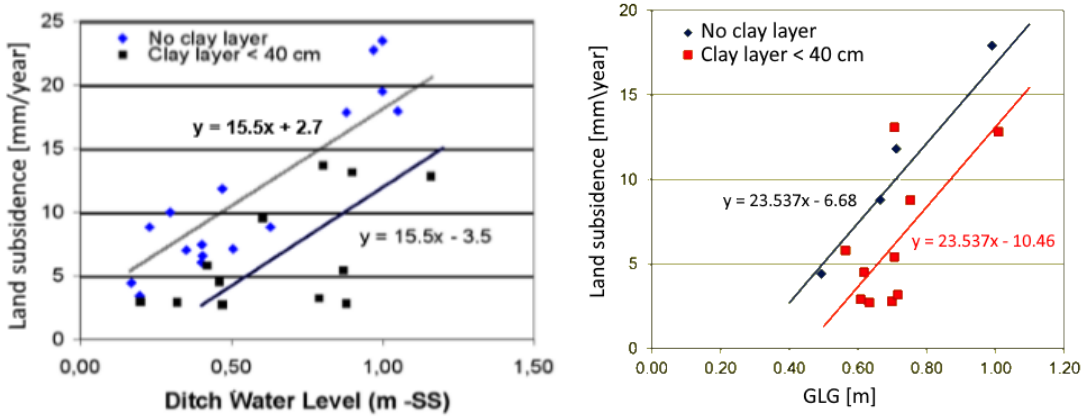

(a) Relations DWL to land subsidence

(b) Relations GLG to land subsidence

Figure 4.2: Relationships found by Van den Akker et al. (2007) in the Zegveld polder

For a peat soil without clay cover, the following equations can be used to quantify land subsidence by lowering of the shallow groundwater level:

$$\Delta L = 15.5 \cdot DWL + 2.7, \tag{4.5}$$

$$\Delta L = 23.537 \cdot GLG - 6.68, \tag{4.6}$$

where DWL is the ditch water level and GLG is the average lowest groundwater level. For a peat soil with a thin clay layer (< 40 cm) cover two slightly different equations can be used to quantify land subsidence by lowering of the shallow groundwater level:

$$\Delta L = 15.5 \cdot DWL - 3.5, \tag{4.7}$$

$$\Delta L = 23.537 \cdot GLG - 10,47. \tag{4.8}$$

These equations are commonly used in land subsidence assessments in the Netherlands, because the input data required is often available. Querner et al. (2012) mentioned in their study that this relation can only be used for situations with similar climate conditions as in the Netherlands. Van Hardeveld et al. (2017) used an modelling equation which was obtained by combining the two relations from Van den Akker et al. (2007). An average clay thickness of 0.2 m at the Zegveld location was assumed to come to a combined formulation of the equations

$$\Delta L = 23.45 \cdot GLG - 18.34 \cdot CL - 6.68, \tag{4.9}$$

in which, ΔL is the rate of soil subsidence [mm year^{-1}], GLG is the average deepest groundwater table level [m below surface] and CL is the thickness of a potential clay layer on top of the peat layer [m]. In the research from Van Hardeveld et al. (2017) a time step of 5 years was used for parameter adjustment because it is stated this time step best reflects the average readjustment period of surface water levels in Dutch peatlands.

Zanello et al., 2011

Zanello et al. (2011) used an improved version of the modelling approach from Stephens et al. (1984) in their study to irreversible peat subsidence in the Zennare Basin. They chose this approach because the equation does includes the effect of temperature. The modelling approach was adjusted so local agricultural practices (ploughing) and carbon fraction changes over the long term could also be included. To do this a corrective factor is introduced in

$$S^*(T,h) = S(T,h)\frac{\epsilon_{u,\tau}}{\epsilon_{u,\tau_0}}, \tag{4.10}$$

where $S^*(T,h)$ is the subsidence rate considering the available carbon matter [cm year^{-1}], $S(T,h)$ is the subsidence rate as calculated by Stephens et al. (1984) [cm year^{-1}], $\epsilon_{u,\tau}$ is the carbon fraction of the peat above the water table level at time t [-] and ϵ_{u,τ_0} is the carbon fraction of the peat above the water table level at time t_0 [-]. $\epsilon_{u,\tau}$ can be calculated with

$$\epsilon_{u,\tau} = \epsilon_{u,\tau_0} - \left(1 - \frac{\rho_l \cdot \epsilon_l}{\rho_u}\right)\frac{\tau_0 - \tau}{\tau^\star}, \tag{4.11}$$

where ρ_l is the bulk density of the peat soil below the water table [kg m^{-3}], ϵ_l is the organic matter fraction of the peat soil below the water table [-], ρ_u is the bulk density of the peat soil above the water table [kg m^{-3}], τ_0 is the peat thickness at time t_0 [cm], τ is the peat thickness at time t [cm] and $\tau^\star$ is the reference thickness of the initial peat above the water table [cm].

Hoogland et al., 2012

Hoogland et al. (2012) used a model to forecast land subsidence in the polder Groot-Mijdrecht to see how long and where agricultural land use will still be possible in the future. This model included an overall calculation of the subsidence rate, as also other subsidence components where included through the parameter C,

$$\frac{dE(s,t)}{dt} = -K \cdot fO(s,t) \cdot \{E(s,t) - W(s,t)\} - C, \tag{4.12}$$

in which $dE(s,t)$ is the subsidence rate [mm year^{-1}], $E(s,t)$ is the surface elevation at location s and time t [mm], $W(s,t)$ is the regulated surface water level at location s and time t [mm], $fO(s,t)$ is the fraction of the upper part of the soil profile where sufficient oxygen is available for oxidation, K is the fraction of peat thickness that oxidises [year^{-1}] and C is the additional subsidence rate due to other processes [mm year^{-1}]. $fO(s,t)$ is calculated using the equation below, which uses a parameter for the maximum depth were sufficient aeration occurs, D:

$$fO(s,t) = \begin{cases} \frac{P(s,t)}{D} & P(s,t) \leq D \\ 1 & P(s,t) > D. \end{cases} \tag{4.13}$$

In their research this parameter D was approximated by the groundwater level depth in dry periods, which was estimated to be 0.80 m based on (Van den Akker et al., 2007). The parameters K and C were found based on a model calibration with project data from the polder Groot-Mijdrecht, where $K = 0.0105$ [year^{-1}] and $C = 0.68$ [mm year^{-1}]. A positive aspect of this model is that it includes a factor to account for the influence of oxygen supply on the subsidence rate. Taking the parameter C out of equation 4.12 gives an equation that can be used to estimate subsidence from compression by oxidation.

Fokker et al., 2019

Fokker et al. (2019) used a modified version of the equation used by Van der Meulen et al. (2007). The modification is the consideration of admixed clastic sediments, because only the organic material oxidises. They calculated the height reduction from oxidation with

$$\Delta h_{ox} = (1 - e^{-V_{ox} \cdot \Delta t}) \cdot (h(t) - \lambda_{r,ox} h_0), \tag{4.14}$$

in which Δh_{ox} is the reduction of peat thickness above the phreatic water level [m], V_{ox} is the rate of oxidation [m m^{-1} year^{-1}], Δt is the increase in time [year], $h(t)$ is the total thickness of peat above phreatic water level [m], $\lambda_{r,ox}$ is the fraction of the initial thickness which consists of admixed clastic sediments [-] and h_0 is the initial thickness in [m].

This equation also uses the parameter V_{ox}, but in this research parameters are extracted from project data from Flevoland, through Ensemble Smoothing with Data Assimilation (ES-MDA). Two estimates are done for each parameter, one based on a Koppejan settlement model approach, and one based on a NEN-Bjerrum settlement model approach. The values found in their study are listed in table 4.1.

Table 4.1: Estimated values for the parameters of the oxidation equation for peat from Fokker et al. (2019). Number in the brackets is the standard deviation in units of the last digit.

Parameter	NEN-Bjerrum estimate	Koppejan estimate	Unit
V_{ox} Peat	0.0123 (17)	0.0088 (16)	m m^{-1} year^{-1}
$\lambda_{r,ox}$ Peat	0.09 (30)	0.088 (26)	-

Bootsma et al., 2020

Bootsma et al. (2020) described a modelling approach that can be selected in the subsidence model Atlantis, where the volume loss by oxidation is calculated by an organic-mass based approach. The height reduction in a time step is calculated by

$$\Delta L^{ox} = \Delta M_{org} \hat{V}, \tag{4.15}$$

where ΔL^{ox} is the height reduction by oxidation [m], ΔM_{org} is the change in organic mass [kg] and $\hat{V}$ is the specific volume of oxidation [m^3/(kgm^2)]. The change in the organic matter content over one time step is calculated with

$$\Delta M_{org} = -\alpha_m L \Delta t, \tag{4.16}$$

where α_m is an empirical constant which is estimated based the project data from Van den Akker et al. (2007), which represents the constant rate of organic mass loss [kg year^{-1}], L is the current height of the unsaturated zone [m], and Δt is the time step [year]. To use equation 4.15 the parameter $\hat{V}$ can be calculated with

$$\hat{V} = \frac{0.5}{F_{org} \rho_{bulk}} \left(1 + erf\left(\frac{F_{org} - 0.2}{0.1}\right)\right), \tag{4.17}$$

where F_{org} is the organic mass fraction and ρ_{bulk} is the dry bulk density. These parameters are updated each time step, based on the organic mass loss. The initial dry bulk density can be calculated using an equation from Erkens et al. (2016):

$$\rho_{bulk}(t_0) = \frac{100}{F_{org}(t_0)} \left(1 - e^{-\frac{Forg(t_0)}{0.12}}\right), \tag{4.18}$$

where $F_{org}(t_0)$ is the organic mass fraction at time t = 0 [-]. The updated F_{org} can be calculated based on the updated M_{org}, equation 4.20. The updated organic mass content is calculated with

$$M_{org}(t + \Delta t) = M_{org}(t) + \Delta M_{org}(t), \tag{4.19}$$

$$F_{org} = \frac{M_{org}}{M_{org} + M_{min}}, \tag{4.20}$$

where M_{org} is the organic mass content and M_{min} is the mineral mass content. The updated dry bulk density, which is used in equation 4.17, can be calculated based on the updated L and M_{org} by using

$$\rho_{bulk} = \frac{M_{org} + M_{min}}{L}. \tag{4.21}$$

The initial organic mass content can be calculated with formula 4.22. M_{min} (the mineral mass content) stays constant over time and can be calculated with equation 4.23,

$$M_{org} = F_{org}(t_0) \cdot \rho_{bulk}(t_0) \cdot L(t_0), \tag{4.22}$$

$$M_{min} = (1 - F_{org})\rho_{bulk} L. \tag{4.23}$$

A positive aspect of this approach is that soil properties can be more accurately represented by working with organic mass content and bulk densities. Moreover, this approach can also be used for organic clays because of its organic mass based approach. To use this model characteristics of the soil need to be known. A limitation is that the value of the parameter α_m is not given in the paper, and no indication of a possible value in the Netherlands is provided in this research.

Overview models oxidation

Table A.3 in appendix A.3 shows an overview of the characteristics of the above mentioned oxidation modelling techniques.

4.3. Discussion

Degradation of organic material, especially the aerobic component, is known to be relevant for land subsidence in the Netherlands, and is incorporated in most subsidence models through one of the equations introduced in the previous section. Based on theoretical knowledge, it is assumed that the subsidence calculated by these equations follows mostly from the loss of water of the soil, through a decrease in water retention capacity caused by the degradation of the organic material. This factor is often not specifically mentioned in the subsidence studies. For area type 2, the natural and agricultural lands, this submodel is expected to be an important factor for the overall model results.

Relevance organic matter degradation Netherlands

Figure 4.3 shows the estimated SOM content in the upper 0.3 m of the Dutch soils. Hotspots with a high percentage of SOM in the topsoil are found in the western and northern parts of the Netherlands. Conijn and Lesschen (2015) showed that within the type 2 areas, grasslands generally contain more SOM than croplands and nature areas. As explained in sections 2.3 and 4.1, it is not only the SOM content but also the stability of the material and the resistance against further decomposition, that are relevant in determining the potential relevance of an oxidation component.

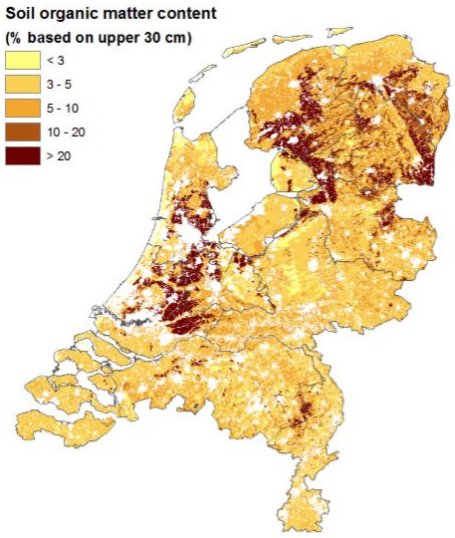

Figure 4.3: Estimated SOM content in the upper 0.3 m of the soil in the Netherlands (Lesschen et al., 2012)

In the Netherlands, generally organic soils can be found where the SOM is of high stability and age and the degree of humification is high. These organic soils are relatively stable against further decomposition, and only a change in the system, like the introduction of oxygen, can induce a higher degradation rate.

Modelling approach

Different oxidation models described in section 4.2 each have their own positive and negative aspects. All models use a parameter that in a way characterizes a rate of the oxidation process, examples for this are V_{ox}, k, K and α_m. This is based on a hypothesis from Kortleven (1963) who argued that per year a fraction of the organic mass is decomposed and leaves the soil through this process. Influencing factors like temperature, pH, water content, soil properties and the composition of organic matter are included indirectly in this parameter.

Most approaches do not directly include the influence of a higher temperature on the decomposition rate. The only exception here is the approach of Stephens et al. (1984), which was also used by Zanello et al. (2011). Oxygen supply is most often assumed to be sufficient throughout the unsaturated zone of the soil, only Hoogland et al. (2012) included a factor that accounted for the maximum depth where sufficient aeration occurs in the unsaturated zone.

There are many characteristics related to the soil properties and the composition of the organic matter that influence the decomposition rate, as mentioned in section 4.1. Zanello et al. (2011), Fokker et al. (2019) and Bootsma et al. (2020) all used a factor to consider a fraction or mass of mineral particles admixed in the organic soil layers, ε_l, $\lambda_{r,ox}$ and M_{min}. In the approach of Fokker et al. (2019) this factor $\lambda_{r,ox}$ actually characterises the height of the soil layer that remains for $t \rightarrow \infty$. From a theoretical perspective, it makes sense that there a certain height of the soil remains, but this might be more than only height from the mineral particles, as some SOM can be stabilised by the soil matrix and remains unavailable for degradation.

Based on the evaluation of the oxidation models and their parameters, it is seen that generally two parameters are used in the oxidation models, excluding the temperature based approaches. One to characterise the rate of the degradation process and one to characterise the height of the unsaturated soil layer that remains after long periods of time. This general behaviour is visualised in figure 4.4.

The model of Hoogland et al. (2012) does include the first parameter, but similarly to the model of Van der Meulen et al. (2007) does not include a second parameter characterising the height remaining at large timeframes. Instead, this model has an extra parameter characterising the maximum depth where aerobic degradation can occur without being restrained by oxygen deficiency, which partly decouples

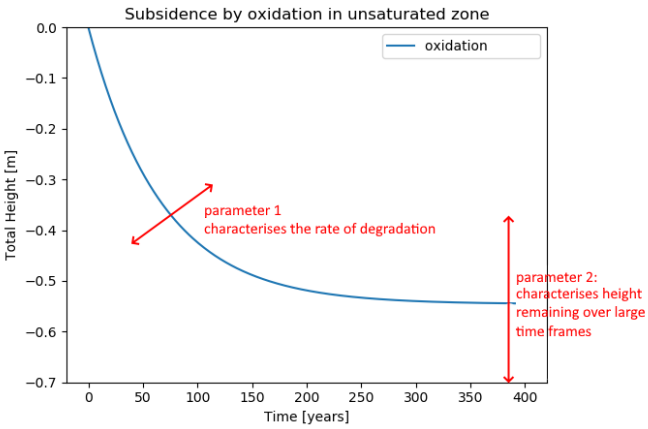

Figure 4.4: Characteristic oxidation curve determined by two model parameters

the boundary between aerobic and anaerobic degradation from the groundwater level.

As can be seen, these models are based on a simplified version of reality, where there is a complex interaction between soil environment, the microorganisms responsible for degradation of organic material and water retention of the soil. This is not only identified for subsidence studies, biochemical studies found this as well. Zak et al. (2019) looked at carbon turnover in rewetted peatlands in Germany and concluded that it is not sufficient to look at measurements of single parameters (nutrient availability, pH, redox-conditions, etc.) only to come up with an estimation for this, due to the high complexity of driving factors and possible metabolic processes. Vermeulen and Hendriks (1996) stated that models based on the hypothesis from Kortleven (1963) (using a rate of oxidation parameter) have proved suitable for engineering applications.

Considering the modelling techniques evaluated in section 4.2 some techniques are less suitable for this study than others. First, the approach of Van den Akker et al. (2007) will not be used to evaluate oxidation specifically, because the result of this equation includes all subsidence components as a result to drainage of peat soil as it is based on subsidence measurements. These equations are used to compare results for all subsidence processes together. The temperature based approaches can only be used when soil temperature data is available for a location close to the project. Ros et al. (2012) mention that the Arrhenius function and the Q10 function both give an overestimation of mineralisation rate for temperatures <15°C. Temperatures below 15°C are relevant part of the year for the Netherlands. An overestimation of the aerobic degradation subsidence component with temperature based models can thus be expected. Moreover, it is uncertain whether this approach only includes compression by oxidation, or also includes other subsidence components, as it was calibrated based on subsidence measurements. The modelling approach from Bootsma et al. (2020) is not used in this study, because no information is available on organic matter content of the considered soils, which is essential for this mass based approach.

Anaerobic decomposition

When anaerobic decomposition is evaluated in literature, this is mostly related to water quality or nutrient availability in the peatlands, and not from a land subsidence perspective. No existing modelling approaches were found for a subsidence component by anaerobic degradation of organic material. Some studies mentioned an indication of the ratio between aerobic and anaerobic degradation rates. Groenendijk et al. (2005) and Kemmers and Koopmans (2010) showed that anerobic processes are about 30 to 50% less efficient than aerobic degradation. Hendriks and van den Akker (2012) estimated that the contribution of anaerobic degradation to the overall degradation of the peat can maximum be around 10%. A possible approach to include anaerobic degradation is using a factor to calculate a rate of degradation parameter for the anaerobic process. This is further evaluated in section 8.2.2.

To be able to accurately predict the anaerobic decomposition, more knowledge on the principles of

anaerobic degradation in peat lands is needed. When more knowledge is available, a model including soil chemistry and the availability of electron acceptors other than oxygen should be evaluated. Soil models mentioned for this aspect are often more focused on the nutrient availability and solute flow in the soil and not designed from a land subsidence perspective. Examples of two models often encountered in literature are SWAP (Soil-Water-Atmosphere-Plant) and ANIMO (Agricultural Nutrient Model).

5

Compression by shrinkage

Shrinkage of soil can also contribute to measured subsidence over time. Compression of soil by shrinkage is a decrease in soil volume through a decrease in water content. More specifically, it is the contraction of soil layers above the water table, following the development of negative pore water pressures in the unsaturated zone of the soil as the soil dries. A loss of water can be caused by components like:

- *Evapotranspiration:* the sum of evaporation and transpiration components. Evaporation is the loss of water from the soil to the atmosphere. The driving force for this process is the difference between water vapour pressure in the atmosphere and at the soil surface. Transpiration is a loss of water from plants where the water is released as water vapour. Transpiration rates can be different for different plants, but also depend on energy supply, wind and the vapour pressure gradient.

- *Soil sealing:* the covering of soil with impermeable material, like buildings, asphalt, pavements, parking lots, etc. This limits infiltration of water in the soil.

- *Dewatering:* drainage of groundwater. Through this process the groundwater level is lowered, which causes a loss of water in the upper part of the soil.

- *Excessive groundwater use:* when more groundwater is used than recharged, this leads to a loss of water. Groundwater can be used for industrial purposes, irrigation purposes, etc.

Shrinkage can be divided in a reversible and a non-reversible component, where the non-reversible components is most important for long term subsidence considerations. Non-reversible shrinkage can be seen as a final process of soil structure forming processes. Often initial dewatering holds the non-reversible shrinkage part, after which shrinkage and swelling become more reversible. An important characteristic of soil shrinkage is that the ratio of shrinkage does not have to be similar in all directions. On a macroscopic level, total shrinkage shows in two ways, through shrinkage cracks and subsidence of the surface.

There are four phases of shrinkage, through which soil volume decreases when soil dries. These four phases are listed below. The first phase is only relevant for a well structured soil, the others are relevant for both well structured and non structured soils.

- *Structural shrinkage:* When a shrinkage process is interrupted by addition of water, the soil starts to partially swell. Resuming drainage then influences the shrinkage where this youngest water is drained first. The soil can start to shrink by reaching a denser packing of the soil aggregates through large pores which were previously filled with this youngest water. Reeve and Hall (1978) showed that the total volume change in this shrinkage phase is dependent on organic carbon levels and structural development of the soil and that the volume change in this phase is often negligible compared to the total loss of water.

- *Normal / basic / proportional shrinkage:* This is the volume decrease due to water loss from the soil aggregates, where the soil starts to become unsaturated. Soil particles assume a denser packing, as water between these particles is lost. The volume decrease of the soil is then equal to the water loss.

- *Residual shrinkage:* In this phase, air enters the aggregate soil system and the aggregates are not fully saturated anymore. The volume still decreases but now the volume loss does not match water loss anymore, because the mineral particles cannot move any closer together. Due to the air in the aggregate soil system, the soil starts to have a lighter colour.

- *Zero shrinkage:* In this last phase the soil particles have reached their densest configuration. No volume decrease will occur anymore upon further extraction of water.

These four phases are often shown in soil shrinkage characteristic curves (SSCCs), which show the relation between soil water content and soil volume. An example of two SSCCs are shown in figure 5.1.

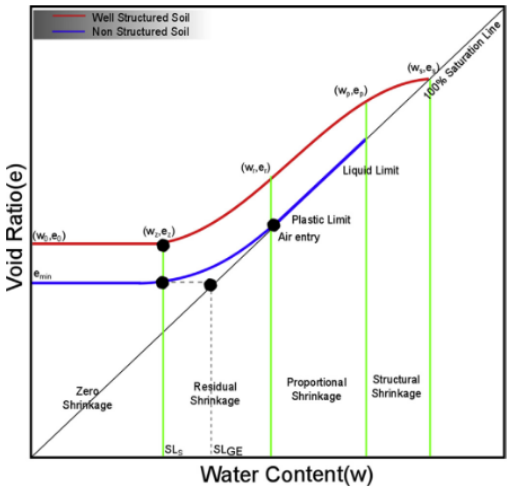

Figure 5.1: SSCCs for both a well structured and a non structured soil, from Mishra et al. (2019), who modified the curve from (Cornelis et al., 2006).

To understand fully how the soils behave upon drying, two different stages of the shrinkage principles should be understood. The first stage is the link between water content changes and three-dimensional volume changes, which is shown through the SSCC. The second stage is a link between this three-dimensional volume change to the shrinkage consequences: development of cracks and surface subsidence. For this second stage Bronswijk (1990) developed a general relation between the volume change by shrinkage and the subsidence of the soil volume, see equation 5.1. This is based on a soil cube with initial volume V $[m^3]$ and initial sides z $[m]$, shown in figure 5.2.

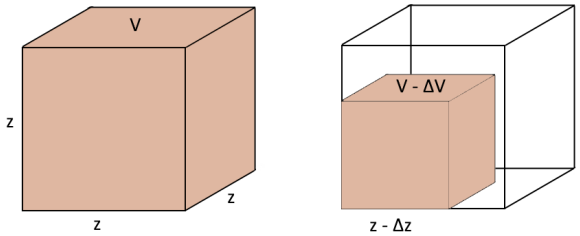

Figure 5.2: Reference situation for the development of equation (5.1), based on figure from Bronswijk (1990)

$$1 - \frac{\Delta V}{V} = (1 - \frac{\Delta z}{z})^{r_s}, \tag{5.1}$$

where r_s is a dimensionless geometry factor, also seen in the study from Rijniersce (1983), that functions as a distribution factor for cracking and surface subsidence:

$$\begin{cases} r_s = 1 & subsidence\ without\ cracking \\ 1 < r_s < 3 & subsidence\ dominates\ cracking \\ r_s = 3 & isotropic\ shrinkage \\ r_s > 3 & cracking\ dominates\ subsidence \\ r_s \to \infty & cracking\ without\ subsidence. \end{cases} \tag{5.2}$$

General factors influencing shrinkage of soil aggregates are: clay content, clay mineralogy, composition of cation exchange complex and organic matter content and environmental circumstances. The environmental circumstances influence actual shrinkage while the other factors determine the potential shrinkage of the soil. These factors will be further discussed below:

Clay content and mineralogy
Clay content and mineralogy are often mentioned in relation with shrinkage and swelling of soils. More specifically, it is the expansible mineral content of soil that is important. Two soils with the similar clay contents, can still behave very different based on the mineralogy of the clay particles. Different type of clay minerals exist and they can be categorized in five main groups: the koaline group, smectite group, illite group, chlorite group and a group with others. The smectite group of clay minerals is associated with strong shrinkage and swelling behaviour, as the distance between smectite sheets strongly varies depending on the amount of water in the soil. The size of the normal shrinkage phase is strongly related to the expansible mineral content of the soil.

- **The cation exchange complex (CEC)**
  The CEC of a soil indicates the amount of cations that can be exchanged per a mass of soil. This CEC is caused by various negative charges on the surface of soil particles, where especially clay particles and soil organic matter play a role. Thomas et al. (2000) showed that the value of the CEC can be an indicator of shrinkage/swelling potential, where in general higher CEC values were found for high and very-high shrinking/swelling soils compared to moderately shrinking/swelling soils. Meimaroglou and Mouzakis (2019) mentioned that the CEC showed a stronger correlation with linear shrinkage than clay content, as the CEC depends both on clay content and mineralogy. The CEC value increases with an increasing expansive clay mineral content.

Organic matter content
There appears to be no consensus on the role of organic matter to shrinkage of soils. Reeve and Hall (1978) indicated a positive correlation between the organic carbon content and soil shrinkage, while Gray and Allbrook (2002) found no relation between these two. A factor that might play a role in these controversial finding is the interaction between soil water and SOM, where a degradation of SOM also causes a loss of soil water that was associated with this SOM.

Environmental conditions
Occurring environmental conditions and the hydraulic state of the soil can influence what shrinkage or swelling of soil actually occurs, with respect to its potential shrinkage.

- **Type of vegetation**
  Trees and vegetation take up moisture from the soil. The type of vegetation influences the depth of the roots and the evapotranspiration rates. Mitchell and Van Genuchten (1992) showed that the roots of plants also have another effect on in-situ shrinkage behaviour of soil. Roots can have an anchoring function for soil mass, through which they affect cracking patterns and thus affect the overall shrinkage.

- **Depth of the layer in the profile**
  Shrinkage of soil can be different for different depths considered. The influence of vegetation is largest in the top part of the soil and decreases with depth. The type of vegetation influences the depth of the roots. Moreover, deeper layers are closer to the water table level and will thus be influenced more by capillary rise.

- **Climatic conditions**
  Evapotranspiration rates influence the water content of soil, where higher rates cause a loss of water and thus influence soil shrinkage. Evapotranspiration rates are influences by climatic conditions like temperature, wind and humidity. Temperature and air movement show a positive correlation with shrinakge, as temperature or air movement increases and other factors stay constant then the evapotranspiration component will increase. Humidity of the air around the vegetation and soil has a negative correlation, a higher humidity will decrease evapotranspiration.

- **Seasonal variation**
  The strong seasonal variation of shrinkage is commonly seen. Seasons with more precipitation cause a rise in the actual groundwater level and thus increase water content in a part of the soil. Dry seasons, however, can cause an additional lowering of the groundwater and thus enlarge the part of soil susceptible to soil shrinkage. Moreover, temperature, wind conditions and humidity also vary seasonally.

5.1. Shrinkage of clay soils

As mentioned before, clay soils contain a certain amount and type of clay minerals. Clay minerals are plate-like shaped crystals which are build from smaller platelets and these platelets are surrounded by water molecules. For clay minerals with strong swelling/shrinkage behaviour the distance between these platelets is influenced by the amount of water in the soil.

Clay soils with a high expansive clay mineral content are called expansive clays. Expansive clays have two different structure levels, a macrostructure level and a microstructure level (Gens and Alonso, 1992). The microstrucure is formed by clay minerals that form arrangements of individual particles. These arrangements can further join together and create clay aggregates. This internal structure of the soil aggregates is seen as the microstructure. On a macrostructure level, the soil skeleton formed by these aggregates together with other soil grains is considered. Different types of pores can be identified, based on this double-level structure. Micropores correspond with intra-aggregate pores, while macropores are inter-aggregate pores. A visualization of this double-layered structure is shown in figure 5.3.

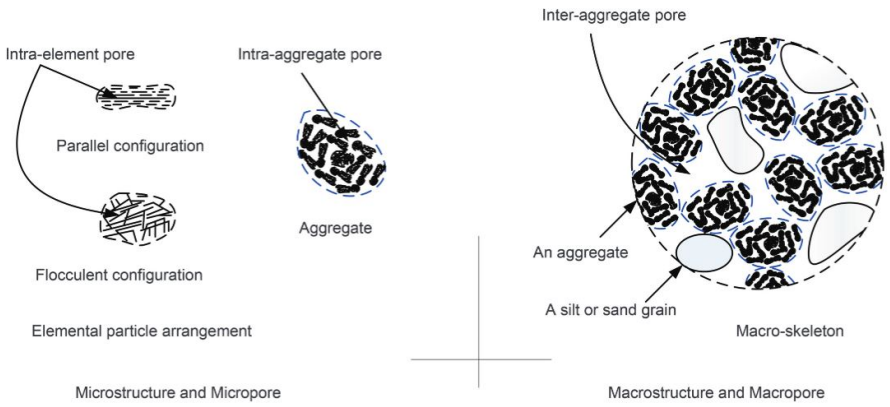

Figure 5.3: Schematization of double-level structure in expansive soils (Wang and Wei, 2015)

Considering shrinkage and swelling cycles of expansive clays, Wang and Wei (2015) showed that strains can be separated into two components, a reversible and a non-reversible component, based on results from Alonso et al. (1999), Nowamooz et al. (2009). These two components were explained using

the previously explained double-level structure. The majority of the non-reversible strains were accumulated during the first cycle(s), caused by an irreversible change of the macrostructure. The reversible deformation behaviour of aggregates caused the reversible strains.

Bronswijk and Evers-Vermeer (1990) showed SSCCs for seven representative clay soil profiles in the Netherlands, that came from varying locations. Overall, the courses of the shrinkage processes varied strongly between the different profiles considered.

5.2. Shrinkage of organic soils

The shape of SSCCs for organic soils is different from clay soils. Peng and Horn (2013) stated that the SSCCs for organic soils generally only show a structural shrinkage and a normal shrinkage phase, which is connected to the macropore and micropore volume of the soil. Considering an aggregate of an organic soil specifically, Peng and Horn (2013) stated these generally only presented normal shrinkage because of the lack of the macropores. Two examples of SSCCs for organic soils are shown in figure 5.4.

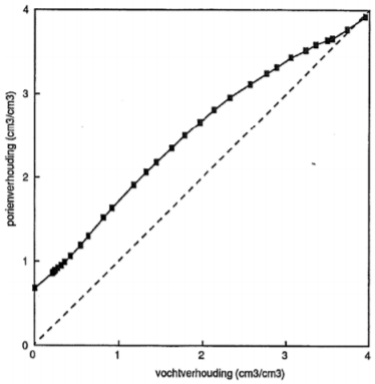

(a) SSCC of an organic soil at the Zegveld polder with an organic matter content of 45% (Van den Akker et al., 2013)

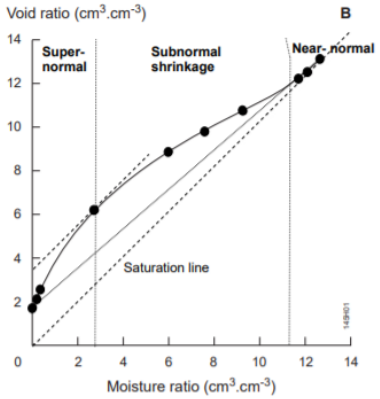

(b) Typical SSCC of a peat (Hendriks, 2004)

Figure 5.4: SSCCs of organic soils

Hendriks (2004) identified three shrinkage stages for peat soils, shown in figure 5.4b, where he used different terminology for these stages: a near-normal shrinkage phase, a subnormal shrinkage phase and a supernormal shrinkage phase. The first represents a state where little air enters the system and volume reduction equals nearly water loss, after this water loss exceeds the reduction in volume and air enters in the macropores, while the micropores remain saturated. In the last phase also the micropores are emptied and the skeleton collapses, the reduction in volume exceeds the water loss.

Shrinkage of organic soils is influenced by the type of organic soil, the degree of decomposition, its bulk density and the loading condition. Gebhardt et al. (2010) stated that shrinkage potential seems to increase with the degree of decomposition of the soil, while it decreases with increasing ash content.

For fibrous organic soils, the fibers themselves also influence their shrinkage behaviour. Fibers shrink most in the transverse direction. Considering a general horizontal orientation of fibers in peat soils, this means these soils will shrink most in vertical direction. For this soil type the ratio of horizontal to vertical shrinkage is related to the orientation and quantity of its fibers (TAW, 1996b).

5.3. Existing modelling techniques

COLE and PLE

The COLE is the coefficient of linear extensibility, which quantifies the swelling and shrinkage potential of a soil layer. It can be calculated with this equation:

$$\text{COLE} = \left(\frac{V_{wet}}{V_{dry}}\right)^{1/3} - 1, \tag{5.3}$$

where V_{wet} is the volume of a soil aggregate in a wet state and V_{dry} is the volume of a soil aggregate in the dry state. Most important here is the definition of dry and wet state, as these can vary for different countries and studies. Bronswijk and Evers-Vermeer (1990) used defined V_{wet} as the volume of an aggregate at saturation and V_{dry} as the volume of an aggregate at a pressure head of -16000 cm.

The best fit of a formula calculating the COLE based on clay content for the study from Bronswijk and Evers-Vermeer (1990) was

$$\text{COLE} = 0.002552 \cdot \text{clay content} + 0.0118 \qquad r^2 = 0.59, \tag{5.4}$$

where the COLE for the purpose of international comparison was defined with V_{wet} being the volume at a pressure head of -333 cm and V_{dry} being the volume at an oven-dry state. Another fit presented considers also the organic matter content [m%] of the soil (Bronswijk and Evers-Vermeer, 1990):

$$\text{COLE} = 0.002636 \cdot \text{clay content} + 0.006 \cdot \text{organic matter content} - 0.171 \qquad r^2 = 0.71. \tag{5.5}$$

Based on the COLE value, magnitude of shrinkage can be ranked in one of three classes:

Table 5.1: Magnitude of shrinkage classes based on COLE values (Grossman et al., 1968)

COLE value	**Magnitude of Shrinkage**
COLE < 0.03	low
0.03 < COLE < 0.06	moderate
COLE > 0.06	high

The potential linear xtensibility (PLE) can be used to quantify soil shrinkage of in-situ soil, with potentials of different layers

$$\text{PLE} = \text{COLE}(1) \times z(1) + \text{COLE}(2) \times z(2) + ... + \text{COLE}(n) \times z(n), \tag{5.6}$$

where $z(n)$ is the thickness of the nth soil horizon. These values indicate the potential shrinkage of a soil, not the actual shrinkage.

Fokker et al., 2019

Subsidence by shrinkage of reclaimed subaqueous soil in the Flevoland polder was considered by Fokker et al. (2019). It was expected that initial groundwater lowering could induce a non-reversible shrinkage mechanism. In a previous study the attempt to match modelled subsidence with measured data failed without application of this shrinkage component (Fokker et al., 2015). They chose to implement a relationship similar to the one they proposed to model subsidence from oxidation. This is based on the approximation that the rate of shrinkage is proportional to the exposed volume of soil susceptible to this, which is a similar concept as degradation of organic material. The height reduction from shrinkage of soil was calculated with

$$\Delta h_{sh} = (1 - e^{-V_{sh} \cdot \Delta t}) \cdot (h(t) - \lambda_{r,sh} h_0), \tag{5.7}$$

in which Δh_{sh} is the reduction of clay thickness above the phreatic water level [m], V_{sh} is the rate of shrinkage [m m^{-1} year^{-1}], Δt is the increase in time [a], $h(t)$ is the total thickness of clay above phreatic water level [m], $\lambda_{r,sh}$ is the fraction of the initial thickness that represents the residual thickness [-] and h_0 is the initial thickness in [m].

Based on a qualitative statement from Schothorst (1982) and the residual thickness factors $\lambda_{r,sh}$ being in line with studies from De Glopper (1969, 1987), it was concluded that this modelling approach seemed reasonable. Values for V_{sh} and $\lambda_{r,sh}$, for clay and organic clay, were found based on project data from Flevoland through ES-MDA. For these four parameters two values are available, one based on a NEN-Bjerrum estimate and one based on a Koppejan estimate. Table 5.2 shows the values found in this research for Flevoland.

Table 5.2: Estimated values for the parameters of the shrinkage equation for clay and organic clay from Fokker et al. (2019). Number in the brackets is the standard deviation in units of the last digit.

Parameter	**NEN-Bjerrum estimate**	**Koppejan estimate**	**Unit**
V_{sh} Organic Clay	0.138 (6)	0.133 (9)	m m^{-1} year^{-1}
V_{sh} Clay	0.27 (2)	0.17 (2)	m m^{-1} year^{-1}
$\lambda_{r,sh}$ Organic Clay	0.469 (12)	0.478 (15)	-
$\lambda_{r,sh}$ Clay	0.67 (2)	0.66 (3)	-

5.4. Discussion

The timescale evaluated is an important characteristic with respect to a contribution of compression by shrinkage behaviour to land subsidence, as soil shrinkage has a strongly seasonal aspect. The development of both reversible and non-reversible strains complicates the situation. The only modelling approach of a shrinkage component that was found in land subsidence studies was the approach from Fokker et al. (2019). This approach does not include a reversible component.

Both shrinkage of clay soil and organic soil are relevant in the soft soil region of the Netherlands. Bronswijk and Evers-Vermeer (1990) evaluated the SSCC curves from seven different clay profiles in the Netherlands. It was stated that some of the Dutch clay soils *"belong to the strongest swelling-shrinking soils of the world"* (Bronswijk and Evers-Vermeer (1990), p.192), but the actual shrinkage of the clay soils is restricted by the climatic conditions. Fokker et al. (2019) only derived shrinkage modelling parameters for organic clay and clay soils. Shrinkage of peat soil was not included in this study.

Compression by shrinkage can contribute to land subsidence in the grass and agricultural lands, where the shrinkage of organic and clay soils can be triggered through lowering of the groundwater levels. A non-reversible shrinkage component is introduced here. Kechavarzi et al. (2010) and Schwärzel et al. (2002) suggest that SSCCs of peat soils depend on the combined influence of the intensity of drainage and degree of decomposition, where less decomposed peat soils are more vulnerable to shrinkage. Following the general lack of this component in land subsidence evaluation studies, it is assumed that the oxidation models presented in section 4.2 model the coupled process of volume loss from shrinkage and degradation of the SOM. It is a strong simplification of reality, where a more complex interplay between different forces and components is relevant. To be able to accurately model what happens with peat soil at a specific location, following groundwater level lowerings, specific details need to be known. An interaction between the SSCC curve of organic soils and its oxidation process should be considered, based on the current state of degradation of the soil.

Another type of projects where shrinkage can be relevant is when dredged materials are used. They can also show a relevant non-reversible shrinkage component, as this is part of the final process of structure forming of soil.

6

Interaction between subsidence components

Generally speaking, soil consists of three components. These are the solid, liquid (water) and gaseous (air) phases. In the unsaturated part of the soil all three phases can be present. In the saturated part, the availability of gaseous components is determined by their diffusion coefficients in water. In figure 6.1 these three soil phases are shown, also the processes that can potentially create a decrease in mass/volume for this phase are mentioned.

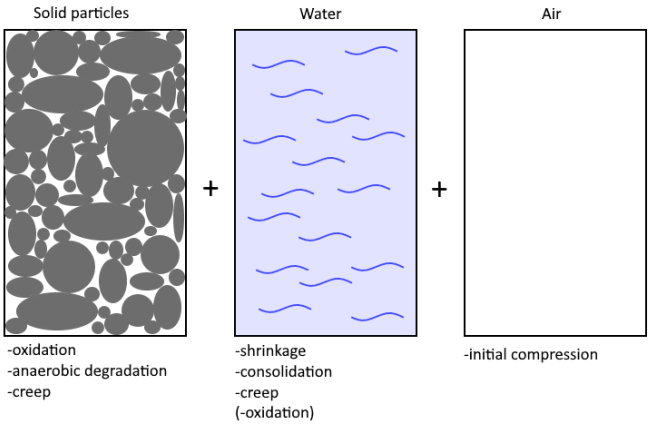

Figure 6.1: Components of soil with their potential causes of decrease in their volume/mass

6.1. Coupling compression by degradation of SOM and shrinkage

Considering the unsaturated part of the soil, oxidation of organic material and shrinkage are two important components. Shrinkage is the decrease in volume through a loss in water (see also chapter 5) and oxidation is associated with a loss of organic material (see chapter 4). Generally speaking, it can thus be said that the volume decrease originates from two different parts of the soil and the components can be added. However, reality is more complex. Through the loss of organic material, the soil also loses a part of its water retention capacity and oxidation therefore does not only cause a loss of organic material, but also a loss in water, as water that cannot be retained anymore evaporates or drains off. This is the reason why oxidation is also listed as an influencing factor for water in figure 6.1. Zain (2019) showed that in-situ oxidation of organic soil results in volumetric compression and this was mainly due a decrease in water content and the loss of solid matter was only a minor part of the volumetric compression. Moreover, extensive shrinkage behaviour (cracks) influences availability of oxygen throughout the soil, which

can increase the rate of degradation. This raises the question whether subsidence by compression from oxidation and subsidence by compression from shrinkage can be calculated separately and added.

Fokker et al. (2019) included both shrinkage and oxidation components. In this study the modelling approaches were treated as independent from each other. Peter Fokker mentioned that the uncertainties were already large and coupled behaviour potentially has been considered implicitly trough the values of the parameters used in this study, which were based on subsidence measurements (Personal contact with Peter Fokker, 07-05-2020).

6.2. Coupling compression by shrinkage and loading

Peng et al. (2012) concluded that compaction cannot influence shrinkage behaviour significantly for expansive clays, due to the double structure level. Loading under a constant water content or suction level (mechanical stress) influences dominantly the macropores, where loading through a variation in water content (hydraulic stress) mostly influences the microporosity.

6.3. Coupling compression by loading and degradation of SOM

Compression by degradation of SOM can influence the structure of organic soils, therefore the question is raised what the impact of degradation is on compression by loading behaviour. In standard settlement calculations the potential impact of degradation of organic matter is not accounted for.

Creep strain in organic and peat soils is often attributed to the dual-porosity concept (Zhang and O'kelly, 2013). It is assumed that during primary consolidation most water is expelled from the macropores in the structure, and that during the secondary consolidation water is expelled from the micropores into the macropores. A factor to pay attention to here is the degradation of organic material itself. In some studies this degradation is incorporated in the explanation for creep in organic soils, and this can cause confusion in terminology.

A simple factor that should be considered for the coupling between the two components is the difference between fibrous peat and amorphous peat. Zhang and O'kelly (2013) mentioned that when amorphous peat is considered, the material can be considered isotropic, but for fibrous peat peat structural anisotropy should be considered in constitutive models.

Van Paassen et al. (2020) showed with laboratory tests that compression and consolidation parameters can be significantly affected by oxidation of organic soils. Oxidized soil samples had lower compression and recompression indices, and a smaller initial void ratio. Zain (2019) also studied the influence of degradation of SOM on the compression behaviour of a natural organic soil. Different soil samples were used for consolidation tests. Both studies from Van Paassen et al. (2020) and Zain (2019) simulated in-situ oxidation by using hydrogen peroxide. Several findings from this research are listed below:

- It was found that there was an increase in the C_α parameter after the degradation of the organic material, but a reduction in the primary settlement. The explanation for the increase in C_α was that the degradation process creates additional voids in the soil, which can cause additional volume reduction.

- Another finding from this study was that the combination of creep and degradation of SOM seemed to increase the consolidation coefficient values for the next loading step in the tests. In general it is believed that permeability of the soil governs the consolidation coefficient. However, in this study it was found that the permeability value actually had decreased after creep and degradation of SOM. An explanation for the decrease in permeability could be the increase in the volume of gas bubbles in the soil.

- A stiffer material response for consecutive loading steps was found for the samples subjected both to creep and oxidation, compared to samples only subjected to creep

The results suggested that these effects were mostly related to the effect of entrapped gas bubbles in the soil, as a result of the degradation of SOM (Zain, 2019).

7

Subsidence monitoring techniques

Different monitoring techniques have been used across the projects that will be evaluated. In this chapter the most important techniques will be discussed. It is important to know the accuracy of the methods used and their limitations, to correctly interpret the measurements used in this study.

7.1. Interferometric Synthetic Aperture Radar (InSAR)

InSAR is a technique which is commonly used to monitor deformations of infrastructure, the land surface and buildings with a level of accuracy on the millimeter scale. It is an active satellite system, where the satellite send a signal with a wavelength in the order of a couple of centimeter to the Earth's signal and measures the reflected signal. Figure 7.1 shows a simple visualisation of this principle.

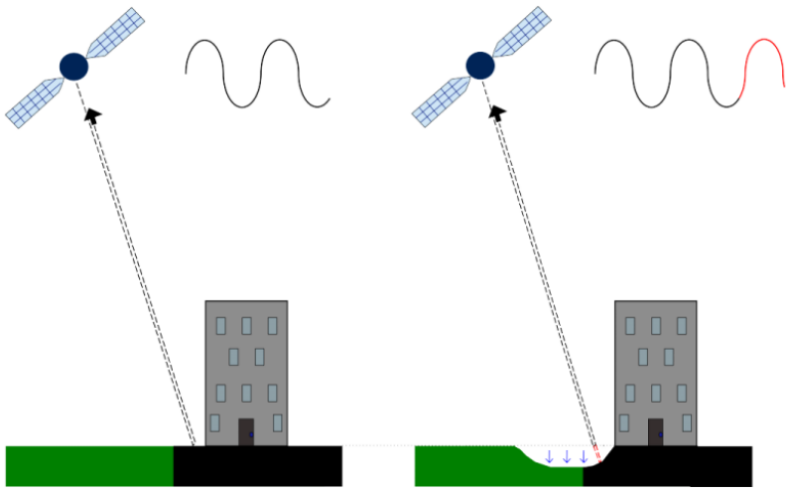

Figure 7.1: Principle of InSAR measurement before and after subsidence (SkyGeo, 2020)

InSAR is not suitable for all terrains, as not all objects on the surface of the earth reflect the signal well enough. If a reflection is roughly similar for every satellite image, the location is recognizable and the displacement can be tracked over time by combining series of different satellite acquisitions. Objects that reflect well are infrastructure, buildings and other hard surfaces. Objects that show change over time (like vegetation) cause difficulties as the location is not always recognizable. Other errors of InSAR measurements are shown in figure 7.2.

Category	Character	Type	Origin
Phase errors	Random broad-band, characterized by interferometric correlation	Thermal noise	Radar system
		Quantization noise	
		Ambiguity/sidelobenoise (multiplicative)	
		Baseline decorrelation	Electromagnetic field correlations
		Volumetric decorrelation	
		Temporal decorrelation	
		Misregistration noise	Processor
		Number noise	
	Slowly varying systematic	Receiver phase instabilities	Radar system
		Atmosphere	Propagation path
		Ionosphere	
	Data dependent, systematic and/or random	Phase unwrapping errors	Processing
		Source DEM errors	Differential processing
Metrology errors	Generally systematic, can be random if platform motion is severe and uncompensated	Baseline error	System geometry uncertainty
		Platform position error	
		Range error	
Data gaps	Terrain dependent	Layover	Image distortion
		Shadow	

Figure 7.2: Errors of InSAR and their sources (Bürgmann et al., 2000)

7.2. Laser Imaging Detection and Raging (LiDAR)

Laser Imaging Detection and Raging or LIght Detection And Raging is a method where the distance to the surface or an object is measured with laser pulses. The principle of radar methods and LiDAR is the same, but LiDAR uses laser light and radar uses radio waves. Airborne LiDAR or airborne laser scanning is a method where a laser scanner is attached to an aircraft and during the flight 3D point measurements of the surface are taken, see figure 7.3.

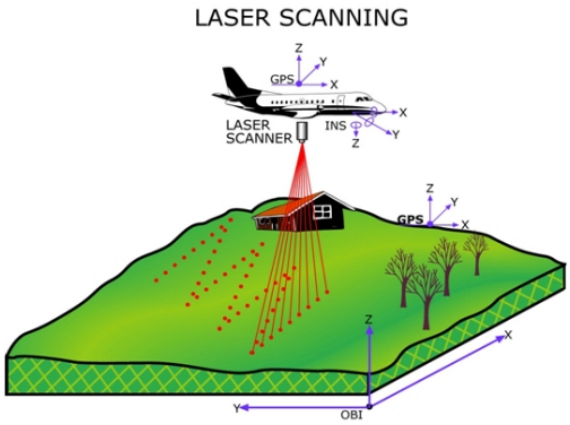

Figure 7.3: Principle of LiDAR measurements (Hasan, 2014)

Measurements are obtained in different flight strips, that are slightly overlapping, which are later merged together. To do this, these strips are georeferenced with on-board navigation sensors that monitor the location of the plane and the movements of the scanner (an Inertial Navigation System (INS) and a Global Navigation Satellite System (GNSS)).

One of the most important issues with airborne laser scanning is the strip adjustment, which is the elimination of misalignment and offset between these overlapping flight strips (Sande et al., 2010). Another disadvantage of LiDAR is the limitation on the use of this method in nighttime or cloudy weather.

Different types of errors for LiDAR applications are discussed in literature, where it is concluded that there are in general three different sources of errors (Crombaghs et al., 2000): (1) the individual sensors (scanners, INS, GNSS) and their integration, (2) properties of the target surface (its geometry and reflection) and (3) the post-processing (filtering and interpolation). The first one can be further detailed into four different categories of sensor errors:

- A random error for each point, due to the measuring uncertainty of the laser scanner itself.
- The GPS observation includes a random error as well, which is then the same for all point measurements done within the time interval of this GPS observation.
- An error per flight strip, caused by the GPS/INS-system.
- Per block of measurements a ground control point is used to correct measurements. Errors in the measurement of the ground control point thus influence the error of the LiDAR obtained points.

7.3. Zakbaken

A 'zakbaak' is a simple object that consists of a steal plate (0.5 to 2 m^2) with a vertical pipe on top of it. It can be used to monitor changes in elevation of soil layers, or the 'klink' of an embankment.

The plate is placed at the bottom of the to be constructed embankment. After/during constructing the embankment, there will be settlements of the subsoil caused by the loading. The plate of the zakbaak will settle with the subsoil. The height of the top of the pile is monitored, measured at several moments in time. Measurements are commonly done by hand, an example of which is shown in figure 7.4. This measurement by hand is a source of human error. Other methods of measuring the settlement of the zakbaken are getting more attention, as for example the electric zakbaken where plates are placed in the subsoil without the pile and measurements can be extracted continuously, or 'soilspect' where a digital measuring station is placed on top of the zakbaken.

Figure 7.4: A zakbaken placed in to monitor the settlement of a sand body (Roolvink, 2015)

II

Projects

8

Krimpenerwaard

The Krimpenerwaard polder is a part of the Netherlands where land subsidence has received a lot of attention. It is currently a location for subsidence related studies for agricultural purposes (see Proeftuin Krimpenerwaard) and the land subsidence itself has been evaluated in several studies, (Acacia Water, 2019, Muntendam-Bos et al., 2009, Rackwitz, 2019). However, this is often on a general scale and not on a local scale evaluating the contribution of the different physical processes. In this study two smaller project locations are selected, the size of one plot of grassland.

Subsidence measurements and model results are compared at for these project locations, to see if subsidence can accurately be modelled using existing modelling techniques. Also contributions of different subsidence components to overall subsidence are evaluated for this area type. To do this, different models from part I of this study have been implemented.

Explanation on the location selection, the development of water levels over time and the values used as height measurements over time is given in appendix B. The project locations within the Krimpenerwaard polder are shown in figure 8.1.

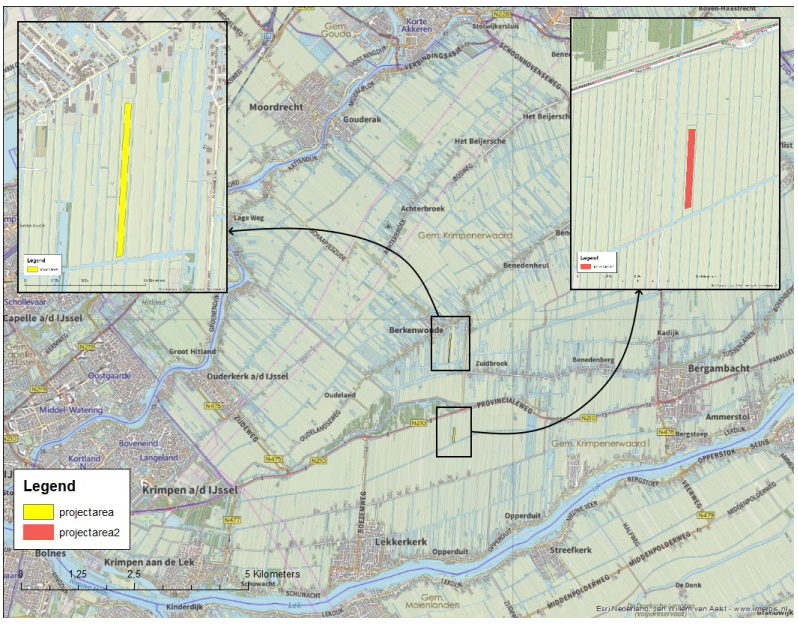

Figure 8.1: Locations of the two project areas within the Krimpenerwaard polder

8.1. Soil Profile

For both project locations a soil profile representative of the initial situation (1984) has been assumed based on site investigation available in the area. The soil profiles used as input are shown in figure 8.2. In appendix B.4 the assumptions used to come to these estimated initial soil profiles are explained.

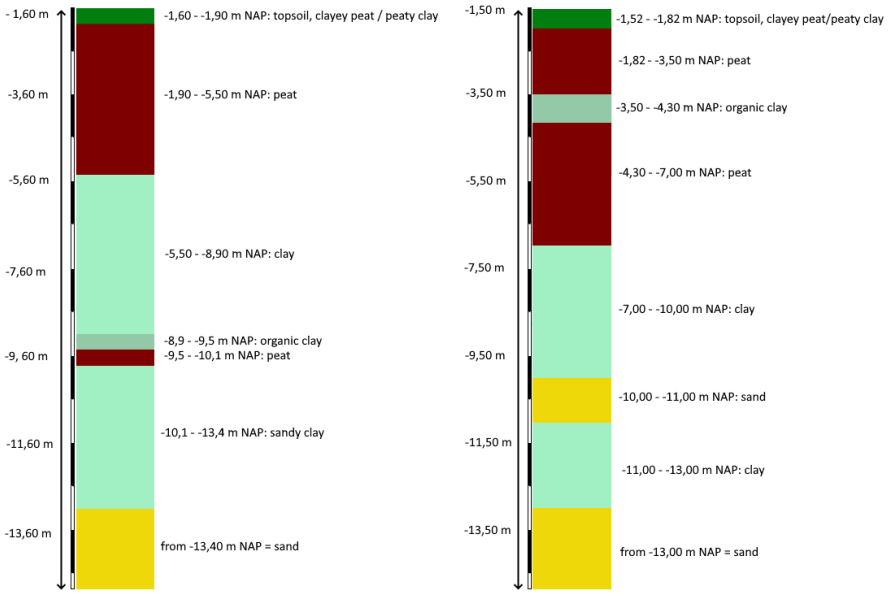

(a) Project area 1 (b) Project area 2

Figure 8.2: Initial soil profiles used for subsidence calculation Krimpenerwaard

8.2. Methodology

The analysis and modelling of subsidence was based on python code. In this section, first the overall modelling approach and then different parts of the model are explained.

8.2.1. Total model

Model

The model calculates subsidence as a result of different components specified in chapters 3, 4 and 5 over time. For each time step, the reduction in height is calculated based on several submodels. These submodels all return a height change based on a subsidence component for that specific time step, considering the current boundary conditions. Figure 8.3 shows a visualization of this process.

This time step based approach allows coupling of different submodels. Moreover, the part of the soil profile that is vulnerable to aerobic degradation of SOM and shrinkage is adjusted every time step. Subsidence of the surface level is the sum of subsidence components of all layers below. All layers until the Pleistocene sandlayers are considered.

Input

Input parameters needed for the different subsidence components can roughly be categorised in:

- Soil profile, soil parameters & layer discretization (number of smaller evaluated layers within a soil layer);
- Water levels over time & hydraulic head in deeper sand layers;
- Time parameters (total time to be evaluated, starting year, time step, etc.);
- Surface elevation measurements over time.

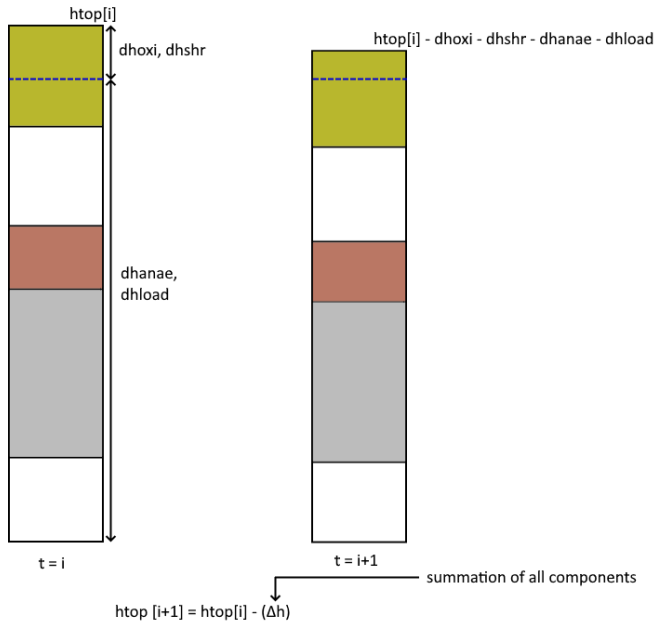

Figure 8.3: Time step based model approach

Output
Output of the model is:

- Graph showing subsidence of the toplayer over time as modelled by the different submodels, surface elevation measurements in time and land subsidence modelled with the equations from Van den Akker et al. (2007);
- Graph showing the contributions of different subsidence components over time, together with surface elevation measurements in time;
- Table giving contributions of different subsidence components to total subsidence from the model in for the end situation, both in numbers and percentages;
- Graphs from submodels (effective stresses over time, oxidation detail plots, etc.).

8.2.2. Submodels

Aerobic degradation of SOM models
From all models evaluated in section 4.2 four models have been implemented, these are the models from: Stephens et al. (1984), Van der Meulen et al. (2007), Hoogland et al. (2012) and Fokker et al. (2019). The soil profile is evaluated in three different parts to calculate subsidence from aerobic degradation for a time step: 1) layers completely above the water level, 2) layers split in two parts by the water level and 3) layers completely below the water level. The third part does not have a contribution to aerobic degradation, as there is an oxygen deficiency. Characteristics of the aerobic degradation models are:

- Water level increase over time is not possible.
- Different start times of oxidation for different parts of the peat layer are not considered. In reality different parts of the profile already started oxidation before the start of the model. This time aspect could not be implemented in the model. The influence of this aspect for one situation is evaluated in appendix B.6. There it is shown that considering the history of water level lowerings results in a lower initial rate of oxidation and thus a lower value of subsidence by compression by oxidation calculated. For the situation evaluated in the appendix, the difference was approximately 9,5% over a time period of 36 years.

- Based on archeological boorprofiles available the upper 30cm of the soil profile for both project areas is seen as the topsoil, which consists of a peaty clay/clayey peat. It is assumed that this topsoil layer does not contribute to compression from oxidation anymore, as it has been above the water level for a longer period of time and more recalcitrant SOM has accumulated. This assumption is further evaluated in the sensitivity study, section B.9.

- Average monthly soil temperature data at a depth of 0.1m from KNMI location De Bilt is used for the oxidation model of Stephens et al. (1984).

Compression by loading component models
To evaluate subsidence by compression through loading, the Koppejan and NEN-Bjerrum were implemented as submodels. Their modelling principles have been evaluated in section 3. In the model, the soil layers are further split into smaller parts, to calculate the stress changes more accurately. The number of these smaller parts can be specified in the input of the model. Characteristics of the settlement models are:

- Analytical (Terzaghi) consolidation approach (degree of consolidation based on average coefficient of consolidation)

- The change in effective stress is equal to the change in pore water pressure minus the change in total stress, caused by the water level lowering. In some layers this may lead to a decrease in effective stress over time. No swelling calculation is included in the submodels, zero strains are modelled for this scenario.

- A linear distribution of pore water pressures over height is used and it is assumed that the hydraulic head of the sand layer does not change over time.

- Number of sublayers within every layer can be specified in the model input. There is a maximum of sublayers allowed, as otherwise a sublayer will move below the waterlevel over time and the compression by loading submodel is not able to model that situation. The maximum number allowed differs per soil profile and loading situation.

- A POP of 7.5 kPa for all soil layers is used (but this can be adjusted in the submodel).

- Interaction with the other submodels is one-sided. At t=0, all stresses over time are calculated based on the initial soil profile and the water level lowerings over time. Influence of oxidation and anaerobic degradation on the calculation of soil stresses over time is not incorporated. The other submodels are influenced by the compression by loading results, as this influences what part of the soil profile lies above or below the water level over time.

At this moment the NEN-Bjerrum model can only be used with lower C_α values than calculated based on the koppejan parameters. Otherwise, some unrealistic large creep settlements are modelled. Values mentioned by Fokker et al. (2019) in his study are used. This limitation of these models was also recognised by Bootsma et al. (2020), as he mentioned about the isotache model that: *"it overcomes limitations of the Koppejan model but requires more sensitive parameter tuning to avoid spurious effects of anomalously high creep rates and initial subsidence rates"* (Bootsma et al. (2020), p.3). The abc isotache model gave very high initial creep rates, which immediately caused an overestimation of subsidence. Therefore, this model is not used for this project.

Anaerobic degradation of SOM model
For subsidence by anaerobic decomposition of organic matter, no existing model was found. Therefore a submodel was developed based on theoretical knowledge and assumptions.

The rate and magnitude of anaerobic decomposition of SOM depend on different factors, similar to aerobic decomposition. Zander et al. (2020) studied spatial variability of organic matter degradability in tidal Elbe sediments. The ratio of aerobic to anaerobic degradation in river sediments over time found in this study is shown in figure 8.4 and can be modelled with

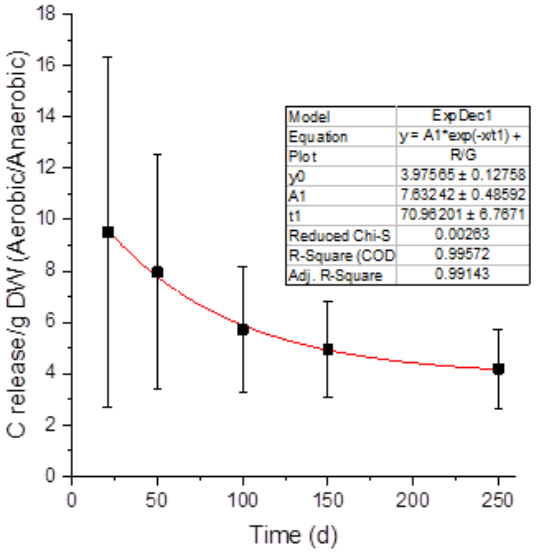

Figure 8.4: Ratio aerobic and anaerobic degradation over time, Zander et al. (2020)

$$y = A1 * exp^{\frac{-x}{t1}} + y0, \tag{8.1}$$

where y is the ratio of aerobic decomposition to anaerobic decomposition in river sediment [-], x is time [days] and $A1$, $t1$ and $y0$ are coefficients. Their values are mentioned in figure 8.4. The peat soils in this study are old, therefore it can be expected that for the peat soils of the Krimpenerwaard the ratio of aerobic to anaerobic degradation has already reached the value of y0.

To model the contribution of anaerobic degradation the aerobic degradation rate is divided by the factor y0, to come to the anaerobic degradation rate. The modelling framework from Fokker et al. (2019) is used, where now the anaerobic degradation rate V_{an} is used instead of the aerobic degradation rate V_{ox}:

$$\Delta h_{an} = (1 - e^{-V_{an} \cdot \Delta t}) \cdot (h(t) - \lambda_{r,an} h_0). \tag{8.2}$$

Characteristics of the anaerobic degradation model implemented are:

- An important assumption that is used in this approach is that anaerobic degradation only applies to the soil part between the groundwater level as indicated by the peilbesluiten and the GLG. This has been implemented to account for the unavailability of suitable electron acceptors for the degradation at greater depth. This zone faces variations of water content over time, which is can also have an accelerating effect on the degradation of SOM Denef et al. (2001).
- The rate between oxidation and anaerobic degradation is based on the study Zander et al. (2020).
- $\lambda_{r,an} = \lambda_{r,ox}$, the part of the soil that is unavailable for decomposition is the same for the aerobic as the anaerobic situation.

Van den Akker Approach

Last, the equations of (Van den Akker et al., 2007) are compared with the measurements and the other model results. These equations are based on actual field measurements, meaning that all physical components are implicitly incorporated in this model, see section 4.2. Two approaches are possible: using the DWL or the GLG. It is assumed that the DWL is equal to the groundwater levels mentioned in the reports from the waterboard.

The equations from Van den Akker et al. (2007) are based on two different scenarios, a scenario where the peat layer extends until surface level and a scenario where the peat layer is covered with a thin clay layer (<40 cm). At these project locations the topsoil layer of clayey peat/peaty clay is interpreted as a thin clay layer covering the peat layer. Therefore the equations based on this clay covered situation have been used, see section 4.2.

8.3. Results

Both project locations have been evaluated with the model. Groundwater levels, hydraulic head of the sand layer, soil profile and soil parameters used as input can be found in appendices B.3, B.4.1, B.4.2 and B.5. Other settings used in the model for this evaluation are shown in appendix B.7.

The evaluation of the results consists of different steps. First, differences between different submodels for both project areas are shown. Figure 8.5 shows the settlements modelled with the NEN-Koppejan and the NEN-Bjerrum settlement models. Figure 8.6 shows the differences and similarities between the included oxidation models for the project areas. The Stephens oxidation submodel was evaluated with a time step of $\frac{1}{12}$ year, as it uses monthly averaged temperatures. Other oxidation submodels use a time step of 0,5 year.

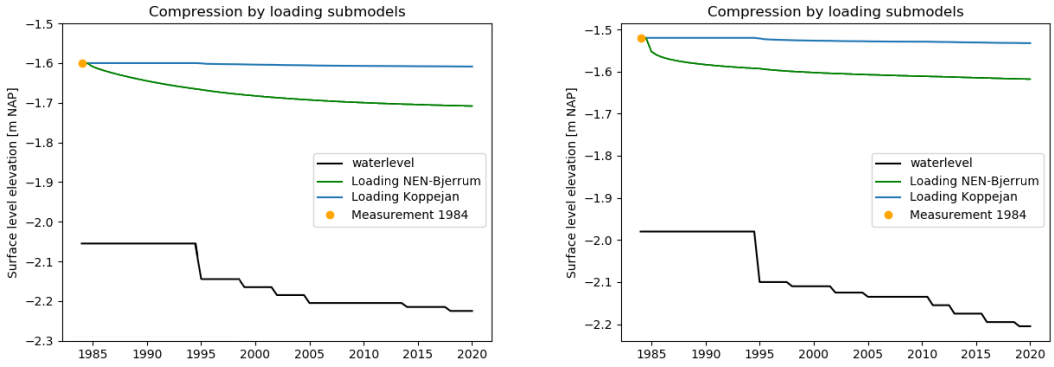

(a) Project Area 1

(b) Project Area 2

Figure 8.5: Comparison compression by loading submodels: Koppejan and NEN-Bjerrum.

Compression by loading results are verified with D-Settlement, see appendix B.8. Large differences can be seen between the model results of compression by loading, figure 8.5. This is due to several reasons:

- Initial creep rates:
  - The Koppejan settlement model does not model an initial creep rate, as creep strain is only introduced after a loading component. Therefore the model does not model any settlements up until the first water level lowering. This is not realistic, as in reality there have already been previous water level lowerings, which also introduced a creep strain component.
  - The NEN-Bjerrum model works with the isotache principle, and therefore does model an initial strain. However, this is not based on contributions of previous water level lowerings, but based on the POP value used. The creep rate in the first years of the modelling time is quite large, caused by the relative small OCR for deeper soil layers in the model. It is expected, that due to this initial high creep strain, the model overestimates the total settlement. In the sensitivity study, appendix B.9 it is shown that using a higher POP for the NEN-Bjerrum settlement model limits this initial creep.
- Creep parameters:

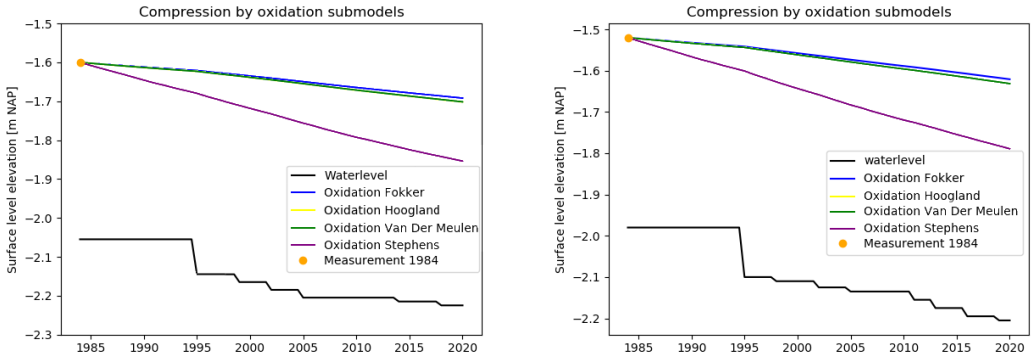

(a) Project Area 1

(b) Project Area 2

Figure 8.6: Comparison compression by oxidation submodels: Fokker et al. (2019), Van der Meulen et al. (2007), Hoogland et al. (2012) and Stephens et al. (1984). The Koppejan loading model was used in this model setting.

– It should be remembered during the comparison of these submodels that the value of C_α is not based on the Koppejan creep parameters, but values are used from the study of Fokker et al. (2019).

Considering compression from oxidation models it can be seen that three models (Van der Meulen et al. (2007), Fokker et al. (2019) and Hoogland et al. (2012)) show similar results. The yellow line which models the result from Hoogland et al. (2012) is not visible because it gives exactly the same result as the submodel from Van der Meulen et al. (2007). Only the model from Stephens et al. (1984) shows a large difference. It is likely that subsidence from oxidation is inaccurate and overestimated using the submodel from Stephens et al. (1984). One of the reasons for this is that parameters for Everglades peat soil are used, as parameters for Dutch peat soil were not available. The second reason could be that the average yearly temperatures are below 15 °C. Ros et al. (2012) stated that models based on the Arrhenius function and the Q10 function give a likely overestimation of mineralisation rates for soil temperatures in the Netherlands (<15°C). Moreover, it is questioned whether this model only calculates subsidence as a result of compression by oxidation or includes other components as well.

For the evaluation of project areas 1 and 2 the Fokker submodel for oxidation is used. From the three comparable submodels this one is the most extensive because it includes the factor λ_r. The temperature based oxidation calculation is not included because it is not representative for this situation and the other two submodels (Hoogland et al. (2012) and Van der Meulen et al. (2007)) are not included because they give similar results as the Fokker submodel. Both compression by loading submodels are included in the evaluation. For anaerobic degradation of SOM only one submodel is available.

8.3.1. Project area 1

Figure 8.7 and 8.9 show the model results for project area 1. In figure 8.7 and figure 8.8 the contributions of different components over time are shown, with different submodels used. Other combinations of submodels are possible as well. Tables 8.1 and 8.2 show the contributions of different components to land subsidence over 36 years as modelled. Figure 8.9 shows a comparison of the subsidence modelled with the submodels to the land subsidence calculated with the Van den Akker et al. (2007) equations.

The contribution of different components to total subsidence is different for the two situations. When the Koppejan loading submodel is used it is shown that compression by oxidation contributes most. In contradiction compression by loading contributes most to subsidence when the NEN-Bjerrum loading submodel is used. This contribution decreases over time. The total model result for the Koppejan approach tends more towards the AHN2 measurement, where the model with the NEN-Bjerrum approach tends more towards the AHN3 measurement. For both approaches the model outcome lies within the range of uncertainty of both measurement points.

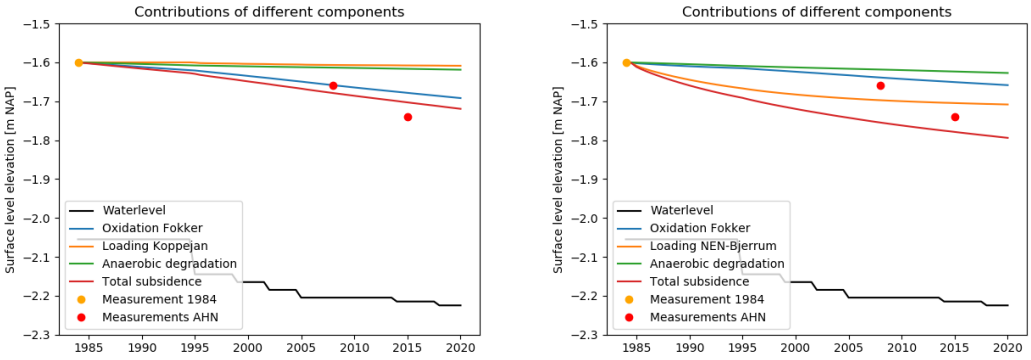

(a) Koppejan loading submodel

(b) NEN-Bjerrum loading submodel

Figure 8.7: Contributions of different subsidence components over time, considering different submodels

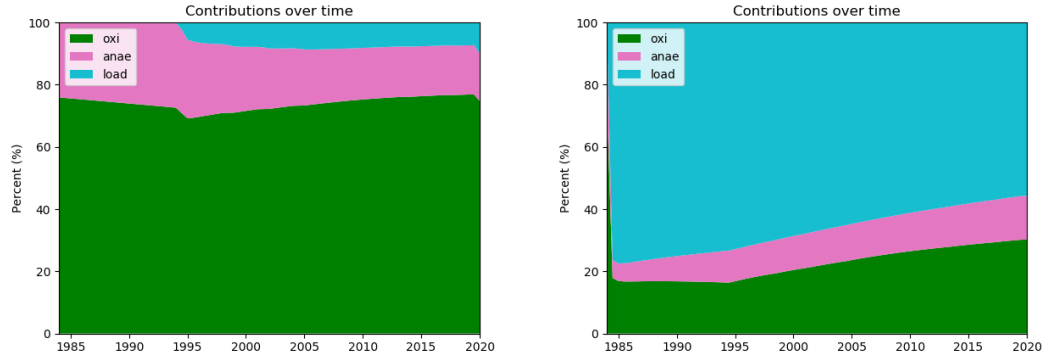

(a) Koppejan loading submodel

(b) NEN-Bjerrum loading submodel

Figure 8.8: Contributions of different subsidence components over time as percentages, considering different submodels

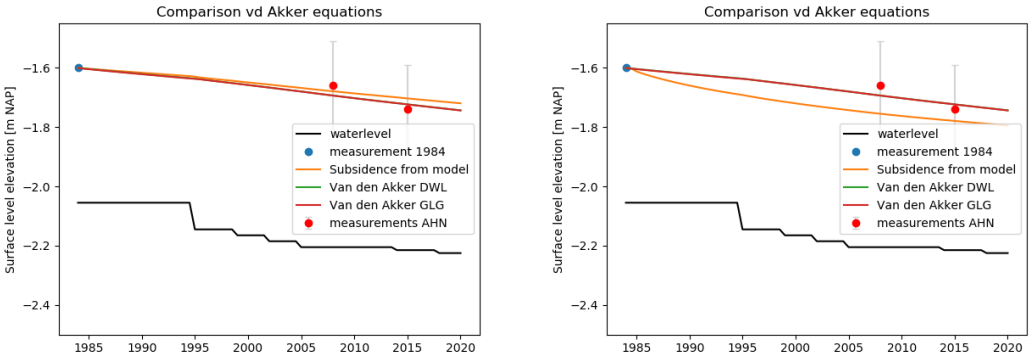

(a) Koppejan loading submodel

(b) NEN-Bjerrum loading submodel

Figure 8.9: Comparison of model results with Van den Akker et al. (2007) equations approach

Applying the equations from Van den Akker et al. (2007) to this project area gives results that agree well with the subsidence measurements, if the topsoil is considered as a a thin clay layer which covers the peat layer. Applying the equations for a situation without a clay layer will lead to an overestimation of the subsidence.

Table 8.1: Contributions of subsidence components over an evaluated time period of 36 years - Koppejan loading submodel - project area 1

Subsidence component	**Subsidence [m]**	**Percentage of total subsidence [%]**
Aerobic degradation (oxidation)	0,092	76,90%
Anaerobic degradation	0,019	15,82%
Compression by loading	0,009	7,73%
Total subsidence	0,119	

Table 8.2: Contributions of subsidence components over an evaluated time period of 36 years - NEN-Bjerrum loading submodel - project area 1

Subsidence component	**Subsidence [m]**	**Percentage of total subsidence [%]**
Aerobic degradation (oxidation)	0,059	30,16%
Anaerobic degradation	0,027	14,06%
Compression by loading	0,108	55,78%
Total subsidence	0,194	

Figure 8.10 shows project area 1 on the land subsidence map of the Netherlands 2.0, which was launched on 8 September 2020. It can be seen that some data points north of the project area are available, circled in blue. The measurements from these data point are compared to the land subsidence computed by the model. The first measurement of the subsidence map datapoints is placed at the nearest calculation point of the model, as the dataset of skygeo only contains subsidence to a reference point and not the initial NAP height used for their measurements. The result of this comparison is shown in figure 8.11.

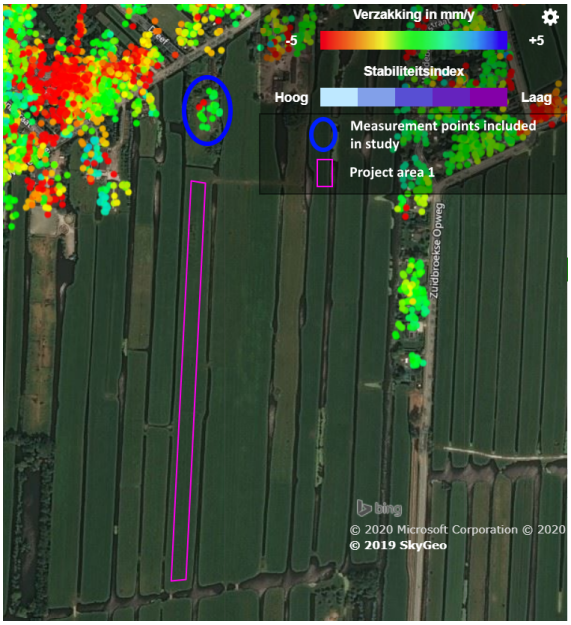

Figure 8.10: Indication bodemdalingskaart measurement points considered and project area 1 location

The data points from the Bodemdalingskaart 2.0 near project area 1 show a wide range of subsidence. Figure 8.11 shows that the modelled subsidence over the time period of the measurements (2015 - 2019) falls in the range of the measurement points for both model approaches. The measurement points used belong to a small plot north of the project area, where a house is located. Some of the measurement points belong to the house, some measured subsidence of the surface around the house. It is unknown whether this plot was raised in the past. Strictly speaking these measurements thus do not represent the situation which was evaluated with the model (area type 2, grass and agricultural land). Therefore

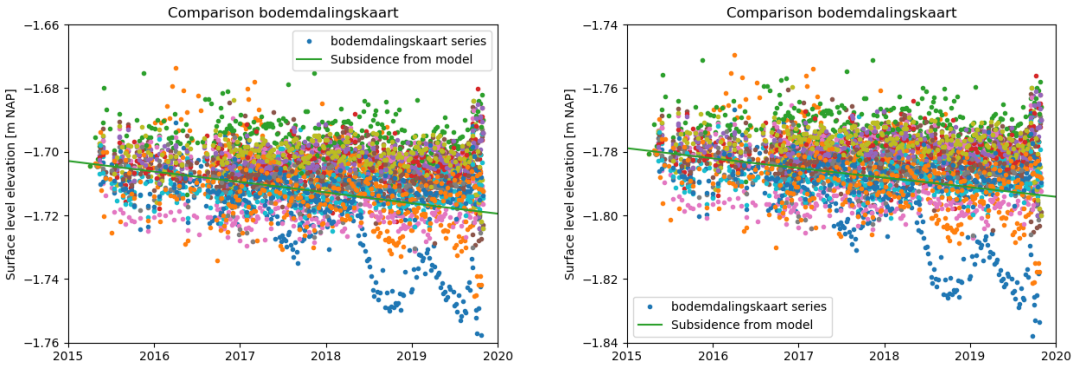

(a) Koppejan loading submodel

(b) NEN-Bjerrum loading submodel

Figure 8.11: Comparison model result with bodemdalingskaartmeasurement points

the comparison of the measurement points with the model results might not be valid.

8.3.2. Project area 2

Figure 8.12, figure 8.13 and 8.14 show the model results for project location 2. Tables 8.3 and 8.4 show the contributions to land subsidence as modelled over 36 years. Figure 8.14 shows a comparison of the subsidence modelled with the submodels to the land subsidence modelled with the Van den Akker et al. (2007) equations. No measurement points from the Bodemdalingskaart 2.0 near this project area were available to validate the model result.

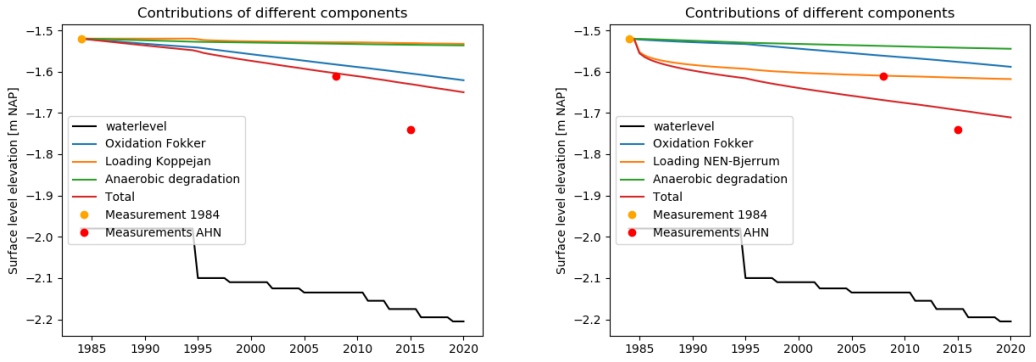

(a) Koppejan loading submodel

(b) NEN-Bjerrum loading submodel

Figure 8.12: Contributions of different subsidence components over time, considering different submodels

Table 8.3: Contributions of subsidence components over an evaluated time period of 36 years - Koppejan loading submodel - project area 2

Subsidence component	**Subsidence [m]**	**Percentage of total subsidence [%]**
Aerobic degradation (oxidation)	0,101	77,65%
Anaerobic degradation	0,016	12,64%
Compression by loading	0,013	9,72%
Total subsidence	0,130	

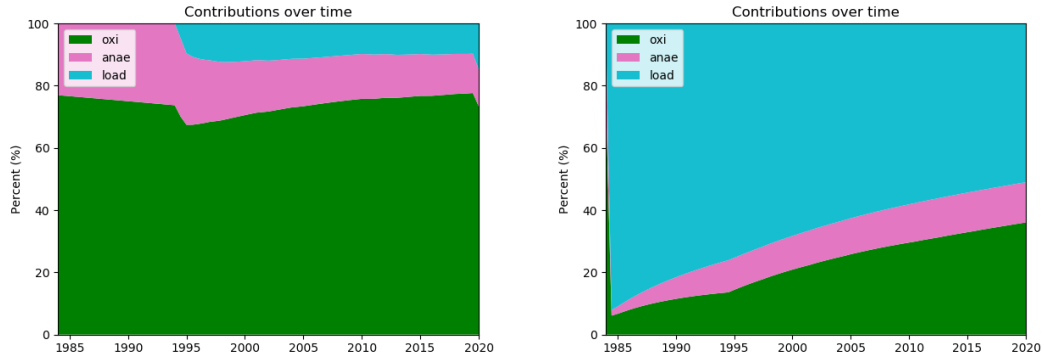

(a) Koppejan loading submodel

(b) NEN-Bjerrum loading submodel

Figure 8.13: Contributions of different subsidence components over time as percentages, considering different submodels

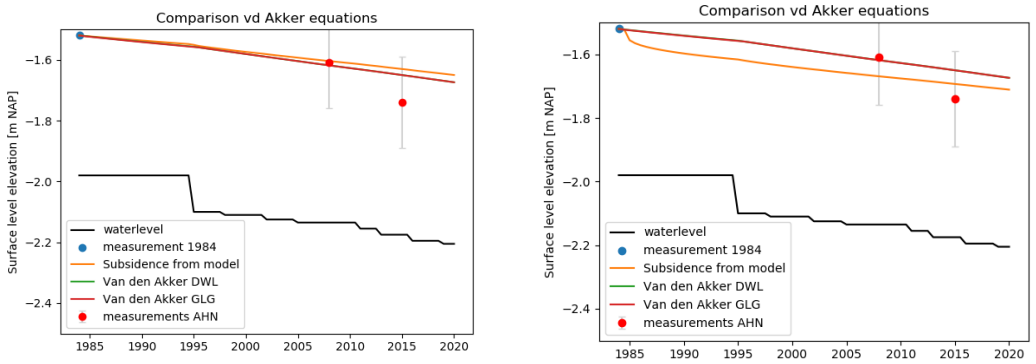

(a) Koppejan loading submodel

(b) NEN-Bjerrum loading submodel

Figure 8.14: Comparison of model results with Van den Akker et al. (2007) equations approach

Table 8.4: Contributions of subsidence components over an evaluated time period of 36 years - NEN-Bjerrum loading submodel - project area 2

Subsidence component	**Subsidence [m]**	**Percentage of total subsidence [%]**
Aerobic degradation (oxidation)	0,068	35,93%
Anaerobic degradation	0,025	12,82%
Compression by loading	0,098	51,25%
Total subsidence	0,191	

The graphs show similar results in terms of contributions of processes as for project area 1. Again the Koppejan submodel approach approximates the AHN2 measurement and not the AHN3 measurement. The NEN-Bjerrum submodel approach does approximate the AHN3 measurement more than AHN2.

8.4. Discussion

To be able to discuss the results presented in the previous section a sensitivity study has been performed. This shows the influence of variation model parameters on the model results. This study is included in appendix B.9.

Different components of subsidence are relevant in this study area. Schothorst (1977) concluded that for grass and agricultural lands about 65% of the total subsidence was caused by oxidation and shrinkage of soil, while only 35% was caused by compression by loading. In all situations evaluated in

the section above, different percentages were found, but this is also influenced by the contribution of an extra component in the study (anaerobic degradation). Percentages of contributions are also influenced by the reference time period that is considered. When the Koppejan submodel is used the contribution of compression by loading is initially 0%, as there has not been a water level lowering. This causes the graphs 8.8a and 8.13a to be very different in the beginning to graphs 8.8b and 8.13b. The figures all show an increasing contribution of compression by oxidation over time, after the first water level lowering.

Looking at the contributions over the total time span evaluated, see tables 8.1, 8.2, 8.3 and 8.4, it can be seen that the different compression by loading submodels lead to different results. In the approach with the Koppejan submodel compression by oxidation has the largest contribution to total land subsidence which corresponds with the findings from Schothorst (1977). A difference with the findings from Schothorst (1977) is that here the influence of compression by oxidation often exceeds 65%. When the NEN-Bjerrum submodel is used the largest contribution comes from compression by loading.

One of the disadvantages of the Koppejan settlement model is the use of the superposition principle, which the NEN-Bjerrum settlement model does not have. However, the NEN-Bjerrum model has large initial creep predictions, which seem not to be realistic. In the sensitivity study it is shown that the POP value used has a large influence on this initial creep. Based on this evaluation it seems preferential to use a higher POP value (±20) when evaluating subsidence in the grass and agricultural lands. Still, differences between the two compression by loading models remain substantial.

The evaluation of the V_{ox} parameter in the sensitivity study showed the importance of this parameter. The value of this parameter used for soil layers above the water level has a large influence on the model results. Also, the impact of the assumption that topsoil does not contribute to subsidence through oxidation anymore is shown to have impact on the results. For the other non-temperature based oxidation models, a value with a similar meaning as V_{ox} is included. This model parameter is therefore an important factor for the overall model results and should be studied further in the future to improve the accuracy of modelling predictions, see chapter 13.

The model parameter V_{ox} also has an influence on the compression by anaerobic degradation model results. This is because V_{an} is calculated based on V_{ox}. This submodel approach has not been verified with measurements of anaerobic degradation and should be used with care. The possible contribution to land subsidence from anaerobic degradation remains a topic of interest. The submodel can be updated in the future when more theoretical knowledge about the relevance of this component in the dutch peatlands is available.

Based on the results together with the sensitivity analysis, it can be seen that multiple modelling approaches seem to give reasonable outcomes. Through variations with the V_{ox} parameter and the POP value a reasonable model fit that agrees with the measured subsidence can be obtained. The equations from Van den Akker et al. (2007) approximate the measurements at both locations, but these equations should be used with care since they include all subsidence components indirectly and thus are only valid in similar situations as where on the situation they have been based on.

Uncertainties

When evaluating the overall model results, there are multiple factors that should be considered as they possibly have influenced the model results:

- Soil profiles:
  - Average soil profiles have been used, based on site investigation available from DINOLoket. In reality, there is a variation of the soil profile within the project area. Variation of soil parameters has been explored in section B.9, but variation in soil layers and depths themselves has not been evaluated.
  - In appendix B.4 the difficulties for determining an average soil profile for location 2 are mentioned, as the available site investigation data from DINOloket shows a lot of variation. The influence of the soil profile on the model outcome is large, as all submodels are influenced by this. It is expected that the model results of project area 1 are more accurate than the ones for project area 2. For project area 1 the data from DINOloket showed more similarities.
- Compression by loading submodels:

  - At the moment all models use the analytical approach as consolidation model, whereas a numerical approach might be more accurate. Differences between these two consolidation models were evaluated in section 3.2.3
  - No tertiary compression of peat soil is modelled, it is assumed that the potential contribution from this component is small and this does not have a significant impact on the modelling results.

- Overall model approach:
  - A submodel for shrinkage of soil above the groundwater level is not included, as it is expected that this factor is actually included in the commonly used oxidation models, that model response of peat soil to drainage. This response to drainage is in reality far more complex than the simplified equations of the presented models, as coupled behaviour between the soil structure and soil hydrology governs the problem.
  - In chapter 6 it was indicated that degradation of SOM could have influence on the compression by loading model parameters. This coupling is not accounted for, the model parameters are not adjusted over time.
  - The use of the 'vigerende peilen' as groundwater levels should be questioned. For the typical Dutch landscapes some bulging of the water level within the peatland plots can be expected. Figure 8.15 shows an example of this situation. This has to do with the hydrodynamic conditions of the area. A simple approach to consider this factor could be to add an additional height to the groundwater levels that are used as input to the model. For project area 1 an additional height of 0,15 cm added to the groundwater levels would cause a huge reduction in compression by oxidation calculated. In total, the subsidence modelled with the Koppejan Fokker approach is then 0,069 m instead of 0,119 m.

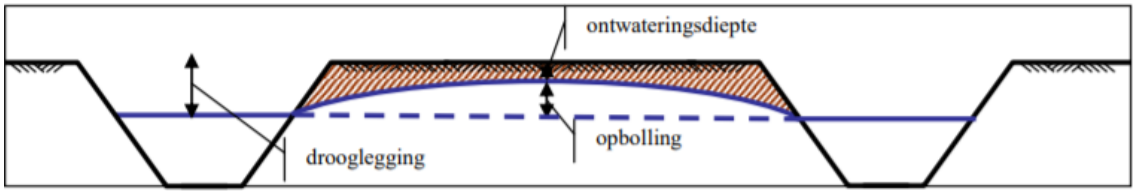

Figure 8.15: Bulging component in relation to groundwater level in a standard situation (dutch: opbolling) (Van Vemden-Versprille, 2013)

  - Using the groundwater level as the boundary between the aerobic and anaerobic zones in the soil is a general point of discussion for these type of models. The groundwater levels used in the model are a simplification of reality, as average values are used and no such a stable groundwater level exists. Moreover, many studies discuss the use of the groundwater level as the boundary between the oxic and anoxic zones (Deppe et al., 2010, Estop-Aragonés et al., 2012, Kechavarzi et al., 2010), because in reality this is more connected to the pore volume available for gas transport (the air-filled porosity, AFP). Estop-Aragonés et al. (2012) looked at the relation between the water table and the AFP and concluded that the general assumption that the water table is an important control for the presence of oxygen in peat is true, but that *"this is much less thight in the unsaturated zone then often assumed"* (Estop-Aragonés et al. (2012), p.12). They mention that in fact the presence of oxygen in the peat soil depends more on the soil physical properties and the duration and intensity of drainage. These soil physical properties are unknown in this project, and therefore this simplified approach based on the water table level was used.

For the comparison with the AHN measurements, it is important to also evaluate the error of the measurements themselves. A method that is commonly used to evaluate the AHN2 and AHN3 measurements, is to subtract the AHN3 measurements from the AHN2 measurements. This shows the differences between the datasets, where the differences can orginate from technical differences in the AHN

products or from changes of the landscape between the measurement times. Different studies shows that this subtracting of the two datasets reveals a pattern of lines (Rackwitz, 2019, van Meijeren, 2017). van Meijeren (2017) showed that this pattern corresponds with the flight trajectories of the AHN2. It seemed that zones where two flight trajectories overlap in AHN2 have a higher terrain height. This correspondence with the flight trajectories of AHN3 was not found. Small errors introduced by the GNSS and INS equipment were mentioned as the likely source for this deviations. Figure 8.16 shows the result of subtracting the AHN3 dataset from the AHN2 dataset. A yellow colour (negative value) means that there has been an increase in height over time and a blue colour (positive value) means that there was a decrease in height over time. A pattern with lines can be seen in this dataset, and thus it is expected that some errors are included in the datasets used in the evaluation of the project results.

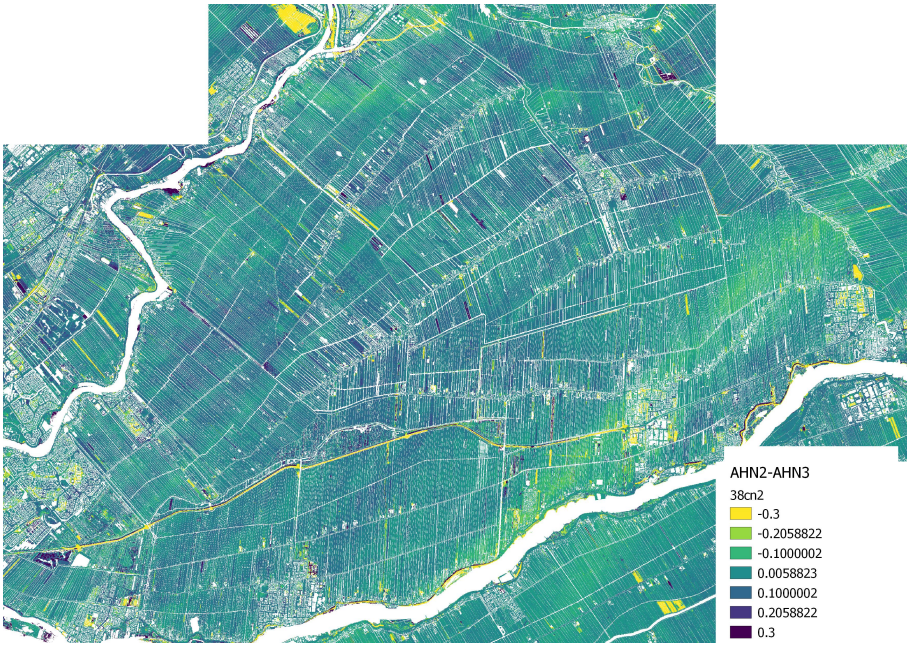

Figure 8.16: AHN3 subtracted from AHN2 for the Krimpenerwaard polder

9

A5 Badhoevedorp

From 2001 to 2003 an embankment for the extension of the A5 road in Badhoevedorp was created using dredged material from the river called 'de Zaan'. This dredged material had first ripened in a field for approximately three years and was then used for the construction of the extension of the road. Two times an investigation was done to find the characteristics of from this material, the first being in jan/feb 2001 and the second more detailed one in may/jun 2001. Also after the construction of the embankment some samples of the material were taken.

The embankment was constructed in layers of 0,3 m in height, to ensure good compaction throughout the embankment. Figure 9.1 shows an overview of the construction process of this project over time. Table 9.1 shows the details of the timing of the different constructed parts of the embankment.

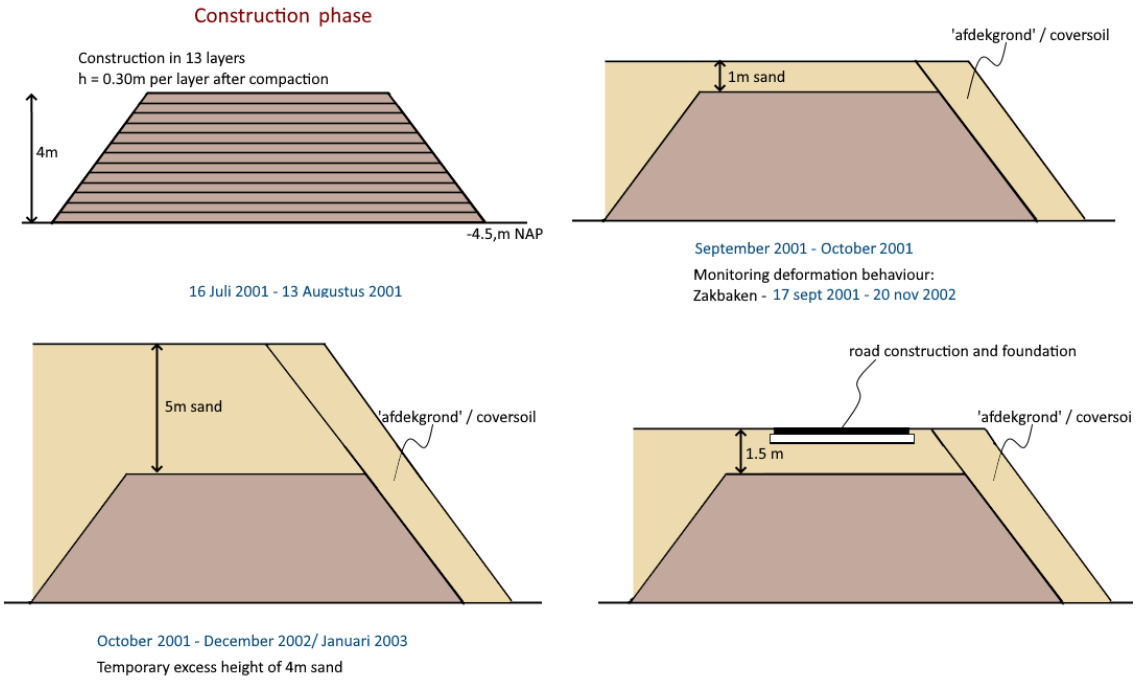

Figure 9.1: Overview of project (construction phases) A5 Badhoevedorp

After the construction, subsidence of the embankment itself was measured using zakbaken during the application of a temporary surcharge. Measurements from six zakbaken are available. The time span of

Table 9.1: Dates of construction embankment and sand layers and period of monitoring

Layer	**Date**	**Time since start construction [days]**	**Thickness [m]**
embankment0	17 july 2001	0	0,3
embankment1	18 july 2001	1	0,3
embankment2	19 july 2001	2	0,3
embankment3	20 july 2001	3	0,3
embankment4	24 july 2001	7	0,3
embankment5	25 july 2001	8	0,3
embankment6	26 july 2001	9	0,3
embankment7	30 july 2001	13	0,3
embankment8	31 july 2001	14	0,3
embankment9	1 august 2001	15	0,3
embankment10	2 august 2001	16	0,3
embankment11	3 august 2001	17	0,3
embankment12	9 august 2001	23	0,3
start monitoring	17 september 2001	63	-
sand1	17 september 2001	63	1,0
sand2	1 october 2001	77	4,0
end monitoring	20 november 2002	492	-

the monitoring data is 15 months in total, in these 15 months 10 measurements were done per zakbaak. Data on the subsidence of the subsoil of this construction was not available, and this component is thus not included in this study. This project is evaluated in this land subsidence study to get a better understanding of the subsidence components for an embankment.

For the klink of the embankment itself, different potential subsidence mechanisms can be evaluated, in connection with the origin of the material. These are:

- *Compression from a (temporary) loading component:* settlements caused by the sand layers. These are one permanent sand layer of 1 m thickness and 4 m of sand used as temporary excess height.
- *Compression of soil by its own weight:* the layers of the embankment that have been constructed first and have a lower position in the embankment are compressed by the weight of the layers above that were constructed later.
- *Shrinkage of the soil:* it is a possibility that some non-reversible shrinkage behaviour of soil as the final stage of the ripening process has had a contribution to the measured subsidence. In the report from this project (Bisschop, 2003) it is stated that it was expected that the cover soil would limit the influence of shrinkage of the dredged material.
- *Compression following aerobic degradation of organic material:* the organic content of the material exceeded the general guideline of 5%. In the report it is stated that the influence of degradation of organic material is expected to be small, because of the overburden layer.

9.1. Methodology

To evaluate subsidence of the constructed embankment, different steps have been used. First the settlement as a result of the loading by its own weight and the temporary excess height is calculated. To model the subsidence from compression by loading the change of effective stress over time is calculated. The unit weight of the 13 constructed layers is calculated based on the in-situ density of each layer, see table C.1.

The layer which is constructed first (layer 0) eventually has the highest effective stress and the last layer constructed (layer 12) has the lowest effective stress. Layer 0 is loaded by all other constructed layers and layer 12 is only loaded by the sand layers. Using the effective stress development over time,

settlements are calculated using the Koppejan settlement model and the analytical consolidation approach. The drainage length is adjusted every time a new layer of the dredged material is constructed, and is assumed to be half the height of the total embankment over time.

The Koppejan settlement model is used, because these model parameters are given in the report (Bisschop, 2003). A range of the Koppejan parameters is indicated, and therefore a sensitivity analysis could be performed.

After this step, the settlement from compression by the temporary excess height only is calculated with D-Settlement. In this calculation the construction of the embankment itself is not considered, but the embankment is a complete structure from the start of the model. Using this tool, also the NEN-Bjerrum settlement model and the numerical consolidation approach can be applied. The NEN-Bjerrum model parameters are calculated based on the Koppejan parameters, see appendix C.2. The abc isotache model is excluded, as its model parameters are not available and could not be calculated.

Based on the two calculations done above, an estimation of the relevance of other subsidence components can be done. This depends on how well the calculated subsidence scenarios already approximate the measurements of the zakbaken. All calculations are based on a one-dimensional scenario, whereas the embankment is actually a two-dimensional construction. This creates an uncertainty in the model results.

9.2. Results

9.2.1. Evaluation 1: Compression by loading (own weight and sand layers)

Using the approach explained in the previous section, subsidence was calculated over time. Both compression by the loading components (sand layers) and compression of soil by its own weight were taken into account. A range of Koppejan model parameters is used to evaluate the scenario. This range is indicated in table C.2. Figure 9.2 shows the results with the use of these parameters. The black dotted lines indicate the time period in which subsidence measurements are available from the zakbaken. The first measurement points are placed at the location of the modelled subsidence at the start of the monitoring time.

The graphs show that using the Koppejan settlement model and the analytical consolidation approach leads to an overestimation of the subsidence. Even with the maximum settlement model parameters (thus a minimal calculated subsidence) the model overestimates the subsidence, see table 9.2.

Another scenario is also evaluated. The application of saturated soil mechanics principles is questionable for this case, where the embankment is constructed above the groundwater level. As explained in chapter 3 consolidation is the dissipation of excess pore water pressures over time. It can be questioned whether these excess pore water pressures exist in this situation. A scenario is evaluated where consolidation settlements are neglected and only creep plays a role. The modelled subsidence for this scenario is shown in figure 9.3 and table 9.2. The subsidence calculated with only creep falls in the range of the measured subsidence.

Table 9.2: Subsidence in monitored time period modelled with different model scenarios and the range of Koppejan parameters

		Subsidence modelled [m]		
		Minimum parameters	Average parameters	Maximum parameters
Model Scenario	Normal	0,370	0,314	0,263
	Only creep	0,147	0,118	0,097
Range of subsidence measured by zakbaken [m]			0,004 - 0,183	

9.2.2. Evaluation 2: Compression by loading (temporary excess height)

In the second step the construction of the layers with dredged material over time is neglected. The embankment is modelled as a construction of 13 layers, with different unit weights for each constructed layer. The other model parameters used for each layer do not differ. Two loading steps are relevant in this situation, the construction of the sand layer with 1 m thickness and the construction of the tempo-

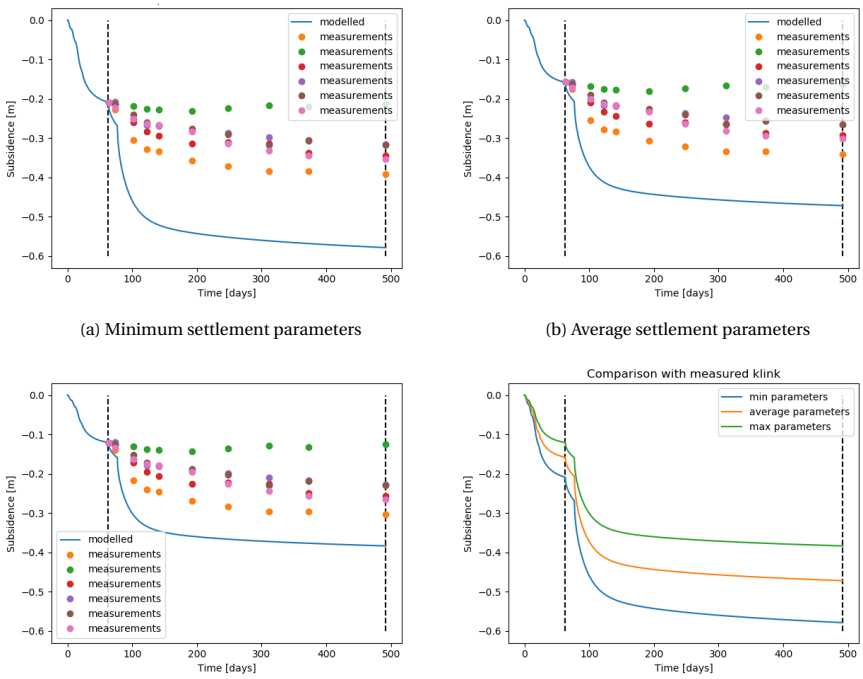

(a) Minimum settlement parameters

(b) Average settlement parameters

(c) Maximum settlement parameters

(d) Comparison results

Figure 9.2: Modelled subsidence from compression by loading with Koppejan model using a range of settlement parameters, as indicated in report (Bisschop, 2003)

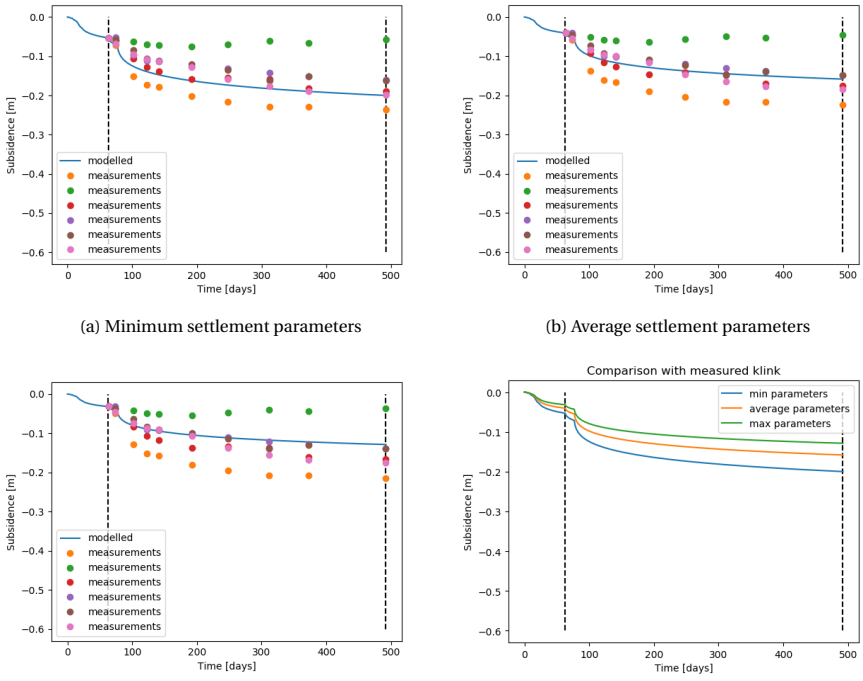

(a) Minimum settlement parameters

(b) Average settlement parameters

(c) Maximum settlement parameters

(d) Comparison results

Figure 9.3: Modelled subsidence from compression by loading with Koppejan model using a range of settlement parameters and the assumption that only creep plays a role

rary excess height sand layer, which has a thickness of 4 m. During the monitoring time of the zakbaken, the excess height was not removed and therefore this height remains until the end of the model.

Model parameters used for the Koppejan and NEN-Bjerrum settlement models are shown in tables C.2 and C.3 in the appendix. The average parameters indicated in these tables were used. It should be noted that the parameter C_α could not directly be calculated based on the Koppejan model parameters, and is thus based on a value from NEN-EN1997-1 (2019). The results of the calculation of compression by loading component are shown in figure 9.4 and in table 9.3.

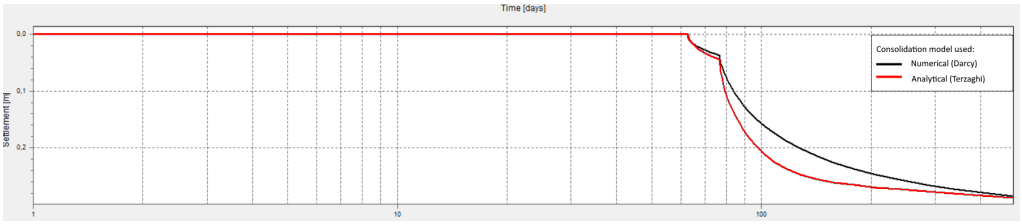

(a) Koppejan settlement model

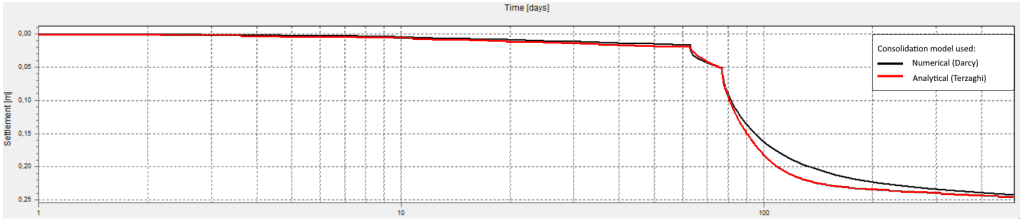

(b) NEN-Bjerrum settlement model

Figure 9.4: Results A5 Badhoevedorp calculation D-Settlement

Table 9.3: Differences between compression by loading component calculated with different settlement and consolidation models

Settlement model	**Consolidation model**	**Settlement after 492 days [m]**	
		Normal	*Only creep*
Koppejan	Analytical (Terzaghi)	0,289	0,095
Koppejan	Numerical (Darcy)	0,285	0,095
NEN-Bjerrum	Analytical (Terzaghi)	0,245	0,112
NEN-Bjerrum	Numerical (Darcy)	0,242	0,112
Range of subsidence measured by zakbaken [m]		0,004 - 0,183	

Figure 9.4 shows that the main difference between the numerical and the analytical consolidation approach is degree of consolidation over time. A difference between the two settlement models is that the NEN-Bjerrum settlement model calculates an initial settlement component, while the Koppejan model only calculates settlement after a loading component.

Both settlement models predict a larger subsidence from only compression by loading from the sand layers than was measured with the zakbaken. The influence of the compression by the own weight of the construction is relatively small, compared to the compression by the sand layers as loading components. This can be seen from looking at the differences between the calculated subsidence with the Koppejan settlement model and the analytical consolidation approach in table 9.2 and 9.3.

9.2.3. Evaluation 3: Contribution other components

From the calculations in the previous steps it can be seen that the subsidence of the embankment itself is overestimated using the settlement models. Therefore, it seems that no other subsidence component has been relevant over the time span evaluated or that potential other components do not have a significant influence. For shrinkage and degradation of organic matter these assumptions are evaluated

with respect to knowledge from the literature study.

Shrinkage
The dredged material has ripened for three years before it was used as construction material for the embankment. As mentioned in chapter 5, most irreversible shrinkage occurs in the initial phase after dewatering, but it is possible that some irreversible shrinkage occurred during the monitoring period. Gebert and Groengroeft (2019) analysed long-term soil ripening processes in a dike constructed from dredged material, and found vertical shrinkage cracks in the dredged material, but environmental settings differed from the embankment constructed in this project.

A simple calculation is used to evaluate possible irreversible shrinkage of the dredged material with the Fokker et al. (2019) shrinkage modelling approach. The equation from Fokker et al. (2019) works with the principle that $V_{sh} = 0,17$ year^{-1}, which means that 17% of the thickness of the clay soil layer is lost per year, where a certain thickness characterised by $\lambda_{r,sh}$ is excluded. The thickness of the dredged material in the ripening basin is unknown, therefore the calculation is done with the total thickness of the embankment (3,9 m). Figure 9.5 shows this simple calculation with the parameters as found by Fokker et al. (2019). The black dotted lines indicate the time interval that subsidence of the embankment was monitored. The subsidence from shrinkage in this time interval is approximately 0,108 m according to this calculation.

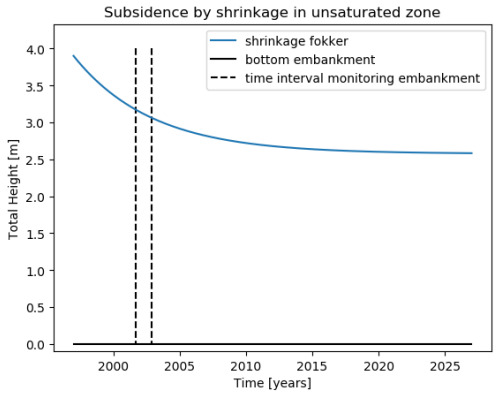

Figure 9.5: Evaluation possible non-reversible shrinkage component A5 embankment with Fokker shrinkage modelling approach

This modelling approach is based on a subsidence study for subsidence in area type 2 in Flevoland, model parameters are based on this study as no other values are available. The use of this model is questionable, as this project has different characteristics and it was applied as a first estimate for shrinkage of layers for recently reclaimed land, not man made embankments. In this project the dredged clay had ripened for a period of approximately three years before it was used as construction material. Details from this process are not available, only that the ripening process was actively supported. This is not included in this simple calculation based on a situation without enhanced ripening of soil and thus the shrinkage calculated during the monitoring period here is probably overestimated.

Another factor that can be looked at is the consistency index. In TAW (1996a) a minimum consistency index is indicated as requirement for clay used as construction material. It is mentioned that when $I_c \geq 0.6$ shrinkage will be limited. This was the case for the dredged clay used for the embankment. Based on this factor and the findings in the previous two evaluations, it is assumed that the influence of non-reversible shrinkage was limited.

Degradation of organic material
Bisschop (2003) mentioned that the organic material content in the embankment was higher than allowed, as the maximum allowed content is 5% and a range between 6.3-9.3% was reported for this construction, with an average content of 7.7%.

Diffusion of oxygen into the soil is expected to be limited, because compaction of the material was applied which lowers air-filled porosity. It is assumed that the use of a cover soil has further influenced the availability of oxygen, but no information is available on the soil which was used for this cover layer. Through these influencing factors the availability of oxygen is assumed to be limited, which means anaerobic conditions can occur. Anaerobic degradation of organic components in the dredged material can lead to gas production, which could influence stability of the embankment.

As mentioned in section 4.1 there are several stabilizing mechanisms which prevent the degradation of organic material. One of the mentioned mechanisms was stabilization through interaction with the soil matrix. It is expected that the clay particles stabilized the organic matter available in the dredged clay soil and thus limited organic matter was available for degradation. Gebert et al. (2019) looked at the rate of gas production of contaminated dredged sediment samples from a landfill and found that for the samples analysed the largest part of the organic matter was bound in organo-mineral compounds, which influenced the rate of anaerobic gas production. This suggested that during the pre-treatment of the material in dewatering fields, the readily available pool of organic matter had already been depleted. A similar situation could have occurred for the construction of the embankment of the A5. However, a small contribution to subsidence from anaerobic degradation of organic components, which has lead to gas production, cannot be excluded.

9.3. Discussion

A general range between 3 to 5 mm was mentioned for accuracy of these type of measurements in Vermilion Energy (2020). This is a small number compared to the overall subsidence values calculated in this section.

Figures 9.2 shows an overestimation of the subsidence calculated where two components were considered, the compression of soil by its own weight and the compression from loading by the two constructed sand layers. This is modelled with the Koppejan settlement model and the analytical consolidation approach. The Koppejan settlement model uses the superposition principle, which has proven to be incorrect. The principle means that settlement curves for each loading component over time are superposed. This can be part of the reason that the Koppejan settlement model overestimates the subsidence of the embankment. However, the NEN-Bjerrum model does not work with this superposition principle, but also showed an overestimation, see table 9.3. Therefore the superposition principle cannot be the only reason for the overestimation of the subsidence.

An evaluation where only creep components are considered shows subsidence results which lie in the range of measurements from the zakbaken. However, a solid theoretical background for this evaluation is lacking, but it is used as a first simplified approach to account for the unsaturated situation. In unsaturated soil mechanics both permeability of soil for air and for water play a role. The use of the model parameters from the laboratory results should also be questioned, as it is expected that these are based on saturated soil samples.

As explored in section 9.2.3 a small contribution from further ripening of the soil, which is a complex interplay of mechanisms leading to soil formation, cannot be excluded. But since the overall subsidence of the embankment is overestimated with the evaluations in steps 1 and 2, it seems logical that no other subsidence components played a significant role.

Uncertainties:

- A large simplification of the situation evaluated was done in with respect to the two-dimensional effects. In this study only one-dimensional subsidence components are calculated and two-dimensional effects are neglected. The exact locations of the zakbaken with respect to the embankment are unknown. It is assumed that part of the large variation of the measurements with the zakbaken is caused by differences between the locations of the zakbaken.

- In the report no details of the loading components are given. In Bisschop (2003) it is stated that the constructed sand layers are approximately 1 m and 4 m thick. No exact numbers are available.

10

N3 Dordrecht

The N3 in Dordrecht is a road where monitoring data are available for a long period of time (1995 - 2017). Interpretation of the subsidence measurements help understanding land subsidence in infrastructure and living areas (area type 3). Figure 10.1 shows the three project locations of the N3 that have been analysed. It is estimated that the road is constructed around 1980 at all these locations.

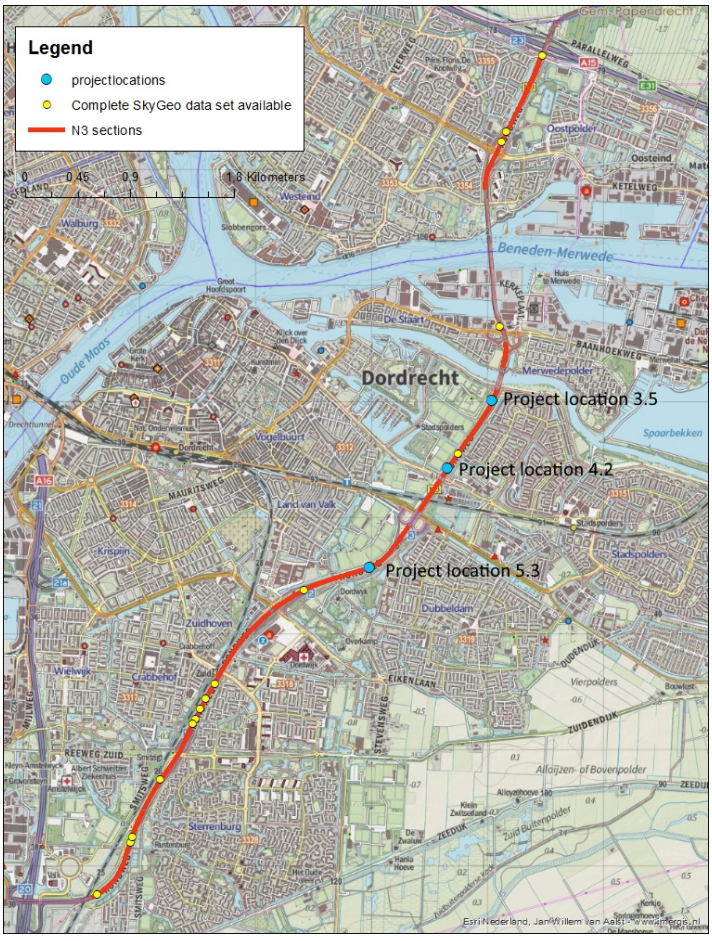

Figure 10.1: Locations of the three project locations along the N3 trajectory

The selection of these project locations is explained in appendix D. The subsidence measurements, site investigation data, the hydraulic situations and settlement model parameters are also evaluated in this appendix.

10.1. Soil profile

Subsidence at these locations is calculated for the specific soil profiles of these project locations. Based on borings from 1950, a geological profile from Deltares and CPT profiles from 2018 initial soil profiles for all three project locations have been estimated. The soil profiles used as input are shown in figure 10.2. In appendices D.5.1, D.6.1 and D.7.1 the results of the borings and CPTs are shown and the assumptions used to come to these estimated initial soil profiles are explained.

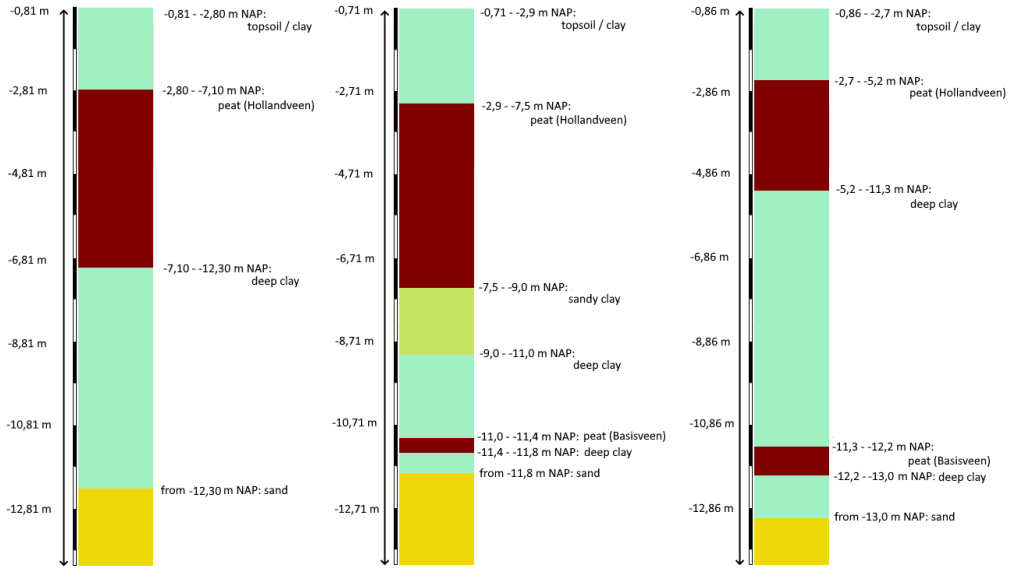

(a) Location 3.5 (b) Location 4.2 (c) Location 5.3

Figure 10.2: Initial soil profiles used for subsidence calculation

10.2. Methodology

As shown in the previous section, soft soil layers are present at the project locations. The peat layers are located below the water level and therefore it is expected that compression by oxidation had no contribution in the measured subsidence. The construction of the road has lead to an increase in total stress at the project locations by the embankment and pavement construction.

To model compression by loading subsidence the software D-Settlement was used. This model includes all consolidation and settlement models described in section 3. Input for the models is based on available site investigation data from before and after construction of the road. This is further explained in appendix D.

The fit for settlement module of D-Settlement is used to fine-tune the model outcome. This module allows the user to manipulate the settlement prediction of the model by using fit factors. These fit factors represent a factor with which a model parameter, or a ratio of model parameters is multiplied. In this process equal weights are used for the different fit factors. During the fitting of the model two key performance indicator (KPI) parameters are checked, the coefficient of determination and the ratio primary-secondary settlement. The coefficient of determination shows the correlation factor for the fit. The closer the value gets to 1,0 the better the match between the measurement points and the prediction by D-Settlement. For the ratio between primary and secondary settlement 70 - 30 % or 60 - 40 % is indicated as a normal range. These percentages are based on a quick calculation with parameters

from the table NEN 2b from NEN-EN1997-1 (2019), explained in appendix D.9. Based on a visual representation together with these KPI's, fit factors that create the best fit with the measurement points are obtained.

By using the fit for settlement approach, it is automatically assumed that all measured subsidence comes from compression by loading that was caused by the construction of the road. It is uncertain whether this assumption is valid. It would mean that secondary compression (creep) would be the only component contributing to subsidence over long time frames. By comparing the fit factor that influences modelled creep for all locations more knowledge can be obtained relating to this assumption. A higher correction for the creep parameter than for the other input parameters could indicate that another subsidence component has also played a role in measured subsidence at these locations.

10.3. Results

Results are shown in terms of fit factors for the settlement parameters of the different models. Also, model results for the different settlement models can be compared. For all three project locations, the Koppejan, NEN-Bjerrum and abc isotache settlement models are used. In total nine evaluations have been done. The numerical consolidation model is used for the NEN-Bjerrum and abc-isotache settlement models. the analytical consolidation approach is used for the evaluation with the Koppejan settlement model.

10.3.1. Location 3.5

Fit factors found with the fit for settlement module of D-Settlement are shown in table 10.1. Figure 10.3 shows the fits of the different models with the measurements points. Using these fit factors from table 10.1, the 'new' model parameters could be calculated. For all model scenarios the new model parameters are shown in table 10.2.

Table 10.1: Fit factors found with D-Settlement to fit the settlement curve with the measured subsidence at location 3.5, showing all three settlement models

ABC isotache		**NEN-Bjerrum**		**Koppejan**	
Fit factors		**Fit factors**		**Fit factors**	
Ratio primary swelling / virgin (a/b)	1,000	Reloading / Compression ratio (RR/CR)	1,000	Primary compression ratio (C'p/Cp)	1,000
Primary compression constant (b)	0,980	Compression ratio (CR)	0,956	Above preconsolidation pressure (1/C'p)	0,948
Ratio secondary / primary (c/b)	1,300	Ratio Compression (C_α/CR)	1,300	Primary / secular ratio (C'p/C's)	1,100
Preconsolidation stress (POP or OCR)	1,000	Preconsolidation stress (POP or OCR)	1,000	Preconsolidation stress (POP or OCR)	1,000
Vertical permeability (kv)	2,950	Vertical permeability (kv)	5,000	Vertical permeability (kv)	2,500
KPI's		**KPI's**		**KPI's**	
Coefficient of determination	1,000	Coefficient of determination	1,000	Coefficient of determination	0,987
Ratio primary-secondary settlement [%]	74 - 26	Ratio primary-secondary settlement [%]	79 - 21	Ratio primary-secondary settlement [%]	66 - 34

Figure 10.3 shows that with all settlement models a reasonable fit with the measurement can be obtained. For all settlement models the largest fit factor was needed for the vertical permeability in the model. To get the ratio of primary to secondary settlement near the logical range, the parameter that determines the primary settlement (b, CR, 1/C'p) is lowered and the ratio parameter (c/b, C_α/CR, C'p/C's) is increased.

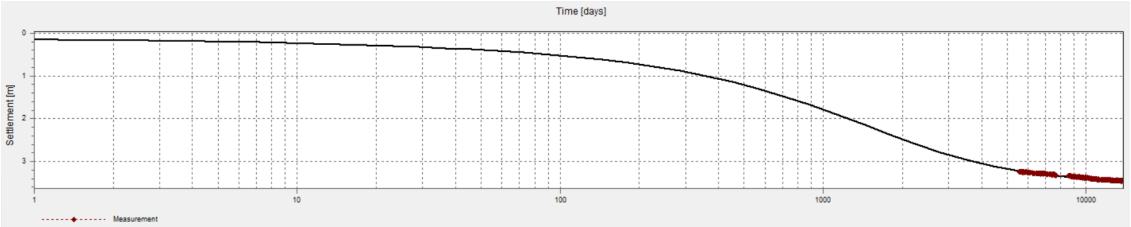

(a) ABC isotache model fit complete

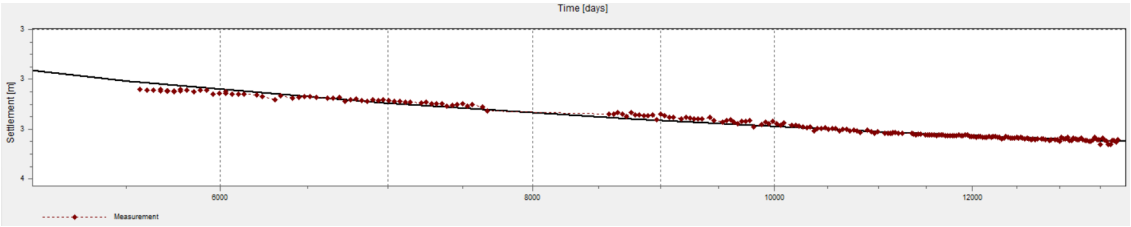

(b) ABC isotache model fit detail

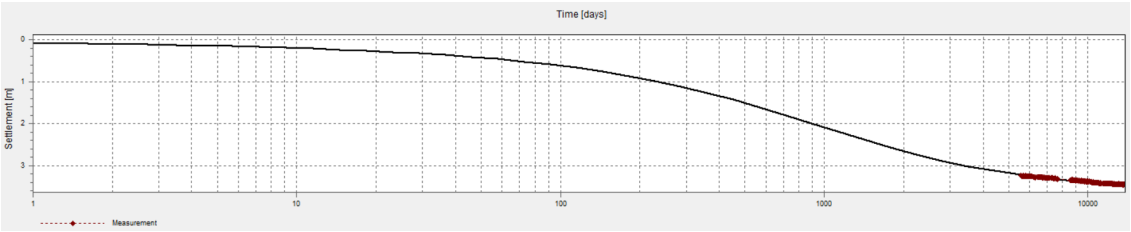

(c) NEN-Bjerrum model fit complete

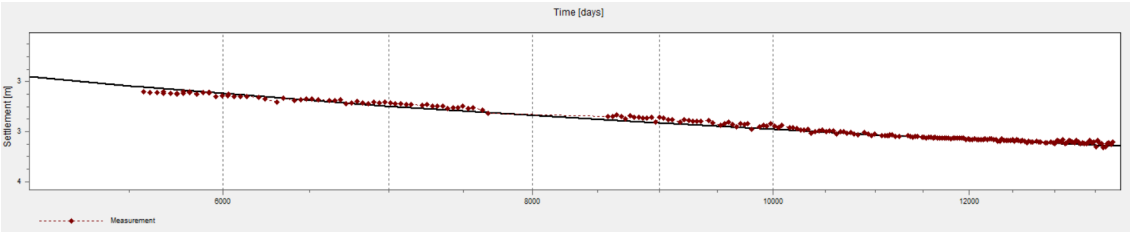

(d) NEN-Bjerrum model fit detail

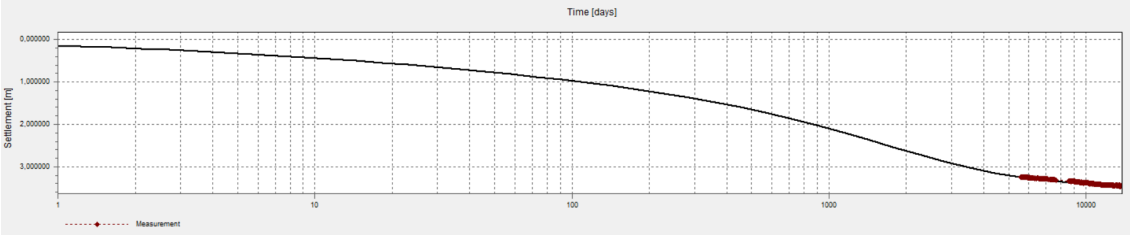

(e) Koppejan model fit complete

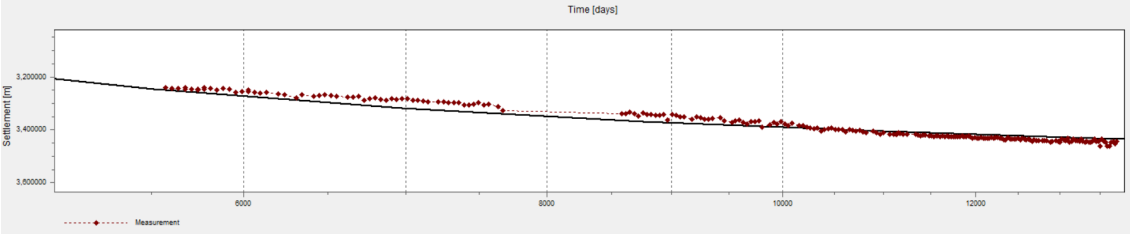

(f) Koppejan model fit detail

Figure 10.3: Fits obtained with D-Settlement for location 3.5

Table 10.2: New model parameters for location 3.5 with fit correction

ABC isotache model						
soil layers	**a**	**b**	**c**	**POP**	**cv**	
topsoil / clay	0,00946	0,03433	0,00160	8,00	5,75E-07	
peat (Hollandveen)	0,03071	0,23510	0,02097	8,00	2,60E-07	
deep clay	0,01889	0,14124	0,00829	13,00	4,57E-08	
NEN-Bjerrum model						
soil layers	**RR**	**CR**	**C_α**	**POP**	**cv**	
topsoil / clay	0,01777	0,11234	0,00353	8,00	9,75E-07	
peat (Hollandveen)	0,07840	0,40497	0,03958	8,00	4,40E-07	
deep clay	0,03134	0,27476	0,01641	13,00	7,75E-08	
Koppejan model						
soil layers	**Cp**	**Cs**	**C'p**	**C's**	**POP**	**cv**
topsoil / clay	146,7	1337,9	33,1	46,2	8,00	4,88E-07
peat (Hollandveen)	53,6	115,0	6,6	81,3	8,00	2,20E-07
deep clay	58,0	270,4	9,8	134,4	13,00	3,88E-08

10.3.2. Location 4.2

Fit factors found with the fit for settlement module of D-Settlement are shown in table 10.3. Figure 10.4 shows the fits of the different models with the measurements points. Using these fit factors from table 10.3, the 'new' model parameters could be calculated. For all model scenarios the new model parameters are shown in table 10.4.

Again, with all settlement models a reasonable fit with the measurements is obtained. For all settlement models the largest fit factor was needed for the vertical permeability in the model. For the abc isotache and NEN-Bjerrum models a larger correction of this parameter was needed than for location 3.5. To get the ratio of primary to secondary settlement near the logical range, the parameter that determines the primary settlement (b, CR, 1/C'p) is lowered and the ratio parameter (c/b, C_α/CR, C'p/C's) is increased, similarly as for location 3.5.

Table 10.3: Fit factors found with D-Settlement to fit the settlement curve with the measured subsidence at location 4.2, showing all three settlement models

ABC isotache		**NEN-Bjerrum**		**Koppejan**	
Fit factors		**Fit factors**		**Fit factors**	
Ratio primary swelling / virgin (a/b)	1,000	Reloading / Compression ratio (RR/CR)	1,000	Primary compression ratio (C'p/Cp)	1,000
Primary compression constant (b)	0,915	Compression ratio (CR)	0,930	Above preconsolidation pressure (1/C'p)	1,142
Ratio secondary / primary (c/b)	1,300	Ratio Compression (C_α/CR)	1,300	Primary / secular ratio (C'p/C's)	1,000
Preconsolidation stress (POP or OCR)	1,000	Preconsolidation stress (POP or OCR)	1,000	Preconsolidation stress (POP or OCR)	1,000
Vertical permeability (kv)	5,000	Vertical permeability (kv)	6,000	Vertical permeability (kv)	2,000
KPI's		**KPI's**		**KPI's**	
Coefficient of determination	0,999	Coefficient of determination	0,999	Coefficient of determination	0,999
Ratio primary-secondary settlement [%]	74 - 26	Ratio primary-secondary settlement [%]	74 - 26	Ratio primary-secondary settlement [%]	63 - 37

Table 10.4: New model parameters for location 4.2 with fit correction

ABC isotache model						
soil layers	**a**	**b**	**c**	**POP**	**cv**	
topsoil / clay	0,00883	0,03205	0,00149	8,00	9,57E-07	
peat (Hollandveen)	0,02868	0,21951	0,01958	8,00	4,39E-07	
sandy clay	0,03093	0,07307	0,00352	5,00	3,38E-07	
deep clay	0,01764	0,13187	0,00774	13,00	7,75E-08	
peat (Basisveen)	0,06460	0,19683	0,01458	8,00	1,85E-07	
deep clay	0,01764	0,13187	0,00774	13,00	7,75E-08	
NEN-Bjerrum model						
soil layers	**RR**	**CR**	**C_α**	**POP**	**cv**	
topsoil / clay	0,01728	0,10929	0,00343	8,00	1,17E-06	
peat (Hollandveen)	0,07627	0,39396	0,03850	8,00	5,26E-07	
sandy clay	0,01954	0,14385	0,00730	5,00	4,06E-07	
deep clay	0,03049	0,26729	0,01596	13,00	9,30E-08	
peat (Basisveen)	0,06994	0,30243	0,02920	8,00	2,22E-07	
deep clay	0,03049	0,26729	0,01596	13,00	9,30E-08	
Koppejan model						
soil layers	**Cp**	**Cs**	**C'p**	**C's**	**POP**	**cv**
topsoil / clay	121,7	1337,9	27,5	42,2	8,00	3,9E-07
peat (Hollandveen)	44,5	115,0	5,5	74,3	8,00	1,75E-07
sandy clay	32,9	350,3	13,8	40,1	5,00	1,35E-07
deep clay	48,2	270,4	8,1	122,8	13,00	3,10E-08
peat (Basisveen)	16,0	74,3	85,0	44,3	8,00	7,4E-08
deep clay	48,2	270,4	8,1	122,8	13,00	3,10E-08

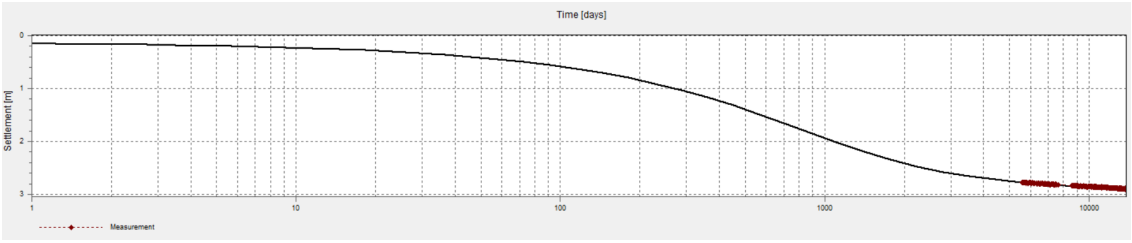

(a) ABC isotache model fit complete

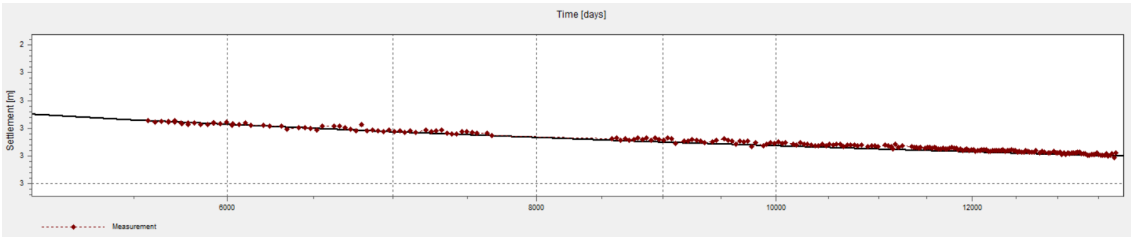

(b) ABC isotache model fit detail

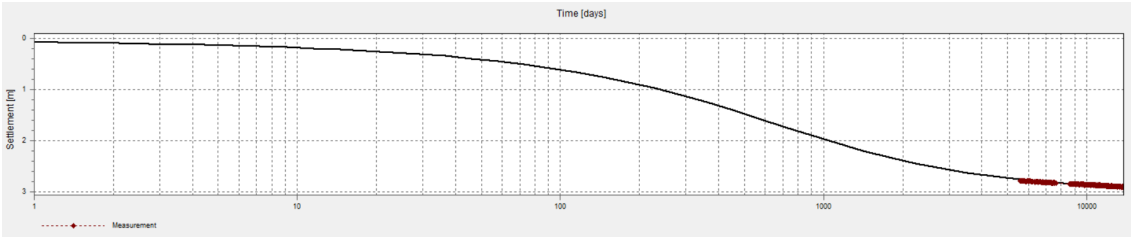

(c) NEN-Bjerrum model fit complete

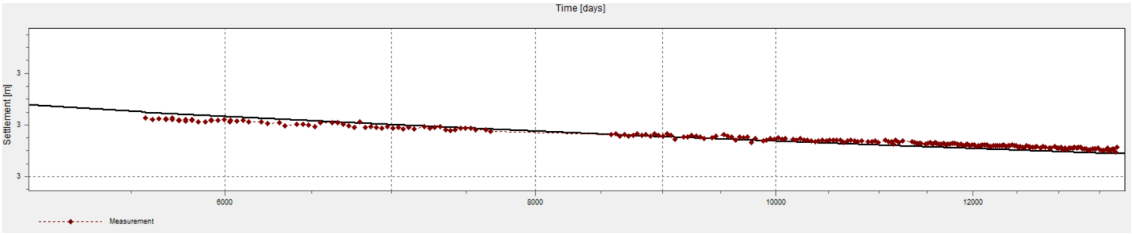

(d) NEN-Bjerrum model fit detail

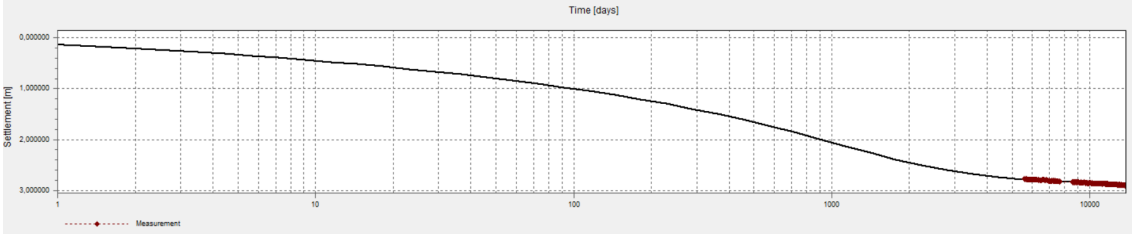

(e) Koppejan model fit complete

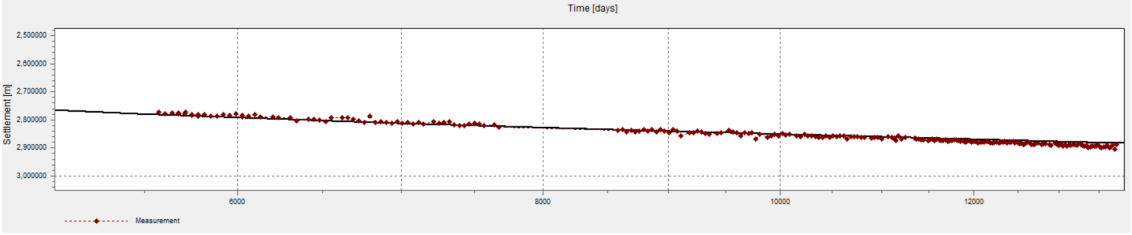

(f) Koppejan model fit detail

Figure 10.4: Fits obtained with D-Settlement for location 4.2

10.3.3. Location 5.3

Fit factors found with the fit for settlement module of D-Settlement are shown in table 10.5. Figure 10.5 shows the fits of the different models with the measurements points. Using these fit factors from table 10.5, the 'new' model parameters could be calculated. For all model scenarios the new model parameters are shown in table 10.6.

Table 10.5: Fit factors found with D-Settlement to fit the settlement curve with the measured subsidence at location 5.3, showing all three settlement models

ABC isotache		**NEN-Bjerrum**		**Koppejan**	
Fit factors		**Fit factors**		**Fit factors**	
Ratio primary swelling / virgin (a/b)	1,000	Reloading / Compression ratio (RR/CR)	1,000	Primary compression ratio (C'p/Cp)	1,000
Primary compression constant (b)	1,250	Compression ratio (CR)	1,220	Above preconsolidation pressure (1/C'p)	1,300
Ratio secondary / primary (c/b)	1,300	Ratio Compression (C_α/CR)	1,300	Primary / secular ratio (C'p/C's)	1,300
Preconsolidation stress (POP or OCR)	1,000	Preconsolidation stress (POP or OCR)	1,000	Preconsolidation stress (POP or OCR)	1,000
Vertical permeability (kv)	3,500	Vertical permeability (kv)	5,000	Vertical permeability (kv)	2,900
KPI's		**KPI's**		**KPI's**	
Coefficient of determination	1,000	Coefficient of determination	1,000	Coefficient of determination	1,000
Ratio primary-secondary settlement [%]	75 - 25	Ratio primary-secondary settlement [%]	75 - 25	Ratio primary-secondary settlement [%]	60 - 40

Table 10.6: New model parameters for location 5.3 with fit correction

ABC isotache model						
soil layers	**a**	**b**	**c**	**POP**	**cv**	
topsoil / clay	0,01207	0,04378	0,00204	8,00	6,83E-07	
peat (Hollandveen)	0,03917	0,29988	0,02675	8,00	3,07E-07	
deep clay	0,02409	0,18016	0,01058	13,00	5,43E-08	
peat (Basisveen)	0,08825	0,26890	0,01992	8,00	1,28E-07	
deep clay	0,02409	0,18016	0,01058	13,00	5,43E-08	
NEN-Bjerrum model						
soil layers	**RR**	**CR**	**C_α**	**POP**	**cv**	
topsoil / clay	0,02267	0,14337	0,00450	8,00	9,75E-07	
peat (Hollandveen)	0,10005	0,51680	0,05051	8,00	4,38E-07	
deep clay	0,04000	0,35064	0,02094	13,00	7,75E-08	
peat (Basisveen)	0,09174	0,39673	0,03830	8,00	1,83E-07	
deep clay	0,04000	0,35064	0,02094	13,00	7,75E-08	
Koppejan model						
soil layers	**Cp**	**Cs**	**C'p**	**C's**	**POP**	**cv**
clay	106,9	1337,9	24,1	28,5	8,00	5,66E-07
peat	39,1	115,0	4,8	50,2	8,00	2,54E-07
clay	42,3	270,4	7,1	83,0	13,00	4,50E-08
peat	14,1	74,30	6,1	57,5	8,00	1,06E-07
clay	42,3	270,4	7,1	83,0	13,00	4,50E-08

The largest fit factor is used for the vertical permeability at this location as well. Here the value of the parameter governing primary settlement (b, CR, 1/C'p) is not lowered but it is increased. This creates a

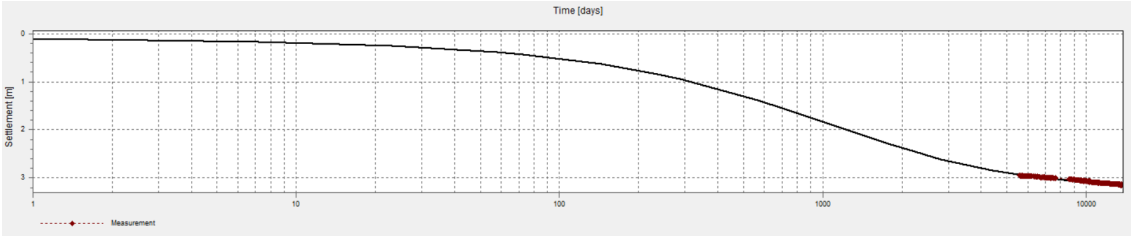

(a) ABC isotache model fit complete

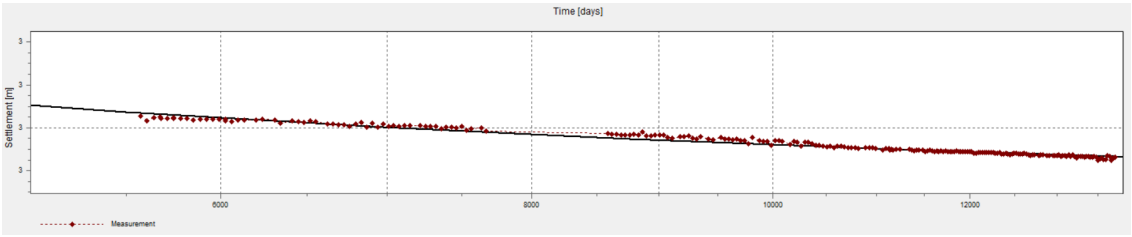

(b) ABC isotache model fit detail

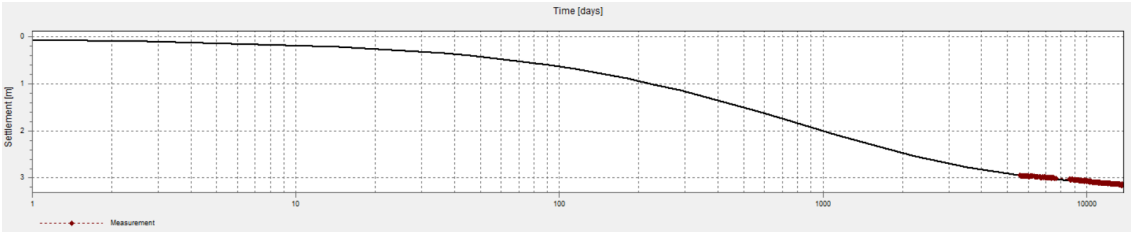

(c) NEN-Bjerrum model fit complete

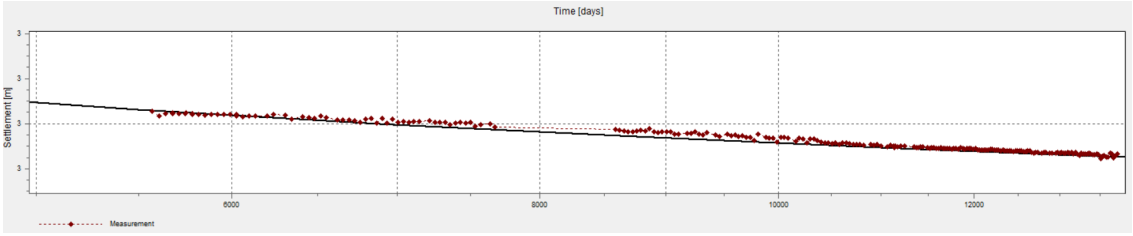

(d) NEN-Bjerrum model fit detail

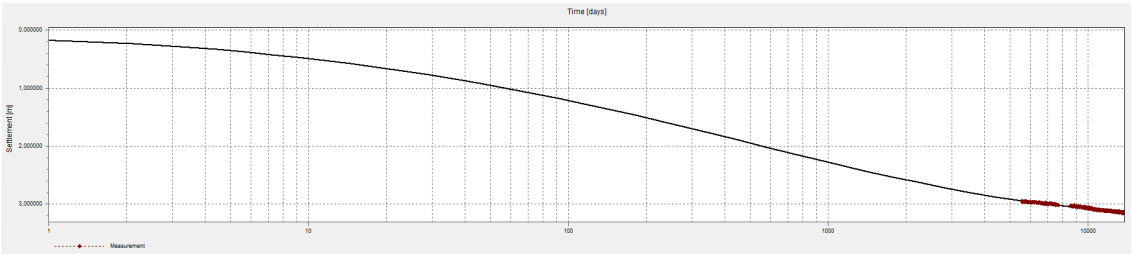

(e) Koppejan model fit complete

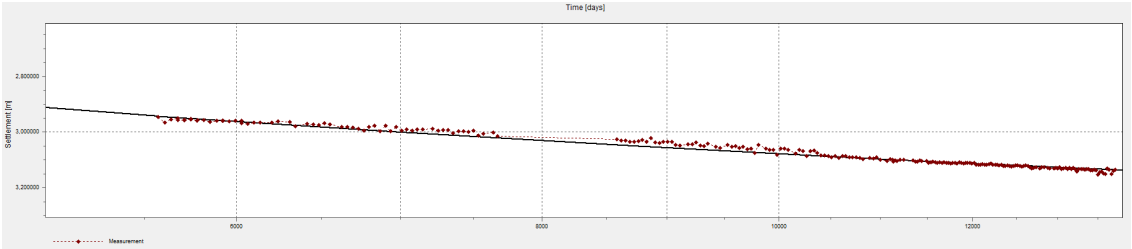

(f) Koppejan model fit detail

Figure 10.5: Fits obtained with D-Settlement for location 5.3

difference compared to the other two locations. The parameter governing the ratio between secondary and primary compression was also increased for all three settlement models.

10.3.4. Comparison fitted parameters

The obtained settlement model parameters for all locations are compared. Figures 10.6, 10.7 and 10.8 show the values per soil parameter for all soil layers. The original input value is plotted with a green dot, the crosses represent the parameter values of the different locations obtained after the correction with the fit factors. The black lines represent the range of variation of the soil parameter in the laboratory results. The parameters of the basisveen peat layer and the sandy clay layer were based on only one sample, therefore no range of laboratory results is indicated.

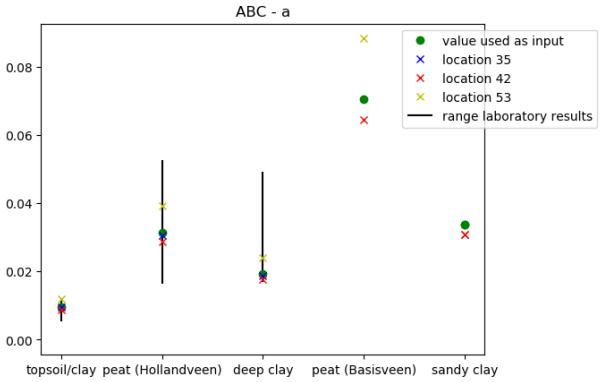

(a) parameter a

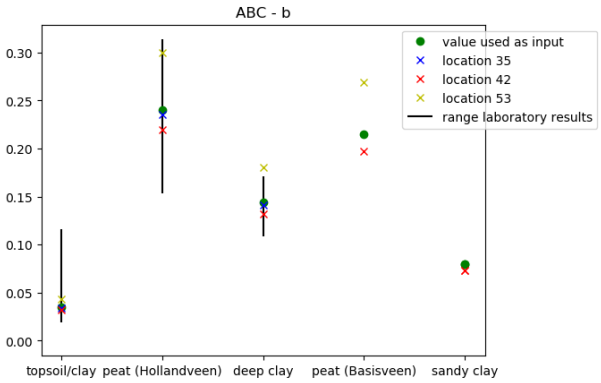

(b) parameter b

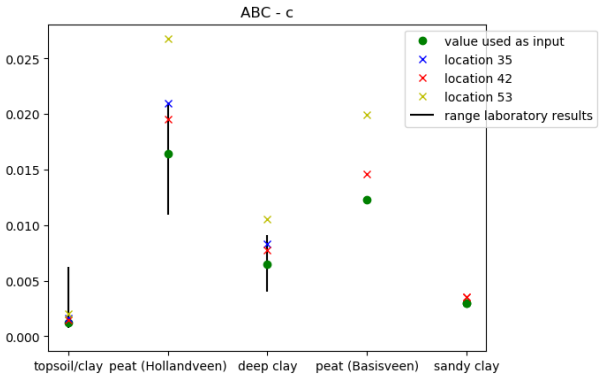

(c) parameter c

Figure 10.6: Obtained abc isotache parameter values with fit for settlement module

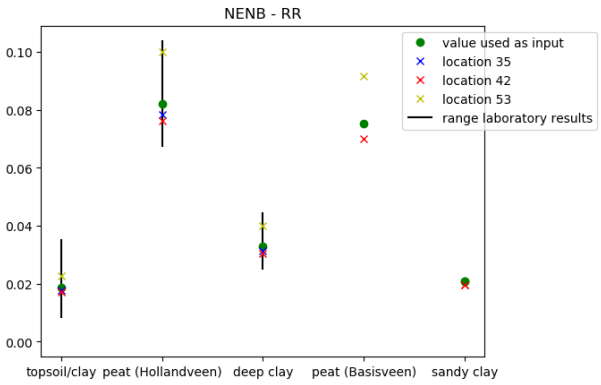

(a) parameter RR

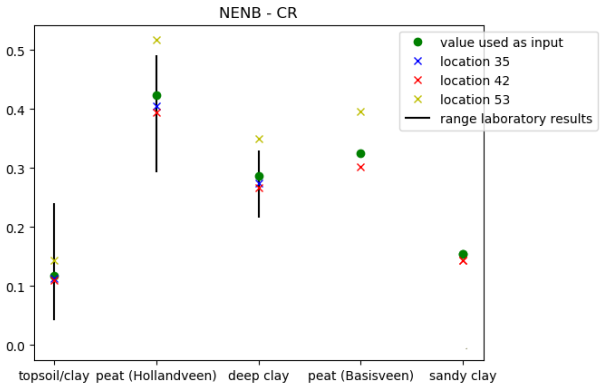

(b) parameter CR

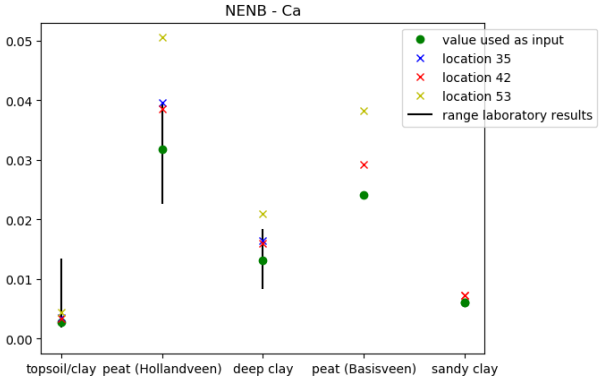

(c) parameter Ca

Figure 10.7: Obtained NEN-Bjerrum parameter values with fit for settlement module

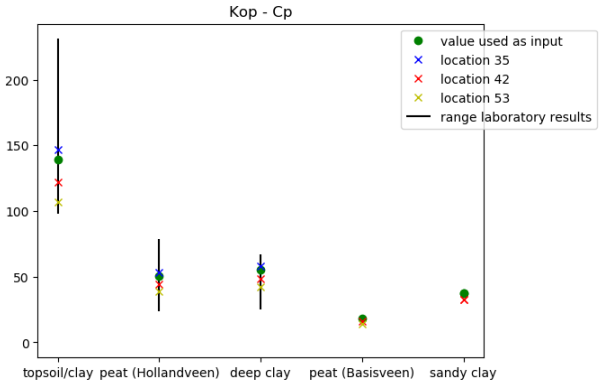

(a) parameter Cp

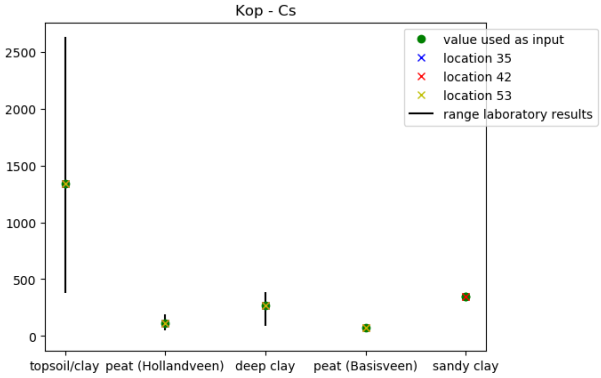

(b) parameter Cs

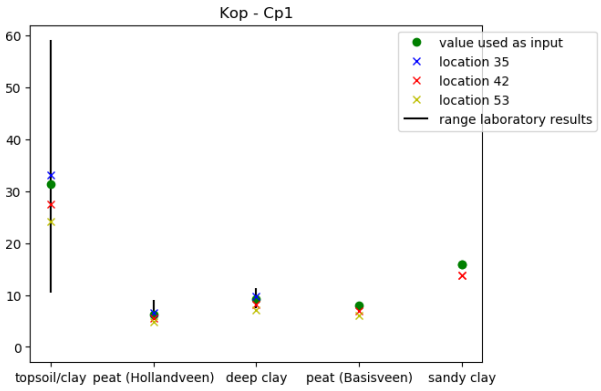

(c) parameter C'p

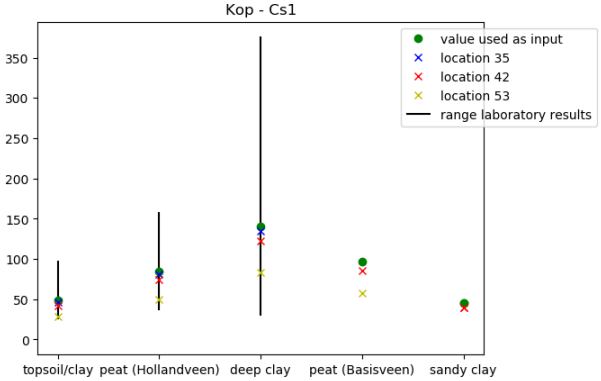

(d) parameter C's

Figure 10.8: Obtained Koppejan parameter values with fit for settlement module

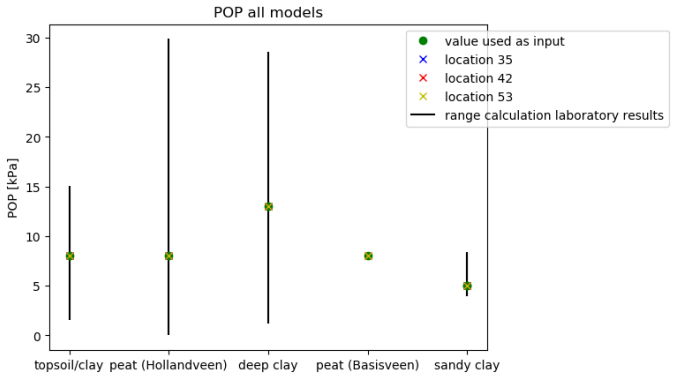

(a) parameter POP

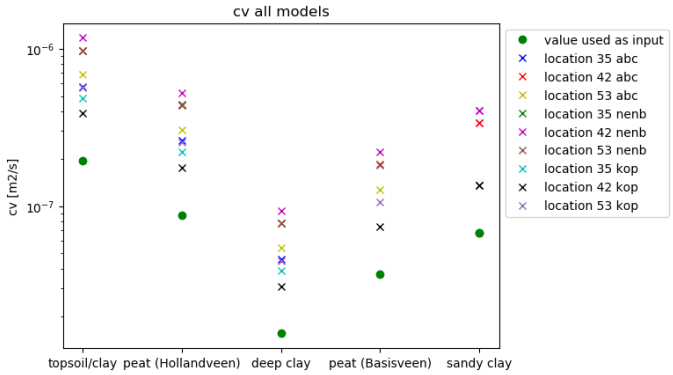

(b) parameter cv

Figure 10.9: Obtained POP and cv parameter values with fit for settlement module

For all parameters some variation can be seen across all locations analysed. Only the parameters Cs and the POP value show the same value for all situations. A fit factor of 1,0 for the POP was used in all models, which causes the same outcome of this parameter. Parameter Cs in the Koppejan model is not corrected by a fit factor thus the initial value is kept for all locations.

For the abc isotache model it can be seen that all results from location 3.5 and 4.2 lie within the range of the laboratory results. For location 5.3 the obtained parameter values do not always fall in this range, parameter b of the deep clay layer and parameter c for the hollandveen peat layer and the deep clay layer lay outside of the range encountered in the laboratory study. The results for the NEN-Bjerrum model show a similar pattern. Some parameters from the model for location 5.3 lie outside of the range encountered in the laboratory study. These are the b and c parameter values for the hollandveen peat layer and the deep clay layer. The obtained model parameters for the Koppejan model all fall in to the range of values encountered in the laboratory study.

Location 5.3 shows different parameter values than the other locations with all settlement models used. This location is the only location where fit factors larger than one were used for the primary settlement parameters. As the other parameters are corrected based on a ratio with this primary settlement parameter, it makes sense that this difference shows in all model parameters.

10.4. Discussion

Table 10.7 shows a general indication of the differences in loading components and subsidence measured at each location. This is based on information specified in appendix D. It can be seen that location 5.3 shows different behaviour than the other two locations. Comparing this location with location 4.2 shows that more subsidence is measured at location 5.3 than at location 4.2 but the total thickness of the construction elements is less.

Table 10.7: General comparison of loading situation per project location

	Location 3.5	**Location 4.2**	**Location 5.3**
Thickness clay construction element [m]	0,55	-	-
Thickness sand construction element [m]	7,85	6,80	4,60
Thickness road construction elements (both slag and asphalt together) [m]	0,70	0,68	0,63
Total subsidence since start of construction [m]	3,44	2,89	3,14

A reason could be the difference in the soil profiles between the two locations, see figure 10.2. One difference between the soil profiles for location 4.2 and 5.3 is the sandy clay layer which is present at location 4.2 but absent at location 5.3. As from a sandy clay in general less settlement contribution is expected compared to normal clay, this has had influence on the different behaviour between the locations. Another difference between the soil profiles is the thickness of the peat layer. At location 4.2 the thickness of the peat layer is larger than at location 5.3. Based on this only more settlement would be expected from location 4.2 compared to location 5.3. But regardless of both differences in the soil profiles 10.6, 10.7 and 10.8 show that a correction for the model parameters of location 5.3 is still needed to obtain a good fit with the measurements.

Fit factors were needed for all evaluated scenarios to come to the best fits with the measurements. A small correction is observed for the secondary settlement parameters at all locations, which causes an slight increase in creep. This correction is not extreme, but noticeable compared with the corrections for other parameters. It indicates that a small contribution from another subsidence component cannot be excluded. Hoefsloot (2015) also reported an underestimation of creep based on parameters from laboratory tests for the construction of two embankments at the Bloemendalerpolder. In this study it is mentioned that gas development in the peat layer could have caused additional subsidence. Overall, compression by loading seems to be the subsidence component that governs the subsidence behaviour.

An additional evaluation was done for location 3.5. The subsidence for location 3.5 was calculated with a model that includes a potential anaerobic degradation component. The Koppejan settlement model and the analytical consolidation approach model settings have been used. The values based on laboratory test of the model parameters are used for all parameters apart from the consolidation coefficient. As no fit was possible with these initial values, the corrected parameters (which already include a fit factor) are used for the c_v. The anaerobic degradation calculated with this model is based on the submodel for the Krimpenerwaardpolder. A important difference is that here no bottom limit for the zone of anaerobic degradation is used, which means that the whole peat layer is vulnerable to anaerobic degradation. This would represent a worst case scenario, where the anaerobic degradation is not limited by any depth. Figure 10.10 shows the result of the modelled subsidence for different scenarios with the subsidence measurements. A time step of 0,25 years was used in the model.

Sometimes anaerobic degradation of peat soil is listed as a possible cause for secondary compression in peat soils. To see the influence of this on the model results, three scenarios have been evaluated with the previously mentioned anaerobic degradation model. The first scenario shows the model results from only the Koppejan settlement model, figure 10.10a and 10.10b. The second scenario is a scenario where no creep contribution is calculated for the peat layer and anaerobic degradation is included, figures 10.10c and 10.10d. It can be seen that this model slightly underestimates the subsidence measured. Last, a model scenario is used where both creep and anaerobic degradation of the peat layer are included. In this scenario the subsidence is overestimated with approximately 9,9%, figures 10.10e and 10.10f. Based on these results it seems anaerobic degradation could contribute to creep of peat soil, but the approach holds a large factor of uncertainty. The use of the anaerobic degradation submodel seems questionable because this model has not been tested and was purely based on assumptions. Moreover, the creep calculation is based on creep parameters from laboratory test. These tests are generally performed on small soil samples with short time periods, and thus it is expected that no anaerobic degradation component is included in this parameter.

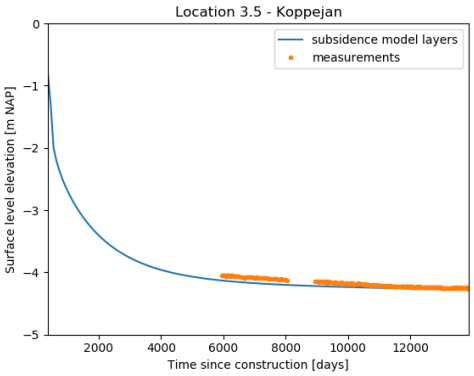

(a) No anaerobic degradation

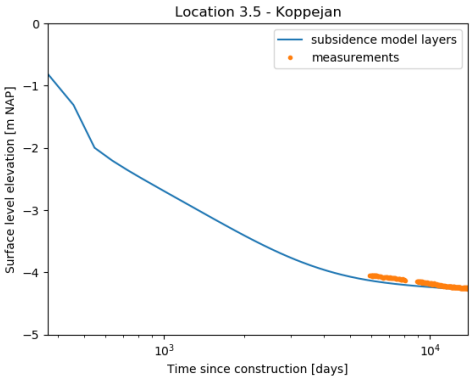

(b) No anaerobic degradation - logarithmic time scale

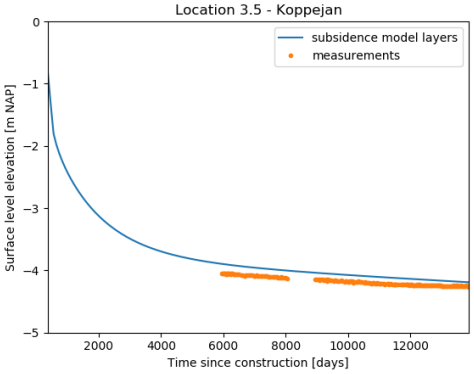

(c) No creep peat layer, including anaerobic degradation

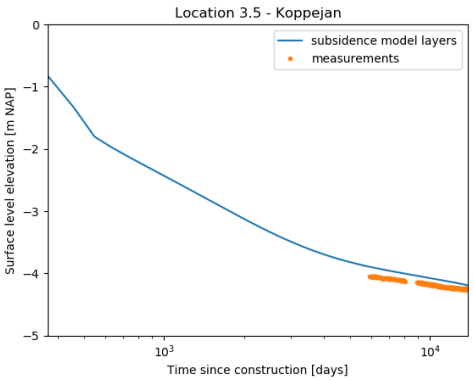

(d) No creep peat layer, including anaerobic degradation - logarithmic time scale

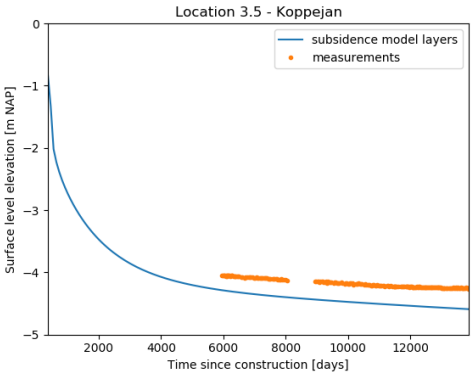

(e) Both creep and anaerobic degradation

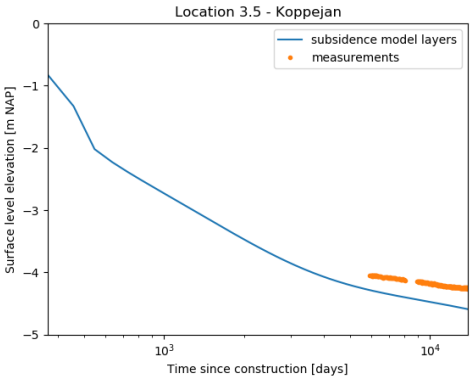

(f) Both creep and anaerobic degradation - logarithmic time scale

Figure 10.10: Different scenarios evaluated with Koppejan settlement model and anaerobic degradation submodel

Uncertainties

When evaluating the results of this chapter, there are multiple factors that should be considered:

- Average soil profiles and settlement parameters have been used, based on site investigation available. In reality, spatial variability of soil characteristics influences soil behaviour. This variability is shown through the range of values obtained in the laboratory study.
- The initial soil profiles are based on site investigation data from 1950. The construction of the road is estimated to have been in 1980. Potential influence of subsidence components in those

30 years are not calculated. As the peat layers were already below the water level it is expected that there was no influence from compression by oxidation in this time period. Moreover, it is assumed that all non-reversible shrinkage of the topsoil has already occurred before 1950.

- Consolidation coefficients:
  - Not all consolidation coefficients used in the calculations represent the loading situation. Often, a value of the consolidation coefficient was only available for the last loading step of the laboratory test. This explains high correction factors needed for the vertical permeability, as this is probably underestimated in general by using the values from this step.
  - Because consolidation coefficients were used in the calculation, the vertical permeability of the soil layers was not adjusted during the model calculations. Using a strain dependent permeability is more realistic, especially for the peat layers. This strain dependent permeability approach could not be applied because the initial vertical permeability (k0) is unknown. Using the k10 value mentioned in the laboratory report only resulted in a larger correction being needed for the vertical permeability.
- Overall fit factors are used, because no option for individual fit factors per layer is available. Therefore all layers are corrected with the same factor. This means that the ratio of input parameters between the soil layers themselves remained the same, and this ratio cannot be corrected.
- As explained in appendix D some assumptions were used to merge the three individual data sets of measurement points. The merged data set will probably deviate slightly from reality.
- The groundwater level used in the calculations was based on the water levels as indicated by the waterboard over time in the relevant water level area, the 'vigerende peilbesluiten'. Another source of information about the groundwater levels is also available, measurements by Geonius from hydraulic head monitoring wells. It is assumed that the water levels indicated by the waterboard were more realistic. Water levels reported in the boorprofiles next to the road often agreed more with these water levels than the ones observed by Geonius. The measurements in the monitoring well at location 3.5 indicated a shallow groundwater level higher than the initial height of the soil profile, which is assumed to be unrealistic. It could be that certain deviations in the water level at specific locations are missed by using general water levels from the waterboard.
- Times of loading have been estimated based on the website 'topotijdreis', as no detailed information on the time of construction of the road was available. Moreover, in the model it is assumed that all loading components are placed at the same time (day 0). Because of the length of the whole time period evaluated these assumptions still approximate reality. Dependent on the design of the road, there could be up to 1,5 year in time difference between the load components.
- The influence of aging of soil is neglected in the calculations. Due to ageing it is expected that soil can show a stiffer response over time, but modelling parameters are not adjusted here. Moreover, no tertiary compression component is evaluated.
- The uncertainty in the InSAR measurements is assumed to be negligible. Infrastructure is known to give a good reflection of the signal and on the website from SkyGeo it is mentioned that the surface deformation can be determined with millimeter precision (SkyGeo, 2020).

Another interesting observation from this analysis is related to the use of the numerical or analytical consolidation approach. Using the Darcy consolidation model together with the Koppejan settlement model lead to a large underestimation of the vertical permeability. Therefore very high values of the fit factor (±30) for this component were necessary for this combination of models. When the Koppejan settlement model was combined with the Terzaghi consolidation model, no extreme correction was needed.

11

Markermeerdikes

The final project evaluated in this study includes three project areas along the trajectory of the Markermeerdikes. Measurements of the crest height of the dikes are available over a long time period. At some locations the first known crest height even comes from the year 1890. This long timespan makes it an interesting location to evaluate with respect to land subsidence over time. The dikes have the function to protect the hinterland from high water events, this height is even more important. Also one calculation is done to evaluate subsidence of the hinterland at the scale of one grassplot, with the same methodology as for the Krimpenerwaard polder project. All project locations for the Markermeerdikes are shown in figure 11.1.

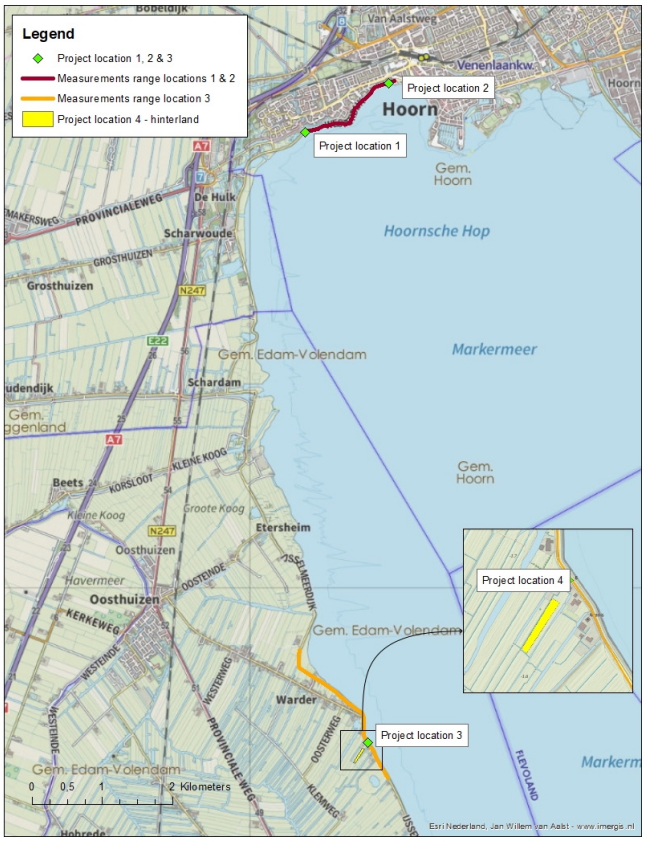

Figure 11.1: Project locations Markermeerdikes

This project is evaluated to see if knowledge from the previous evaluated projects can help in calculating subsidence for a more complicated situation, where different processes are expected to have had influence on the overall subsidence measured. An important boundary condition of this evaluation is that only one dimensional calculations have been done, though the dike is a two dimensional construction. The selection of the project locations and the evaluation of available information is explained in appendix E.

11.1. Soil profile

Many assumptions are used to come to the initial soil profiles used for the project locations. These are explained in appendix E.4. The initial profiles are shown in figure 11.2. For project locations 1 and 2 this profile represents the situation in 1890, for project location 3 it represents the situation in 1916. Location 4 is the estimated soil profile from a grass plot in 1994 behind the dike at location 3.

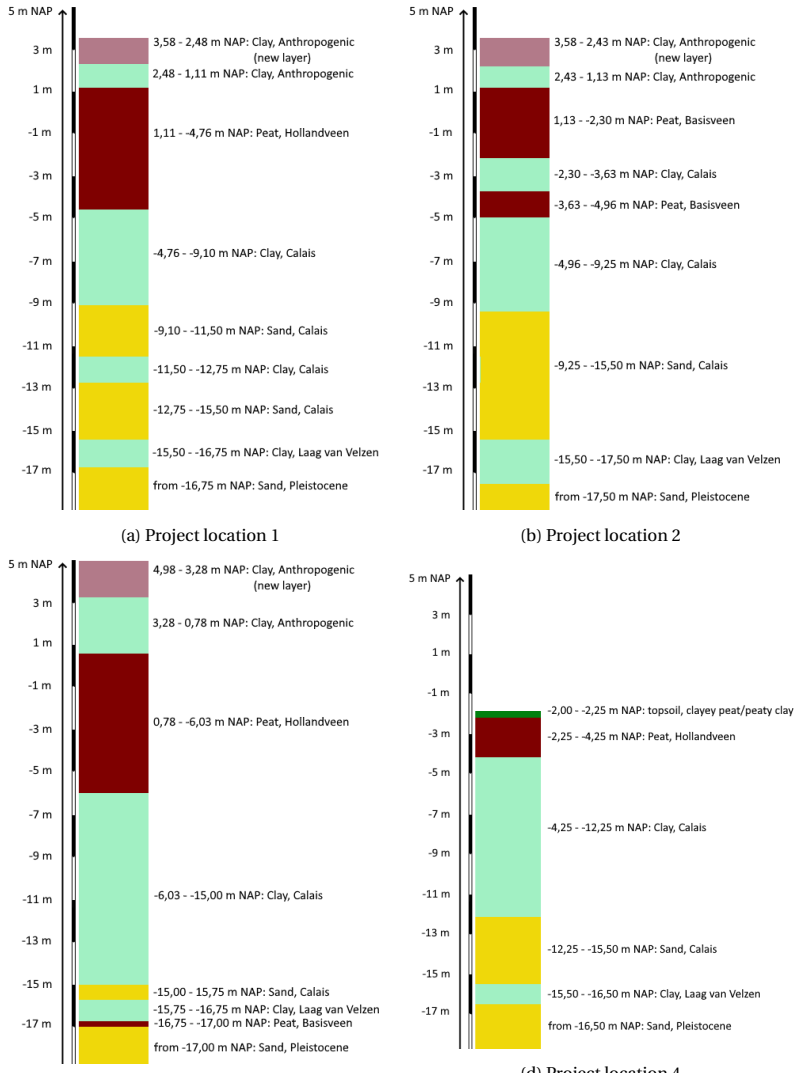

(a) Project location 1

(b) Project location 2

(c) Project location 3

(d) Project location 4

Figure 11.2: Initial soil profiles used for subsidence calculation Markermeerdikes

11.2. Methodology

11.2.1. Total model

Model

The model calculates subsidence as a result of different components over time. For each time step, the reduction in height is calculated based on several submodels. Figure 11.3 shows a visualization of this process. It is similar to the Krimpenerwaard modelling approach, though in this model an additional component is included, compression by of soil by its own weight, and shrinkage is assumed to only be relevant for the new constructed soil layer.

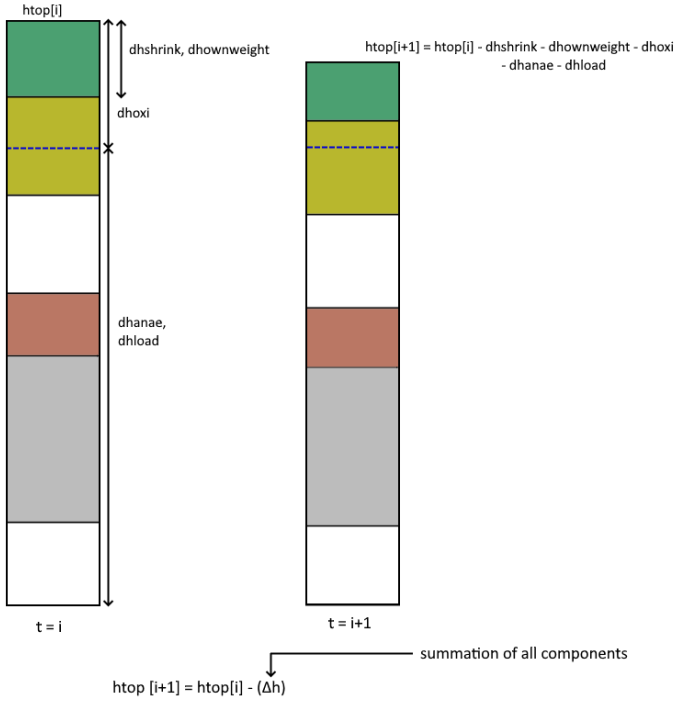

Figure 11.3: Time step based model approach Markermeerdikes

Input

Input parameters needed for the different subsidence components can roughly be categorised in:

- Soil profile, soil parameters & layer discretization (number of smaller evaluated layers within a soil layer);
- Water level in the crest & hydraulic head in deeper sand layers;
- Time parameters (total time to be evaluated, starting year, time step, etc.);
- Surface elevation measurements over time;
- Loading details (height of constructed layer, unit weight, etc.).

Output

Output of the model is:

- Graph showing the contributions of different subsidence components over time, together with surface elevation measurements in time;
- Table giving contributions of different subsidence components to total subsidence from the model in for the end situation, both in numbers and percentages;
- Graphs from submodels (effective stresses over time, etc.).

11.2.2. Submodels

Submodels for three components could be used from the Krimpenerwaard modelling approach with either no or minor adjustments. These are listed below:

- **Compression by oxidation:** No changes from the Krimpenerwaard modelling approach.
- **Compression by anaerobic degradation:** Reevaluation of the assumption about the GLG. For the Krimpenerwaard project it was assumed that the zone vulnerable for anaerobic degradation was limited by the water level and the GLG of the area. For the Markermeerdikes this zone is estimated a different way. Two water levels for the crest of the dike are provided by Alliantie Markermeerdijken for all project locations, the daily average and the normative high water level (MHW in Dutch). It is assumed that the difference between these two values can also be used calculate the normative low water level. This level is then used as the bottom level of the zone where anaerobic degradation is possible.
- **Compression by loading:** The calculation of the change in effective stress is updated, as this is now caused by an added loading component instead of a lowering of the water level. Also the option to use different POP values for different soil layers is added in the code.

Other submodels had to be added, as they were not revelant for the situation considered at the Krimpenerwaard polder. These are:

- **Compression by shrinkage:** The modelling approach from Fokker et al. (2019) has been implemented in the model. As mentioned before, it is assumed that shrinkage only plays a role for the newly constructed soil layer (upper layer). This is based on the assumption that non-reversible shrinkage for all other soil layers has already completed.
- **Compression by own weight:** To calculate compression by own weight in the new constructed layer, the layer is subdivided in a number of sublayers. Compression by its own weight is then calculated for each sublayer, where all sublayers above are considered as the loading component.

11.2.3. Evaluated scenarios

Different scenarios are evaluated to see the influence on the model result. In each scenario one aspect of the normal scenario is changed. Based on the results of the different scenarios a best fit scenario could be estimated. The scenarios are:

- *Normal scenario:* Parameters used are shown in appendix E.5. Both the Koppejan and NEN-Bjerrum settlement model are used. The constructed soil layer is seen as a clay layer vulnerable to compression by shrinkage.
- *Oxidation scenario:* The constructed soil layer is seen as organic soil vulnerable to compression by oxidation, parameters $V_{ox} = 0,015$ year^{-1} and $\lambda_{r,ox} = 0,09$ are used for this layer. This scenario is only evaluated with the Koppejan settlement model.
- *Shrinkage organic clay scenario:* The constructed soil layer is seen as organic soil vulnerable to compression by shrinkage, parameters $V_{sh} = 0,133$ year^{-1} and $\lambda_{r,sh} = 0,478$ are used for this layer. This scenario is only evaluated with the Koppejan settlement model.
- *Reduced C_α scenario:* C_α values for all soil layers are based on the results from Fokker et al. (2019) instead of the values from the report Alliantie Markermeerdijken (2018). Only evaluated with NEN-Bjerrum settlement model.
- *Increased POP scenario:* All POP values are increased with a value of 10 kPa. This scenario is only evaluated with the NEN-Bjerrum settlement model.
- *Only creep from above water level:* Settlements originating from the unsaturated soil part are calculated by only considering creep settlement. This scenario is based on the findings from the A5 Badhoevedorp. Both Koppejan and NEN-Bjerrum settlement models are used.

- *Best fit scenario:* Using the output of the previous scenarios a best fit parameter set is constructed and tested on all locations. Changes in the best fit scenario compared to the normal parameters scenario are:
  - The constructed soil layer is seen as an organic soil vulnerable to compression by an interplay of oxidation and shrinkage, where parameters used are $V_{ox} = 0,015$ year^{-1} and $\lambda_r = 0,478$.
  - The coefficient of consolidation for the Calais clay layers is changed from $1E-07$ m^2/s to $5E-08$ m^2/s. A value of $1E-07$ m^2/s is assumed to be on the high side for a clay soil.
  - The C_α values for all soil layers are based on the results from Fokker et al. (2019) instead of the values from the report Alliantie Markermeerdijken (2018).
  - Settlements originating from the unsaturated soil part are calculated by only considering creep settlement.

11.3. Results

For all project locations the model result is compared with subsidence measurements available. Model settings are shown in appendix E.7. First differences between the compression by loading and the compression by oxidation submodels are evaluated. For the evaluation of the oxidation submodels, the Koppejan loading model is used. The differences between the loading submodels are shown in figure 11.4a and the differences between the oxidation submodels are shown in figure 11.4b.

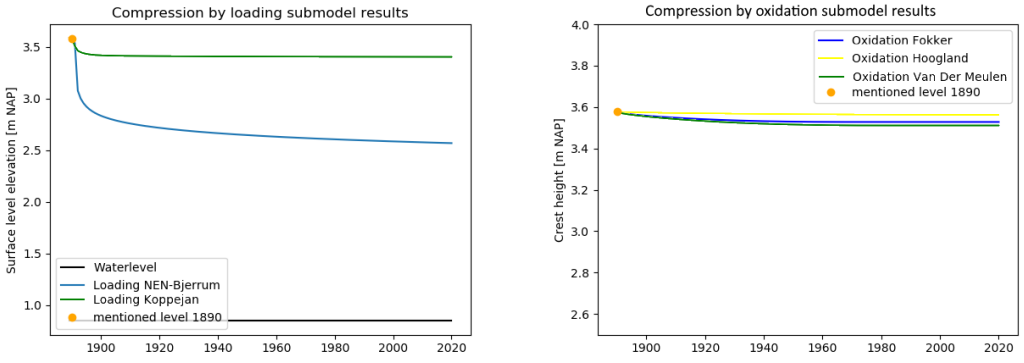

(a) Project location 1

(b) Project location 1

Figure 11.4: Comparison compression by loading and oxidation submodels for project location 1. Oxidation models evaluated with the Koppejan loading model was used in the model setting to evaluate the oxidation models.

Large differences can be seen between the NEN-Bjerrum and the Koppejan submodel results. The NEN-Bjerrum predicts a larger initial settlement, than the Koppejan model. This is due to a high creep contribution in the first years. Moreover, a difference can be seen between the slope of the model predictions over longer timescales. It should be noted that the Cs and C's Koppejan model parameters are not calculated directly from the C_α parameter value, but estimated based on an excel tool from Arcadis.

The oxidation models from Fokker et al. (2019) and Van der Meulen et al. (2007) predict similar results, only a small difference can be seen, which is caused by the factor λ_r included in the Fokker submodel but not in the Van der Meulen submodel. The Hoogland model gives a different outcome, because the water level lies below the critical depth of oxygen diffusion which was assumed in the study from Hoogland et al. (2012). The oxidation component is corrected with a factor to account for a potential oxygen deficiency. This critical depth was estimated for a polder area, and it is not sure whether the use of this value is valid here. The Fokker submodel is used for analysis done in this chapter.

Results of the total subsidence calculation for all project locations are shown in table 11.1. Also the differences in results between the used scenarios are shown in this table. Results for each project location are further discussed below.

Table 11.1: Total subsidence results, all scenarios

Model scenario	**Total subsidence calculated [m]**		
	Project location 1 (Δt = *130 year*)	*Project location 2* (Δt = *130 year*)	*Project location 3* (Δt = *104 year*)
Normal - Koppejan	0,768	0,833	1,620
Normal - NEN-Bjerrum	1,479	1,455	2,758
Oxidation - Koppejan	1,161	1,216	1,784
Shrinkage OC - Koppejan	0,940	1,006	1,792
Adjusted C_α - NEN-Bjerrum	0,881	0,933	2,099
Adjusted POP - NEN-Bjerrum	1,251	1,248	2,414
Only creep above gwl - Koppejan	0,744	0,809	1,585
Only creep above gwl - NEN-Bjerrum	1,451	1,427	2,722
Best fit - Koppejan	0,767	0,803	1,216
Best fit - NEN-Bjerrum	0,892	0,919	1,713

11.3.1. Project location 1: dike 20 dp 29

The results for all scenarios evaluated are shown in appendix E.8.1. Here only the comparison of the model outcome with the measurements for the normal and best fit scenario are presented, see figure 11.5.

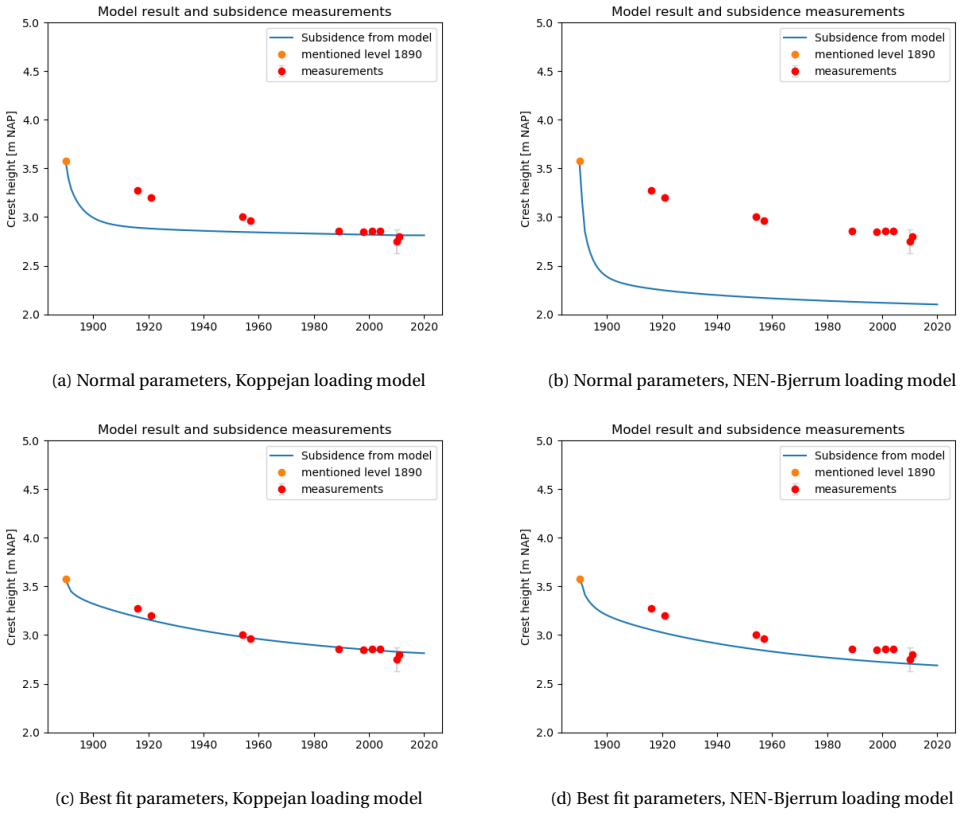

(a) Normal parameters, Koppejan loading model

(b) Normal parameters, NEN-Bjerrum loading model

(c) Best fit parameters, Koppejan loading model

(d) Best fit parameters, NEN-Bjerrum loading model

Figure 11.5: Project location 1: dike 20 pole 29

The total subsidence calculated over the time span of 130 years with the Koppejan approach approximates the measurements from 1980 onwards, but the subsidence before this time period is overestimated. With the best fit scenario parameters, this effect is minimized. The NEN-Bjerrum approach

overestimates subsidence with the normal scenario, but it can be seen that this is reduced using the best fit parameters.

11.3.2. Project location 2: dike 20 dp 14

The results for all scenarios evaluated are shown in appendix E.8.2. Here only the comparison of the model outcome with the measurements for the normal and best fit scenario are presented, see figure 11.6.

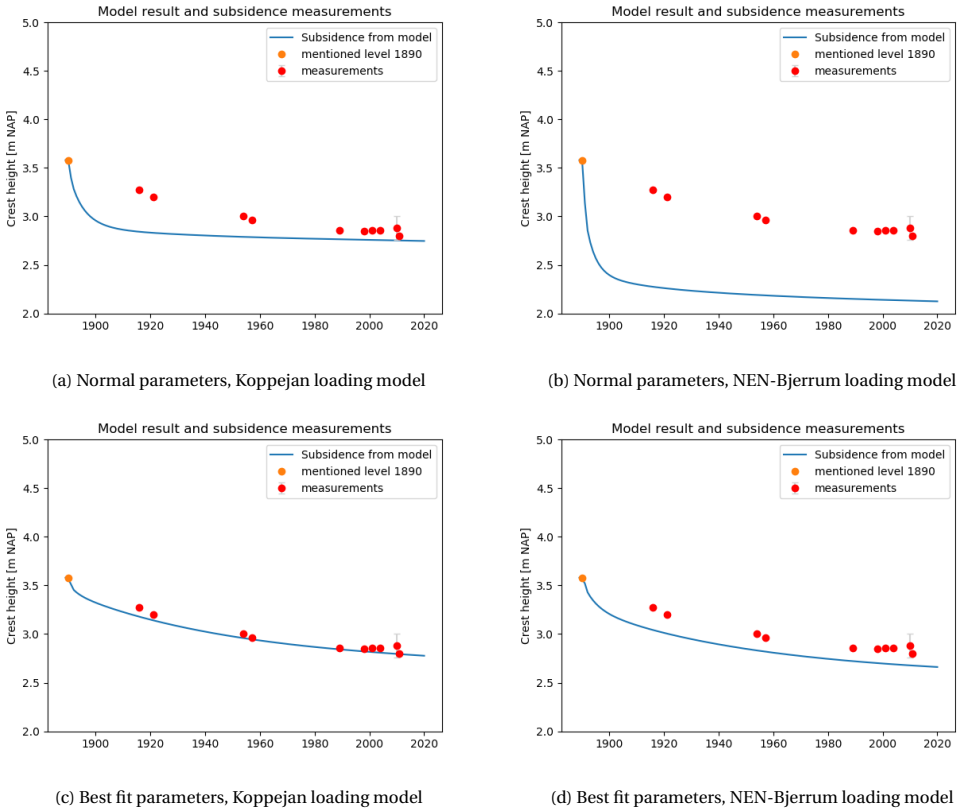

(a) Normal parameters, Koppejan loading model

(b) Normal parameters, NEN-Bjerrum loading model

(c) Best fit parameters, Koppejan loading model

(d) Best fit parameters, NEN-Bjerrum loading model

Figure 11.6: Project location 2: dike 20 pole 14

A similar pattern in the results can be seen for project location 2 and project location 1.

11.3.3. Project location 3: dike 23 dp 60

Again, only the comparison of the model outcome with the measurements for the normal and best fit scenario are shown in figure 11.7. All other model results are shown in appendix E.8.3.

At this location many assumptions were used to come to an representative soil profile that could be used as input, and also characteristics of the loading component are unknown. It can be seen that with the used assumptions the subsidence is overestimated with the normal scenario. Using the best fit parameters and the Koppejan approach the subsidence is underestimated, while the use of the NEN-Bjerrum approach still shows an overestimation.

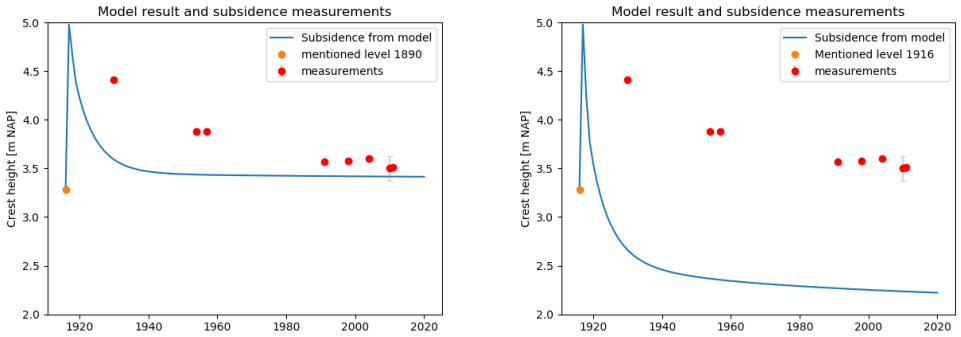

(a) Normal parameters, Koppejan loading model

(b) Normal parameters, NEN-Bjerrum loading model

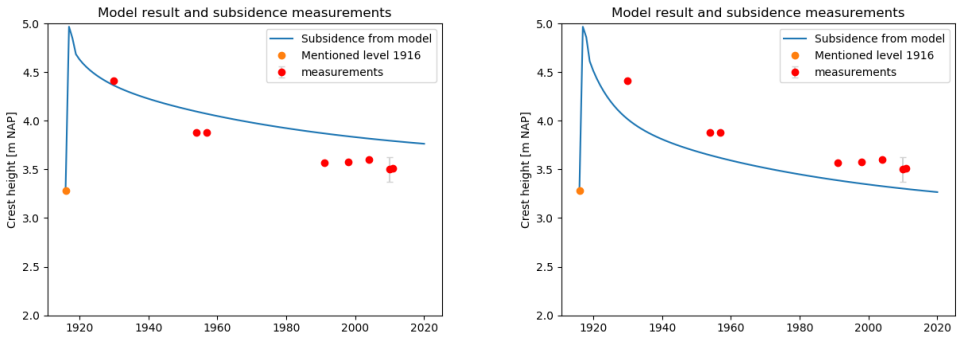

(c) Best fit parameters, Koppejan loading model

(d) Best fit parameters, NEN-Bjerrum loading model

Figure 11.7: Project location 3: dike 23 pole 60

11.3.4. Project location 4: hinterland of dike 23 dp 60

The model from that was used to evaluate subsidence in the Krimpenerwaard polder is used to evaluate subsidence of project location 4, a grassplot behind the dike. Input parameters are given in appendix E.5.4. The modelled subsidence is compared with the AHN2 and AHN3 measurements, see figure 11.10. The modelling equations from Van den Akker et al. (2007) are applied as well. The contributions over time are shown in figures 11.8 and 11.9.

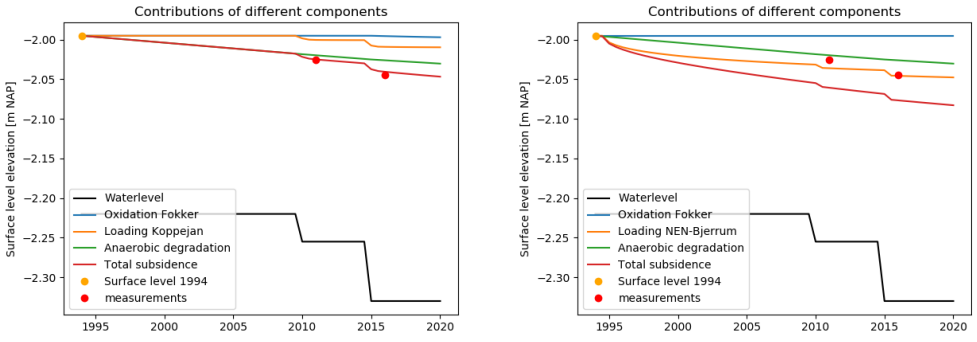

(a) Koppejan approach

(b) NEN-Bjerrum approach

Figure 11.8: Contributions of different subsidence components over time

Both approaches show different results. Using the Koppejan approach, there is no contribution from compression by loading before the first lowering of the water level in the modelled time period. The peat

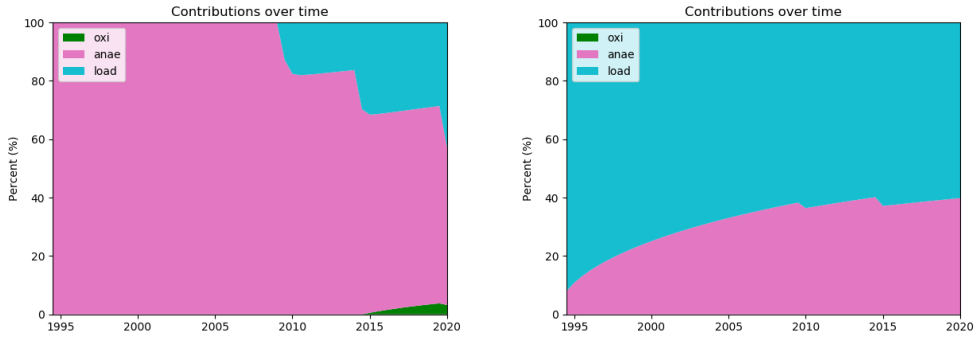

(a) Koppejan approach

(b) NEN-Bjerrum approach

Figure 11.9: Comparison of model results with Van den Akker et al. (2007) equations

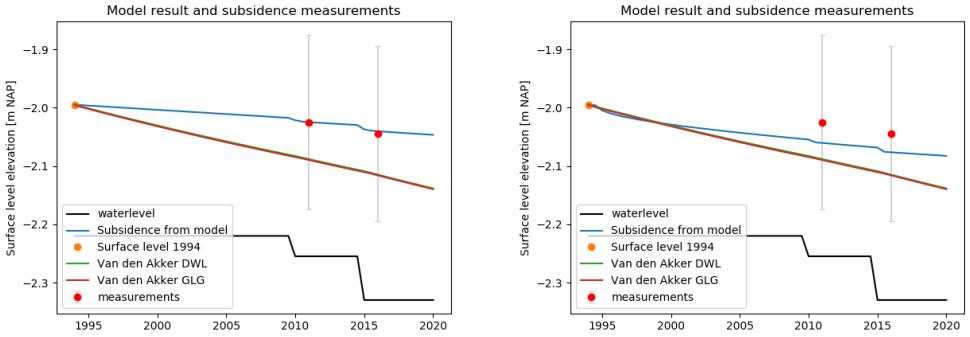

(a) Koppejan approach

(b) NEN-Bjerrum approach

Figure 11.10: Comparison of model results with Van den Akker et al. (2007) equations

layer also lies below the water level in the beginning of the model, and thus is the only contribution to subsidence from compression by anaerobic degradation of SOM. With the last water level lowering a small part of the peat layer ends up in the unsaturated zone and therefore a small contribution from compression by oxidation can be seen. The NEN-Bjerrum approach does have a contribution from compression by loading from the start. The peat layer remains below the water level in this situation. Both model results approximate the measurement points and lie within the range of uncertainty given for these measurements. The equations from Van den Akker et al. (2007) seem to overestimate the subsidence at this location, but the results also lie in the range of uncertainty.

11.4. Discussion

Many assumptions have been used in the evaluation of subsidence at different locations along the Markermeerdikes. The assumptions influence the outcome of the model to a large extent. An important component that influences the model results in all scenarios is the vulnerability of the newly constructed soil layer to subsidence processes. If this layer is seen as a clay layer and corresponding shrinkage parameters are used, the initial rate of subsidence seemed to be too high but the total amount of subsidence approximates the measurements. If this layer is seen as a peat layer, vulnerable for compression by oxidation, the rate of subsidence is better but the total amount of subsidence is overestimated. In the best fit scenarios the material is classified as an organic clay where the rate of oxidation for a peat soil is used, but the residual thickness factor is based on an organic clay. The combination of these parameters is not directly from Fokker et al. (2019). This subsidence component contributes between approximately 55 to 70% of the final subsidence calculated with the best fit parameters for locations

1 and 2. It contributed between 45 and 55% for project location 3. This assumption that governs the shrinkage/oxidation behaviour of the soil layer thus has a large influence on the model results.

Another subsidence component that contributes to the best fit subsidence modelled is compression by loading. This is the second largest contributor for project locations 1 and 2 and the main contributor for location 3. At location 3 a thicker soil layer is applied, and the higher contribution from this component makes sense.

The NEN-Bjerrum approach consistently overestimates subsidence for all scenarios considered. The overestimation was limited by using C_α values from the study from Fokker et al. (2019) instead of the values from Alliantie Markermeerdijken (2018). The values of C_α from Alliantie Markermeerdijken (2018) are based on test samples from locations across the trajectory from Hoorn to Edam. This makes the observation that subsidence could better be approximated using the parameters from Fokker et al. (2019) interesting. All other settlement model parameters are based on Alliantie Markermeerdijken (2018). The report is from 2018, so parameter values used are representative for the current situation of the dikes, and not necessarily for the soil profile at the start of the model. Because no other information was available, these parameters are still used in the model.

The assumption that settlement from the unsaturated zone of the soil can be estimated by calculating only creep settlement did not significantly influence the compression by loading component. For the best fit scenarios the influence is approximately a reduction of 2 to 4 cm for all locations. Initial creep settlements modelled by the NEN-Bjerrum approach account for a large part of the total settlement and these are not reduced by this assumption. For the Koppejan approach the impact of this reduction by 2-4 cm is larger as the overall computed settlement is smaller.

The model approach for anaerobic degradation has not been verified and is built as a first estimation. It is based on assumptions and theoretical knowledge. For project location 4, the Koppejan and NEN-Bjerrum approaches show different results in terms of contributions to subsidence, but compression by anaerobic degradation plays a role for both. As this has not been tested there is a large uncertainty in this outcome.

Comparing project locations 3 and 4 the contrast in contributions to overall subsidence at these locations is clear. At the crest of the dike, compression by oxidation/shrinkage of soil and compression by loading seem to be the dominant components. Compression by loading as a result of water level lowerings over time and compression by anaerobic degradation are indicated as dominant components for subsidence of the hinterland. For both projects assumptions on the parameters V_{ox}, V_{an} and V_{sh} of soil layers determine the outcome of the model.

No perfect fit could be obtained where the modelled outcome lies in the range of uncertainty of all measurement points for all locations. But with the best fit scenario used, a better outcome is found than with the normal parameters scenario. As locations 1 and 2 show similar characteristics and the best fit scenario at location 3 does not give a model that fits all measurement points, the results should be used with caution. Another reason for this is that the input of the models is based on many assumptions. Best would be to test leading assumptions on multiple other locations as well, but the options are limited by the availability of data. Some of the key aspects of uncertainty in this evaluation are indicated below.

Uncertainties:

- No two-dimensional effects are evaluated in this study. Only one-dimensional subsidence aspect have been included. This is an important point of uncertainty. Since dikes are two-dimensional constructions, adding a two-dimensional evaluation would be valuable.

- Subsidence measurements:

  - Different files with subsidence measurements over time were provided by Alliantie Markermeerdijken. Sometimes these files contained contradicting information. For crest height measurements in 2011 variations up to 2 cm were found in different files.

  - Crest height measurements from the file used are indicated over a section of the dike. Variation within this section is not indicated. Project locations 1 and 2 lie within the same section

of the dike for subsidence measurement available. The distance between the two locations is approximately 1,6 km and differences in soil profiles can be seen.

The assumption regarding compression by shrinkage/oxidation of the constructed soil layer influences the model results to a large extent, as mentioned before. At project locations 1 and 2 the soil layers constructed in 1890 are assumed to be similar at both locations, and thus similar subsidence results are modelled. Using the same set of measurement points for both locations influenced the results because this way a similar fit was observed for both locations. Measurements from the project locations themselves instead of the range would have been more useful for this project.

- The methodology used to obtain the crest height measurements is unknown and thus an assumption has been used that they are obtained using levelling.
- Average values for the AHN measurements at project location 4 were used. In the chapter about the Krimpenerwaard project the comparison of AHN2 and AHN3 was evaluated. Flight patterns in one of the data sets can have influenced the values used as measurement points for this project.
- In 2005 there has been a correction of the NAP level. In this study all values from before 2005 are corrected with -0,02 m to account for this NAP correction. For some data sources (crest height measurements, groundwater levels over time, etc.) it is unknown whether this component was already included.

- Soil profiles:
  - Initial soil profiles were estimated based on many assumptions to be able to use the model. When the soil profiles from 2010 as computed by the model are now compared with the soil profiles of the crest from Alliantie Markermeerdijken, differences can be found.
  - Already in 1918 observations of subsidence of the Markermeerdikes near Hoorn were mentioned in a letter. Some of the old boorprofiles belonging to project locations 1 and 2 showed the belt of seaweed around -2,25 to -2,75 m NAP. This material belongs to an old technique used for the construction of dikes. In the letter it is mentioned that when assumed this material was originally constructed around highwater level this shows a subsidence component from approximately 3 m. In the soil profile provided by Alliantie Markermeerdijken all shallow peat material in the crest of the dike belongs to the Hollandveen peat layer. Based on the archaeological information it is assumed that a part of this peat layer is formed by anthropogenic organic construction material. Variability of the peat layer itself has not been considered in this study.

- Project location 3:
  - At this location characteristics of the loading component, as the timing, the soil type and the thickness of the constructed layer are unkown. In the model these are all based on assumptions. These assumptions have governed the outcome of the model.
    - ◇ In one document, plans for the construction of the dike in 1918 are mentioned. A new crest height of 3,90 m is indicated in this document. It is assumed that these plans were not carried out, because the crest height measured in 1930 is higher than the height indicated in the plans. This aspect was discussed with an archaeologist from the Markermeerdikes who argued that this could potentially be a writing error or measurement error. This was evaluated by comparing 1930 measurements from surrounding sections. These sections all showed a similar pattern with a higher 1930 measurement value and thus it was assumed that the construction plans from 1918 are not carried out.

- The water level at the crest of the dike used in the model is based on hydraulic characteristics of the current situation. In the model it is assumed that the water levels are representative for full time period considered.

III

Conclusions and Recommendations

12

Conclusion

Different research questions are provided in section 1.4. These are answered in this chapter based on the projects evaluated in part II from this thesis and background information provided in part I.

12.1. Conclusions subquestions

What is the result of the comparison of project data for grass and agricultural areas (area type 2) and residential areas and infrastructure (area type 3) to the land subsidence model result (sum of all individual components over time)?
The used modelling approach, which consists of mostly existing modelling techniques, approximates the measurement points of the AHN for the project locations evaluated in the category grass and agricultural lands. In general, it can be seen that compression by degradation of organic matter plays the largest role in these areas. However, some points still remain unclear.

- This conclusion is based on the modelling approach at the Krimpenerwaard polder, but a grassland plot at the hinterland of the Markermeerdikes has been used to check the model. Compression by anaerobic degradation showed to be the dominant subsidence component at the grassplot behind the Markermeerdikes. This is a difference with the Krimpenerwaard plots where compression by oxidation is the largest contributor to subsidence, caused by differences in soil profile and water levels.

- The role of compression by anaerobic degradation in land subsidence is not well understood, and the modelling approach used here has not been checked against measurements up to now.

- It should be remembered that it is assumed that the compression by oxidation submodels also include irreversible shrinkage of peat. These submodels all calculate the loss of thickness of an organic soil layer based on a rate of oxidation parameter. From the sensitivity analysis, see appendix B.9, it can be seen that the value used for this parameter influences the results to a large extent.

- The formulas from Van den Akker et al. (2007) also approximate the measurements for grass and agricultural lands well and seem suitable to predict subsidence for these areas in the Netherlands. These formulas predict land subsidence based on a ditch water level or average lowest groundwater level (dutch: GLG). However, no contribution from separate components can be found with this calculation method which remains its largest disadvantage.

Commonly used settlement models are suitable to approximate subsidence measurements for residential areas and infrastructure projects analyzed. However, the evaluation of the N3 Dordrecht showed that creep (and thus long-term subsidence) was slightly underestimated by the model. The settlement models overestimated klink at the embankment constructed at the A5 Badhoevedorp.

- For the N3 Dordrecht some parameter fine-tuning was needed to obtain the best fit with the measurements, where a higher correction was needed for the creep component than for the primary consolidation component. The values for the consolidation coefficients had to be increased consistently, the availability of laboratory-based parameter values influenced this as often only values of the highest load step were available, and the overall consolidation coefficient had thus been underestimated.
- The embankment at the A5 Badhoevedorp is constructed above the groundwater level and thus unsaturated soil mechanics should be used. It is expected that consolidation of the material caused by its own weight occurs fast due to its unsaturated character. This explains the better fit obtained when only creep settlements were calculated. Influence of a final part of soil ripening processes is difficult to estimate based on currently existing subsidence modelling techniques.

What is the result of the comparison of project data for dikes (area type 1) to the land subsidence model result (sum of all individual components over time)?
Modelled subsidence over time for the Markermeerdikes overpredicts the rate of subsidence. It is possible to obtain a better fit with the subsidence measurement, by modifying the rate of compression by oxidation/shrinkage of the constructed soil layer, decreasing the consolidation coefficient, using C_α parameter values from the study from Fokker et al. (2019) and calculating only creep in the unsaturated zone.

- The evaluation of the three dike locations indicate a large contribution of compression by oxidation/shrinkage of the new applied soil layer and compression by the loading of the subsoil, but the contribution of compression by oxidation/shrinkage is based on assumptions. The nature of the soil used as construction material influences the relevance of different subsidence components. If the soil is interpreted as clay layer it is vulnerable to compression by shrinkage, if it is seen as organic soil layer then compression by oxidation is relevant.
- To model compression by shrinkage of a clay layer, only one existing one-dimensional model was found in subsidence studies. This approach from Fokker et al. (2019) has only been used to evaluate subsidence in Flevoland and its results could not be compared with other models.
- Even with the adjustments listed no fit could be found that worked well for all three locations. It is expected that neglecting the two-dimensional aspect of the dike embankment in this subsidence evaluation has played a role. Moreover, many uncertainties regarding the initial soil profiles, the details of the load components and the validity of the measurements influenced the evaluation of all project locations.

How sensitive are model results to potential variation of input and model parameters, due to heterogeneity of soil?
Modelling subsidence on a project scale has implications for the use of model parameters. Average parameters are used for the models, which are often based on samples from multiple locations. Due to the variability of the subsurface these average parameters might not be representative for the soil profile of the specific locations considered. All models used are sensitive to variations in input and model parameters, though variation in some parameters has more influence on the subsidence results than other parameters.

- The model parameters for the compression by oxidation/shrinkage submodels are based on average values indicated in literature, which makes it difficult to find the influence of heterogeneity of organic soil. The results for these submodels are very sensitive to a variation in the rate of oxidation or rate of shrinkage parameter, as could be seen in the sensitivity study for the Krimpenerwaard polder and the model results for the Markermeerdikes.
- Variability of settlement parameters has been considered for the Krimpenerwaardpolder, the A5 Badhoevedorp and the N3 Dordrecht. At the Krimpenerwaardpolder the impact of a variation in settlement model parameter is smaller than the variation in compression by oxidation/shrinkage parameters. For the N3 Dordrecht and the A5 Badhoevedorp variation could be evaluated based on laboratory test results.

Can it be assumed that there are no other effects contributing to subsidence than primary and secondary consolidation when soft soil layers (soft clays and peat) are pushed below the groundwater level?
Using subsidence measurements of the N3 Dordrecht, this question was evaluated for residential areas and infrastructure. Peat layers at all locations are located below the groundwater levels already from the start of the evaluated time span. The results of this analysis indicate that the contribution from another component in this situation cannot be excluded, but the influence on total subsidence is not significant as primary and secondary compression govern subsidence behaviour.

- This conclusion is based on a slight underestimation of creep based on laboratory parameters used as input for settlement models. An underestimation of creep settlements based on laboratory parameters is also reported by Hoefsloot (2015) for the construction of two embankments in the Bloemendalerpolder, where gas development in the peat layer was listed as possible cause for this underestimation. A difference with this study is that the correction needed in this study is smaller than the correction needed for the best fit at the Bloemendalerpolder, where an approximately 2.1 times larger creep contribution was used in order to approximate subsidence measurements of the embankment.

- A component that complicated the answer to this question is that the cause of secondary compression in different soil types remains a point of discussion in literature. Anaerobic degradation of organic matter is sometimes listed as a possible cause for creep settlements in peat soil. The separation of different components then becomes difficult and terminology is important with respect to this point.

For grass and agricultural areas, it is assumed that there can be another subsidence contribution from below the groundwater level, compression by anaerobic degradation of organic matter.

- Because the submodel used for this component has not been verified, conclusions regarding compression by anaerobic degradation should be used with caution. Recommendations regarding this point can be found in chapter 13.

What happens with the subsidence rate in grass and agricultural areas when shallow groundwater table lowering stops and the water table is not lowered any further from the current level?
Subsidence in this situation will go on, until all organic components available for degradation are degraded (in the aerobic or anaerobic zone). Mineral particles or organic matter that is stabilized and unavailable for degradation will represent a thickness of organic soil layers that remains. Organic soil below the zone where anaerobic degradation can occur will not be degraded. The rate of oxidation and anaerobic degradation will go down over time. Stopping the groundwater table lowering decreases the contribution from compression by loading, as only a creep component will remain which is small.

- The answer to this question is based only on the functionality of the submodels implemented in the Krimpenerwaard model approach and not on any measurements.

How does a shift from grass and agricultural areas to residential areas, infrastructure or dikes influence the already existing land subsidence rate?
Compression by degradation of organic matter plays the largest role in the existing subsidence rate for grass and agricultural areas with organic soil layers. When a loading component is introduced to the system this changes and compression by loading becomes more relevant. The change in the subsidence rate itself is determined by characteristics of the soil profile and the load component that is applied. The contribution from compression by oxidation is reduced as pushing these layers below the groundwater level limits the availability of oxygen. Assuming a situation where all organic soil layers are pressed below the water level and primary consolidation has completed, the subsidence rate is determined by creep but the influence of another component (potentially anaerobic degradation) cannot be excluded.

12.2. General conclusions

How do different shallow land subsidence processes contribute to total land subsidence for areas with different land uses over time, measured on a project scale and can these be modelled accurately on this project scale using existing modelling techniques?

Subsidence in residential areas and infrastructure is dominated by compression by loading. However, the contribution of another long-term subsidence component cannot be excluded based on the project evaluated in this study. Settlement models are suitable to estimate subsidence behaviour in this area type, as the potential influence of another component is small.

For grass and agricultural areas contributions of different components are dependent on the soil profile and water levels, but compression by degradation of organic matter is found as dominant subsidence component in the evaluated areas. Multiple modelling approaches are tested, and outcomes lie within the range of uncertainty of the subsidence measurements. The main uncertainty lies here with the empirical compression by oxidation, shrinkage and anaerobic degradation models used. Subsidence from these components remains difficult to distinguish based on a total subsidence signal only. The settlement models implemented are commonly used and also showed suitable for residential areas and infrastructure. The equations from Van den Akker et al. (2007), which are widely used for subsidence predictions in the Netherlands and are based on field measurements in a grass and agricultural area, give satisfactory results for the project areas evaluated.

When organic material has been used for the construction of dikes in the past, not only compression by loading is relevant, but different components seem to influence total subsidence. No accurate outcome for all locations evaluated could be obtained with the existing modelling techniques. It is assumed that to obtain a better fit for all locations two-dimensional effects should be considered and more characteristics of the load components are needed. However, it can be concluded that for dikes using subsidence rates based on the land subsidence map of the Netherlands, or adding a subsidence rate from nearby grass and agricultural lands is not representative for considering 'land subsidence'. This term here is used as a collective term that represents all other subsidence components than compression by loading.

Overall, comparing total subsidence for four different projects with modelled predictions showed that unravelling an overall subsidence signal into its separate contributing components remains challenging. In theory, an infinite amount of combinations of submodels could lead to a similar agreeable result. Therefore in the assumptions made in this study, differences in outcome are imposed. In general, existing modelling techniques could be used to approximate subsidence measurements, but the nature of the models themselves is sometimes questioned as these often do not include or distinguish all relevant influences and couplings between subsidence components.

13

Recommendations

- To fully understand subsidence behaviour in the Netherlands on a local scale a different type of subsidence measurements is needed, which allows separation between contribution to subsidence from different soil layers. At the moment Deltares is involved in a research project where subsidence in a soil profile is measured with extensometers, levelling, LiDAR and InSAR in a grass and agricultural area. The extensometers can provide information on the depth that subsidence originates from. The outcome of this study will provide valuable information for future subsidence modelling studies. It is recommended to also use a similar subsidence measurement approach for the other area types analyzed in this project. This way assumptions done in this study can be verified or rejected.
- It is recommended that more project locations should be evaluate to verify the conclusions from this study. Looking at different dike locations could help understand subsidence for this area type. Because subsidence components are location specific and depend on the soil structure and soil hydrology, it is recommended to use locations with different characteristics.
- Modelling approaches:
  - At the moment the interaction between the compression by loading and the compression by oxidation and shrinkage submodels is one-sided. The oxidation, anaerobic degradation and shrinkage submodels are influenced by results from compression by loading as it changes the position of the water level in the soil profile, but the compression by loading submodels are not influenced by the other submodels. Coupling between soil structure and soil hydrology actually governs the problem. Therefore it is recommended to develop a modelling approach where a full coupling of these effects can be considered. The oxidation submodel from Bootsma et al. (2020) which is included in Atlantis is a good starting point of this new modelling approach, as it includes an estimation of density of the soil over time. This should then be connected to the compression by loading submodels, where changes in density influence the mechanical behaviour of the soil, to develop a fully coupled approach.
  - The assumptions used for the evaluation of compression by anaerobic degradation should be tested. Main components to be evaluated are the rate of anaerobic degradation (V_{an}) and in what part of the soil profile anaerobic degradation can be relevant. It is recommended to update the submodel of anaerobic degradation when more information is available.
  - Compression by oxidation and shrinkage governed subsidence behaviour of the Krimpenerwaard polder and the Markermeerdike project locations. Model parameters for these submodels should be evaluated. It is expected that better model results can be obtained when location specific characteristics are included in these parameters. It is useful to obtain rate of oxidation parameters and rate of shrinkage parameters for different soil types with standardized laboratory tests. The models and tests should include influence of temperature,

depth in the soil profile and pH on these parameters, improving modelling site specific oxidation and shrinkage.

- The calculation for shrinkage of clay soil should be improved. At this moment the only model that could be implemented easily was the model from Fokker et al. (2019). In their study this model was also used as a first estimate or approximation, and it is therefore not certain if this model is representative for a prediction of subsidence caused by this mechanism in other areas.

- Settlement models:
  - In this study no strain dependent permeability was used. When there is a shift from grass and agricultural lands to dikes or residential areas and infrastructure, the use of a strain dependent permeability can be beneficial to optimize subsidence predictions. Hoefsloot (2015) compared the use of different settlement models and consolidation models for settlement prediction of two embankments constructed on soft soils and reported a best fit with the numerical consolidation approach, using strain dependent permeability.
  - The fit for settlement module in D-Settlement works with equal fit factors for all soil layers. Because Hoefsloot (2015) indicated gas development as a possible source for a higher correction in creep parameter needed, it would be beneficial to see if a good fit with the measurements at the N3 Dordrecht can be obtained by correcting the creep parameters for only the peat soil layer(s). This could provide clarity on the source of possible additional subsidence measured.

- Terminology:
  - Due to the interdisciplinary aspect of land subsidence, definitions of terms used in studies should be given. This limits misinterpretation and makes it easier to identify what can actually be concluded from these researches.
  - Oxidation components in subsidence studies should be clearly defined. Often it is not clarified in that shrinkage and oxidation for organic soil following drainage are interconnected. It is assumed that when the term oxidation is used in subsidence studies, the term often represents the full response of organic soil to drainage, which includes the loss of water and degradation of organic matter.

Bibliography

Acacia Water. 2019. Bodemdaling krimpenerwaard. *Eindrapport*, AW256AR190951.

Addiscott, T. 1983. Kinetics and temperature relationships of mineralization and nitrification in rothamsted soils with differing histories. *Journal of Soil Science*, 34(2):343–353.

Alexander, M. et al. 1961. Introduction to soil microbiology. *Introduction to soil microbiology.*

Alliantie Markermeerdijken. 2018. Ontwerpbasis zetting do. *AMMD-003443*.

Alonso, E., Vaunat, J., and Gens, A. 1999. Modelling the mechanical behaviour of expansive clays. *Engineering geology*, 54(1-2):173–183.

Arrhenius, S. 1889. Über die dissociationswärme und den einfluss der temperatur auf den dissociationsgrad der elektrolyte. *Zeitschrift für physikalische Chemie*, 4(1):96–116.

Bailey, V. L., Pries, C. H., and Lajtha, K. 2019. What do we know about soil carbon destabilization? *Environmental Research Letters*, 14(8):083004.

Beckwith, C. W., Baird, A. J., and Heathwaite, A. L. 2003a. Anisotropy and depth-related heterogeneity of hydraulic conductivity in a bog peat. i: laboratory measurements. *Hydrological processes*, 17(1): 89–101.

Beckwith, C. W., Baird, A. J., and Heathwaite, A. L. 2003b. Anisotropy and depth-related heterogeneity of hydraulic conductivity in a bog peat. ii: modelling the effects on groundwater flow. *Hydrological processes*, 17(1):103–113.

Beuving, J. and van den Akker, J. 1996. Maaiveldsdaling van veengrasland bij twee slootpeilen in de polder zegvelderbroek; vijfentwintig jaar zakkingsmetingen op het roc zegveld. Technical report, SC-DLO.

Bishop, A. and Lovenbury, H. 1969. Creep characteristics of two undisturbed clays. *Proc. 7th ICSMFE Mexico*, 1:29–37.

Bisschop, F. 2003. Proefophoging a5 te badhoevedorp met klei uit baggerspecie. *in opdracht van Dienst Weg- en Waterbouwkunde (DWW) - Ballast-Ham Nederland - Rijkswaterstaat (RWS) – Ministerie van Verkeer en Waterstaat*, DWW-2003-091.

Bjerrum, L. 1967. Engineering geology of norwegian normally-consolidated marine clays as related to settlements of buildings. *Geotechnique*, 17(2):83–118.

Blume, H.-P., Brümmer, G. W., Horn, R., Kandeler, E., Kögel-Knabner, I., Kretzschmar, R., Stahr, K., and Wilke, B.-M. 2016. *Scheffer/schachtschabel: Soil Science*. Springer-Verlag.

Boelter, D. 1968. Important physical properties of peat materials. In *In: Proceedings, third international peat congress; 1968 August 18-23; Quebec, Canada.[Place of publication unknown]: Department of Engery, Minds and Resources and National Research Council of Canada: 150-154*.

Boersma, C. 2015. Dossier land subsidence in peat areas. *Delta Life*, pages 9–17.

Bootsma, H., Kooi, H., and Erkens, G. 2020. Atlantis, a tool for producing national predictive land subsidence maps of the netherlands. *Proceedings of the International Association of Hydrological Sciences*, 382:415–415.

Bronswijk, J. 1990. Shrinkage geometry of a heavy clay soil at various stresses. *Soil Science Society of America Journal*, 54(5):1500–1502.

Bronswijk, J. and Evers-Vermeer, J. 1990. Shrinkage of dutch clay soil aggregates. *NJAS wageningen journal of life sciences*, 38(2):175–194.

Brouns, K., Verhoeven, J. T., and Hefting, M. M. 2014. The effects of salinization on aerobic and anaerobic decomposition and mineralization in peat meadows: the roles of peat type and land use. *Journal of environmental management*, 143:44–53.

Brouns, K., Keuskamp, J. A., Potkamp, G., Verhoeven, J. T., and Hefting, M. M. 2016. Peat origin and land use effects on microbial activity, respiration dynamics and exo-enzyme activities in drained peat soils in the netherlands. *Soil Biology and Biochemistry*, 95:144–155.

Bunnell, F., Tait, D., Flanagan, P., and Van Clever, K. 1977. Microbial respiration and substrate weight loss—i: A general model of the influences of abiotic variables. *Soil Biology and Biochemistry*, 9(1): 33–40.

Bürgmann, R., Rosen, P. A., and Fielding, E. J. 2000. Synthetic aperture radar interferometry to measure earth's surface topography and its deformation. *Annual review of earth and planetary sciences*, 28(1): 169–209.

Campbell, C., Myers, R., and Weier, K. 1981. Potentially mineralizable nitrogen, decomposition rates and their relationship to temperature for five queensland soils. *Soil Research*, 19(3):323–332.

Conijn, J. and Lesschen, J. 2015. Soil organic matter in the netherlands: Quantification of stocks and flows in the top soil. Technical report, Plant Research International, Business Unit Agrosystems Research.

Cornelis, W., Corluy, J., Medina, H., Diaz, J., Hartmann, R., Van Meirvenne, M., and Ruiz, M. 2006. Measuring and modelling the soil shrinkage characteristic curve. *Geoderma*, 137(1-2):179–191.

Crombaghs, M., Brügelmann, R., and de Min, E. J. 2000. On the adjustment of overlapping strips of laser altimeter height data. *International Archives of Photogrammetry and Remote Sensing*, 33(B3/1): 230–237.

Crooks, J., Becker, D., Jefferies, M., and McKenzie, K. 1984. Yield behaviour and consolidation. i: Pore pressure response. In *Sedimentation Consolidation Models—Predictions and Validation*, pages 356–381. ASCE.

CROW. 2004. Betrouwbaarheid van zettingsprognoses. *Report No.204*.

De Glopper, R. 1969. Shrinkage of subaqueous sediments of lake ijssel (the netherlands) after reclamation. In *Proc. First Int. Symp. On Land Subsidence*, pages 192–201.

De Glopper, R. 1987. *Subsidence in the Recently Reclaimed IJsselmeerpolder" Flevoland"*. Rijksdienst voor de IJsselmeerpolders.

De Jong, G. d. J. 1968. Consolidation models consisting of an assembly of viscous elements or a cavity channel network. *Geotechnique*, 18(2):195–228.

De Rijk, L. 1978. The calculation of secondary settlement in one-dimensional compression. *Delft Progress Report*, 3:237–255.

Degago, S., Grimstad, G., Jostad, H., Nordal, S., and Olsson, M. 2011. Use and misuse of the isotache concept with respect to creep hypotheses a and b. *Géotechnique*, 61(10):897–908.

Deltares. 2016. D-settlement embankment design and soil settlement prediction: User manual. *Version 16.1*.

Den Haan, E. 2003. Het a, b, c–isotachenmodel: hoeksteen van een nieuwe aanpak van zettingsberekeningen. *Geotechniek, oktober*, pages 28–35.

Den Haan, E. and Edil, T. 1994. Secondary and tertiary compression of peat. In *International Workshop on Advances in Understanding and Modelling the mechanical behaviour of Peat*, pages 49–60.

Den Haan, E., van Essen, H., Visschedijk, M., and Maccabiani, J. 2004. Isotachenmodellen: Help, hoe kom ik aan de parameters? *Geotechniek*, januari:62–69. URL `https://www.kivi.nl/uploads/media/5852e278ed184/2004,%20nr1%20-%20GT200401_D-Settlement_isotachenmodellen.pdf`.

Den Haan, E. J. 1994. Vertical compression of soils.

Denef, K., Six, J., Bossuyt, H., Frey, S. D., Elliott, E. T., Merckx, R., and Paustian, K. 2001. Influence of dry–wet cycles on the interrelationship between aggregate, particulate organic matter, and microbial community dynamics. *Soil Biology and Biochemistry*, 33(12-13):1599–1611.

Deppe, M., Knorr, K.-H., McKnight, D. M., and Blodau, C. 2010. Effects of short-term drying and irrigation on co 2 and ch 4 production and emission from mesocosms of a northern bog and an alpine fen. *Biogeochemistry*, 100(1-3):89–103.

Dettmann, U., Bechtold, M., Frahm, E., and Tiemeyer, B. 2014. On the applicability of unimodal and bimodal van genuchten–mualem based models to peat and other organic soils under evaporation conditions. *Journal of Hydrology*, 515:103–115.

Dijk, H. v. 1980. Survey of dutch soil organic matter research with regard to humification and degradation rates in arable land. *Rapport-Instituut voor Bodemvruchtbaarheid*.

Duffy, K., Siderius, K., and Long, M. 2020. Parameterisation of the koppejan settlement prediction model using cone penetration testing and gradient boosting. *Proceedings of the International Association of Hydrological Sciences*, 382:443–443.

Duraisamy, Y., Huat, B. B., and Aziz, A. 2007. Engineering properties and compressibility behavior of tropical peat soil. *American Journal of Applied Sciences*, 4(10):768–773.

DWW. 1991. Handleiding wegenbouw ontwerp onderbouw deel 2 techniek. *Ministerie van Verkeer en Waterstaat*.

Edil, T. B. and Dhowian, A. W. 1979. Analysis of long-term compression of peats. *Geotechnical engineering*, 10:159–178.

Erkens, G., Cohen, K. M., Gouw, M. J., Middelkoop, H., and Hoek, W. Z. 2006. Holocene sediment budgets of the rhine delta (the netherlands): a record of changing sediment delivery.

Erkens, G., van der Meulen, M. J., and Middelkoop, H. 2016. Double trouble: subsidence and co2 respiration due to 1,000 years of dutch coastal peatlands cultivation. *Hydrogeology Journal*, 24(3): 551–568.

Estop-Aragonés, C., Knorr, K.-H., and Blodau, C. 2012. Controls on in situ oxygen and dissolved inorganic carbon dynamics in peats of a temperate fen. *Journal of Geophysical Research: Biogeosciences*, 117(G2).

Fenner, N. and Freeman, C. 2011. Drought-induced carbon loss in peatlands. *Nature geoscience*, 4(12): 895–900.

Fokker, P., Gunnink, J., Koster, K., and de Lange, G. 2019. Disentangling and parameterizing shallow sources of subsidence: Application to a reclaimed coastal area, flevoland, the netherlands. *Journal of Geophysical Research: Earth Surface*, 124(5):1099–1117.

Fokker, P. A., Gunnink, J. L., De Lange, G., Leeuwenburgh, O., and Van der Veer, E. 2015. Compaction parameter estimation using surface movement data in southern flevoland. *Proceedings of the International Association of Hydrological Sciences*, 372:183–187.

Freeman, C., Ostle, N., and Kang, H. 2001. An enzymic 'latch' on a global carbon store: A shortage of oxygen locks up carbon in peatlands by restraining a single enzymes. *Nature*, 409(6817):149–149.

Gebert, J. 2018/2019. Soil properties and processes i: Water retention. *powerpoint, TU Delft*.

Gebert, J. and Groengroeft, A. 2019. Long-term hydraulic behaviour and soil ripening processes in a dike constructed from dredged material. *Journal of Soils and Sediments*, 20(3):1793–1805.

Gebert, J., Knoblauch, C., and Gröngröft, A. 2019. Gas production from dredged sediment. *Waste Management*, 85:82–89.

Gebhardt, S., Fleige, H., and Horn, R. 2010. Shrinkage processes of a drained riparian peatland with subsidence morphology. *Journal of soils and sediments*, 10(3):484–493.

Gens, A. and Alonso, E. 1992. A framework for the behaviour of unsaturated expansive clays. *Canadian Geotechnical Journal*, 29(6):1013–1032.

Gray, C. W. and Allbrook, R. 2002. Relationships between shrinkage indices and soil properties in some new zealand soils. *Geoderma*, 108(3-4):287–299.

Groenendijk, P., Renaud, L., and Roelsma, J. 2005. Prediction of nitrogen and phosphorus leaching to groundwater and surface waters; process descriptions of the animo4. 0 model. Technical report, Alterra.

Grossman, R., Brasher, B., Franzmeier, D., and Walker, J. 1968. Linear extensibility as calculated from natural-clod bulk density measurements. *Soil Science Society of America Journal*, 32(4):570–573.

Hämäläinen, M. 1991. *Principal variations in the chemical composition of peat*. Sveriges Lantbruksuniv.

Harlaar, P. and Lange, K. 2018. Onderzoeksrapport geotechnisch onderzoek t.b.v reconstructie n3. *opdrachtgevers Ministerie van Infrastructuur en Milieu, Rijkswaterstaat, Cluster Aansluitingen*, GA170010.002.R01.v1.0.

Hasan, S. 2014. Mapping remote plants through remote sensing technology and gis. *International Journal of Technical Research and Applications*, 2(2):77–80.

Hassink, J. 1995. *Organic matter dynamics and N mineralization in grassland soils*. PhD thesis, Hassink.

Hendriks, R. 1991. Afbraak en mineralisatie van veen: literatuuronderzoek. Technical report, DLO-Staring Centrum.

Hendriks, R. 2004. An analytical equation for describing the shrinkage characteristics of peat soils. *Proceedings of the 13th International Peat Congress, Tampere, Finland*, In J.Päivänen (Ed.) Wise use of Peatlands.

Hendriks, R. and van den Akker, J. 2012. Effecten van onderwaterdrains op de waterkwaliteit in veenweiden: modelberekeningen met swap-animo voor veenweide-eenheden naar veranderingen van de fosfor-, stikstof-en sulfaatbelasting van het oppervlaktewater bij toepassing van onderwaterdrains in het westelijke veenweidegebied. Technical report, Alterra, Wageningen-UR.

Hijma, M. P., Cohen, K., Hoffmann, G., Van der Spek, A. J., and Stouthamer, E. 2009. From river valley to estuary: the evolution of the rhine mouth in the early to middle holocene (western netherlands, rhine-meuse delta). *Netherlands Journal of Geosciences*, 88(1):13–53.

Hobbs, N. 1987. A note on the classification of peat. *Géotechnique*, 37(3):405–407.

Hoefsloot, F. 2015. Evaluation settlement models test embankments bloemendalerpolder–geoimpuls program.

Hoogland, T., Van den Akker, J., and Brus, D. 2012. Modeling the subsidence of peat soils in the dutch coastal area. *Geoderma*, 171:92–97.

Houkes, C. B. 2016. Review and validation of settlement prediction methods for organic soft soils, on the basis of three case studies from the netherlands. *MSc thesis TU Delft*.

Hsi, J., Gunasekara, C., and Nguyen, V. 2005. Characteristics of soft peats, organic soils and clays, colombo-katunayake expressway, sri lanka. In *Elsevier Geo-Engineering Book Series*, volume 3, pages 681–722. Elsevier.

Huat, B. B., Prasad, A., Asadi, A., and Kazemian, S. 2014. *Geotechnics of organic soils and peat*. CRC press.

Johari, N., Bakar, I., Razali, S., and Wahab, N. 2016. Fiber effects on compressibility of peat. In *IOP Conference Series: Materials Science and Engineering*, volume 136-1, page 012036. IOP Publishing.

Kaczmarek, Ł. and Dobak, P. 2017. Contemporary overview of soil creep phenomenon. *Contemporary Trends in Geoscience*, 6.

Kechavarzi, C., Dawson, Q., and Leeds-Harrison, P. 2010. Physical properties of low-lying agricultural peat soils in england. *Geoderma*, 154(3-4):196–202.

Kemmers, R. and Koopmans, G. F. 2010. Interne eutrofiering en veenafbraak; literatuuronderzoek: effect van toepassing van onderwaterdrains: literatuuronderzoek. Technical report, Alterra.

Kleber, M., Nico, P. S., Plante, A., Filley, T., Kramer, M., Swanston, C., and Sollins, P. 2011. Old and stable soil organic matter is not necessarily chemically recalcitrant: implications for modeling concepts and temperature sensitivity. *Global Change Biology*, 17(2):1097–1107.

Kooi, H. and Erkens, G. 2020. Modelling subsidence due to holocene soft-sediment deformation in the netherlands under dynamic water table conditions. *Proceedings of the International Association of Hydrological Sciences*, 382:493–498.

Koppejan, A. 1948. A formula combining the terzaghi load compression relationship and the buisman secular time effect. *Proc. 2nd ICSMFE, Rotterdam, 1948*, 3:32–37.

Kortleven, J. 1963. *Kwantitatieve aspecten van humusopbouw en humusafbraak*. Pudoc.

Koster, K., Stafleu, J., Cohen, K., Stouthamer, E., Busschers, F. S., and Middelkoop, H. 2018a. Three-dimensional distribution of organic matter in coastal-deltaic peat: Implications for subsidence and carbon dioxide emissions by human-induced peat oxidation. *Anthropocene*, 22:1–9.

Koster, K., Stafleu, J., and Stouthamer, E. 2018b. Differential subsidence in the urbanised coastal-deltaic plain of the netherlands. *Netherlands Journal of Geosciences*, 97(4):215–227.

Kruse, J., Lennartz, B., and Leinweber, P. 2008. A modified method for measuring saturated hydraulic conductivity and anisotropy of fen peat samples. *Wetlands*, 28(2):527–531.

Le, T. M., Fatahi, B., and Khabbaz, H. 2012. Viscous behaviour of soft clay and inducing factors. *Geotechnical and Geological Engineering*, 30(5):1069–1083.

Lesschen, J. P., Heesmans, H., Mol-Dijkstra, J., van Doorn, A., Verkaik, E., van den Wyngaert, I., and Kuikman, P. 2012. Mogelijkheden voor koolstofvastlegging in de nederlandse landbouw en natuur. Technical report, Alterra.

Liingaard, M., Augustesen, A., and Lade, P. 01 2002. observed time dependent behavior of soils.

Liu, M., Zhang, L., Yu, W., and Shen, S. 2007. Decomposition process and residual rate of organic materials c and n in soils. *Ying yong sheng tai xue bao= The journal of applied ecology*, 18(11):2503–2506.

Malinowska, E. E. 2016. Tertiary compression of polish peat. *Scientific Review Engineering and Environmental Sciences*, 2016(4)):507–517.

McCauley, A., Jones, C., and Jacobsen, J. 2009. Soil ph and organic matter. *Nutrient management module*, 8(2):1–12.

Meimaroglou, N. and Mouzakis, C. 2019. Cation exchange capacity (cec), texture, consistency and organic matter in soil assessment for earth construction: The case of earth mortars. *Construction and Building Materials*, 221:27–39.

Mesri, G. 1973. Coefficient of secondary compression. *ASCE J Soil Mech Found Div-v 99*, (SM1):123–137.

Mesri, G. 2003. Primary compression and secondary compression. In *Soil behavior and soft ground construction*, pages 122–166.

Mesri, G. and Godlewski, P. M. 1977. Time and stress-compressibility interrelationship. *ASCE J Geotech Eng Div*, 103(5):417–430.

Mishra, P. N., Scheuermann, A., Bore, T., and Li, L. 2019. Salinity effects on soil shrinkage characteristic curves of fine-grained geomaterials. *Journal of Rock Mechanics and Geotechnical Engineering*, 11(1): 181–191.

Mitchell, A. R. and Van Genuchten, M. T. 1992. Shrinkage of bare and cultivated soil. *Soil Science Society of America Journal*, 56(4):1036–1042.

Mitchell, J. K., Campanella, R. G., and Singh, A. 1968. Soil creep as a rate process. *Journal of Soil Mechanics & Foundations Div*.

Moldrup, P., Olesen, T., Komatsu, T., Schjønning, P., and Rolston, D. 2001. Tortuosity, diffusivity, and permeability in the soil liquid and gaseous phases. *Soil Science Society of America Journal*, 65(3): 613–623.

Muntendam-Bos, A., Kleuskens, M., Bakr, M., De Lange, G., and Fokker, P. 2009. Unraveling shallow causes of subsidence. *Geophysical research letters*, 36(10).

Murayama, S. and Zahari, A. 1991. Biochemical decomposition of tropical peats, paper presented at international symposium on tropical peatland, malaysian agric. *Res. and Dev. Inst., Kuching, Malaysia*, pages 124–133.

Mutalib, A. A. 1992. Characterization, distribution and utilization of peat in malaysia. In *Proceedings of the International Symposium on Tropical Peatland. Kuching, Sarawak, Malaysia, 6-10 May 1991*.

Myhre, G., Shindell, D., Bréon, F., Collins, W., Fuglestvedt, J., Huang, J., Koch, D., Lamarque, J., Lee, D., Mendoza, B., et al. 2013. Climate change 2013: the physical science basis. *Contribution of working group I to the fifth assessment report of the intergovernmental panel on climate change*, pages 659–740.

NEN-EN1997-1. 2019. National annex to nen-en 1997-1 eurocode 7; geotechnical design - part 1: General rules. *Definitieve norm*.

Neumann, B., Vafeidis, A. T., Zimmermann, J., and Nicholls, R. J. 2015. Future coastal population growth and exposure to sea-level rise and coastal flooding-a global assessment. *PloS one*, 10(3):e0118571.

Nowamooz, H., Mrad, M., Abdallah, A., and Masrouri, F. 2009. Experimental and numerical studies of the hydromechanical behaviour of a natural unsaturated swelling soil. *Canadian Geotechnical Journal*, 46(4):393–410.

Parish, F., Sirin, A., Charman, D., Joosten, H., Minaeva, T. Y., and Silvius, M. 2008. Assessment on peatlands, biodiversity and climate change. *Global Environment Center & Wetlands International, with support of UNEP-GEF*.

Peng, X., Zhang, Z., Wang, L., and Gan, L. 2012. Does soil compaction change soil shrinkage behaviour? *Soil and Tillage Research*, 125:89–95.

Peng, X. and Horn, R. 2013. Identifying six types of soil shrinkage curves from a large set of experimental data. *Soil Science Society of America Journal*, 77(2):372–381.

Qualls, R. G. 2004. Biodegradability of humic substances and other fractions of decomposing leaf litter. *Soil Science Society of America Journal*, 68(5):1705–1712.

Querner, E., Jansen, P., and Kwakernaak, C. 2008. Effects of water level strategies in dutch peatlands: a scenario study for the polder zegveld. In *Proceedings of the 13th International Peat Congress: After Wise Use-The future of Peatlands, Tullamore, Ireland, 8-13 June, 2008*, pages 620–623.

Querner, E., Jansen, P., Van Den Akker, J., and Kwakernaak, C. 2012. Analysing water level strategies to reduce soil subsidence in dutch peat meadows. *Journal of hydrology*, 446:59–69.

Rackwitz, U. 2019. Toelichting bodemdalingskaart krimpenerwaard. *Hoogheemraadschap van Schieland en de Krimpenerwaard*.

Reeve, M. and Hall, D. 1978. Shrinkage in clayey subsoils of contrasting structure. *Journal of Soil Science*, 29(3):315–323.

Rezanezhad, F., Price, J. S., Quinton, W. L., Lennartz, B., Milojevic, T., and Van Cappellen, P. 2016. Structure of peat soils and implications for water storage, flow and solute transport: A review update for geochemists. *Chemical Geology*, 429:75–84.

Rijniersce, K. 1983. Een model voor de simulatie van het fysische rijpingsproces van gronden in de ijsselmeerpolders.

Robinson, R. 2003. A study on the beginning of secondary compression of soils. *Journal of testing and evaluation*, 31(5):388–397.

Roolvink, H. 2015. In alle zandlichamen zijn zakbakens geplaatst id479893. *RWS*. URL `https://beeldbank.rws.nl/MediaObject/Details/479893`.

Ros, G., van Schöll, L., and Bussink, D. 2012. Soil for life. *Nutrient Management Institure (NMI) Report*, 1248.N.07.

Sande, C. V. D., Soudarissanane, S., and Khoshelham, K. 2010. Assessment of relative accuracy of ahn-2 laser scanning data using planar features. *Sensors*, 10(9):8198–8214.

Schothorst, C. 1977. Subsidence of low moor peat soils in the western netherlands. *Geoderma*, 17(4): 265–291.

Schothorst, C. 1982. Drainage and behaviour of peat soils. Technical report, ICW Wageningen, The Netherlands.

Schwärzel, K., Renger, M., Sauerbrey, R., and Wessolek, G. 2002. Soil physical characteristics of peat soils. *Journal of plant nutrition and soil science*, 165(4):479–486.

SkyGeo. 2020. Insar technical background. *visited on 04-07-2020*. URL `https://skygeo.com/insar-technical-background/`.

Smernik, R. and Skjemstad, J., 2009. Mechanisms of organic matter stabilization and destabilization in soils and sediments: conference introduction.

Smolders, A., Van Diggelen, J., Geurts, J., Moni, P., Lucasse, E., Roelofd, J., and Lamers, L. 2013. Waterkwaliteit in het veenweidegebied, de complexe interacties tussen oever, waterbodem en oppervlaktewater. *Landschap*, 3:144 – 153.

Stephens, J. C., Allen Jr, L., and Chen, E. 1984. Organic soil subsidence. *Reviews in Engineering Geology*, 6:107–122.

Steur, G., Heijink, W., de Bakker, H., Boersma, O., and Hamming, C. 1991. *Bodemkaart van Nederland, schaal 1: 50000: algemene begrippen en indelingen*. Staring Centrum.

Stouthamer, E., Berendsen, H., Peeters, J., and Bouman, M. 2008. Toelichting bodemkaart veengebieden provincie utrecht, schaal 1: 25.000. *Utrecht, Provincie Utrecht*.

STOWA. 2019. Deltafact bodemdaling. pages visited on 10–02–2020. URL `https://www.stowa.nl/deltafacts/ruimtelijke-adaptatie/adaptief-deltamanagement/bodemdaling`.

Tate, R. L. et al. 1987. *Soil organic matter. Biological and ecological effects*.

TAW. 1996a. Technisch rapport klei voor dijken.[in dutch] delft. *The Netherlands: Technical Advisory Committee for Flood Defence in The Netherlands*.

TAW. 1996b. Technisch rapport: geotechnische classificatie van veen - tr16. Technical report.

Terzaghi, K. 1941. Undisturbed clay samples and undisturbed clays. *Journal of the Boston Society of Civil Engineers*, 28(3):45–65.

Thomas, P., Baker, J., and Zelazny, L. 2000. An expansive soil index for predicting shrink–swell potential. *Soil Science Society of America Journal*, 64(1):268–274.

TNO-GSN. 2016. Online portal for digital geo-information. *Geological survey of the Netherlands*. URL `www.dinoloket.nl/en`.

van Asselen, S., Cohen, K. M., and Stouthamer, E. 2017. The impact of avulsion on groundwater level and peat formation in delta floodbasins during the middle-holocene transgression in the rhine-meuse delta, the netherlands. *The Holocene*, 27(11):1694–1706.

Van Asselen, S., Erkens, G., Stouthamer, E., Woolderink, H. A., Geeraert, R. E., and Hefting, M. M. 2018. The relative contribution of peat compaction and oxidation to subsidence in built-up areas in the rhine-meuse delta, the netherlands. *Science of the Total Environment*, 636:177–191.

Van Baars, S. 2003. Soft soil creep modelling of large settlements. In *2nd International Conference on Advances in Soft Soil Engineering and Technology, Kuala Lumpur, Malaysia*, pages 361–371.

Van de Plassche, O. 1982. Sea-level change and water-level movements in the netherlands during the holocene. *PhD. Thesis, Vrije Universiteit (VU) Amsterdam. Mededeling Rijks Geologische Dienst*, 36: 1–93.

Van den Akker, J., Beuving, J., Hendriks, R., and Wolleswinkel, R. 2007. Maaivelddaling, afbraak en co2 emissie van nederlandse veenweidegebieden. *Leidraad Bodembescherming, afl*, 83:83.

Van den Akker, J., Hendriks, R., and Pleijter, M. 2012. Co2 emissions of peat soils in agricultural use: calculation and prevention. *Agrociencia-Sitio en Reparación*, 16(3):43–50.

Van den Akker, J., Hendriks, R., Frissel, J., Oostindie, K., and Wesseling, J. 2013. Gedrag van verdroogde kades: Fase b,c,d, ontstaan en gevaar van krimpscheuren in klei- en veenkades. *Alterra Wageningen UR*. URL `edepot.wur.nl/297906`.

Van den Born, G., Kragt, F., Henkens, D., Rijken, B., Van Bemmel, B., Van der Sluis, S., Polman, N., Bos, E. J., Kuhlman, T., Kwakernaak, C., et al. 2016. Dalende bodems, stijgende kosten: mogelijke maatregelen tegen veenbodemdaling in het landelijk en stedelijk gebied: beleidsstudie. Technical report, Planbureau voor de Leefomgeving.

Van der Meulen, M. J., van der Spek, A. J., de Lange, G., Gruijters, S. H., van Gessel, S. F., Nguyen, B.-L., Maljers, D., Schokker, J., Mulder, J. P., and van der Krogt, R. A. 2007. Regional sediment deficits in the dutch lowlands: Implications for long-term land-use options (8 pp). *Journal of Soils and Sediments*, 7(1):9–16.

Van Hardeveld, H., Driessen, P., Schot, P., and Wassen, M. 2017. An integrated modelling framework to assess long-term impacts of water management strategies steering soil subsidence in peatlands. *Environmental Impact Assessment Review*, 66:66–77.

Van Laarhoven, S. 2017. Influence of loading history on subsurface architecture and subsidence potential for the historical city of gouda, the netherlands. *MSc Thesis, Universiteit Utrecht (UU)*.

van Meijeren, H. 2017. *Assessing the differences between Dutch elevation datasets AHN2 and AHN3*. PhD thesis, MSc thesis.

Van Paassen, L. A., Oliveira, B. R., Zain, N. H., and Jommi, C. 2020. Subsidence of dredged organic sediments in cultivated peatlands. In *E3S Web of Conferences*, volume 195, page 01020. EDP Sciences.

Van Vemden-Versprille, T. 2013. Watergebiedsplan regio greenport boskoop, inventarisatie en knelpunten. *Hoogheemraadschap van Rijnland*, vs. 2.

Vermeulen, J. and Hendriks, R. 1996. Bepaling van afbraaksnelheden van organische stof in laagveen; ademhalingsmetingen aan ongestoorde veenmonsters in het laboratorium. Technical report, DLO-Staring Centrum.

Vermilion Energy. 2020. Bodemdaling statusrapport 2020 - drenthe overijssel friesland. *Versie 1.1*.

von Lützow, M. and Kögel-Knabner, I. 2009. Temperature sensitivity of soil organic matter decomposition—what do we know? *Biology and Fertility of soils*, 46(1):1–15.

Vos, P. 2015. *Origin of the Dutch coastal landscape: long-term landscape evolution of the Netherlands during the Holocene, described and visualized in national, regional and local palaeogeographical map series*. Barkhuis.

Vos, P. and de Vries, S. 2016. Geologisch onderzoek naar de heterogeniteit van de ondergrond onder de markermeerdijk tussen hoorn en amsterdam. *AMMD-002213*.

Wang, G. and Wei, X. 2015. Modeling swelling–shrinkage behavior of compacted expansive soils during wetting–drying cycles. *Canadian Geotechnical Journal*, 52(6):783–794.

Yang, M. and Liu, K. 2016. Deformation behaviors of peat with influence of organic matter. *SpringerPlus*, 5(1):573.

Zain, N. 2019. Effect of oxidation on the compression behaviour of organic soils. *PhD Thesis, Delft University of Technology*. doi: 10.4233/uuid:aa7fe90a-7bf5-4c91-aa3e-c6a594a7d59d.

Zak, D., Roth, C., Unger, V., Goldhammer, T., Fenner, N., Freeman, C., and Jurasinski, G. 2019. Unravelling the importance of polyphenols for microbial carbon mineralization in rewetted riparian peatlands. *Frontiers in Environmental Science*, 7:147.

Zander, F., Heimovaara, T., and Gebert, J. 2020. Spatial variability of organic matter degradability in tidal elbe sediments. *Journal of Soils and Sediments*, pages 1–15.

Zanello, F., Teatini, P., Putti, M., and Gambolati, G. 2011. Long term peatland subsidence: Experimental study and modeling scenarios in the venice coastland. *Journal of Geophysical Research: Earth Surface*, 116(F4).

Zhang, L. and O'kelly, B. 2013. Constitutive models for peat–a review. In *Proceedings of the 12th International Conference on Computational Plasticity–Fundamentals and Applications (COMPLAS XII), Barcelona, Spain, 3rd–5th September 2013*, pages 1294–1304.

Zuur, A. 1958. Bodemkunde der nederlandse bedijkingen en droogmakerijen, deel c: Het watergehalte, de indroging en enkele daarmee samenhangende processen. *Directie Wieringermeer/Landbouwhogeschool, Wageningen, Ned.*

A

Background information

A.1. Classification of organic soils

Organic soils are commonly described by their organic matter content, but there are also other factors that can be used to classify organic soils or peat. Examples are the state of decomposition, the vegetation type of the origin material and the appearance of the soil. Two systems are commonly used to do this for peat soils, the Radforth classification system and the Von Post system (Hobbs, 1987).

The main difference between the two systems is that the Radforth system is developed for engineers with limited knowledge of the botanical component and the Von Post classification system is more detailed. The Von Post system has ten classes, where H1 refers to undecomposed peat and H10 refers to completely decomposed peat.

The fibre content of soils can indicate the degree of humification, where a low fibre content is related to a high degree of humification. Fibres are defined as fragments of plant tissue that are large enough to be retained on a sieve with openings of 0.15 mm in diameter. These fragments should have retained recognisable cellular structure of the original plant material. A classification on the basis of fibre content can be applied for peat soils. This is different from a classification based on organic matter content, as it is possible for soils to have the same organic content but a different fibre content. Three different peat classes are shown in table A.1. Figure A.1 shows a general indication of the three classes in a drained peat soil.

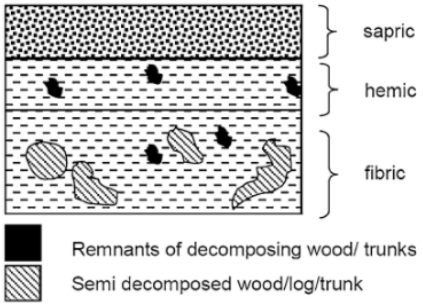

Figure A.1: General morphology of a drained peat soil (Mutalib, 1992)

Another classification of peat that is commonly used in the Netherlands, related to subsidence studies, is the classification based on its origin. This divides peat in three classes: eutrophic, mesotrophic and oligotrophic. Eutrophic peat soils are nutrient rich, mesothrophic peat is lower in nutrient content and oligotrophic peat is the poorest in nutrients. The type of peat is determined by the vegetation of the origin material, which depends on the nutrient richness of the water that is supplied. Oligotrophic conditions occur in an environment where only nutrient poor rainwater enters the system, in contrast, eutrophic conditions are common where nutrient rich water from the river and sea enters.

Designation	Group (Von Post)	Description
Fibrous peat (Fibric)	H1 - H4	Low degree of decomposition, Fibrous structure, >67% fibres, Easily recognised plant structure
Pseudo-fibrous peat (Hemic)	H5 - H7	Intermediate degree of decomposition, Recognisable plant structure 33- 67% fibres
Amorphous peat (Sapric)	H8 - H10	High degree of decomposition, No visible plant structure, Mushy consistency, <33% fibres

Table A.1: Peat classification on the basis of fibre content Von Post (Huat et al., 2014)

A.2. Consolidation models

Approximation formulas degree of consolidation

The degree of consolidation used in the analytical consolidation approach can be calculated with

$$U(t) = 1 - \frac{8}{\pi^2} \sum_{i=1}^{\infty} \frac{1}{(2i-1)^2} \exp\left[-(2i-1)^2 \frac{\pi^2}{4} \frac{c_v t}{h^2}\right]. \tag{A.1}$$

Some approximation formulas for this complicated equation have been developed, three examples are

$$U(t) \approx \frac{2}{\sqrt{\pi}} \sqrt{\frac{c_v \cdot t}{h^2}} \quad \text{for } U < 0.7 \text{ (70\%)}, \tag{A.2}$$

$$U(t) \approx 1 - \frac{8}{\pi^2} \exp\left(-\frac{\pi^2}{4} \frac{c_v \cdot t}{h^2}\right) \quad \text{for } U > 0.5 \text{ (50\%)}, \tag{A.3}$$

$$U(t) \approx \sqrt[6]{\frac{T_v^3}{\left(T_v^3 + 0.5\right)}} \quad \text{with} \quad T_v = \frac{c_v \cdot t}{h^2}. \tag{A.4}$$

A comparison of the three approximation formulas and the full description of degree of consolidation is shown in figure A.2. It can be seen that all formulas approximate the solution very well.

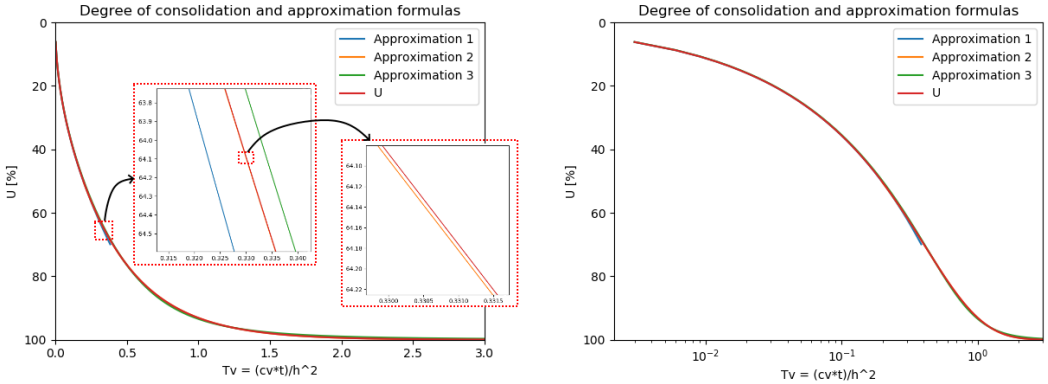

(a) Linear scale x-axis (T_v)

(b) Logarithmic scale x-axis (T_v)

Figure A.2: Comparison full description U(t) (3.6), with approximation formula 1 (A.2), approximation formula 2 (A.3) and approximation formula 3 (A.4)

Comparison consolidation models

Differences between the consolidation models are shown in table A.2, which is based on table 15.1 from Deltares (2016).

Table A.2: Comparison of the two consolidation models, (Deltares, 2016)

	Analytical (Terzaghi)	**Numerical (Darcy)**
Solution method	Analytical	Combination of analytical and numerical
Computation speed	Very fast	Fast
Stability	Unconditional	Unconditional
Final settlements	Accurate	Accurate
Time-dependent settlement	Approximate	Accurate
Parameters	Consolidation coefficient	Consolidation coefficient OR permeability (constant OR strain dependent)
Vertical drains	Approximate	Accurate
Different layers	Approximate	Accurate
Combination with un/reloading	Approximate	Accurate
Submerging effect	Approximate	Accurate
Drained layers	Only deformation, no excess pore pressure	Only deformation, no excess pore pressure
Post-processing	Plots for: - settlements (over time) - stress profiles (initial and final stage)	Plots for: - settlements (over time and depth) - pore water pressures (over time and depth) - stress profiles (over time and depth)

A.3. Overview oxidation models

Name	**Input parameters**	**Model parameters**	**Includes**	**Does not include**	**Known parameters**
Stephens et al., 1984	- temperature T - thickness h	- parameters a and b - reaction rate constant k - threshold temperature T_0	- temperature effect - oxygen supply through thickness h	- influence of pH, water content and nature of soil indirectly in reaction rate constant k	- a and b for Everglades peat soil
Van der Meulen et al., 2007	- timestep Δt - thickness h_{dry}	- rate of peat oxidation V_{ox}	- oxygen supply through thickness h_{dry}	- influence of temperature, pH, water content and nature of soil indirectly in rate of peat oxidation V_{ox}	- V_{ox} for dutch peat soils
Van den Akker et al., 2008	- ditch water level (DWL) OR - average deepest groundwater level (GLG)		- effect of thin (<40 cm) clay layer on top of peat - oxygen supply through relation with ditch water level or average deepest groundwater level	- influence of temperature, pH, water content and nature of soil indirectly in empirical values	
Zanello et al., 2011	- temperature T - thickness h	*above gwl*: - density peat soil - organic matter fraction - peat thickness *below gwl* - density peat soil - organic matter fraction	- nature of soil through organic matter fraction and density - oxygen supply through thickness h	- influence of pH, water content and chemical nature of soil indirectly in reaction rate constant k	

Name	**Input parameters**	**Model parameters**	**Includes**	**Does not include**	**Known parameters**
Hoogland et al., 2012	- Initial surface elevation E_0 - Regulated water surface level W(s,t)	- maximum depth where sufficient aeration occurs D - fraction of peat thickness that oxidises K - additional subsidence rate C	- oxygen supply through parameter D	- influence of temperature, pH, water content and nature of soil indirectly in fraction of peat thickness that oxidises K	- C and K for Groot-Mijdrecht - D estimated based on Van den Akker et al., 2007
Fokker et al., 2019	- timestep Δt - thickness h_{dry}	- rate of oxidation V_{ox} - fraction of initial thickness which consists of admixed clastic sediments $\lambda_{r,ox}$ - initial thickness h0	- oxygen supply through thickness h_{dry} - nature of soil through admixed clastic sediments $\lambda_{r,ox}$	- influence of temperature, pH, water content and chemical nature of soil indirectly in rate of oxidation V_{ox}	- V_{ox} and $\lambda_{r,ox}$ for peat soil in Flevoland
Bootsma et al., 2020	- time step Δt - organic mass fraction at time t_0 $Forg_0$ - initial tickness L_0	- empirical constant α_m	- oxygen supply through thickness L - nature of soil through organic mass fraction Forg	- influence of temperature, pH, water content and chemical nature of soil indirectly in empirical constant α_m	

Table A.3: Overview oxidation modelling techniques

B

Krimpenerwaard

In this appendix, the choice for the location areas in the Krimpenerwaard polder and the determination of the point zero data values is explained. Several trade-offs have been made based on data availability, expected soil investigation availability and possible human intervention.

B.1. Location Choice

Two project areas have been selected based on several criteria, which are explained below. The selected project locations are shown in figure 8.1 in chapter 8.

Data availability

For this study two types of data sets have been provided by the waterboard of the region, data on height measurements from 1984 and reports on the water management strategies over time. For the study location the requirements concerning data availability are:

- Sufficient data points from 1984 data set, no area without 1984 measurement points should be chosen.
- Sufficient data on water level regime over time, no area with an exceptional water level regime should be chosen.

Figure B.1 shows the spatial distribution of the data points from the height measurements in 1984. There is a fairly even distribution of data points along the grass and agricultural part of the Krimpenerwaard polder. Urban areas were avoided during the levelling campaign, and therefore these areas show no data points. Also, the Loetbos has little measurement points. It is reported that the average distance between the data points is 50 meters (Rackwitz, 2019).

A first selection of regions within the Krimpenerwaard polder was made based on the water level areas in the polder and the study of Rackwitz (2019), two water level areas are selected where information can be used for the project area. These are 'Stolwijk en Berkenwoude' and 'Den Hoek en Schuwacht'. Other areas have been eliminated based on the presence of mostly urban areas, or areas with special deviations from the water level.

Soil investigation availability

Through DINOloket, public information about the soil profile at the polder was collected. Different types of information were considered: cone penetration tests (CPTs), and drilling researches (geological and archeological oriented). A combination of all three available soil investigation types is optimal. For the whole Krimpenerwaard area in general, CPTs are mostly located in the urban regions and in the grass and agricultural lands the availability of CPTs is low. Therefore the availability of CPT data mostly governed the location choices of the project.

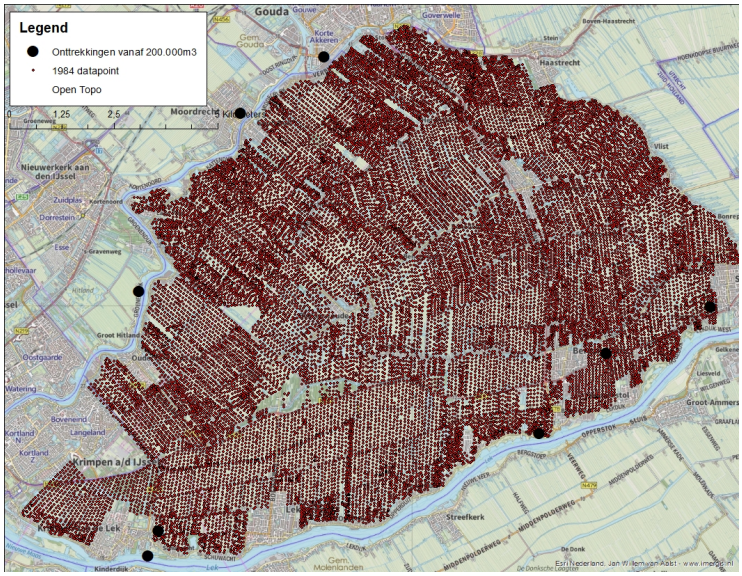

Figure B.1: Distribution of the data points from the measurements in 1984 in the Krimpenerwaard

Figure B.2: Distribution of CPT profiles available in the Krimpenerwaard polder, CPT tests indicated with brown triangles. source: DINOloket

In figure B.2 a certain area with multiple CPT test location is highlighted in red. This is the only region were CPT data is available for grass and agricultural land, probably due to a site investigation for a pipeline. The project locations are thus chosen near this region.

Possible human interventions

Another criteria for selecting the project location is that the height of the project location should not be influenced by any human interventions, other than the lowering of the groundwater table level, as these other interventions are not included in the model. Different known human interventions in the area are considered in the short summary below:

- Groundwater exploitation locations:
  Rackwitz (2019) indicated in his study to overall subsidence of the Krimpenerwaard polder eight locations of groundwater exploitation where more than 200.000 m^3 is pumped up on a yearly basis, see figure B.1. As can be seen, these locations are all around the border of the area. To limit

influence of this subsidence source, project locations away from the border are chosen.

- Dredging depots:
  Some dredging depots are present in the Krimpenerwaard polder, where dredged material from the canals is placed. At these locations the dumping of the dredged material has an influence on the subsidence over time. (Rackwitz, 2019) indicated this in his study as well. To limit the influence of potential dredging maintenance in the region, the project areas have been specified at least 5m from the border with the water around.

- Pipeline:
  A map was constructed showing the values of subsidence between AHN2 and AHN3 (AHN3 was subtracted from AHN2). This map showed a yellow line, which means an increase in height over time, across the polder. After some investigation, it was found that this can probably be linked to the construction of a pipeline through this area. This also explains the straight line orientation of the CPT profiles that are available in the polder, as shown in figure B.2.

- Infrastructure:
  No area should be selected where there is currently infrastructure, as this is not the type of area that is relevant for this project.

- Raisings of the land done by humans:
  Some farmers in the Krimpenerwaard polder have probably raised their land to limit the influence of subsidence on their land. (Rackwitz, 2019) identified some areas where this is expected to have influenced the subsidence between 1984 and 2015 (AHN3).

Based on a comparison between AHN2 and AHN3 for the Krimpenerwaard polder, it was checked that there were no outliers with an increase in height over time near to the project area, that could have been caused by these interventions.

B.2. Calculating surface levels from data series

Based on the location choice, explained in section B.1, the data points used in the model were determined. Three data sets were used (1984 measurements, AHN2 and AHN3). The 1984 measurements have an average distance between the points of 50 meters and AHN2 and AHN3 both have an average point density of 10 points per m^2. Therefore, there are many more AHN2 and AHN3 measured values in the location areas than 1984 measurement points. The data sets of AHN2 and AHN3 were treated similarily in the procedure to extract a data value, while another approach was used for the 1984 dataset.

1984 dataset

Figure B.3 shows the datapoints of the 1984 dataset within and around the project areas. Two different methods were used to calculate the surface level of the project areas at 1984:

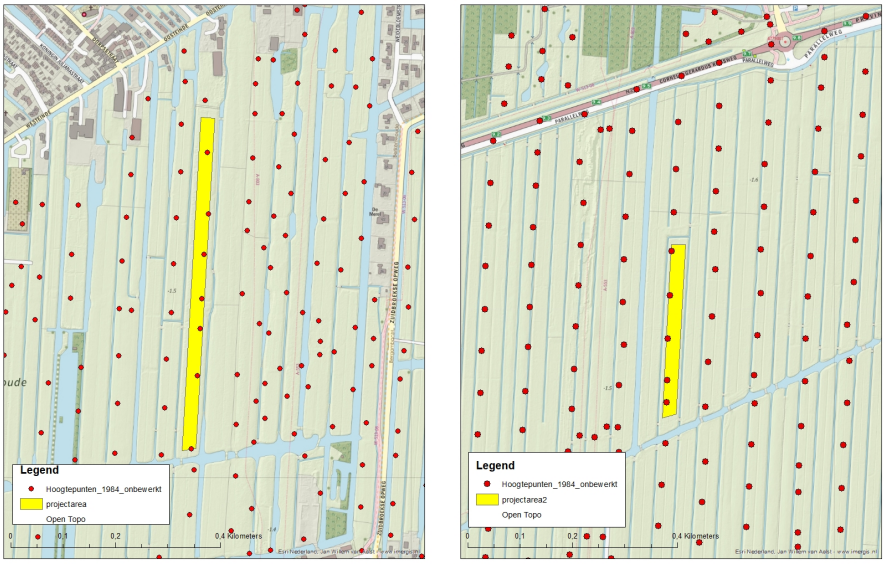

(a) Project area 1 (b) Project area 2

Figure B.3: Project locations with 1984 measurement points in and around the area shown

- Average value of surface level from the datapoints within project areas:
  For project area 1, this meant taking the average of seven values, and for project area 2 the average of five points within the project area was used.

- Average value of surface level from interpolation field values within project areas:
  An interpolation field was created, which is larger than the actual project. This interpolation field was created using the inverse distance weighted (IDW) function in GIS. Here, the distance to the original points is used to interpolate the original measurement points to a field. Limitations of this method are the decrease in quality of the interpolation when the original points are not equally distributed and that the minimum and maximum values only occur at the original points themselves, as all other values are averages. Figure B.4 shows the interpolation fields that were created, it can be seen that the locations of the original points still reflect in this field. A distance coefficient of 5.0 was used in this interpolation.

AHN2 and AHN3

For both datasets the mean value of the digital terrain model (DTM) at the project area was calculated in QGIS. A simple check was done to see if no zero points in the dataset were included, as (van Meijeren, 2017) mentioned some points with a zero value in the data set in the North of the Netherlands. This was not the case.

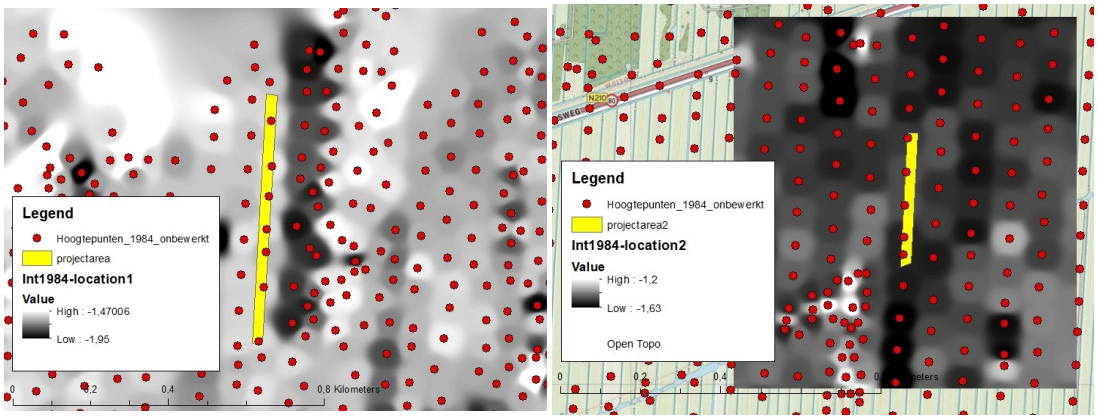

(a) Project area 1

(b) Project area 2

Figure B.4: Project locations with 1984 IDW interpolation field of measurement points in and around the area

Data points height over time

Using the previously explained methods resulted in the following values for height measurements of the project locations, see table B.1.

Table B.1: Surface level measurements based on 1984 measurements, AHN2 and AHN3 data series for both project locations

Project Location	Data series	Average measurement points [m NAP]	Average Interpolation Field [m NAP]
1	1984 AHN2 (2008) AHN3 (2015)	-1,579 -1,663 -1,744	-1,602
2	1984 AHN2 (2008) AHN3 (2015)	-1,530 -1,611 -1,737	-1,528

The NAP correction in the year 2005 is already incorporated in the 1984 values in table B.1. This means that the 1984 values in this table are actually -0,02m lower than the levels computed based on the original measurements. The level computed with the average interpolation field is used as initial surface level.

All measurement points from AHN2 and AHN3 a certain error, the total error for each point includes both a random error (stochastic error) and a systematic error. Moreover, within the project area itself there is also variability of the surface level. It is assumed that the range of uncertainty of the average surface level is similar to the range of uncertainty for an individual AHN measurement. The uncertainty margins for AHN measurements are indicated at the website of the AHN, under the page description of quality. For both AHN measurements a range of uncertainty is used of 15 cm, because it is indicated that minimally 95,4% of the measurement points has this accuracy.

B.3. Groundwater level

For both project locations an evaluation of the water levels over time is needed as an input for the model. A reconstruction of the water levels over time was made based on water management reports provided by the waterboard of the area, Hoogheemraadschap van Schieland en de Krimpenerwaard (HHSK). Table B.2 shows all resources used to come to this overview and table B.3 shows the outcomes of this.

Table B.2: Sources used to come to an overview of maintained waterlevels over time for the two project locations

Name	Source
Jaarverslag Waterkwantiteit 1984	HHK
Jaarverslag Waterkwantiteit 1985	HHK
Jaarverslag Waterkwantiteit 1986	HHK
Jaarverslag Waterkwantiteit 1987	HHK
Jaarverslag Waterkwantiteit 1988	HHK
Jaarverslag Waterkwantiteit 1991 - 1992	HHK
Jaarverslag Waterkwantiteit 1993 - 1994	HHK
Toelichting Peilbesluiten Krimpenerwaard 2011	HHK
Toelichting op het ontwerp peilbesluit Stolwijk en Berkenwoude 1995	HHK
Toelichting op het peilbesluit Den Hoek en Schuwacht 1993	HHK
Verenigde Vergadering (VV) peilbesluit 19 november 1995	HHK

Again, it should be noted that the NAP change in the year 2005 is already incorporated in the data in table B.3. Therefore all values from before 2005 in this table are actually -0,02 m lower than the levels mentioned in the reports. Values reported in are given in reference to the current NAP level. Figure B.5 shows an overview of the data in table B.3.

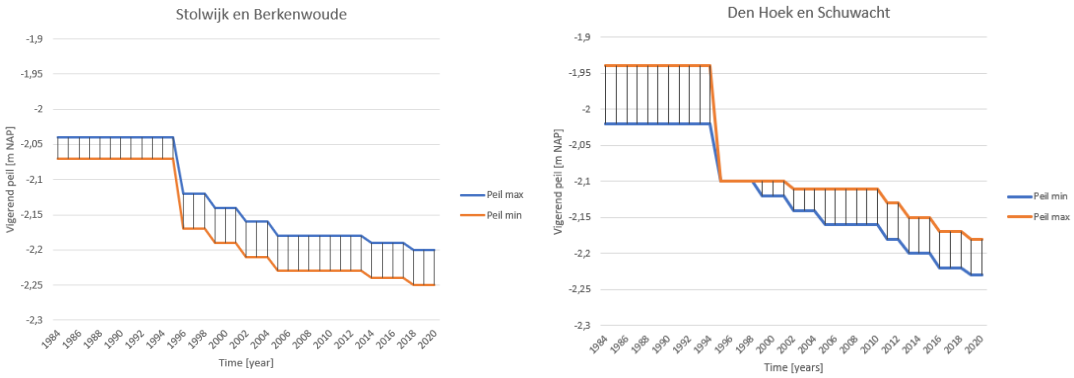

(a) Stolwijk en Berkenwoude (Project area 1)

(b) Den Hoek en Schuwacht (Project area 2)

Figure B.5: Maintained water level in water level area over time, based on HHSK reports

In the model, the average from these minimum and maximum values is used. This is done in order to compensate for the variability within a year. No information was found considering the groundwater levels for project area 2 between 1997 and 2004. These values have been estimated, based on the water level management strategies from the reports and the values around this missing time period, and are therefore shown in orange.

For the Van den Akker et al. (2007) equations, the DWL and GLG are needed. The GLG for the Krimpenerwaarpolder is determined using figure B.6 from Steur et al. (1991). It can be seen that the Krimpenerwaard falls into category II, where the GLG is between 0.5-0.8 m below the surface level. An average value of 0.65 m was used in the model.

Table B.3: Maintained water levels reported. Gray values mean that this level was not specifically mentioned in the report, but based on the other known values this level could be estimated. Orange values mean that this level was not mentioned any of the reports, but based on interpretation of other values and management strategies this value was most logical.

(a) Stolwijk en Berkenwoude (project location 1)

Year	Peil min [m NAP]	Peil max [m NAP]
1984	-2,04	-2,07
1985	-2,04	-2,07
1986	-2,04	-2,07
1987	-2,04	-2,07
1988	-2,04	-2,07
1989	-2,04	-2,07
1990	-2,04	-2,07
1991	-2,04	-2,07
1992	-2,04	-2,07
1993	-2,04	-2,07
1994	-2,04	-2,07
1995	-2,04	-2,07
1996	-2,12	-2,17
1997	-2,12	-2,17
1998	-2,12	-2,17
1999	-2,14	-2,19
2000	-2,14	-2,19
2001	-2,14	-2,19
2002	-2,16	-2,21
2003	-2,16	-2,21
2004	-2,16	-2,21
2005	-2,18	-2,23
2006	-2,18	-2,23
2007	-2,18	-2,23
2008	-2,18	-2,23
2009	-2,18	-2,23
2010	-2,18	-2,23
2011	-2,18	-2,23
2012	-2,18	-2,23
2013	-2,18	-2,23
2014	-2,19	-2,24
2015	-2,19	-2,24
2016	-2,19	-2,24
2017	-2,19	-2,24
2018	-2,20	-2,25
2019	-2,20	-2,25
2020	-2,20	-2,25

(b) Den Hoek en Schuwacht (project location 2)

Year	Peil min [m NAP]	Peil max [m NAP]
1984	-1,94	-2,02
1985	-1,94	-2,02
1986	-1,94	-2,02
1987	-1,94	-2,02
1988	-1,94	-2,02
1989	-1,94	-2,02
1990	-1,94	-2,02
1991	-1,94	-2,02
1992	-1,94	-2,02
1993	-1,94	-2,02
1994	-1,94	-2,02
1995	-2,10	-2,10
1996	-2,10	-2,10
1997	-2,10	-2,10
1998	-2,10	-2,10
1999	-2,10	-2,12
2000	-2,10	-2,12
2001	-2,10	-2,12
2002	-2,11	-2,14
2003	-2,11	-2,14
2004	-2,11	-2,14
2005	-2,11	-2,16
2006	-2,11	-2,16
2007	-2,11	-2,16
2008	-2,11	-2,16
2009	-2,11	-2,16
2010	-2,11	-2,16
2011	-2,13	-2,18
2012	-2,13	-2,18
2013	-2,15	-2,20
2014	-2,15	-2,20
2015	-2,15	-2,20
2016	-2,17	-2,22
2017	-2,17	-2,22
2018	-2,17	-2,22
2019	-2,18	-2,23
2020	-2,18	-2,23

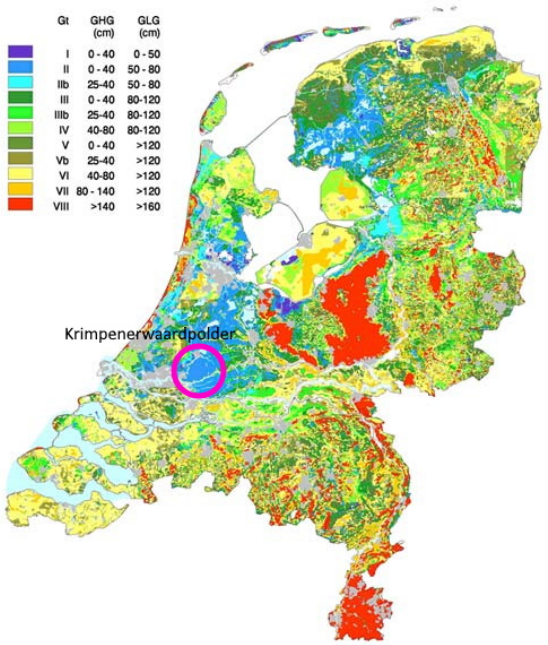

Figure B.6: The groundwater indicator map of the Netherlands, with an estimation for GLG included Steur et al. (1991)

B.4. Soil profile

For both project locations a general representative soil profile was found based on site investigation data from DINOloket. Spatial variation of the soil profile within a project area is not considered.

Three different data sets from DINOloket were used to come to a general soil profile for the project area, CPT data, geological drilling profiles and archeological drilling profiles. Figure B.7 shows the locations of these profiles with respect to the project areas.

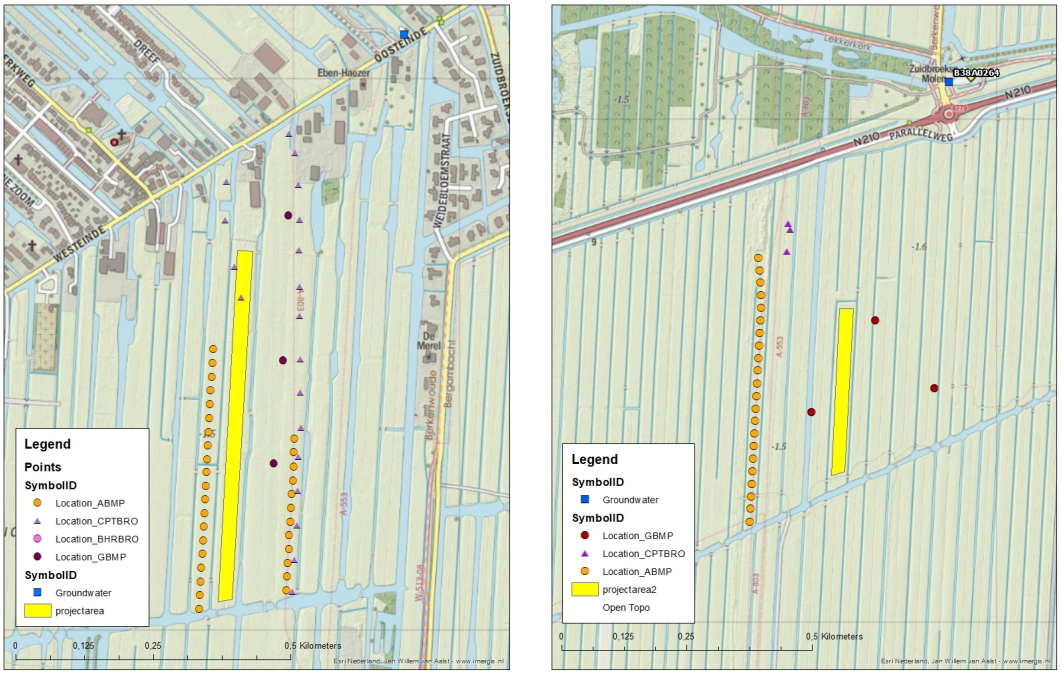

(a) Project area 1

(b) Project area 2

Figure B.7: Locations DINOloket data around project areas

B.4.1. Project area 1

First the three geological boorprofiles near the project area were examined. There is no date specified for when these boorprofiles have been made. A general soil profile was created based on these three profiles, see figure B.8.

After that, the CPT profiles in and around the project area were evaluated. The CPT soil profiles were plotted along an axis running along the length of the project location. This created the following figure. The purple material is identified as loam by D-Foundations, but can be identified as fine sand in the Netherlands.

The CPT investigation was done in the year 2011, which does not match the starting point of the analysis for this project, which is in 1984. Therefore, some adjustments have been done based on the following assumption:

- Thickness of the toplayer (organic clay / decomposed peat) is the same, but then starts at surface level 1984
- Peat layer has decreased in thickness over time, more than the other soil layers

Using an excel tool from Arcadis and the knowledge based on the two previous considered datasets, the following general soil profile was then found for project area 1, see figure B.10.

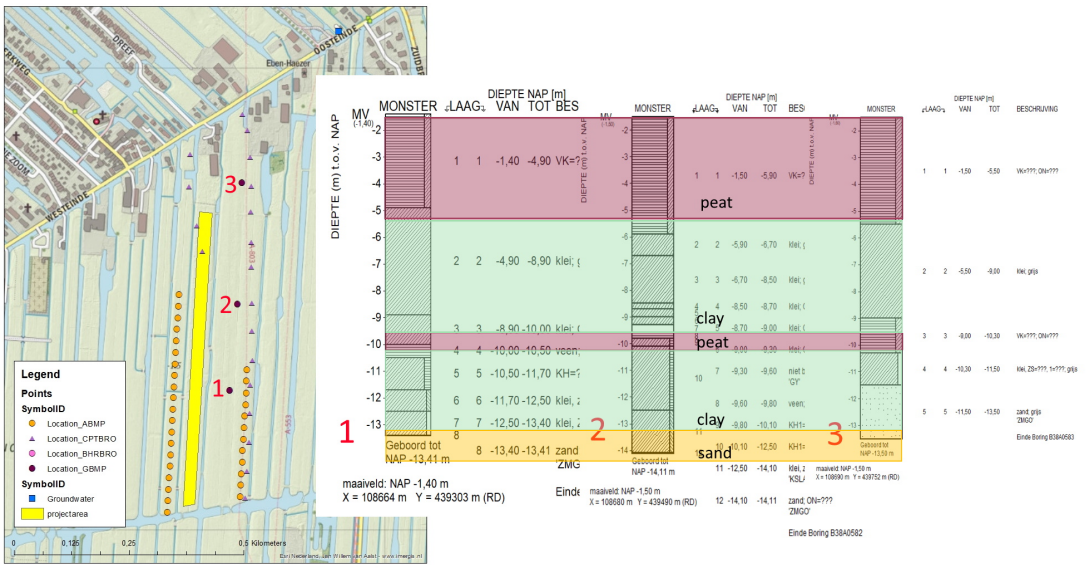

Figure B.8: General interpretation geological drilling profiles project area 1

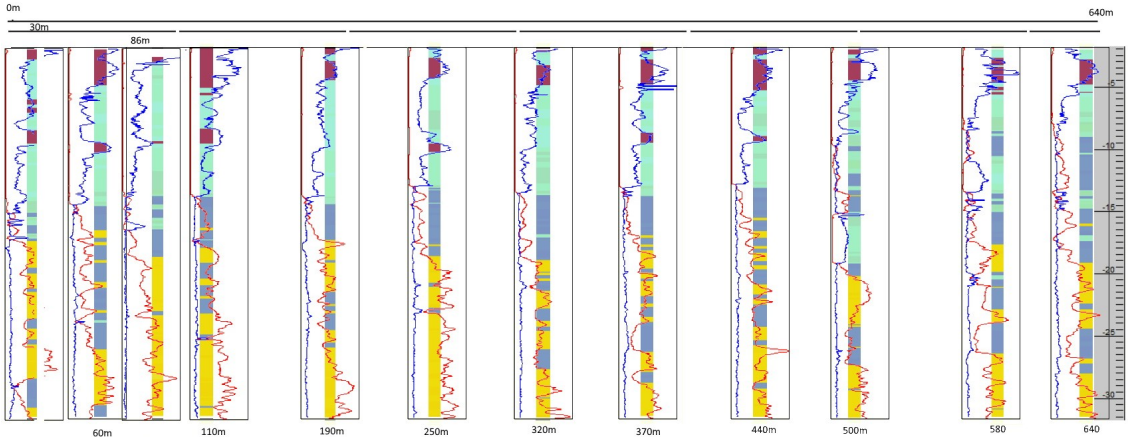

Figure B.9: General interpretation CPT data around project area 1, color index: brown = peat, green = clay, purple = loam, yellow = sand.

The archaeological boorprofiles were used to create a better understanding of the upper peat layer, as these boorprofiles reached only to about -5 to -6 m NAP. It was seen that all boorprofiles generally included an upper layer with a weak or strong clayey peat, then a part nutrient poor peat and towards the bottom of the peat layer the peat has some clayey influences again.

Soil profile: model parameters project area 1

Different model parameters are needed to run the model. Tables B.4, B.5 and B.6 show soil parameters used in submodels.

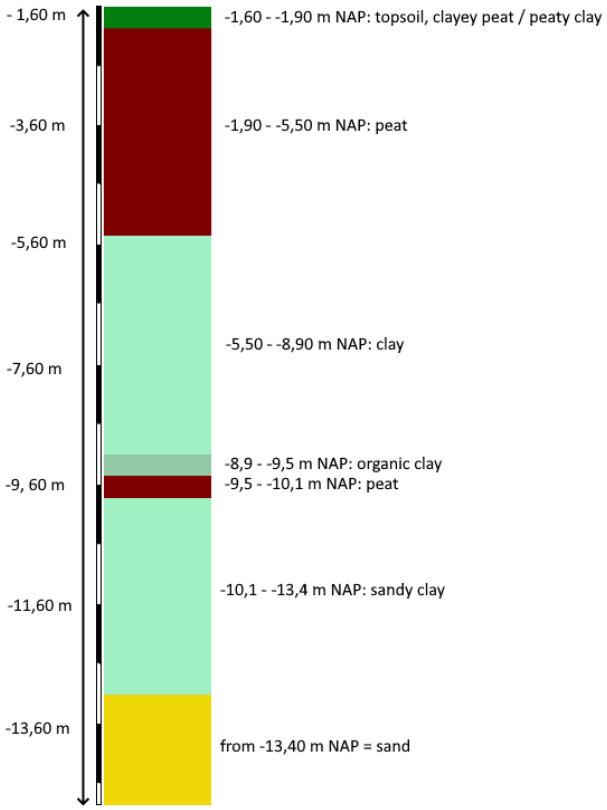

Figure B.10: General soil profile project area 1 used in evaluation

Table B.4: Soil parameters: Oxidation submodels, project area 1

Depth top layer [m NAP]	**Soil Type**	V_{ox} [**year**$^{-1}$]	λ_r [-]	K [**year**$^{-1}$]
-1,6	Topsoil	0	1	0
-1,9	Peat	0,015$^{(a)}$	0,09$^{(b)}$	0,015$^{(a)}$
-5,5	Clay	0	1	0
-8,9	Organic Clay	0	1	0
-9,5	Peat	0,015$^{(a)}$	0,09$^{(b)}$	0,015$^{(a)}$
-10.1	Sandy Clay	0	1	0

(a) Value commonly stated in literature, based on study (Van den Akker et al., 2007)
(b) Value based on results Fokker et al. (2019)

Table B.5: Soil parameters: Loading submodel Koppejan, project area 1

Depth top layer [m NAP]	**Soil Type**	**Cp'** [-]	**Cs'** [-]	**Cp** [-]	**Cs** [-]	$\gamma_{\mathbf{sat}}$ $[kN/m^3]$	$\gamma_{\mathbf{unsat}}$ $[kN/m^3]$	c_v $[m^2/s]$
-1,6	Topsoil	20	75	60	600	13	12	5,50E-08
-1,9	Peat	10	35	30	280	11	5 [(a)]	7,50E-08
-5,5	Clay	19	200	56	1600	15,5	14,5	4,00E-08
-8,9	Organic Clay	16	70	48	560	13,5	12,5	4,50E-08
-9,5	Peat	10	35	30	280	11	5 [(a)]	7,50E-08
-10.1	Sandy Clay	30	250	90	2000	16	15	4,00E-08

All values based on Excel tool from Arcadis
(a) Estimation based on Hsi et al. (2005) and laboratory study N3 samples

Table B.6: Soil parameters: Loading submodel NEN-Bjerrum, project area 1

Depth top layer [m NAP]	**Soil Type**	**RR** [-] [(a)]	**CR** [-] [(a)]	$\mathbf{C}_\alpha$ [-] [(b)]	$\gamma_{\mathbf{sat}}$ $[kN/m^3]$	$\gamma_{\mathbf{unsat}}$ $[kN/m^3]$	c_v $[m^2/s]$
-1,6	Topsoil	0,0384	0,1151	0,0091	13	12	5,50E-08
-1,9	Peat	0,0768	0,2303	0,0060	11	5 [(d)]	7,50E-08
-5,5	Clay	0,0411	0,1212	0,0060	15,5	14,5	4,00E-08
-8,9	Organic Clay	0,0480	0,1439	0,0091	13,5	12,5	4,50E-08
-9,5	Peat	0,0768	0,2303	0,0060	11	5 [(d)]	7,50E-08
-10,1	Sandy clay	0,0256	0,0768	0,004 [(c)]	16	15	4,00E-08

(a) Values calculated from Koppejan parameters, with the use of formulas from Den Haan et al. (2004):

$$\mathrm{RR} = \frac{\ln 10}{C_p} \qquad \mathrm{CR} = \frac{\ln 10}{C_p'} \tag{B.1}$$

(b) Values based on the subsidence study from Fokker et al. (2019). Estimated values for C_α for soil profiles in Flevoland were mentioned here.
(c) Value based on table 2b from NEN-EN1997-1 (2019)
(d) Estimation based on Hsi et al. (2005) and laboratory study N3 samples

B.4.2. Project Area 2

For project area 2 the same methodology was used to come to a general soil profile of the area. First the geological drillings (three in total) were evaluated, then the CPTs (three in total) and last, the archeological drillings to get a better understanding of the peatlayer.

The drilling profiles and CPT profiles are shown along the length of the project area in figure B.11. It can be seen that there is a high variation between the results. The horizontal variation in location between the profiles is indicated in this figure as well.

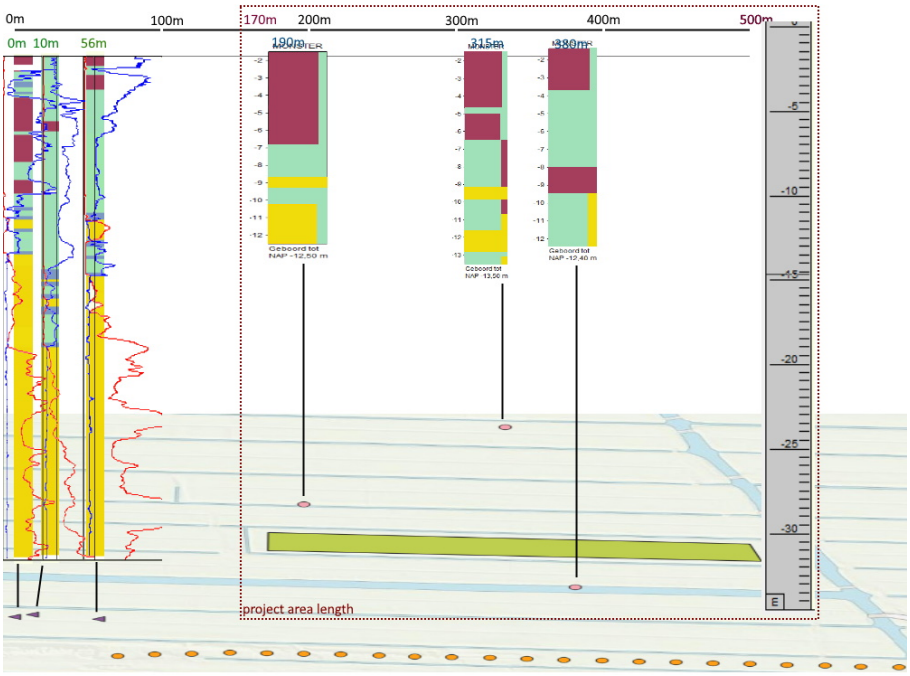

Figure B.11: General interpretation CPT data around project area 2, color index: brown = peat, green = clay, purple = loam, yellow = sand.

The archaeological drilling profiles were inspected to get an idea of the soil profile up to -5 m NAP. Using all the information, a general soil profile was created, see figure B.12.

Since the variation between the site investigations is high, it was difficult to create a general soil profile and an error is probably introduced to the system here.

Soil profile: model parameters project area 2

Tables B.7, B.8 and B.9 show the parameters used in the model for project area 2.

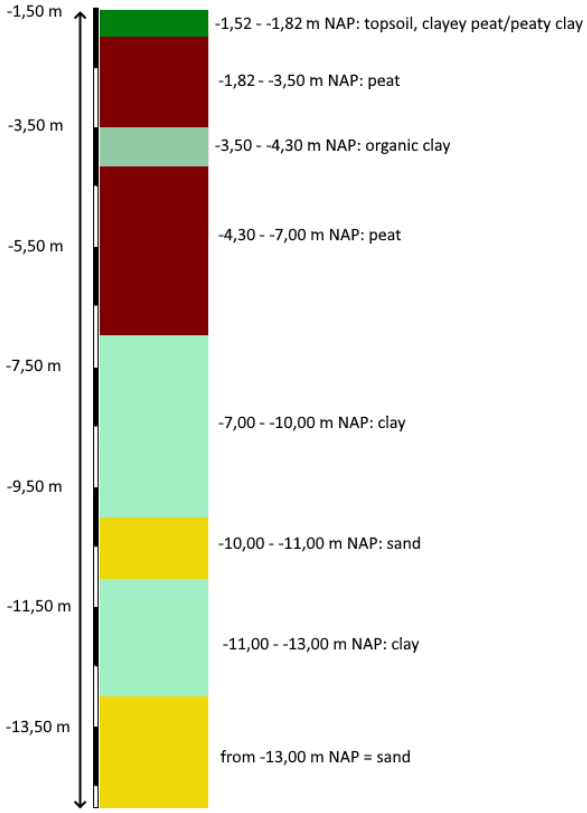

Figure B.12: General soil profile project area 2 used in evaluation

Table B.7: Soil parameters oxidation submodel Fokker, project area 2

Depth top layer [m NAP]	**Soil Type**	V_{ox} [**year**$^{-1}$]	λ_r [-]	K [**year**$^{-1}$]
-1,52	Topsoil	0	1	0
-1,82	Peat	0,015$^{(a)}$	0,09$^{(b)}$	0,015$^{(a)}$
-3,5	Organic clay	0	1	0
-4,3	Peat	0,015$^{(a)}$	0,09$^{(b)}$	0,015$^{(a)}$
-7,0	Clay	0	1	0
-10.0	Sand	0	1	0
-11.0	Clay	0	1	0

(a) Value commonly stated in literature, based on study (Van den Akker et al., 2007)
(b) Value based on results Fokker et al. (2019)

Table B.8: Soil parameters: Loading submodel Koppejan, project area 2

Depth top layer [m NAP]	**Soil Type**	**Cp'** [-]	**Cs'** [-]	**Cp** [-]	**Cs** [-]	$\gamma_{\mathbf{sat}}$ $[kN/m^3]$	$\gamma_{\mathbf{unsat}}$ $[kN/m^3]$	c_v $[m^2/s]$
-1,52	Topsoil	20	75	60	600	13	12	5,50E-08
-1,82	Peat	10	35	30	280	11	$5^{(a)}$	7,50E-08
-3,5	Organic clay	16	70	48	560	13,5	12,5	4,50E-08
-4,3	Peat	10	35	30	280	11	$5^{(a)}$	7,50E-08
-7	Clay	19	200	56	1600	15,5	14,5	4,00E-08
-10	Sand	500	1E+09	1500	1E+09	19	17	drained
-11	Clay	46	435	138	3480	17	16	5,50E-08

All values based on Excel tool from Arcadis
(a) Estimation based on Hsi et al. (2005) and laboratory study N3 samples

Table B.9: Soil parameters: Loading submodel NEN-Bjerrum, project area 2

Depth top layer [m NAP]	**Soil Type**	**RR** [-] $^{(a)}$	**CR** [-] $^{(a)}$	$\mathbf{C}_\alpha$ [-] $^{(b)}$	$\gamma_{\mathbf{sat}}$ $[kN/m^3]$	$\gamma_{\mathbf{unsat}}$ $[kN/m^3]$	c_v $[m^2/s]$
-1,52	Topsoil (Peat, strong clayey)	0,0384	0,1151	0,0091	13	12	5,50E-08
-1,82	Peat (Peat)	0,0768	0,2303	0,0060	11	$5^{(c)}$	7,50E-08
-3,5	Organic clay (Clay, strongly humic)	0,0480	0,1439	0,0091	13,5	12,5	4,50E-08
-4,3	Peat (Peat)	0,0768	0,2303	0,0060	11	$5^{(c)}$	7,50E-08
-7	Clay (Clay)	0,0411	0,1212	0,0060	15,5	14,5	4,00E-08
-10	Sand (Sand, weak clayey)	0,0015	0,0046	0,0001	19	17	drained
-11	Clay (Clay, medium sandy)	0,0167	0,0501	0,0060	17	16	5,50E-08

(a) Values calculated from Koppejan parameters, with the use of formulas from Den Haan et al. (2004):

$$\mathrm{RR} = \frac{\ln 10}{C_p} \qquad \mathrm{CR} = \frac{\ln 10}{C'_p} \tag{B.2}$$

(b) Values based on the subsidence study from Fokker et al. (2019). Estimated values for C_α for soil profiles in Flevoland were mentioned here.
(c) Estimation based on Hsi et al. (2005) and laboratory study N3 samples

B.5. Water head

The water head in the sand layer below the soft soil layers is important in the modelling, because this determines the pore water pressures at the bottom of the evaluated soil profile. For both project locations this water head is determined based on groundwater monitoring information from DINOloket. The locations of the groundwater monitoring locations are shown in figure B.7.

Project area 1

Data from a monitoring well with a filter between -30,61m and -31,61m NAP was used to evaluate the water head for this project location. Measurements between 1979 and 2017 were available and are shown in figure B.13. An average value of -2,373m NAP was used in the model.

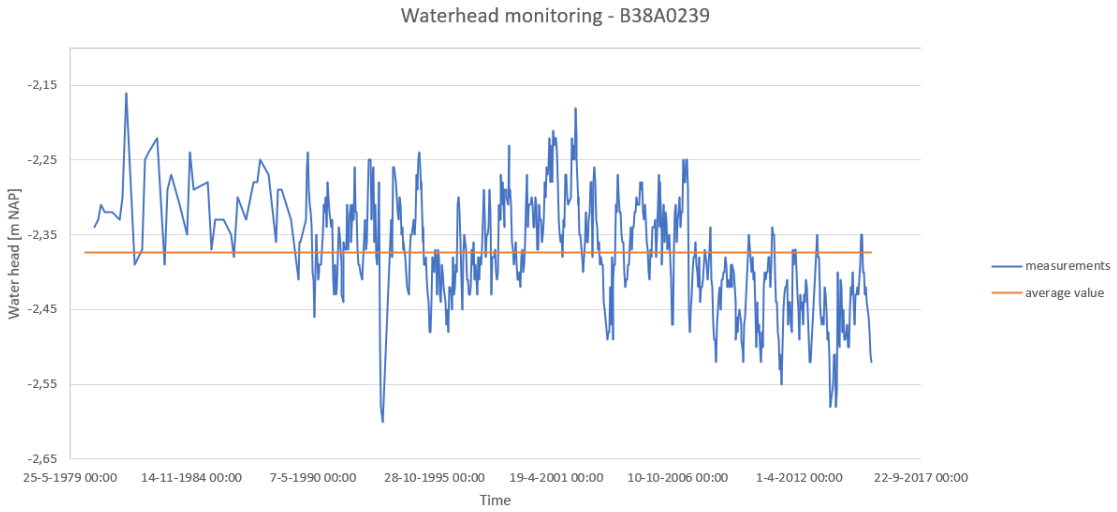

Figure B.13: Measured and average water head over time at well B38A0239

Two checks were done in order to verify this value. First, the average value from other dataseries from the same well, but with a filter at -64,61 to -65,61 m NAP, was compared to the average of the higher filter. The average value of the dataset from the deeper filter is -2,383m NAP, which is close to the value found with the higher filter. Secondly, one of the CPTs with water pressure measurements was used to verify this number. The (linear) line of water pressures in the sand layers is extended to the top to see what head this would give, see figure B.14. It can be seen that this value comes near the average value found above.

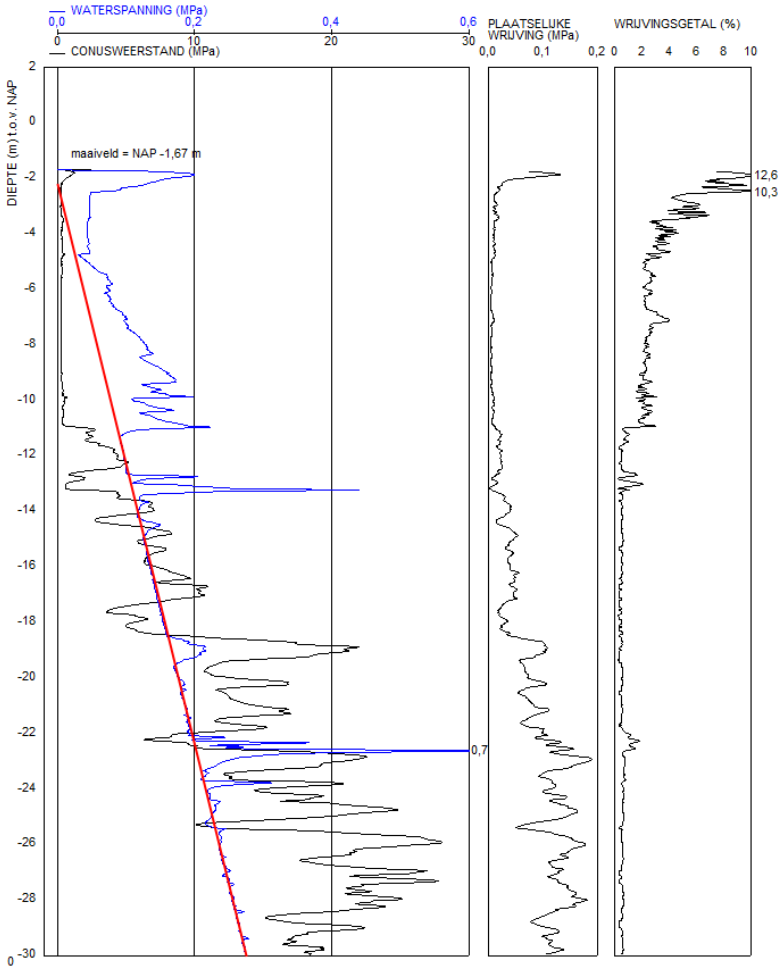

Figure B.14: Interpretation CPT data with water pressure data, project area 1

Project area 2

The same approach was used to determine the water head in the deeper sand layers for project area 2. Data from a monitoring well with filters from -15,09 to -17,09 m NAP and -25,53 to -27,53m NAP was used. Measurements between 1991 and 2011 are shown in figure B.15. An average value of -1.87m NAP was used in the model.
Similar to project area 1, a check was performed using water pressure measurements of a CPT in the sand layers. This check is shown in figure B.16.

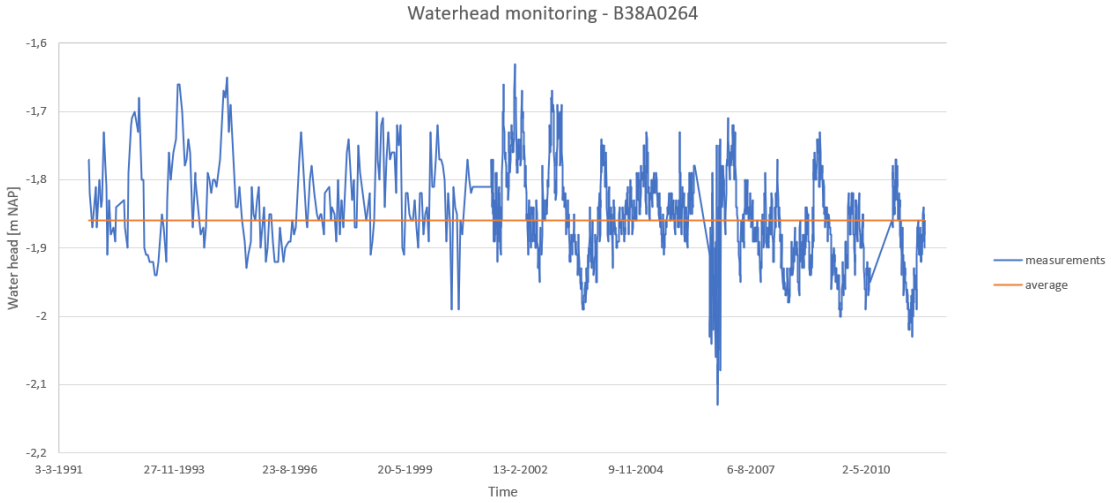

Figure B.15: Measured and average water head over time at well B38A0264

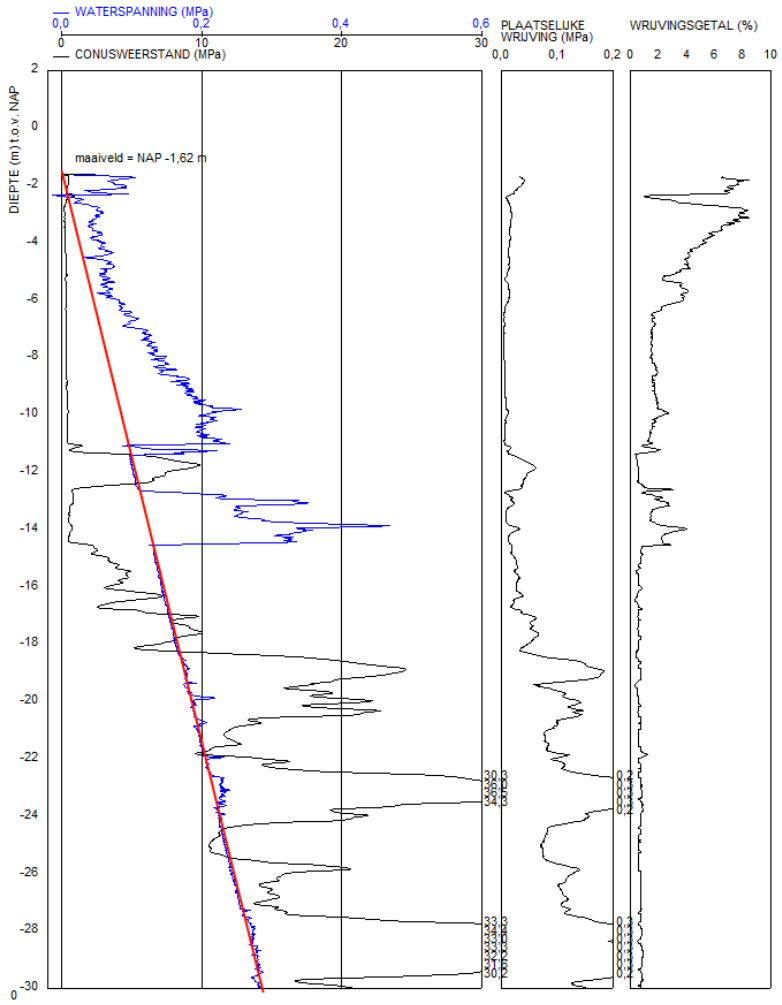

Figure B.16: Interpretation CPT data with water pressure data, project area 2

B.6. Oxidation model evaluation error time

The oxidation submodels included in the python model all work with a time based approach where water level lowerings over time can be accounted for. History of the water level lowerings before modelling time is not accounted for. Moreover, adjustment of the oxidation rate based on the subsidence that already occurred over time is not always accounted for. These two simplifications were made because of modelling purposes.

In this section the error introduced by these simplifications is evaluated. The model results for project area 1 were compared with detailed calculations based on the situation visualised in figure B.17. Different sublayers are identified in this profile, where the layers correspond with the water level lowerings over time. Some assumptions were used to make the two situations comparable.

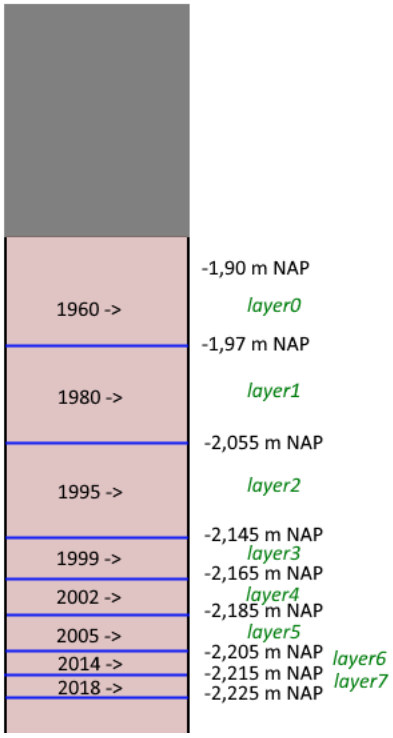

Figure B.17: Oxidation calculation more detail

- The topsoil (upper 30 cm, indicated with grey in figure B.17) does not contribute to subsidence from oxidation anymore.
- No information is available about water level lowerings from before 1960. It is therefore assumed that at 1960 the water level was lowered from -1,90 m NAP to -1,97 m NAP.
- There is no subsidence from compression by loading and compression by anaerobic degradation. Subsidence is calculated only from compression by oxidation, with the use of the Fokker oxidation submodel.

Figure B.18a shows the compression by oxidation components from the sublayers, when also the history (for as far as known) is taken into account. The python model calculates compression by oxidation considering input from only the time zone between the two black striped lines, without using sublayers. Figure B.18b shows a comparison between the compression by oxidation calculations from the detailed approach and from the python submodel. The detailed calculation including the history of the water level lowerings predicts a lower contribution of compression by oxidation, as the initial rate of oxidation

will be lower. The difference after 36 years is shown in table B.10. The difference is approximately 1 cm over 36 years.

Table B.10: Comparison detailed calculation and submodel calculation endresult

Model	**Subsidence from compression by oxidation [m] over 36 years**	
Detailed calculation with history	0,0890	90,43%
Fokker submodel without history	0,0984	100%

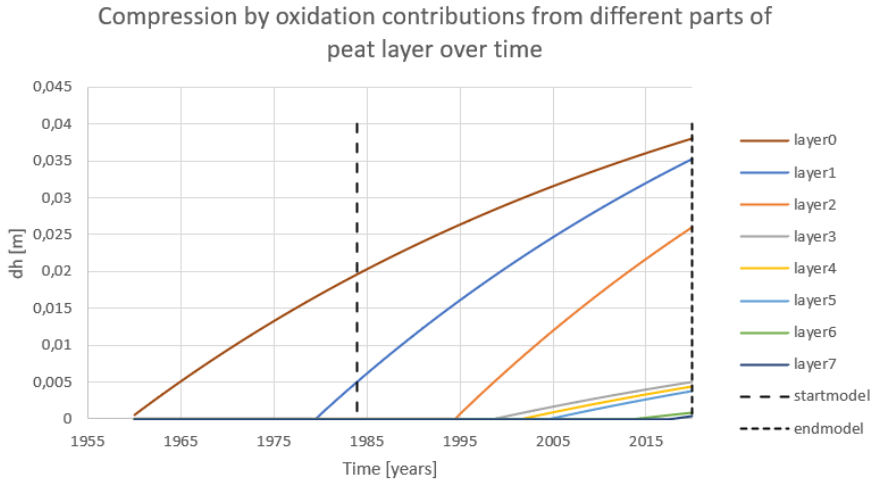

(a) Detailed calculation contributions by compression from oxidation per sublayer over time as indicated in figure B.17. Fokker modelling equation used.

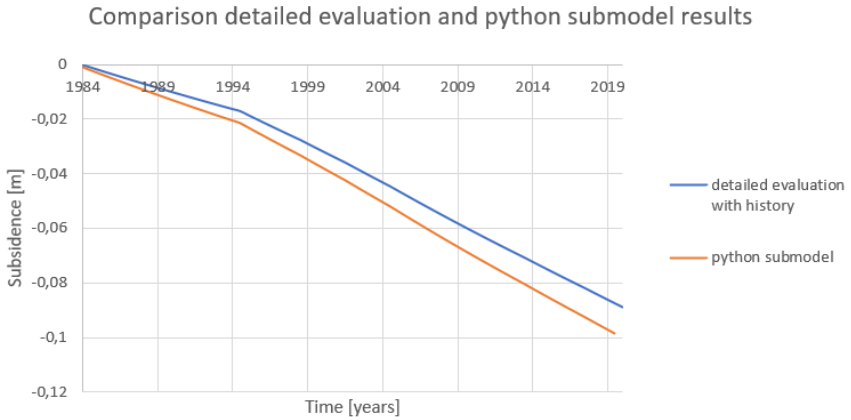

(b) Comparison of submodel result with detailed approach that also considers history of water level lowerings

Figure B.18: Evaluation of neglecting water level lowerings history in python submodel approach

B.7. Model settings used

```
start year = 1984
time period evaluated = 36 years
time step (dt) = 0.5 year
days in a year = 365.25 days

bottom level evaluation project area 1 = -13.4 m NAP
bottom level evaluation project area 2 = -13.0 m NAP

number of evaluated layers within a soil layer = 7
POP = 7.5 kPa
tau0 = 1 day

maximum depth oxygen diffusion in soil profile, parameter D = 0.80 m
```

Figure B.19: Other input settings used in the model to come to the results presented in this section

B.8. Compression by loading comparison with D-Settlement

The results of the compression by loading submodels for project area 1 are compared with D-Settlement models with similar input. The result of this comparison is shown in figure B.20. The koppejan modelling approach shows a small difference, this is because swelling is neglected in the compression by loading submodel and D-Settlement does probably include this. This difference is small and therefore not visible for the NEN-Bjerrum modelling approach, where a larger settlement is modelled.

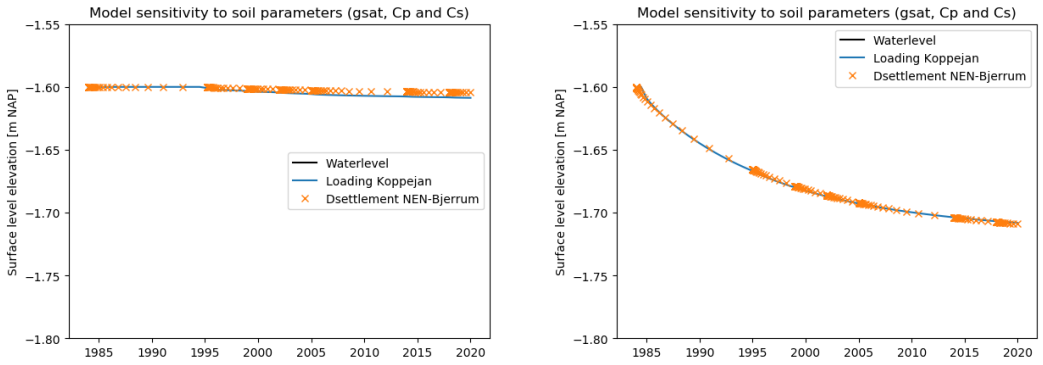

(a) Terzaghi consolidation model and Koppejan settlement model (b) Terzaghi consolidation model and NEN-Bjerrum settlement model

Figure B.20: Comparison of submodel compression by loading results with D-Settlement model results

B.9. Sensitivity study

Different model parameters are used in the submodels, where certain parameters have more influence on the outcome than others. To evaluate the influence of parameters, the model for project location 1 with the Koppejan and Fokker submodels has been used. All results mentioned in this section are based on the 36 years time interval.

Compression by loading model parameters

The sensitivity to the input parameters of the Koppejan settlement model was three different scenarios with variations in Cp, Cs and γ_{sat}. The range of variation for the unit weights is based on an excel tool from Arcadis, where a range of this parameter to be expected is provided for each soil layer (low, high and average values). For the parameters Cp and Cs the range of values is calculated based on some assumptions. These are listed below:

- Variability of these soil parameters can be represented with a normal distribution
- The outer range values of the sensitivity analysis should represent 95% of the normal distribution
- The values of Cp and Cs mentioned in table B.5 represent the mean values of the normal distributions
- The coefficient of variation for in-situ soil parameters is typically $0.1 \leq V \leq 0.3$, here a value of $V = 0.2$ is used.

The standard deviation for each layer can then be calculated using

$$V = \frac{\sigma}{\mu} = 0.2. \tag{B.3}$$

Using the values of the standard deviations, the 95% intervals can be calculated, as '95% of data lies within $\pm 2\sigma$'. The calculation and range of parameters used for the sensitivity study is shown in tables B.11 and B.12.

Table B.11: Range of model parameter Cp in sensitivity study per soil layer

Soil layer	**Cp (μ)**	σ	**Lower limit Cp**	**Upper limit Cp**
topsoil	60	12	36	84
peat	30	6	18	42
clay	56	11,2	33,6	78,4
organic clay	48	9,6	28,8	67,2
peat	30	6	18	42
sandy clay	90	18	54	126

Table B.12: Range of model parameter Cs in sensitivity study per soil layer

Soil layer	**Cs (μ)**	σ	**Lower limit Cs**	**Upper limit Cs**
topsoil	600	120	360	840
peat	280	56	168	392
clay	1600	320	960	2240
organic clay	560	112	336	784
peat	280	56	168	392
sandy clay	2000	400	1200	2800

Variations of the parameters C'_p and C'_s have no impact on the model, as the stress increases remain below the preconsolidation pressure level. Table B.13 shows the settings of Cp, Cs and γ_{sat} for the scenarios evaluated. The results are shown in table B.14 and figure B.21.

Table B.13: Scenarios used in sensitivity analysis Koppejan settlement model

	Low values scenario			**Average scenario**			**High values scenario**		
Soil layer	γ_{sat} **[kN/m^3]**	**Cp**	**Cs**	γ_{sat} **[kN/m^3]**	**Cp**	**Cs**	γ_{sat} **[kN/m^3]**	**Cp**	**Cs**
topsoil	11,7	36	360	13	60	600	14,3	84	840
peat	9,9	18	168	11	30	280	12,1	42	392
clay	14	33,6	960	15,5	56	1600	17,1	78,4	2240
organic clay	12,2	28,8	336	13,5	48	560	14,9	67,2	784
peat	9,9	18	168	11	30	280	12,1	42	392
sandy clay	14,4	54	1200	16	90	2000	17,6	126	2800

Table B.14: Influence of Koppejan model parameters on model results

	Koppejan parameter scenario		
Subsidence component	low values	average values	high values
Compression by oxidation [m]	0,087	0,092	0,093
Compression by loading [m]	0,030	0,009	0,003
Compression by anaerobic degradation [m]	0,020	0,019	0,019
Total subsidence [m]	0,137	0,119	0,115

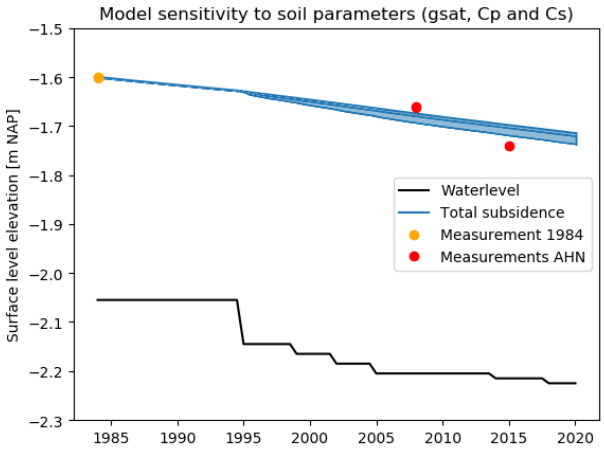

Figure B.21: Modelled results of different inputs of Koppejan settlement model parameters

As can be expected, using lower values of model parameters leads to a higher compression by loading contribution based on the Koppejan settlement model. The increase in this component means that a larger part of the soil profile gets submerged below the groundwater level and therefore does not contribute to the compression by oxidation component. Using lower Koppejan model parameters thus causes a lower contribution from oxidation and a higher contribution from anaerobic degradation. The model parameters will only influence the model results after the first water level lowering (1995). This is the reason why the first part of the solution space (1984-1995) is the same for all scenarios in figure B.21. A variation in the POP parameter is evaluated for the NEN-Bjerrum model instead of the Koppejan model. The reason for this is that the increase in effective stress as result of the water level lowerings is small with respect to the value of the POP, especially in deeper soil layers. Model results of the Koppejan model will thus be similar for the logical range of the POP values. The NEN-Bjerrum model does show variation for different POP values, as this value is used in the initial creep calculation. Table B.15 and figure B.22 show the values of POP analysed and the results.

Using a higher value of the POP parameter results in a lower value of subsidence modelled with the NEN-Bjerrum and Fokker submodels. For higher POP values there is a smaller contribution of initial

Table B.15: Influence of POP value on model results with NEN-Bjerrum submodel

	POP value [kPa]			
Subsidence component	5	7,5	10	20
Compression by oxidation [m]	0,051	0,059	0,065	0,080
Compression by loading [m]	0,129	0,108	0,091	0,047
Compression by anaerobic degadation [m]	0,029	0,027	0,026	0,022
Total subsidence [m]	0,209	0,194	0,181	0,148

creep. This results in a larger part of the soil profile being above the groundwater level, and thus an increase in the compression by oxidation component and a decrease in the compression by anaerobic degradation contribution.

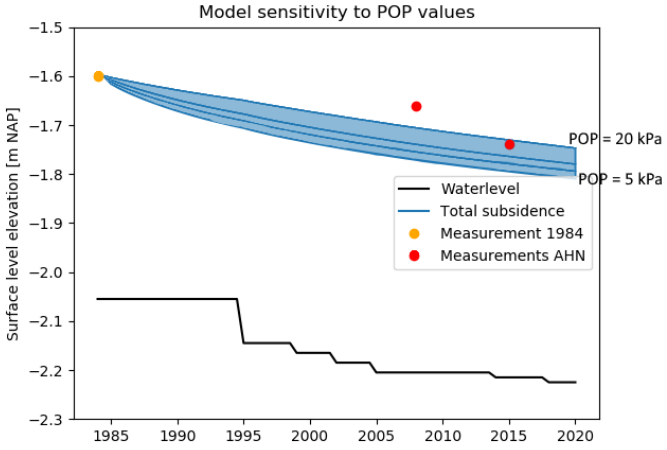

Figure B.22: Modelled results with different values of the POP value, using the NEN-Bjerrum settlement model instead of the Koppejan settlement model

Compression by oxidation model parameters

In figure 4.4 the influence of the V_{ox} parameter (rate of oxidation) was shown in the compression by oxidation submodel results for long time scales. Here different values of this parameter are evaluated. Also the impact of the assumption that the topsoil layer of 30cm is not influenced by compression by oxidation is evaluated. This assumption was mentioned in section 8.2.2. In total seven different scenarios have been evaluated:

- Variation of V_{ox}^{peat}
  - $V_{ox}^{\text{peat}} = 0,0088$ year^{-1}, based on the Koppejan estimate from Fokker et al. (2019) in Flevoland
  - $V_{ox}^{\text{peat}} = 0,0105$ year^{-1}, based on the K value from Hoogland et al. (2012)
  - $V_{ox}^{\text{peat}} = 0,0150$ year^{-1}, based on the value stated by Van der Meulen et al. (2007)
- Variation of V_{ox}^{topsoil}, modelled with $V_{ox}^{\text{peat}} = 0,0150$ and $\lambda_{r,ox}^{\text{topsoil}} = 0,478$, which is based on the $\lambda_{r,sh}^{\text{topsoil}}$ parameter from Fokker et al. (2019).
  - $V_{ox}^{\text{topsoil}} = 0,001$ year^{-1}
  - $V_{ox}^{\text{topsoil}} = 0,005$ year^{-1}
  - $V_{ox}^{\text{topsoil}} = 0,010$ year^{-1}
  - $V_{ox}^{\text{topsoil}} = 0,015$ year^{-1}

The model results from these scenarios are shown in table B.16 and figure B.23. The blue range indicates the solution space for the different values of V_{ox}^{peat}, the green range indicates the solution space for $V_{ox}^{\text{peat}} = 0,0150$ year^{-1} together with different values of V_{ox}^{topsoil}.

Table B.16: Influence V_{ox} parameter values on model result

	V_{ox}^{peat} [year^{-1}]			V_{ox}^{topsoil} [year^{-1}]			
Subsidence component	0,0088	0,0105	0,015	0,001	0,005	0,010	0,015
Compression by oxidation [m]	0,060	0,070	0,092	0,097	0,117	0,139	0,156
Compression by loading [m]	0,009	0,009	0,009	0,009	0,009	0,009	0,009
Compression by anaerobic degradation [m]	0,009	0,012	0,019	0,019	0,021	0,022	0,024
Total subsidence [m]	0,079	0,090	0,119	0,125	0,147	0,170	0,189

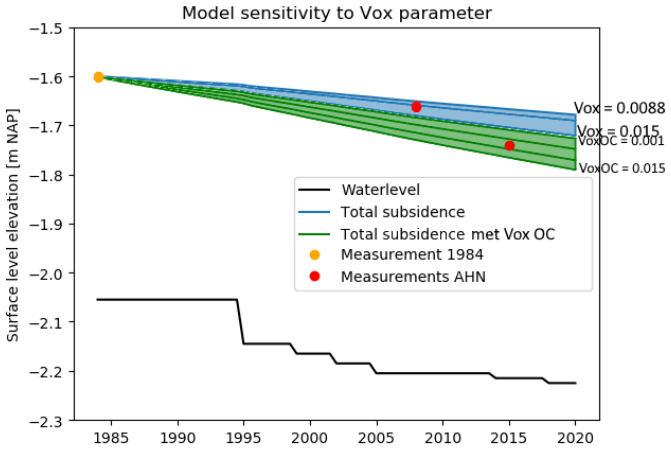

Figure B.23: Modelled results of different input for the V_{ox} parameter

It can be seen that the value of the V_{ox} parameter influences the total subsidence calculated by the model for the full time interval analysed. This parameter influences both the compression by oxidation and compression by anaerobic degradation submodels, as V_{an} is calculated based on V_{ox}. The compression by loading submodel result does not change for different values of V_{ox}, as these settlements calculations are done at the beginning and not coupled with the oxidation model. The influence of the assumption that the topsoil layer does not contribute to subsidence by oxidation anymore ($V_{ox}^{topsoil} = 0$) can clearly be seen in figure B.23. A contribution from this topsoil layer leads to a higher subsidence modelled.

Ratio anaerobic and aerobic degradation

Based on the study from Zander, Gebert and Heimovaraa, the ratio aerobic/anaerobic degradation was assumed to be 3,98/1. This was implemented by dividing the rate of oxidation (V_{ox}) with this factor to find the rate of anaerobic degradation (V_{an}). The variation of values indicated in literature for this ratio is large. Hämäläinen (1991) mentioned that anaerobic degradation of peat soil can be 100 to 1000 times slower than aerobic degradation. Different values of this ratio have been tested, results are shown in table B.17 and figure B.24.

The ratio has an influence on the model results. For a variation from 4 to 10 the influence can be seen, when the ratio is assumed to be much larger (100 to 1000) it can be seen that the influence of anaerobic degradation becomes negligible.

Table B.17: Influence ratio aerobic/anaerobic degradation on model result

	Ratio aerobic/anaerobic degradation			
Subsidence component	3,98	10	100	1000
Compression by oxidation [m]	0,092	0,095	0,096	0,096
Compression by loading [m]	0,009	0,009	0,009	0,009
Compression by anaerobic degradation [m]	0,019	0,007	0,001	7,05E-05
Total subsidence [m]	0,119	0,111	0,106	0,105

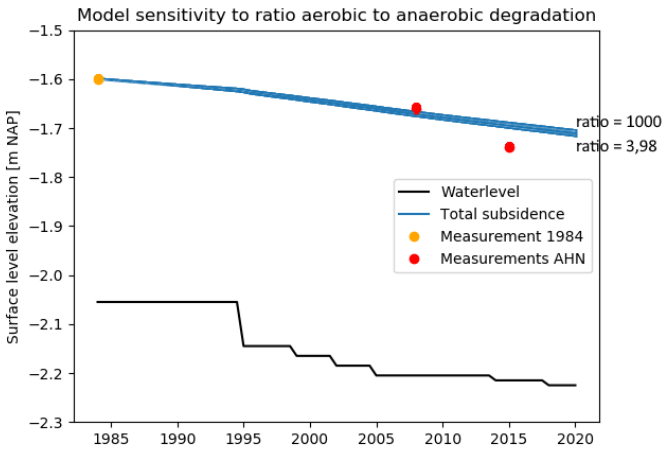

Figure B.24: Modelled results for different values of the ratio aerobic to anaerobic degradation

Water levels

An assumption was used that the average value of the minimum and maximum indicated water levels in the reports from the waterboard was representative for the situation modelled. Here, the influence of this assumption is evaluated. Situations with the minimum and maximum water levels as given in table B.5a are modelled and their results are shown together with the average water level approach as used before, see table B.18 and figure B.25.

Table B.18: Influence water level assumption on model result

	waterlevel situation		
Subsidence component	minimum (highest water level)	average	maximum (lowest water level)
Compression by oxidation [m]	0,101	0,092	0,083
Compression by loading [m]	0,009	0,009	0,008
Compression by anaerobic degradation [m]	0,017	0,019	0,021
Total subsidence [m]	0,0127	0,119	0,112

Only constant minimum and maximum water level values were tested, while in reality this will vary over time. Comparing the three indicated situations over time, not that much variation can be seen on the influence on subsidence. A factor that has influenced this is that the step of water level lowerings have remained the same for all situations.

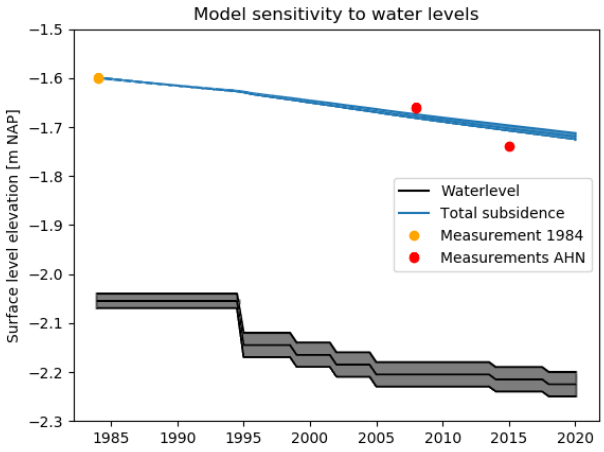

Figure B.25: Modelled results with the minimum, average and maximum water levels indicated as 'vigerende peilen' in the reports from the waterboard

Time step dt

A time step of 0,5 year was used for the results presented in section 8.3. Different values of the time step have been evaluated to determine the sensitivity of this parameter. Table B.19 shows the influence of the time step on the model results.

Table B.19: Influence time step parameter on model result

	dt			
Subsidence component	1 year	0,5 year	1 month	0,5 month
Compression by oxidation [m]	0,09193	0,09186	0,09179	0,09179
Compression by loading [m]	0,00874	0,00870	0,00866	0,00866
Compression by anaerobic degradation [m]	0,01877	0,01889	0,01900	0,01901
Total subsidence [m]	0,11945	0,11945	0,11945	0,11946

As can be seen, the influence on the subsidence is negligible. This is also the reason that no difference could be seen on the plots of the solutions. This plot with the solution space is therefore not included. Using a very small time step leads to long calculation times, while the accuracy only improves little. Therefore the value of 1 or 0,5 year is sufficient.

C

A5 Badhoevedorp

C.1. Subsidence measurements

The subsidence of the embankment measured by the different zakbaken is shown in figure C.1. A large variation in subsidence measured can be seen. The exact locations of the zakbaken are unknown, but it is expected that these locations have had influence on the measured subsidence.

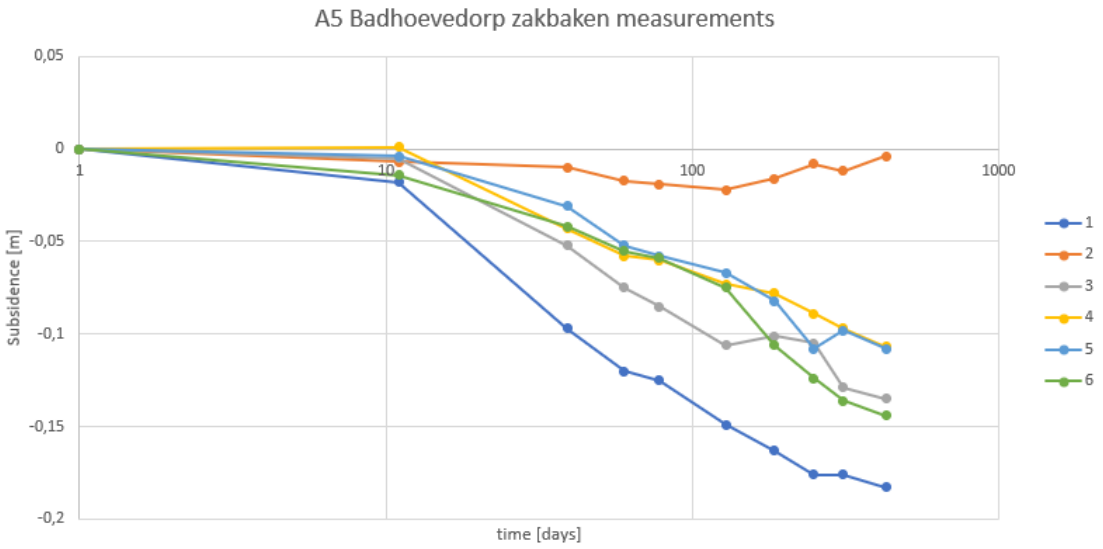

Figure C.1: A5 embankment klink measurements over time

C.2. Model parameters

Model parameters used in the subsidence calculations are indicated in this appendix. Koppejan parameter values are based on triaxial and one-dimensional compression tests executed on soil samples taken from the embankment (Bisschop, 2003). NEN-Bjerrum parameter values were not given in the report but the RR and CR values are calculated based on the Koppejan parameter values with

$$\mathrm{RR} = \frac{\ln 10}{C_p} \qquad \mathrm{CR} = \frac{\ln 10}{C'_p}. \tag{C.1}$$

The value for C_α could not be directly calculated, and thus a value from table 2b from NEN-EN1997-1 (2019) was used.

Table C.1: In-situ density and unit weight of layers of the embankment from (Bisschop, 2003)

Layer	In-situ density [kg/m3]	Unit weight [kN/m3]	Number of samples
0	1581	15,51	10
1	1607	15,77	13
2	1594	15,64	10
3	1603	15,73	10
4	1655	16,24	10
5	1655	16,24	10
6	1717	16,85	10
7	1679	16,47	10
8	1715	16,83	10
9	1721	16,88	10
10	1698	16,66	10
11	1695	16,63	10
12	1745	17,12	10

Table C.2: Range of Koppejan parameters indicated in Bisschop (2003)

Parameter	Minimum	Average	Maximum	Unit	Number of samples
Cp	64,9	88,9	119,0	-	4
Cs	333,3	439,6	555,5	-	4
C'p	22,8	25,0	28,4	-	4
C's	112,4	135,8	158,7	-	4
p_g	33	34	36	kPa	4
c_v (60 kPa)	9,1E-07	9,6E-07	1,0E-06	m^2/s	4

Table C.3: Range of NEN-Bjerrum parameters calculated based on the Koppejan model parameters

Parameter	Minimum	Average	Maximum	Unit	Number of samples
RR	0,03548	0,02590	0,01935	-	-
CR	0,10099	0,09210	0,08108	-	-
Ca		0,005		-	-
p_g	33	34	36	kPa	4
c_v (60 kPa)	9,1E-07	9,6E-07	1,0E-06	m^2/s	4

D

N3 Dordrecht

The first section comprises information regarding the location choice. After this, information about the processing of the SkyGeo measurements and determining the soil profiles is given. Then all input data for the project locations is provided.

D.1. Location choice

The location choice for this project is governed by the availability of data. Information that needs to be available for the analysis is:

- Complete timeseries of SkyGeo measurements (1995 to 2017)
- Geotechnical lab results to determine settlement model parameters
- Indication of soil profile before the construction of the N3 (CPT profile or boorprofile) and the present soil profile

Another restraint is that there is no previous existing embankment at the project locations, for example an old road or harbor area before the construction of the N3. The N3 trajectory can be divided in four different sections, based on the year of construction. Figure D.1 shows for all four section the availability of data and the zones that should be avoided because of a previous loading scenario.

Sections two and four are not used for project locations as there was an indication of previous embankments being present in these sections. Moreover the availability of site investigation data from before the construction of the road is limited. Section one was not chosen as less samples from above the river were analysed in the laboratory compared to section three. It is assumed that soil layers from above and below the river are not comparable.

Section three runs from hectometer poles 3.4 to 6.2. Figure D.1 shows that at the end of this section no soil data from before the construction of the embankment is available. Therefore all project locations were chosen between poles 3.4 and 5.5. Based on availability of the skygeo measurement sets the following three locations were then selected: pole 3.5, pole 4.2 and pole 5.3.

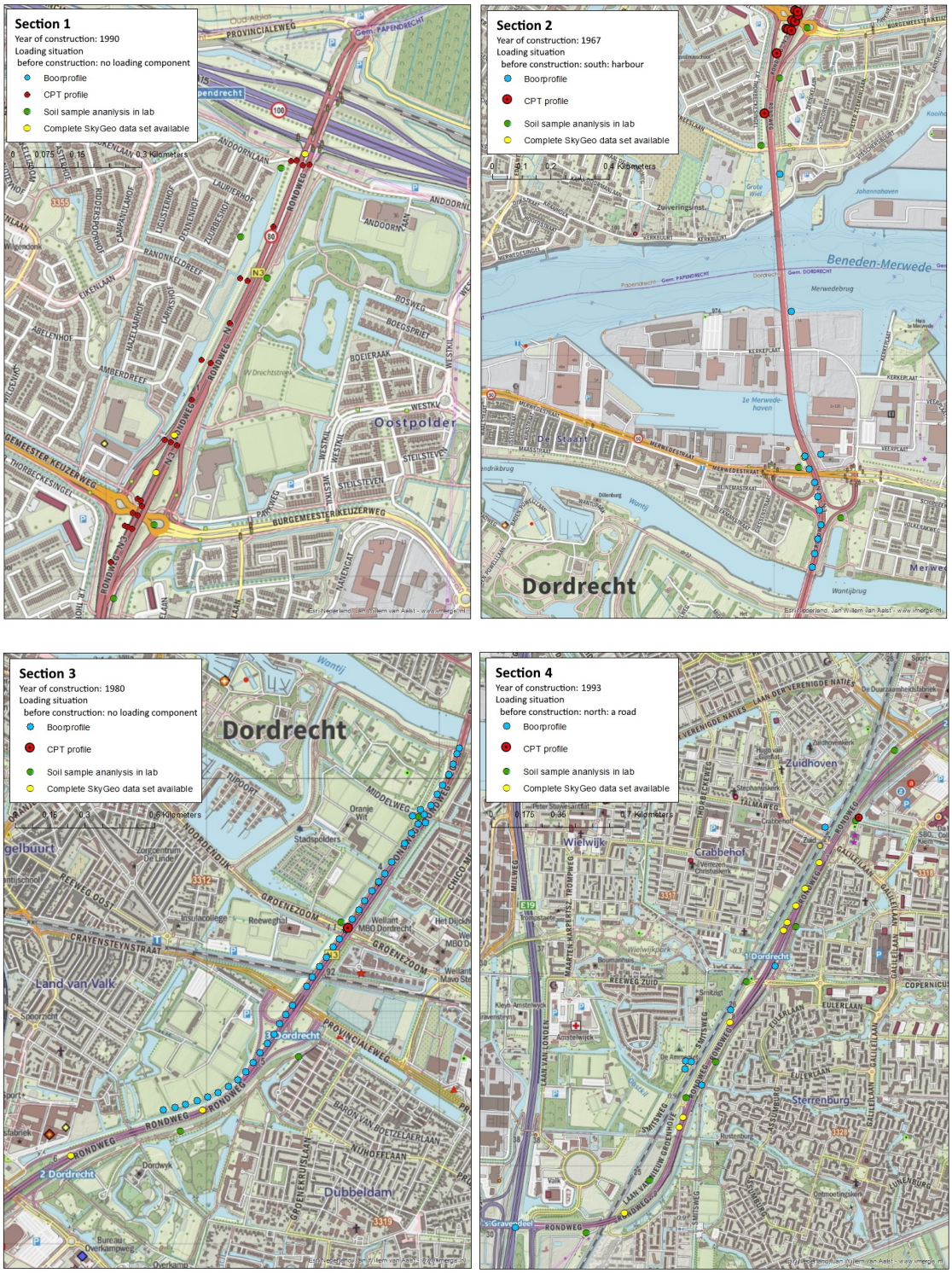

Figure D.1: Four sections of N3 trajectory with available data

D.2. SkyGeo measurements

Subsidence of the N3 is analysed from InSAR data between 1995 and 2017. There are no continuous measurements available. Over time there have been three different measurement periods, of which the second and the third overlap in time. The range of time for each data series is shown in table D.1.

Table D.1: Time characteristics of the three different data series from SkyGeo

Data series	Time start	Time end	Number of measurement points
series 1	4-4-1995	3-1-2001	62
series 2	2-7-2003	8-9-2010	69
series 3	20-6-2010	25-7-2017	99

The three data series do not come from exactly the same location, but three points are selected which lie close to each other. An example of the selection of three data points is shown in figure D.2, where the SkyGeo observation points used for the evaluation at location 1.1 are indicated.

Figure D.2: SkyGeo points available and the three points used to extract data sets indicated for traject 1.1 of the N3

These three data sets are available for all project locations. A similar procedure is followed at each location to come to one data set, where all three are merged together. The procedure is:

- The individual data sets are plotted and a logarithmic trendline is applied.
- The individual sets are manipulated in such a way that their individual logarithmic trendlines all start at zero (zero subsidence).
- The sets are merged together:
  - The starting point of the second data set can be found using the updated logarithmic trendline of the first data set by calculating the starting point of the second trendline with that logarithmic equation.
  - The second and third data sets can be connected based on time, as they have some overlapping measurements.
  - The absolute settlement (in term of subsidence since the start of the construction of the road) at the moment of the last measurement the third data set is determined based on comparison of a recent CPT profile and an old boorprofile or CPT profile. This clearly shows the brought-up anthropogenic soil (sand) and a difference of the level where the soft soil layers start.

D.3. Water level data

The water levels over time have been requested from different water boards along the N3. All project areas fall in the same water level area, and thus only the data available for this area is indicated in table D.2. It can be seen that based on the information available, it seems there has not been a lowering of the groundwater level during the time period evaluated by SkyGeo measurements, but no information is available from before 1999.

Table D.2: Information about the water levels over time, based on information from water boards

Water level area	**Years**	**Vigerend peil [m NAP]**	**Source**
D27.006 (Stadspolders)	2016	-2,00	Waterschap Hollandse Delta - Gebiedsanalyse Dordrecht Stedelijk (2016)
D27.006 (Stadspolders)	1999	-2,00	Waterschap De Groote Waard - Toelichting op het peilbesluit voor het bemalingsgebied STADSPOLDERS (1999)

Geonius reported results from shallow and deeper hydraulic head monitoring wells over time at different locations along the road. The water levels indicated by the deeper monitoring wells were used as hydraulic head for the Pleistocene sandlayers, see table D.3. The water levels indicated by the shallow groundwater level monitoring wells were not used, because it is assumed the water levels from the water board provide a better general estimation.

Table D.3: Phreatic lines used in the calculations for different project locations

Project location	**Phreatic groundwater level [m NAP]**	**Hydraulic head sandlayer**[(a)] **[m NAP]**
3.5	-2.0	-0.40
4.2	-2.0	-0.75
5.3	-2.0	-1.25

(a) Source: Harlaar and Lange (2018) - Appendix 05.02 grondwaterstanden diepe peilbuizen

D.4. Geological profile Deltares

One of the sources of information available for this project is a geological profile constructed by Deltares. This profile is shown in figure D.4, where the hectometer pole numbering indicates the location along the road. Figure D.3 is the legend of the profile.

Figure D.3: Legend for figure D.4

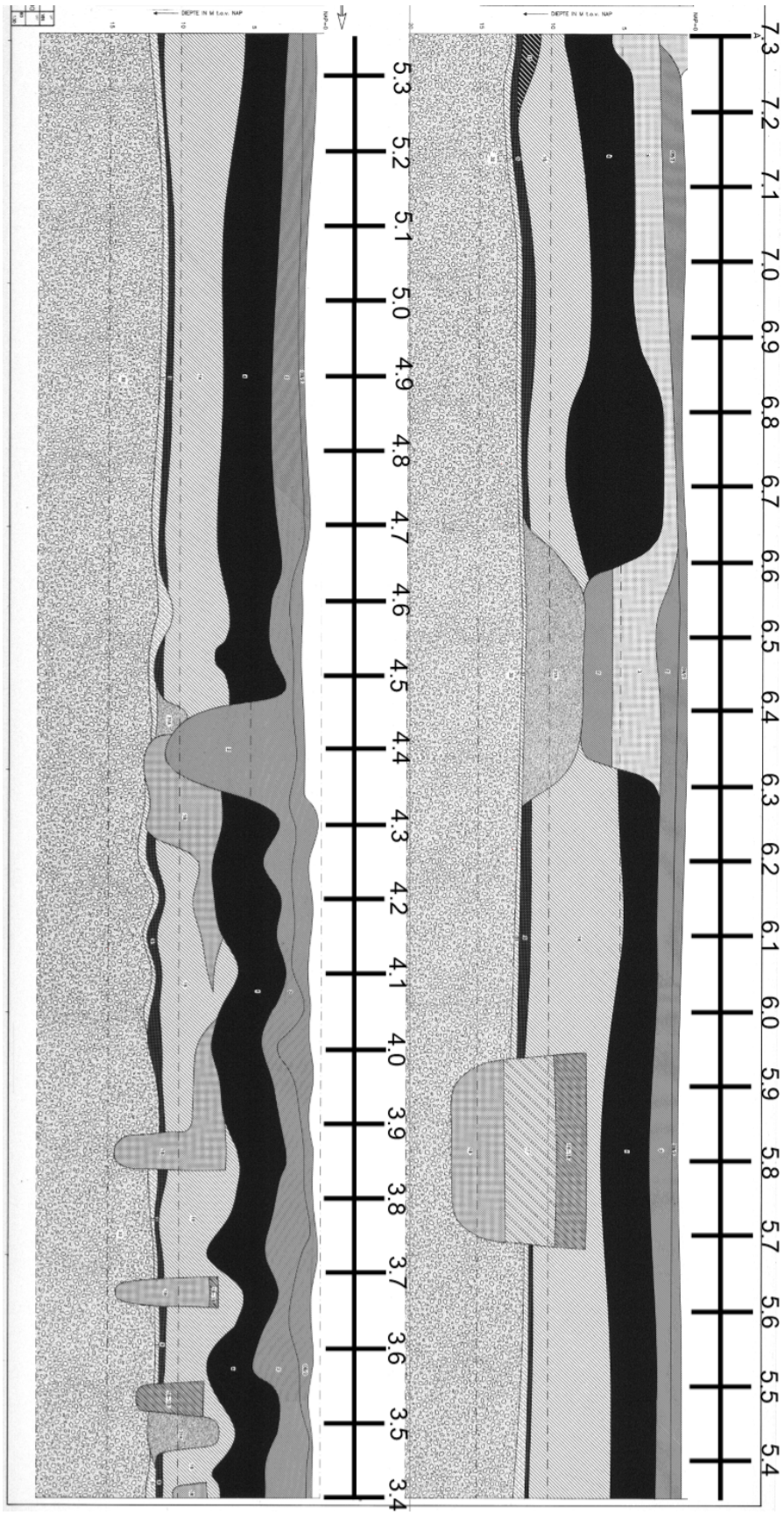

Figure D.4: Geological profile from Deltares showing the middle part of the road (poles 3.4 - 7.3)

D.5. Location 3.5

D.5.1. Soil profiles (before and after construction)

Multiple information sources were used to evaluate the soil profile before and after construction of the road. Figure D.1 indicates multiple boorprofiles executed before the construction of the road being near to this project location. The one closest to location 3.5 was used to evaluate the initial soil profile. The geological profile from Deltares was used to crosscheck this soil profile. A CPT profile from 2018 was used for the evaluation of the change over time. The locations of the profiles used are shown in figure D.5. The profiles themselves are shown in figures D.6 and D.7.

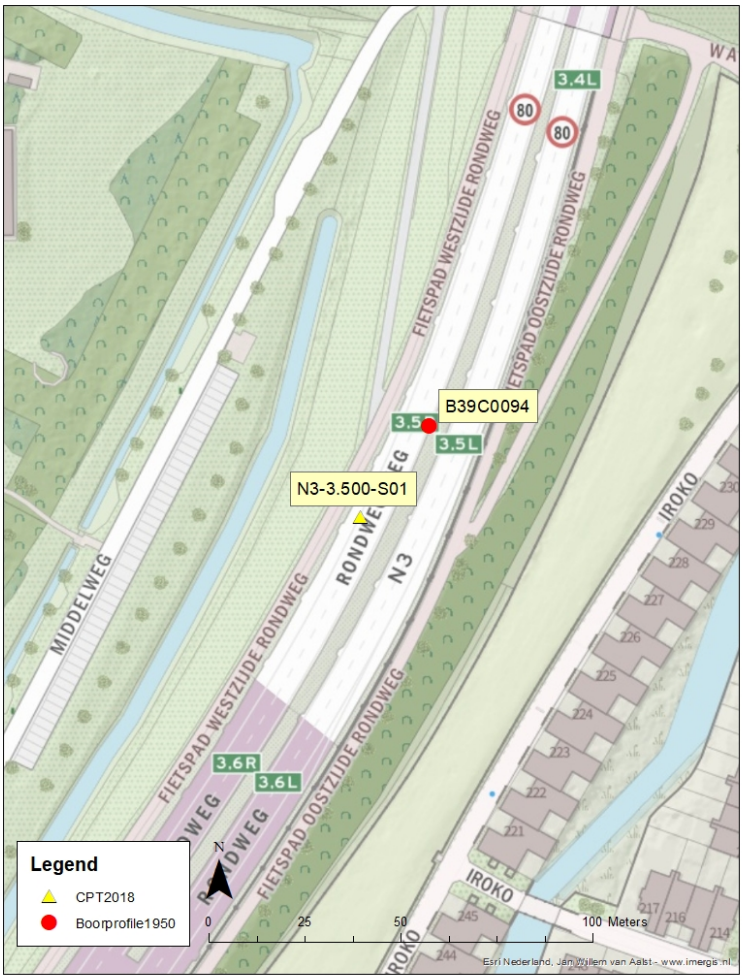

Figure D.5: Overview of locations of soil profiles used for location 3.5

The CPT profile shows the layer of sand that was added as part of the construction of the road. It can be seen that the top of the initial soil profile has been submerged below the water level. Originally the surface level was at -0.81 m NAP (see figure D.6) while the top of this clay layer lies at a deeper level in 2018.

The soil profile as indicated in figure D.8 has been used for as input for the model used in the evaluation. This soil profile is based on the boorprofile, but has a different depth of the sandlayer, based on evaluation of the CPT profile as well.

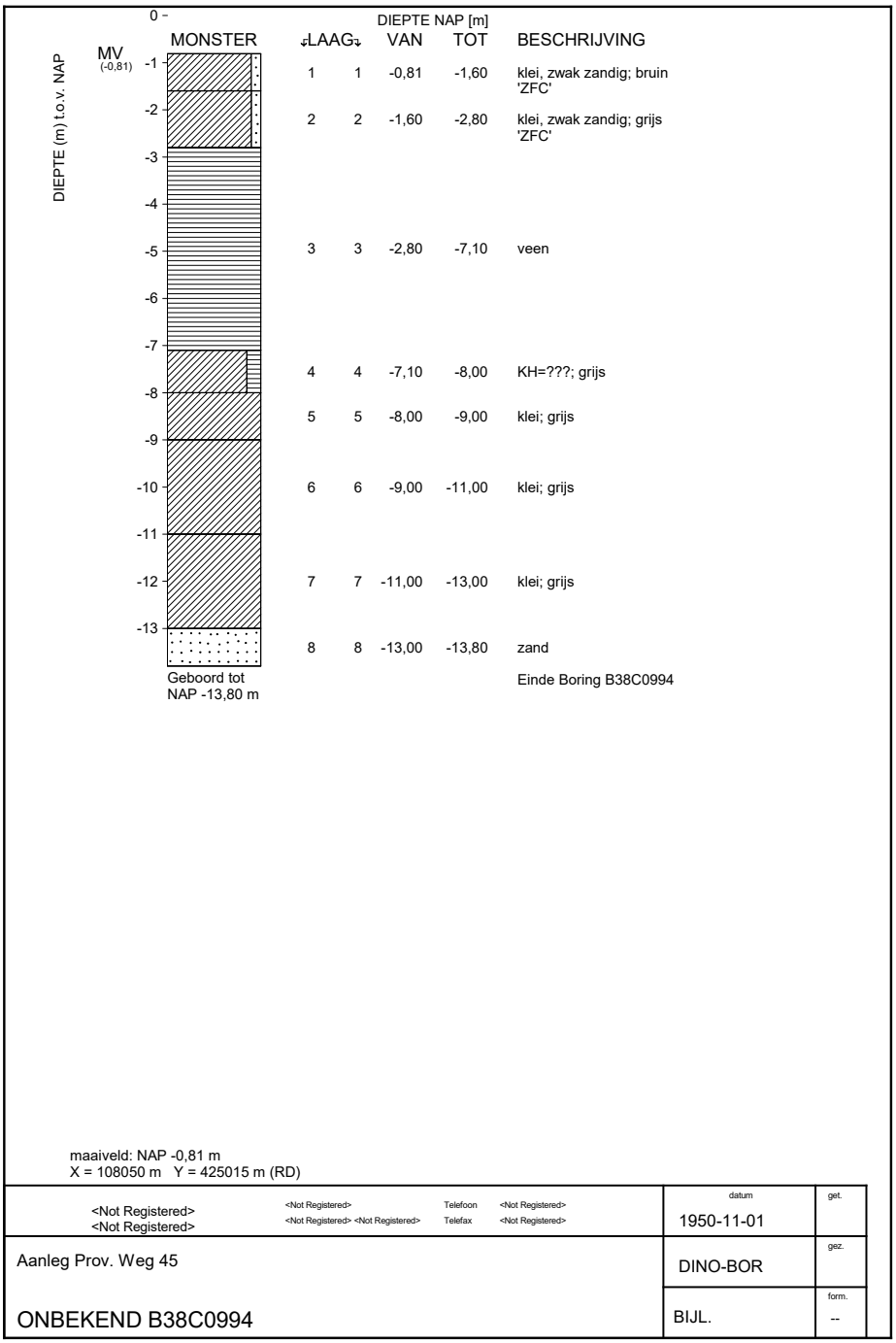

Figure D.6: Boorprofile B38C0094

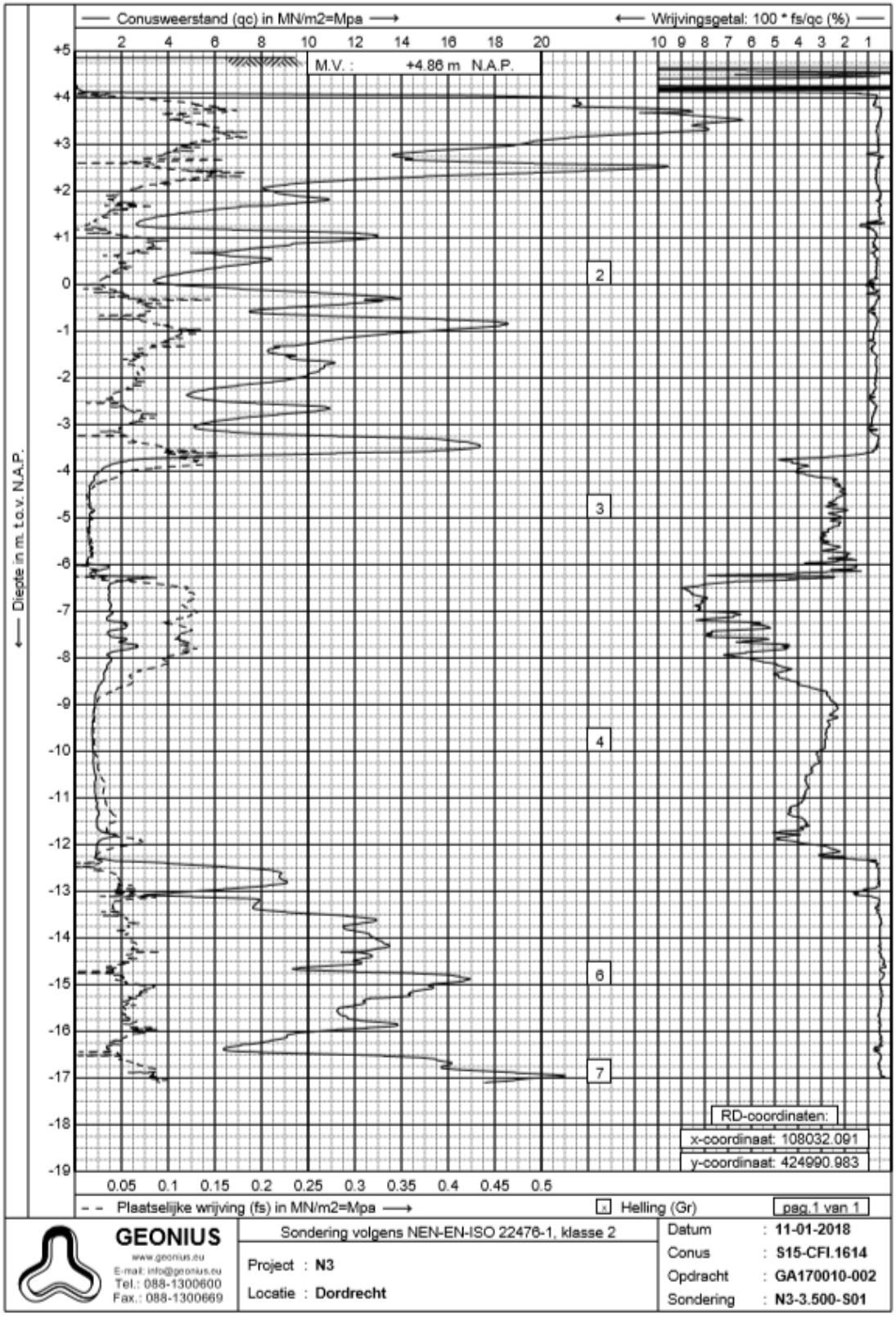

Figure D.7: CPT profile N3-3.500-S01

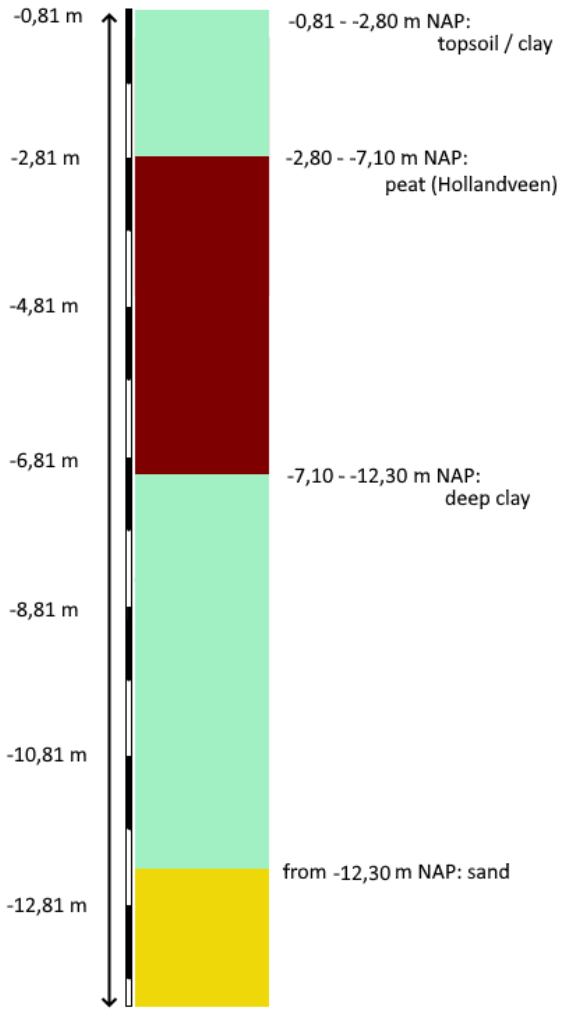

Figure D.8: Initial soil profile used for evaluation location 3.5

D.5.2. Loading situation

Based on the CPT profile and the initial soil profile the loading scenario for location 3.5 was found. It is assumed that there have been four different loading components at this location, forming the construction of the road. These are:

- *Additional clay layer* - Based on a comparison of the thicknesses of the upper clay layer in the initial profile (2m) and the thickness of this layer in the CPT profile from 2018 (2.55m) it is assumed that a clay layer has been put on top of the soil before constructing the road. Furthermore it is assumed that this clay layer is already well compacted and it does not compact any further during the measured time period. This means that the thickness of this additional clay layer is assumed to be 0.55m, to compensate for the difference in thicknesses mentioned before.
- *Sand layer* - A sand layer was used for the construction of the N3. The thickness of this layer was calculated based on the top sand layer shown in the CPT profile and the assumption that the layer itself has not lost volume due to compaction. The thickness is estimated to be 7.85m based on figure D.7.
- *Slag construction element* - Slag was used as part of the foundation for the road. The thickness and unit weight of the slag construction layer is based on an excel sheet from Arcadis with detailed information on road construction elements. The thickness of slag at location 3.5 is 0.465 m and its unit weight is 23 kN/m^3.
- *Asphalt construction element* - Information about the asphalt layer is based on the same excel sheet with detailed information on road construction elements. The thickness of the asphalt layer at location 3.5 is 0.238 m and its unit weight is 18 kN/m^3.

D.5.3. Skygeo measurements

Three separate SkyGeo data sets are available for location 3.5. There might be a small deviation in the exact locations of measured points in the three sets, as explained in D.2. The three individual sets of measurement points are shown in figure D.9. The merged data set is shown in figure D.10.

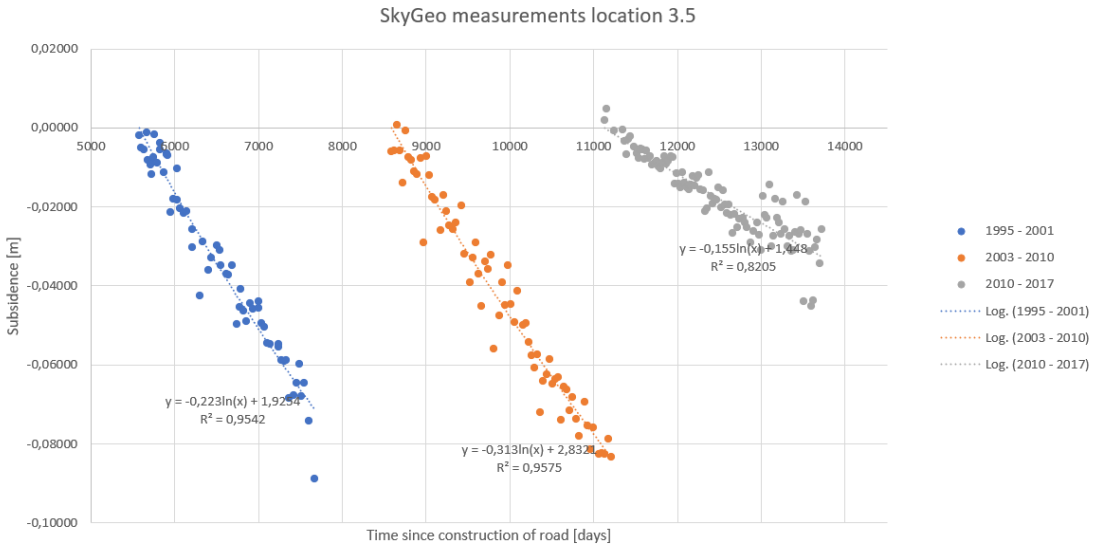

Figure D.9: Individual data sets of SkyGeo subsidence measurement points in time at location 3.5

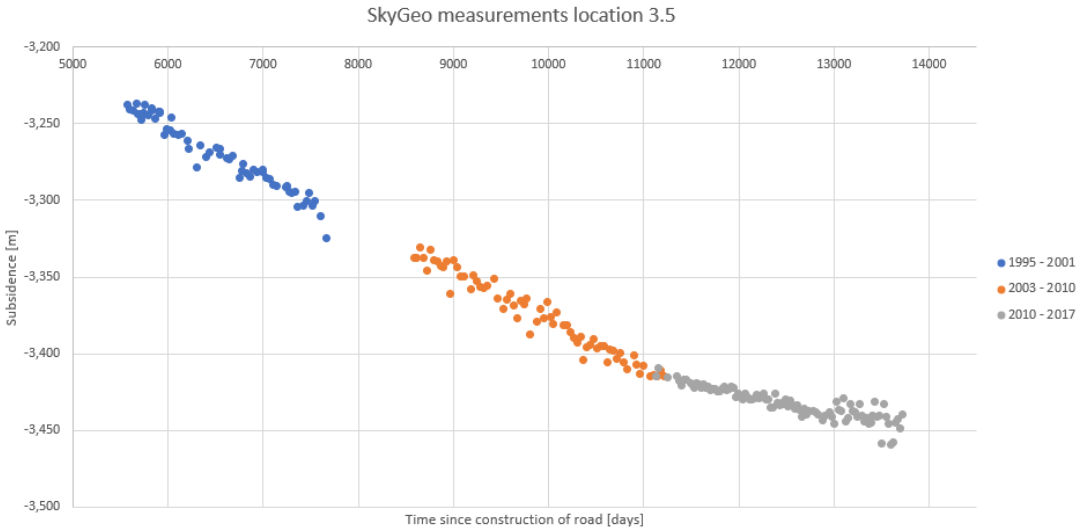

Figure D.10: Merged data set of SkyGeo subsidence measurement points in time at location 3.5

D.6. Location 4.2

D.6.1. Soil profiles (old and new)

The boring closest to location 4.2 together with the historical geological length profile from Deltares were used to evaluate the initial soil profile. A CPT profile from 2018 was used for the evaluation of the change over time. The locations of the profiles used are shown in figure D.11. The profiles themselves are shown in figures D.12 and D.13.

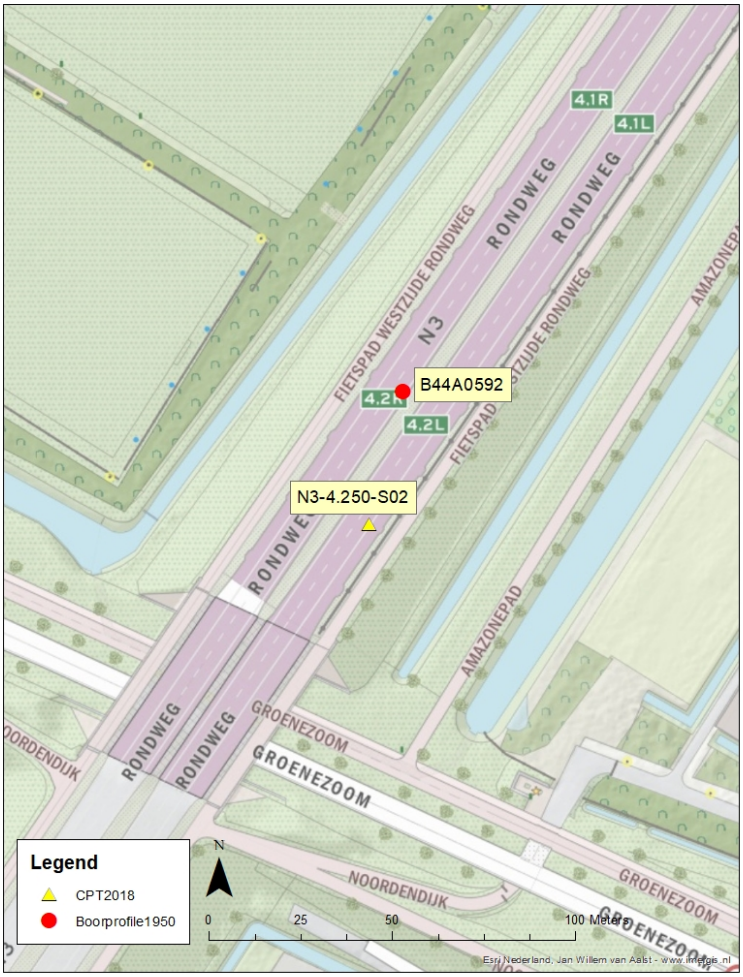

Figure D.11: Overview of locations of soil profiles used for location 4.2

The CPT profile shows the layer of sand that was added as part of the construction of the road. It can be seen that the top of the initial soil profile has been submerged below the water level. Originally the surface level was at -0,71 m NAP (see figure D.12) while the top of this clay layer lies at -3,6 m NAP in 2018 (see figure D.13).

The soil profile as indicated in figure D.14 has been used for as input for the model used in the evaluation. The sequence of soil layers in this profile is based on the geological depth profile from Deltares and the CPT profile. The depths are based on both the boorprofile and the profile from Deltares.

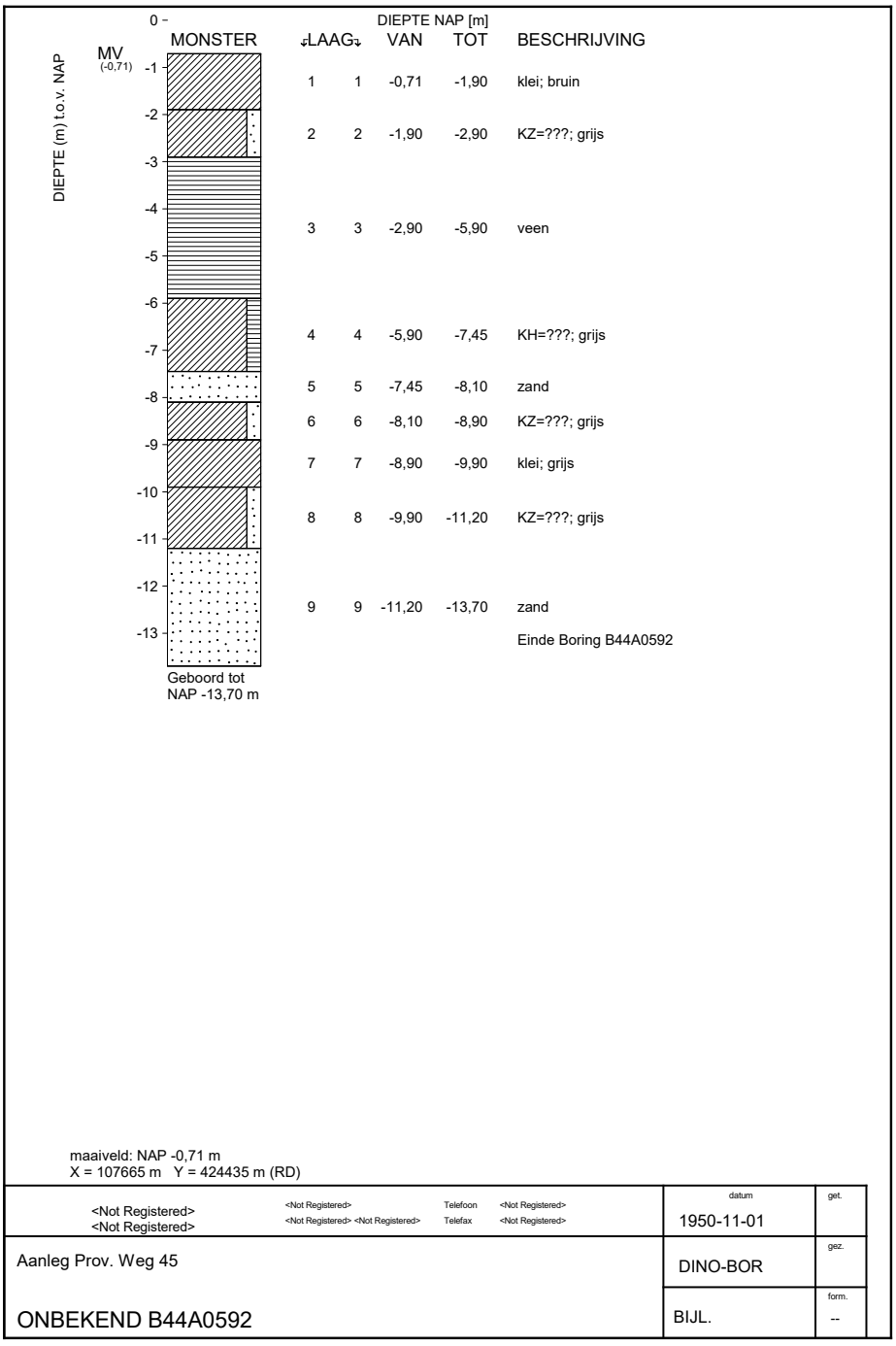

Figure D.12: Boorprofile B44A0591

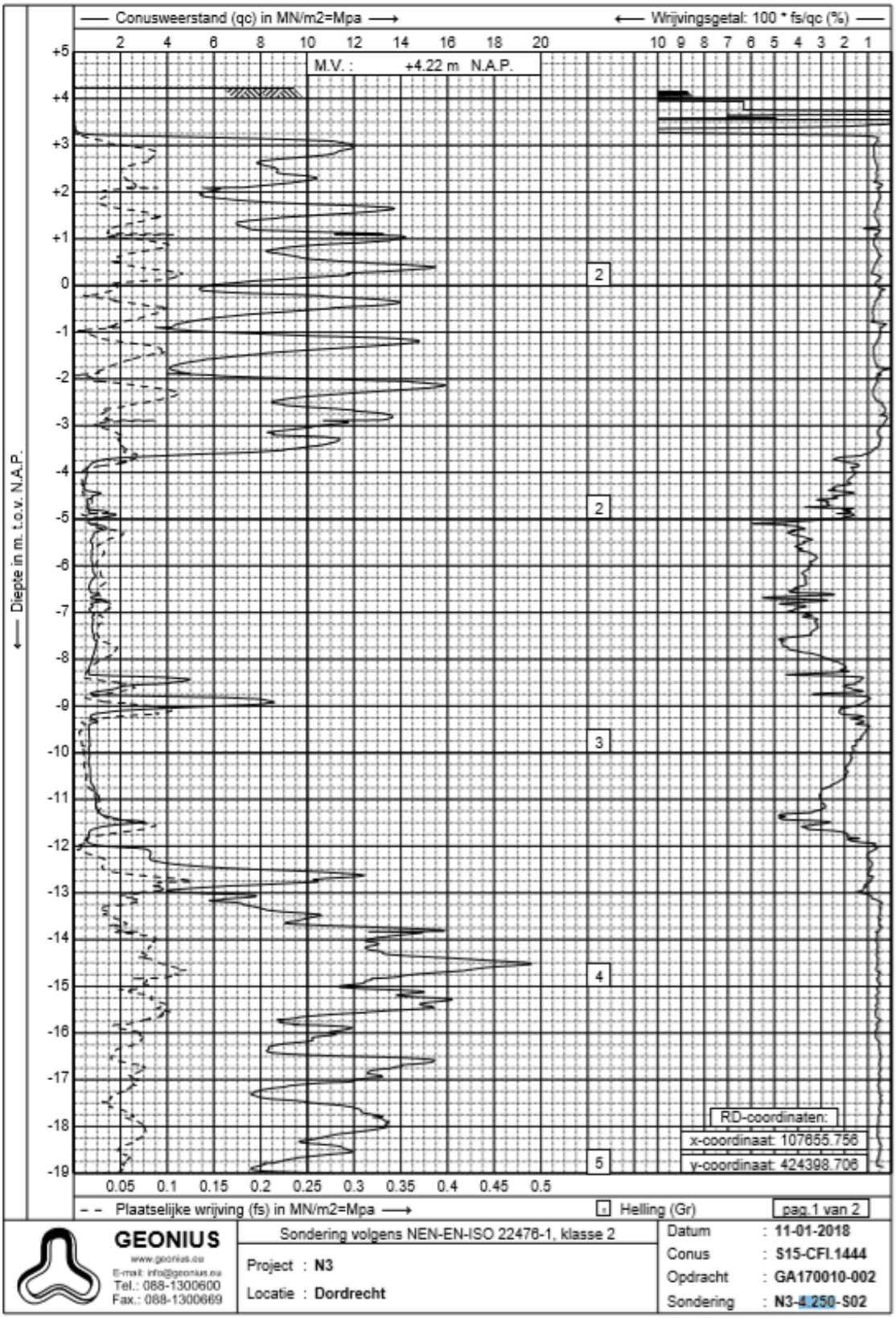

Figure D.13: CPT profile N3-4.250-S02

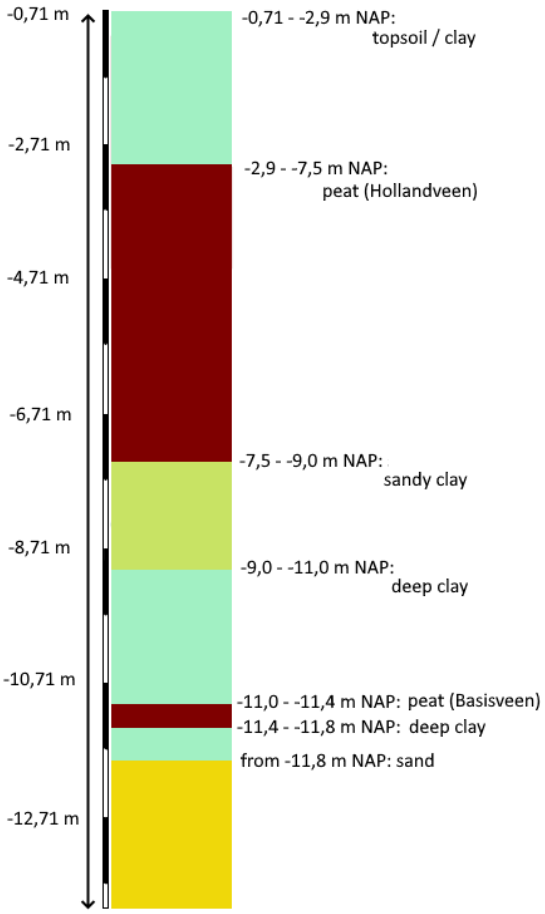

Figure D.14: Initial soil profile used for evaluation location 4.2

D.6.2. Embankment

Based on the CPT profile and the initial soil profile the total thickness of the embankment for location 4.2 was found. It is assumed that there have been three different loading components at this location, forming the construction of the road. These are:

- *Sand layer* - A sand layer was used for the construction of the N3. The thickness of this layer was calculated based on the top sand layer shown in the CPT profile and the assumption that the layer itself has not lost volume due to compaction. The thickness is estimated to be 6,8 m based on figure D.13.
- *Slag construction element* - Slag was used as part of the foundation for the road. The thickness and unit weight of the slag construction layer is based on an excel sheet with detailed information on road construction elements. The thickness of slag at location 4.2 is 0,433 m and its unit weight is 23 kN/m^3.
- *Asphalt construction element* - Information about the asphalt layer is based on the same excel sheet. The thickness of the asphalt layer at location 4.2 is 0,244 m and its unit weight is 18 kN/m^3.

D.6.3. Skygeo measurements

Three separate SkyGeo data sets are available for location 4.2. There might be a small deviation in the exact locations of the measurements in the three sets, as explained in D.2. The three individual sets are shown in figure D.15. The merged data set is shown in figure D.16.

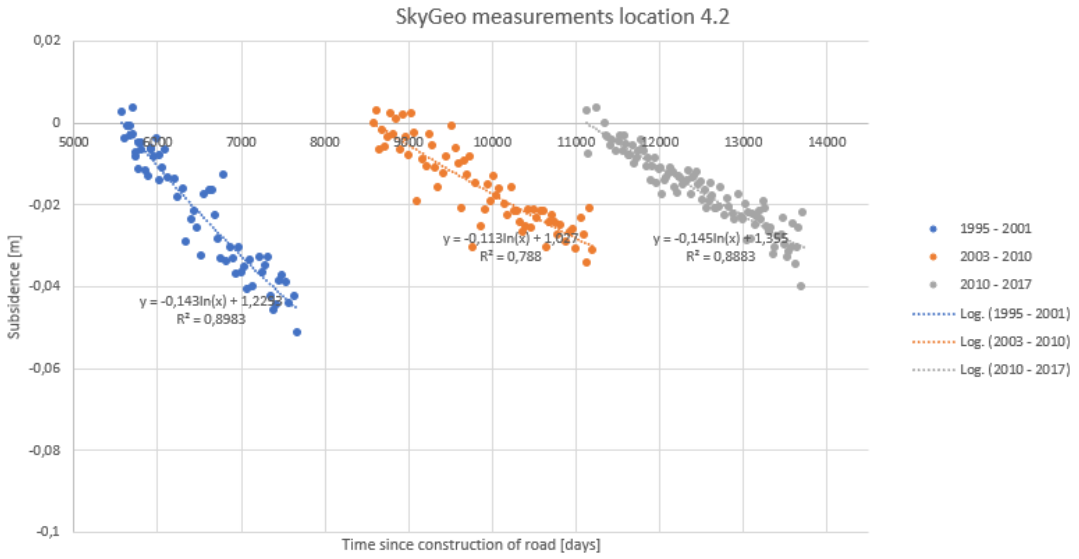

Figure D.15: Individual data sets of SkyGeo subsidence measurement points in time at location 4.2

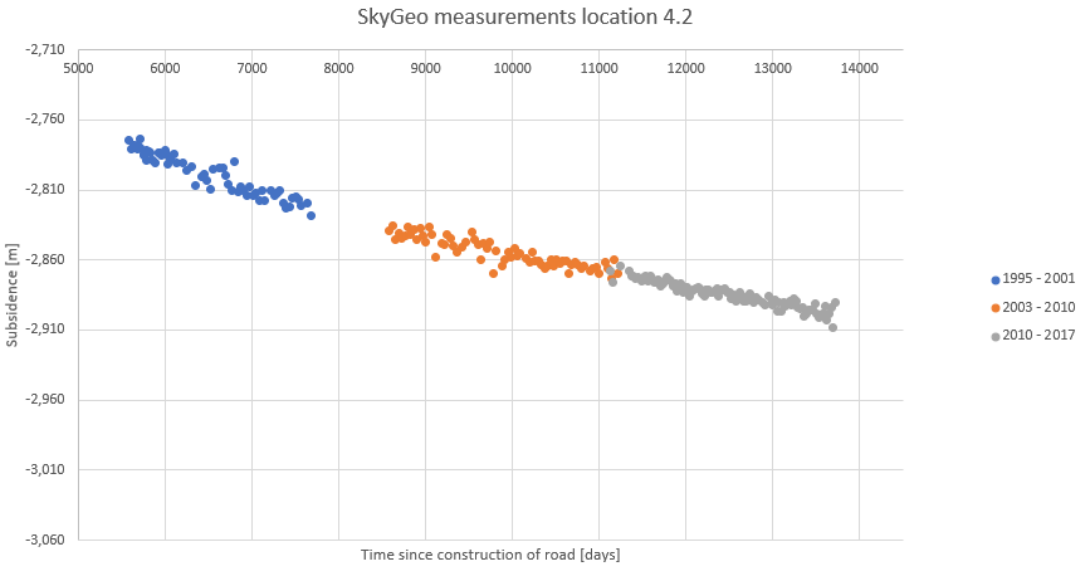

Figure D.16: Merged data set of SkyGeo subsidence measurement points in time at location 4.2

D.7. Location 5.3

D.7.1. Soil profiles (old and new)

The boring closest to location 5.3 together with the historical geological length profile from Deltares were used to evaluate the initial soil profile. A CPT profile from 2018 was used for the evaluation of the change over time. The locations of the profiles used is shown in figure D.17. The profiles themselves are shown in figures D.18 and D.19.

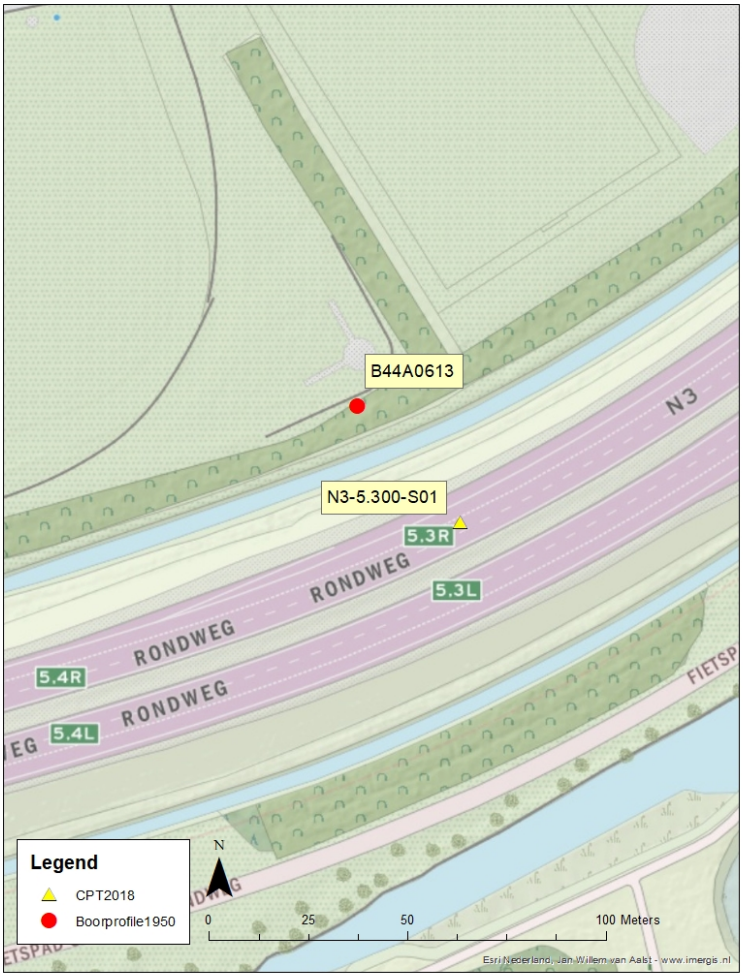

Figure D.17: Overview of locations of soil profiles used for location 5.3

The CPT profile shows the layer of sand that was added as part of the construction of the embankment. It can be seen that the top of the 'old' soil layers has been submerged below the water level. Originally the surface level was at -0,86 m NAP (see figure D.18) while the top of this clay layer lies at -2,9 m NAP in 2018 (see figure D.19).

The soil profile as indicated in figure D.18 has been used for as input for the initial soil profile. The sand layer above the peat layer is not present in the geological profile of Deltares. Therefore this was not included in the initial soil profile. The initial soil profile is shown in figure D.20.

D.7.2. Loading situation

Based on the CPT profile and the initial soil profile the loading scenario for location 5.3 was found. It is assumed that there have been three different loading components at this location, forming the

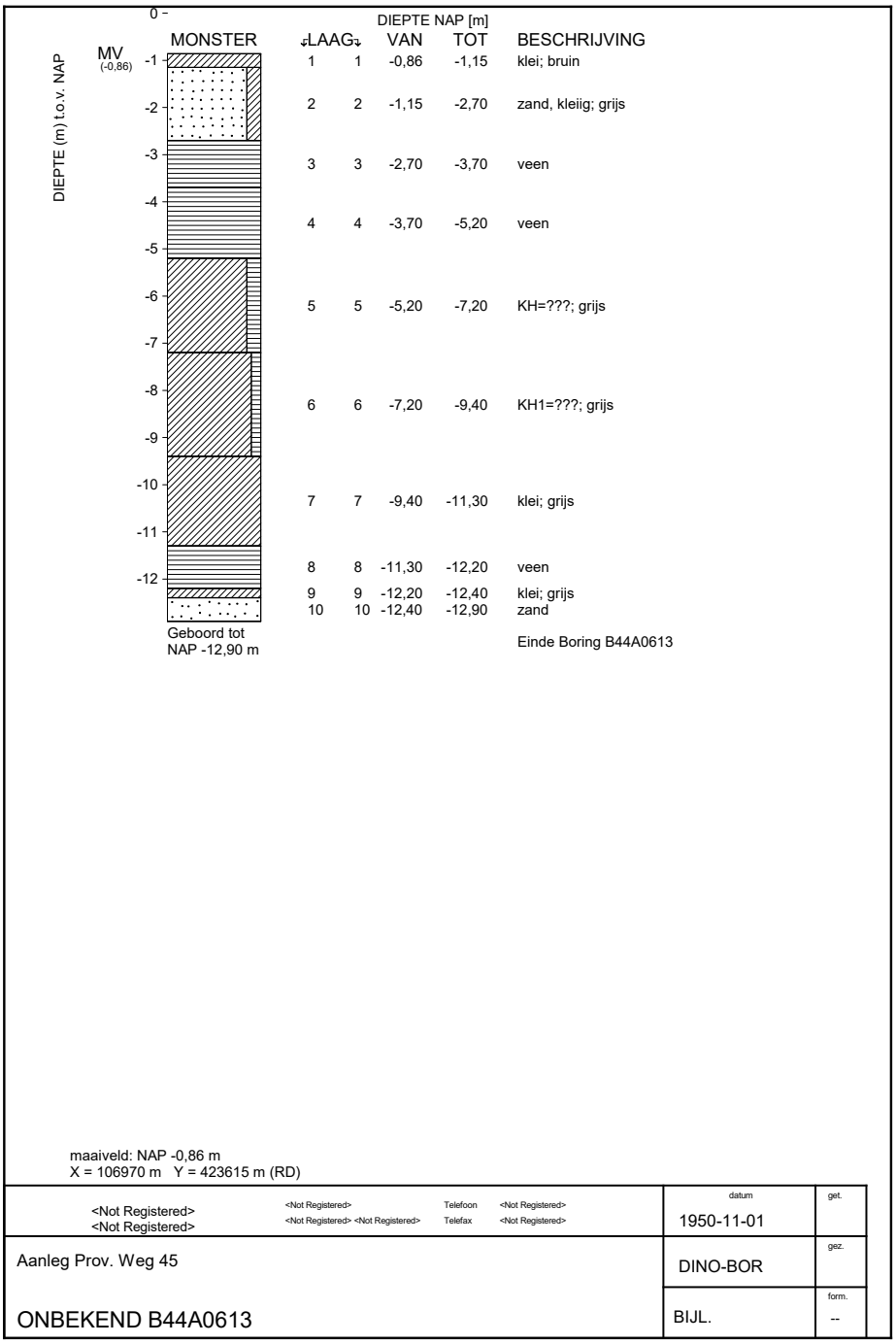

Figure D.18: Boorprofile B44A0613

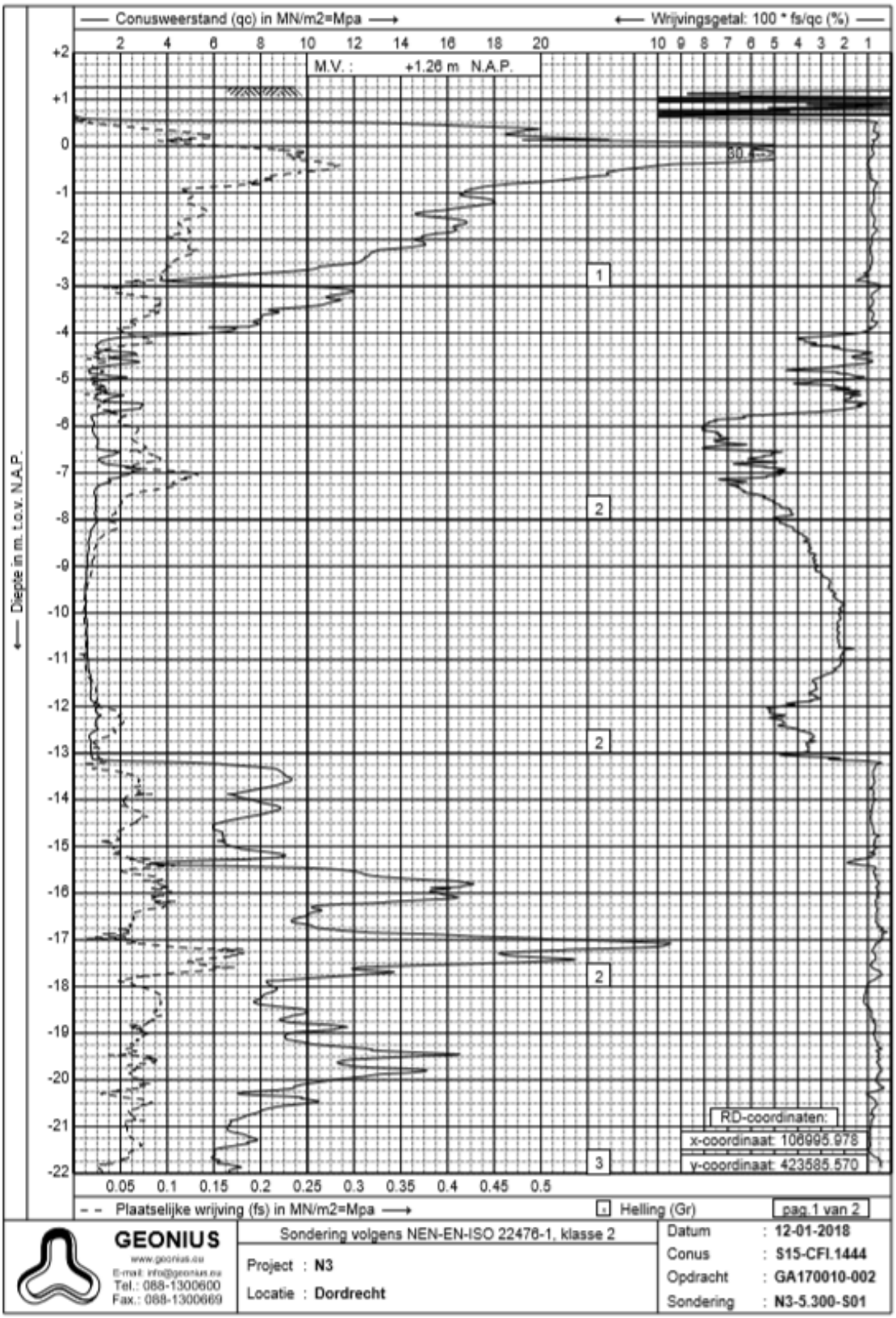

Figure D.19: CPT profile N3-5.300-S01

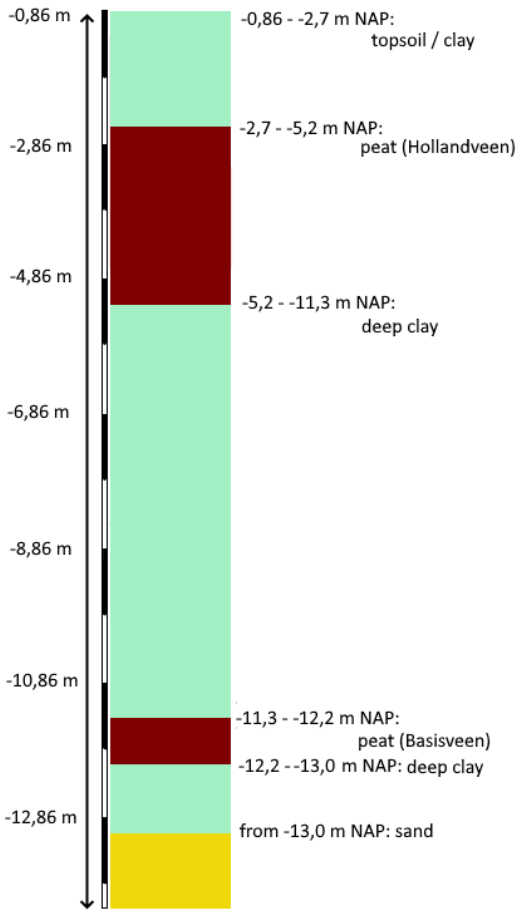

Figure D.20: Initial soil profile used for evaluation location 5.3

construction of the road. These are:

- *Sand layer* - A sand layer was used for the construction of the N3. The thickness of this layer was calculated based on the top sand layer shown in the CPT profile and the assumption that the layer itself has not lost volume due to compaction. The thickness is estimated to be 4,6 m based on figure D.19.
- *Slag construction element* - Slag was used as part of the foundation for the road. The thickness and unit weight of the slag construction layer is based on an excel sheet with detailed information on road construction elements. The average thickness of slag at location 5.3 is 0,397 m and its unit weight is 23 kN/m^3.
- *Asphalt construction element* - Information about the asphalt layer is based on the same excel sheet. The thickness of the asphalt layer at location 5.3 is 0,237 m and its unit weight is 18 kN/m^3.

D.7.3. Skygeo measurements

Three separate SkyGeo data sets are available for location 5.3. There might be a small deviation in the exact locations of measured points in the three sets, as explained in D.2. The three individual sets are shown in figure D.21. The merged data set is shown in figure D.22.

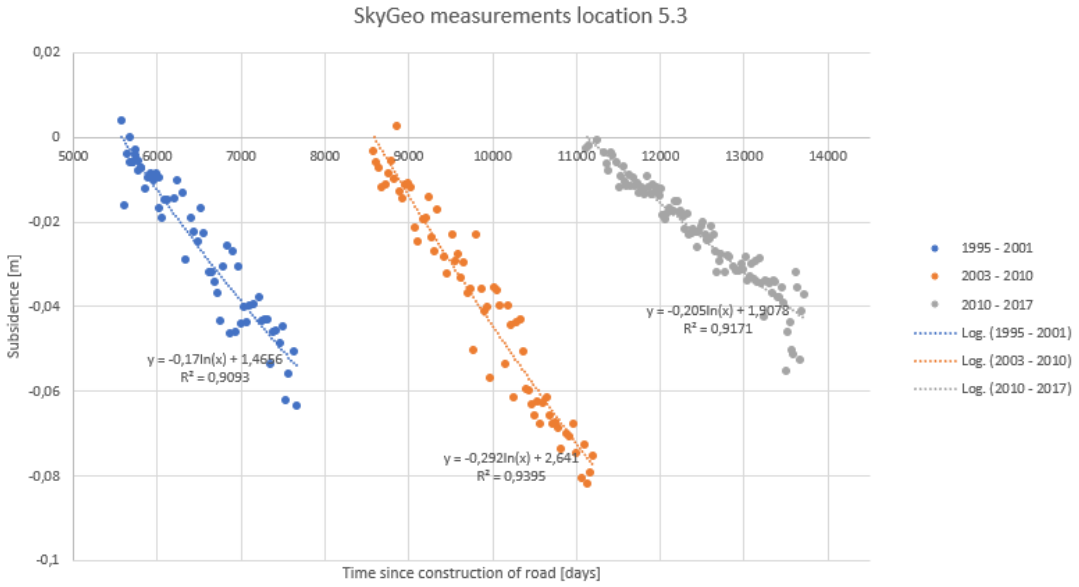

Figure D.21: Individual data sets of SkyGeo subsidence measurement points in time at location 5.3

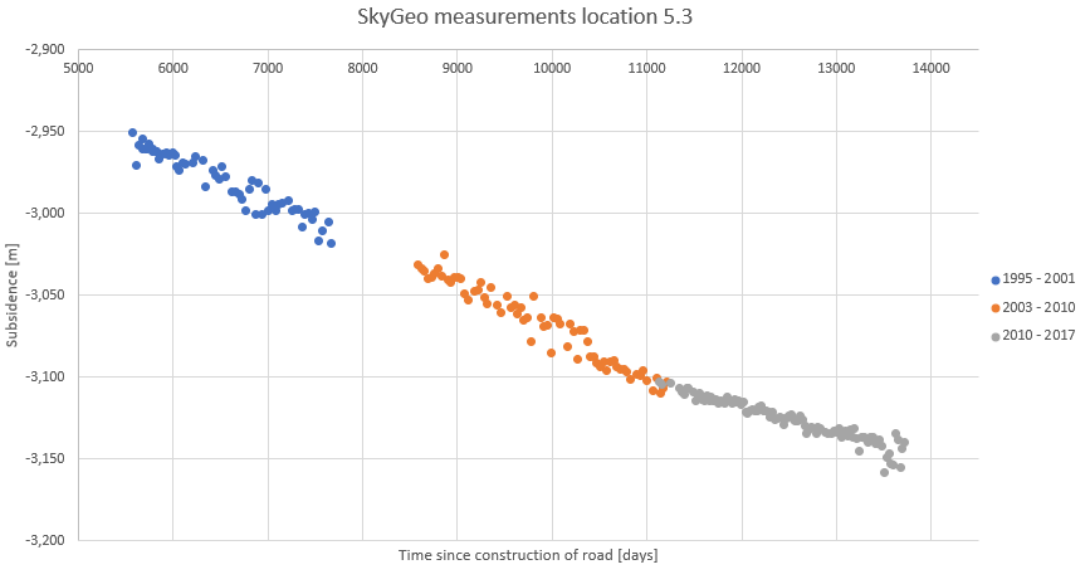

Figure D.22: Merged data set of SkyGeo subsidence measurement points in time at location 5.3

D.8. Soil layers and parameters

In 2018 soil samples were taken for laboratory testing. The locations of the samples are indicated with a green dot in figure D.1. It is assumed that these samples are representative for the initial situation of the soil layers, as the samples are taken next to the road. Test results from laboratory tests on these samples are used to estimate input parameters for the settlement and consolidation models. Different steps were taken to come to the values used.

Not all test results were used in this analysis. The samples from above the river (poles 0.4 to 2.9) and on the other outer end of the trajectory were excluded (poles 8.3 - 9.7). This lead to a data set of 9 locations and 19 samples in total.

Three sources were used to analyse the characterisation of the soil layers. In the laboratory report description of the soil of the samples were given. The depth and location were given as well, and thus the soil layer from which the sample was taken could be estimated based on the geological profile. For all samples density was plotted versus water content, see figure D.23. This shows a clear distinction between the two distinguished soil types (clay and peat).

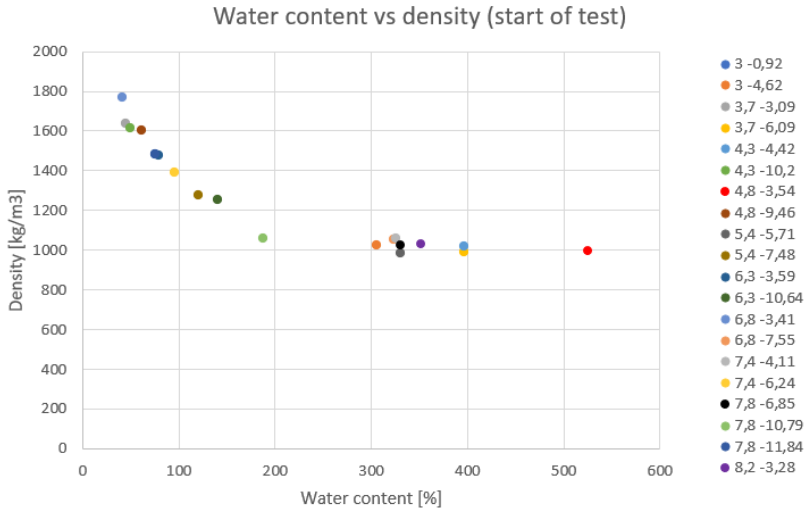

Figure D.23: Water content versus density for soil samples. Legend indicates location (hectometer pole) along the N3 and the depth were the sample was taken.

Using the geological profile from Deltares and the available site investigation data it is assumed that the soil profiles at all project locations can be represented using combinations of five different soil layers. These are a topsoil/clay layer, peat layer (Hollandveen), a deeper clay layer, a deeper peat layer (Basisveen) and a sandy clay layer which is only present at location 4.2. For these five soil types input parameters for the models have been calculated based on laboratory results.

D.8.1. Coefficient of consolidation

The results of the $\sqrt{t}$ method analysis of the coefficient of consolidation for all samples are plotted in figure D.24. The trend lines for the peat layers indicate a decreasing value of c_v with a higher stress level, as expected. For the clay layers there is a large variation in the measured values. For these layers no decreasing trend of c_v with increasing stress level was found. Only one measurement was available for the c_v of the topsoil layer, so no trend line could be plotted.

The consolidation coefficients used were calculated with the following methodology:

- *Topsoil clay layer:* Only one measurement was available, this value is used.
- *Peat layers:* The initial consolidation coefficient is calculated using the trend lines from figure D.24 and an estimate of the initial stress in the soil layer at the project locations.

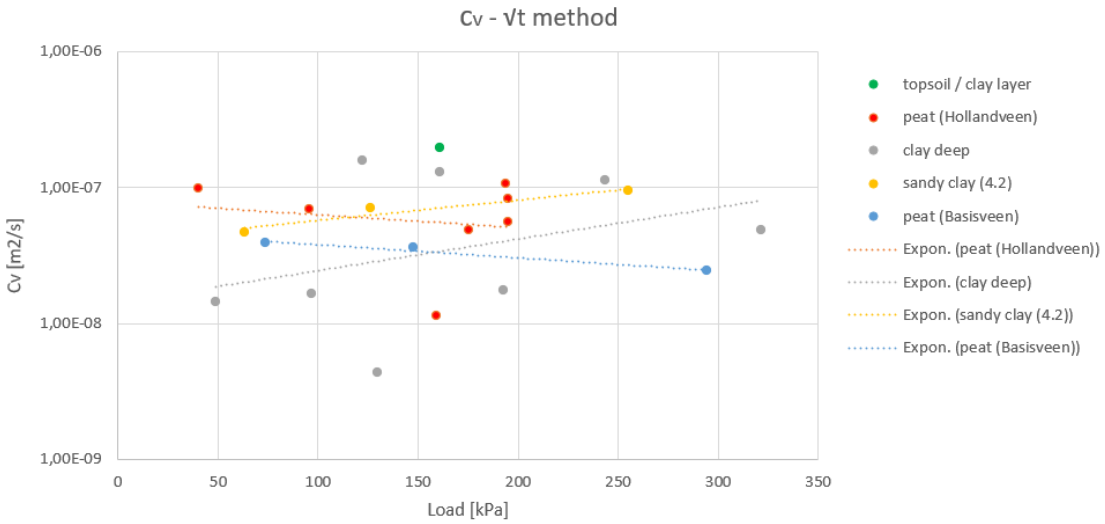

Figure D.24: Coefficient of consolidation lab results ($\sqrt{t}$ method) for the five different soil types.

- *Clay layers:* No clear trend of c_v and load is visible from figure D.24. Therefore the average value of all measured consolidation coefficients of the specified layer is used.

Table D.4 shows the consolidation coefficient values used for the different layers at the project locations.

Table D.4: consolidation coefficients for soil layers at project locations

Location 3.5	c_v [m^2/s]	**Location 4.2**	c_v [m^2/s]	**Location 5.3**	c_v [m^2/s]
Topsoil / clay	1,95E-07	Topsoil / clay	1,95E-07	Topsoil/clay	1,95E-07
Peat (Hollandveen)	8,80E-08	Peat (Hollandveen)	8,77E-08	Peat (Hollandveen)	8,76E-08
Deep clay	1,55E-08	Sandy clay	6,76E-08	Deep clay	1,55E-08
		Deep clay	1,55E-08	Peat (Basisveen)	3,65E-08
		Peat (Basisveen)	3,70E-08	Deep clay	1,55E-08
		Deep clay	1,55E-08		

D.8.2. Settlement model parameters

Model parameters for the different settlement models are indicated for each sample in the laboratory report. In this study average values of multiple samples are used. Tables D.5, D.6 and D.7 show values of settlement model parameters for all soil layers. For parameters c, CR, C_α, C'p and C's the values for the fifth loading step of the laboratory tests were used. It was calculated that this load step best represented the loading situation at the project locations.

Table D.5: abc isotache model parameters based on laboratory test results

Soil layer	**a**	**b**	**c**
Topsoil / clay	0,00965 (4)	0,03503 (3)	0,00125 (3)
Peat (Hollandveen)	0,03134 (8)	0,23990 (8)	0,01646 (8)
Deep clay	0,01928 (4)	0,14412 (5)	0,00651 (5)
Peat (Basisveen)	0,07060 (1)	0,21512 (1)	0,01226 (1)
Sandy clay	0,03380 (1)	0,07986 (1)	0,00296 (1)

(..) indicates the number of samples used to calculate the average value

Table D.6: NEN-Bjerrum model parameters based on laboratory test results

Soil layer	**RR**	**CR**	C_α
Topsoil / clay	0,01859 (4)	0,11752 (4)	0,00284 (3)
Peat (Hollandveen)	0,08201 (8)	0,42361 (8)	0,03185 (8)
Deep clay	0,03278 (5)	0,28741 (5)	0,01320 (5)
Peat (Basisveen)	0,07520 (1)	0,32519 (1)	0,02415 (1)
Sandy clay	0,02101 (1)	0,15468 (1)	0,00604 (1)

(..) indicates the number of samples used to calculate the average value

Table D.7: Koppejan model parameters based on laboratory test results

Soil layer	**Cp**	**Cs**	**C'p**	**C's**
Topsoil / clay	139,03 (4)	1337,85 (4)	31,35 (4)	48,23 (4)
Peat (Hollandveen)	50,79 (8)	114,95 (8)	6,30 (8)	84,83 (8)
Deep clay	55,00 (5)	270,36 (5)	9,26 (5)	140,20 (5)
Peat (Basisveen)	18,30 (1)	74,30 (1)	7,90 (1)	97,10 (1)
Sandy clay	37,60 (1)	350,30 (1)	15,80 (1)	45,80 (1)

(..) indicates the number of samples used to calculate the average value

D.8.3. Pre-overburden pressure

The POP values were calculated for the soil layers based on the preconsolidation pressure from the laboratory tests and the calculated effective stress in the soil profile. Because of the uncertainty of the outcomes, rounded average values were used. Moreover, the calculation of the POP for the deep peat layer (basisveen) lead to impossible (negative) values. Therefore the same POP value as for the Hollandveen peatlayer was used in calculations. All POP values are shown in table D.8.

Table D.8: POP values used for soil layers

Soil layer	**POP [kPa]**
Topsoil / clay	8 (12)
Peat (Hollandveen)	8 (24)
Deep clay layer	13 (5)
Peat (Basisveen)	8 (3)
Sandy clay	5 (3)

(..) indicates the number of samples used to calculate the average value

D.9. Percentage primary - secondary calculation

Three calculations are excecuted for different soil types based on Koppejan model parameters from NEN table 2b from NEN-EN1997-1 (2019). The soil types together with the parameters are shown in table D.9.

Table D.9: Three soil layers with Koppejan parameters from table 2b NEN-EN1997-1 (2019)

Soil layer	**C'p**	**C's**
peat - not preloaded - weak	7,5	30
clay - weak sandy - moderate	20	240
clay - clean - moderate	15	160

The ratio of the primary and secondary contribution is determined by these parameters. Primary settlement is determined by the parameter 1/C'p and secondary settlement is determined by the parameter log(10000)/C's = 4/C's. This can be calculated for all layers to find the range of the percentages that can be expected, see table D.10.

Table D.10: Calculated values ratio primary-secondary settlement

	1/C'p	**4/C's**	**Estimation ratio primary-secondary to be expected**
peat - not preloaded - weak	2/15	4/30	50 - 50
clay - weak sandy - moderate	1/20	4/240	75 - 25
clay - clean - moderate	1/15	4/160	72 - 27

E

Markermeerdikes

E.1. Location choice

In total four locations have been evaluated in this study, 3 project locations of the dike and 1 grass plot of the hinterland. The locations were selected based on availability of information. Different sources of information are considered: archaeological data, crest height measurements and information regarding soil profiles.

Availability of archaeological data determined the project locations to a large extent. A first location selection was based on the availability of old maps of the dike sections. The numbering of the dike segments was different in the past from the current system. Therefore, an archaeological map with the old numbering system was essential to select a project location and to be able to compare it with the current state of the dike. An example of such an old map is shown in figure E.1. Locations 1 and 2 were then chosen because a letter from 5 January 1918 provided useful information on the state of the dike at these locations. Also soil profiles which are expected to be from around this period of time were found for these two locations. Location 3 was chosen because of the availability of a soil profile from 1916.

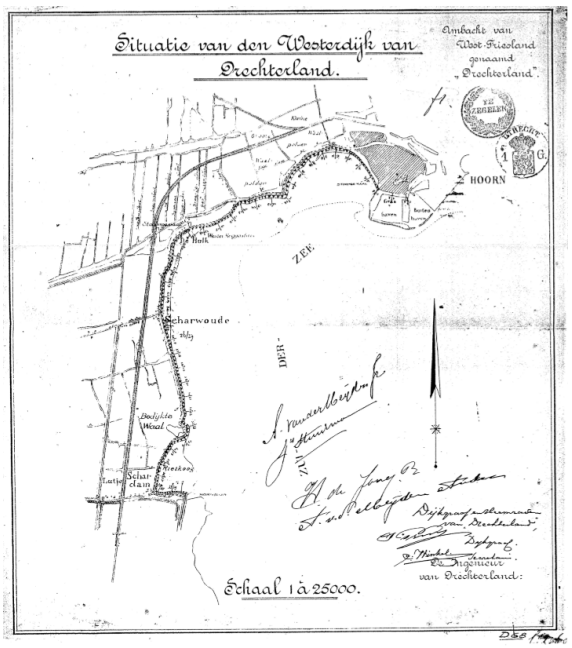

Figure E.1: Old map with dike section numbering from Hoorn to Lutjeschardam

E.2. Crest height measurements

Crest height measurements are available for all sections of the dike between Hoorn and Katwoude. For some sections the earliest mentioned measurement dates from 1916. The latest measurement comes from 2011. For all project locations the crest height measurements over time are plotted below, see figure E.2. Different sources of information have been used, also indicated in the graphs.

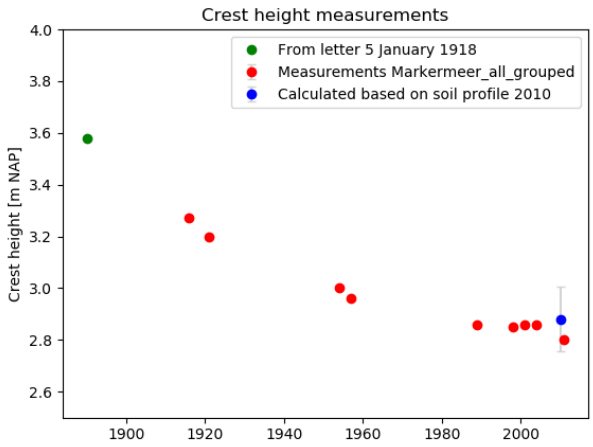

(a) Locations 1 and 2: dike 20 dp 14-29

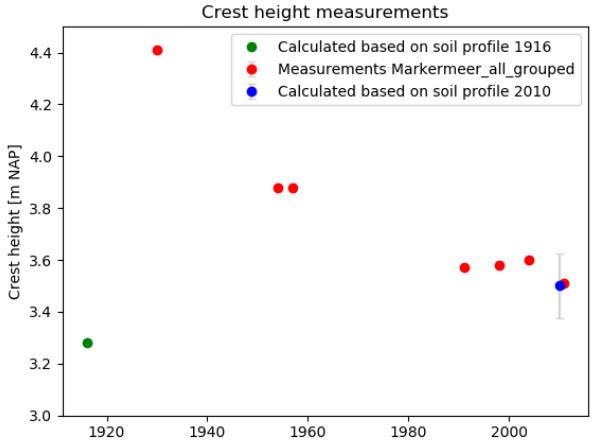

(b) Location 3: dike 23 dp 42-66

Figure E.2: Crest height over time

It is assumed that the measurements were taken by levelling and that the error of the measurements is approximately 4 mm (average of the general range of 3 to 5 mm mentioned by Vermilion Energy (2020)). The error bars of these measurement points cannot be seen on the scale of the figure. Another measurement point is based on the crest soil profile provided, an error range of 0,125 m is considered here, as this value is calculated based on measurements on paper where a 0,5 mm error in the reading means a difference of 0,125 m in reality.

E.3. Project location 4: subsidence measurements and water level data

A plot of grassland was used as project location to also evaluate land subsidence of the hinterland of the dike. AHN measurements are the only surface elevation measurements available for these locations. The average surface level indicated by boorprofiles in and around the project location is used as start point. For both datasets the mean value of the digital terrain model (DTM) at the project area was calculated in QGIS.

Table E.1: Height measurements based on boorprofiles, AHN2 and AHN3 data series

Project Location	Data series	Average measurement points [m NAP]	Uncertainty [m]
4	1994	-1,995	± 0,155
	AHN2 (2011)	-2,025	± 0,15
	AHN3 (2016)	-2,045	± 0,15

The uncertainty of AHN measurements has been evaluated in the Krimpenerwaard appendix section B.2. The uncertainty indicated for the surface level in 1994 is based on the variation encountered for the boorprofile surface levels in/around the project area.

Information regarding the maintained groundwater level over time is provided by the waterboard of the area (HHNK). The sources used to come to this estimation of the groundwater level over time are shown in table E.2. The change of this level over time is shown in figure E.3. Unfortunately the year of the boorprofiles limit the time that can be evaluated with the model, this time period is indicated with the two black lines.

Table E.2: Sources used by HHNK contact person to come to an overview of maintained water levels over time

Name
G. De Vries Az., De zeeweringen en waterschappen van Noord-holland (Haarlem 1864)
G. De Vries Az., De zeeweringen en waterschappen van Noord-holland, tweede druk bew. door J.W.M. Schorer (Haarlem 1894)
G. De Vries Az., De zeeweringen en waterschappen van Noord-holland, derde druk bew. door D. Kooiman (Alphen aan den Rijn 1936)
Jaarboekje voor de provincie Noord-Holland voor de andere jaren dan 1864, 1894 en 1936.
HHNK, Besluit CHI, Peilbesluit Zeevang (2014)

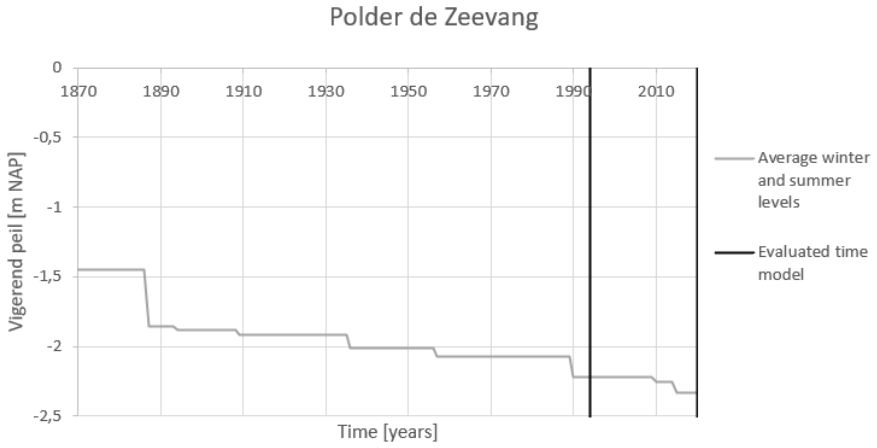

Figure E.3: Maintained water level over time, based on HHNK reports

E.4. Soil profile

Project location 1

Crest height measurements at this location start at 1916, but another source of information also provided knowledge on the new constructed crest height in 1890. Therefore this height is used as the initial crest height, the starting point for the calculations. To calculate subsidence from different components, an estimation of the initial soil profile is constructed. This is done based on several sources of information:

- Soil profile of the crest of the dike in 1918, based on boorprofiles, shown in figure E.4.
- Soil profile of the crest of the dike in 2010, based on CPT and boorprofiles, shown in figure E.5.
- Geological profile description of the subsurface by Deltares (Vos and de Vries, 2016)

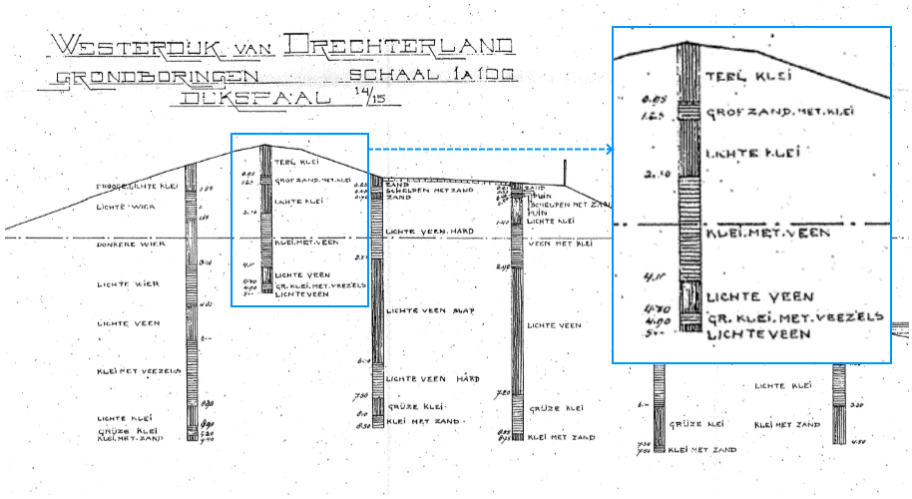

Figure E.4: Boorprofiles 1918 project location 1

An overview of the assumed soil profile over time is shown in figure E.6. Information regarding soil layers shown with black lines is based on site investigation or documents directly. When additional assumptions or calculations are used to come to the constructed profile, these layers are shown with green lines. In the figure the terminology as in the geotechnical profile provided by the Alliantie Markermeerdijken is used. The assumptions used are listed below:

- The upper limit of the Pleistocene sand layer as indicated in the soil profile from 2010 has not changed over time. In other words, it is expected that the level of this sand layer is the same in 1890, 1918 and 2010. The level is assumed to be around -16,75 m NAP, based on the geotechnical profile provided by Alliantie Markermeerdijken.
- The Calais sand layers have not changed in thickness over time. The clay layers below the sand calais layers have changed in thickness, but this is negligible over the time period considered.
- The 'clay with peat' layer indicated in the boorprofile from 1918 is interpreted as part of the Hollandveen layer.
- The boorprofile of the crest of the dike in 1918 reached only to -1,70 m NAP. Therefore the border between the Calais clay layer and the Hollandveen layer has to be estimated. The estimated depth is -4,78 m NAP. This is based on three things:
  - An average depth of the top of the Calais clay layers in the boorprofiles next to the crest (in front and behind the crest). This would indicate a depth of -4,52 m NAP.

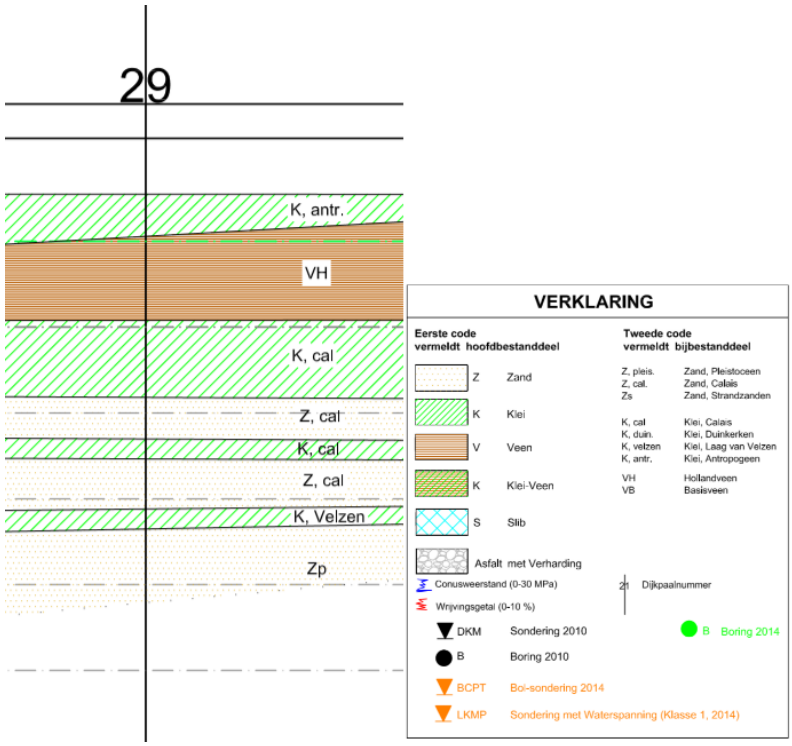

Figure E.5: Soil profile project location 1 based on site investigation 2010

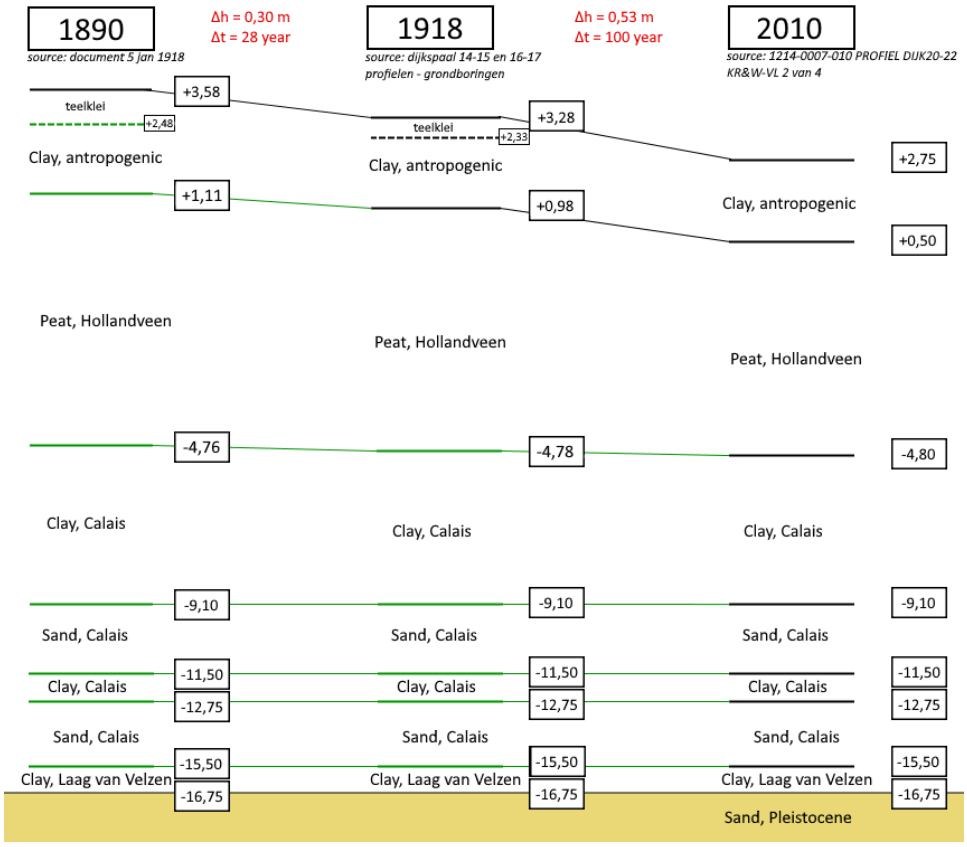

Figure E.6: Estimation soil profile over time location 1: dike 20, pole 29 (not to scale)

  - Mentioned depth of the top of the Wormer clay layers indicated in a letter from 5 January 1918. This would indicate a depth between -3,82 and -5,32 m NAP.
  - Logical thinking, following after the previous mentioned assumptions. Since the subsidence processes between 1918 and 2010 are assumed to be mostly creep and degradation of organic material, it makes sense that most the peat layer has caused most of the subsidence. This is because peat has a higher value of C_α and includes organic material. Therefore, a depth of -4,52 m NAP seems to be too high (as then most subsidence between 1918 and 2010 would originate from the layers below the peat layer).

- It is assumed that the upper soil layer indicated in the boorprofile from 1918 is the layer that was constructed in 1890. The soil type indicated in the boorprofile is 'teelklei', which is interpreted as an organic clay layer.
- Subsidence between 1890 and 1918 originates from a subsidence component of the already existing structure and a subsidence component of the newly applied soil layer in 1890. A ratio between these two components has been assumed. This is that 50% of the subsidence is related to processes regarding the constructed soil layer itself (shrinkage, compression by its own weight) and 50% is related to subsidence from the already existing structure (compression by loading, aerobic/anaerobic degradation of SOM).
  - Through this ratio, the initial thickness of the applied soil layer can be calculated.
  - The other subsidence is divided between the different soil layers:
    - ◇ It is assumed that 75% of the settlement originates from the peat layer
    - ◇ It is assumed that 25% of the settlement originates from the other soil layers
- All calculations/levels originating from the boorprofiles or other information from 1918 are corrected with 0,02 cm to account for the correction of the NAP level in 2005.

Project location 2

The same sources of information are available for project location 2 as for project location 1. To calculate subsidence from different components, an estimation of the initial soil profile is constructed. This is done based on several sources of information:

- Soil profile of the crest of the dike in 1918, based on a boorprofile of the crest, shown in figure E.4.
- Soil profile of the crest of the dike in 2010, based on CPT and boorprofiles, shown in figure E.5.
- Geological profile description of the subsurface by Deltares

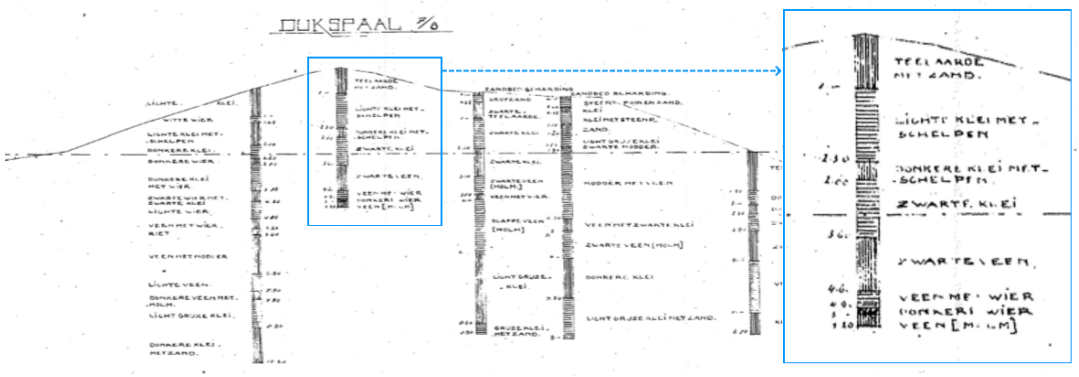

Figure E.7: Boorprofiles 1918 project location 2

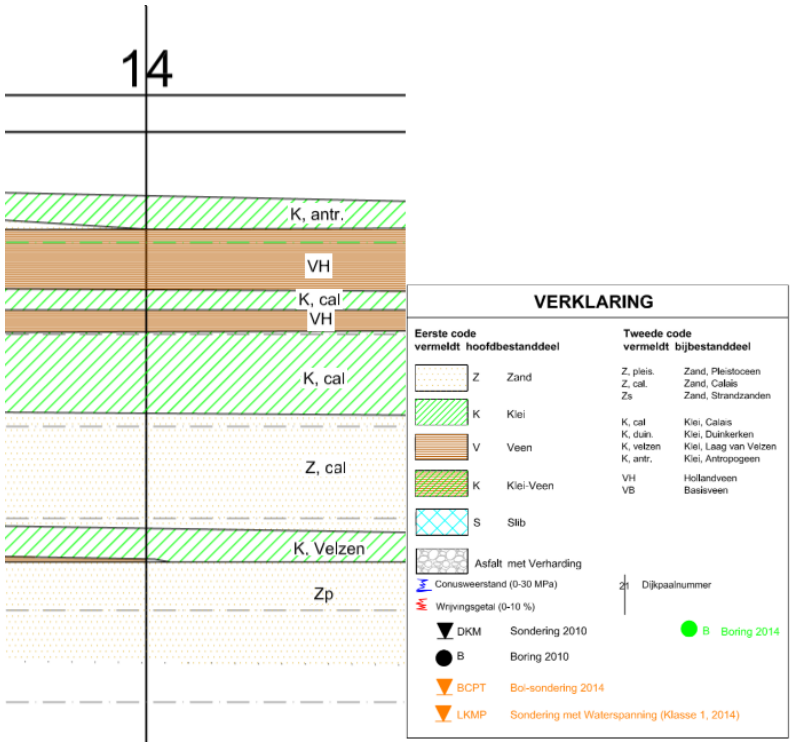

Figure E.8: Soil profile project location 2 based on site investigation 2010

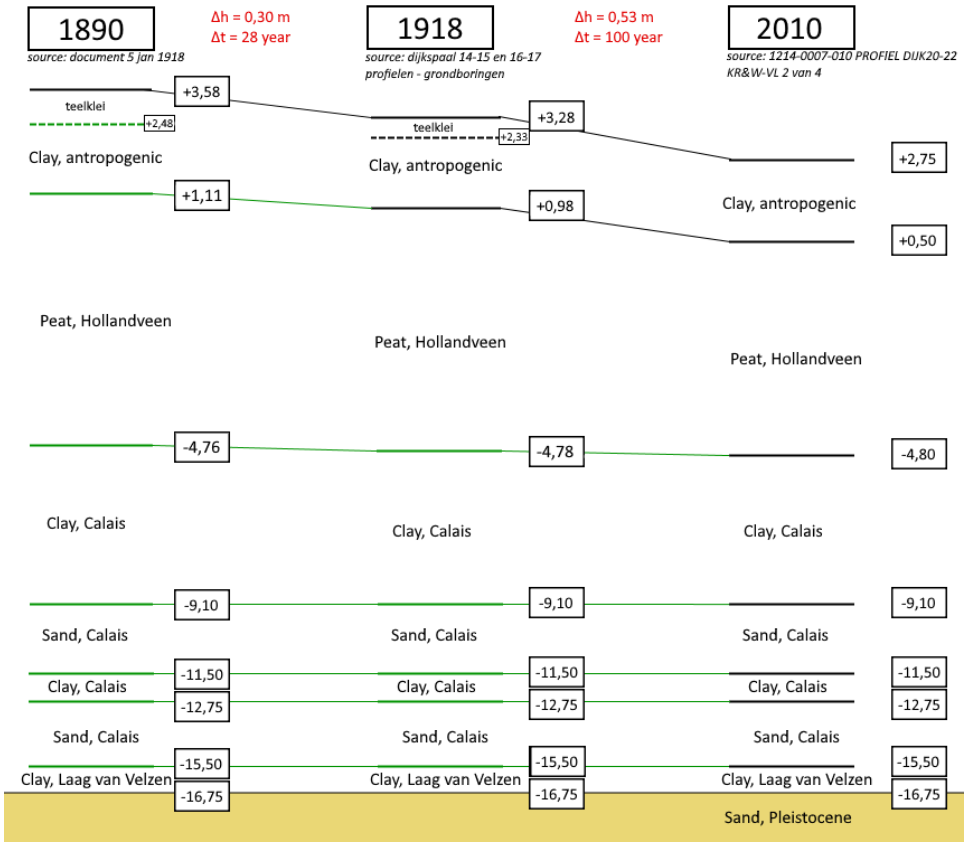

Figure E.9: Estimation soil profile over time location 2: dike 20, pole 14 (not to scale)

An overview of the assumed soil profile over time is shown in figure E.9. This figure uses the same meaning of black and green lines as for project location 1, where black lines indicate information is based on site investigation or documents directly and green lines mean additional assumptions or calculations are used to come to the constructed profile. The assumptions used are listed below:

- The upper limit of the Pleistocene sand layer as indicated in the soil profile from 2010 has not changed over time. In other words, it is expected that the level of this sand layer is the same in 1890, 1918 and 2010. The level is assumed to be around -17,50 m NAP, based on the geotechnical profile provided by Alliantie Markermeerdijken.

- The Calais sand layer has not changed in thickness over time. The clay layer below the sand layer has changed in thickness, but this is negligible over the time period considered.

- The 'black clay' and 'dark clay with shells' layers indicated in the boorprofile from 1918 are interpreted as part of the Hollandveen peat layer. This is done because otherwise the top of the peat layer in the boorprofile from 1918 lies below the top of the peat layer indicated in the soil profile from 2010, which is unrealistic.

- The boorprofile of the crest of the dike in 1918 reached only to -1,90 m NAP. Therefore the border between the Calais clay layer and the Hollandveen layer has to be estimated. The estimated depth is -4,98 m NAP. This is based on three things:

  - An average depth of the top of the Calais clay layers in the boorprofiles next to the crest (in front and behind the crest). This would indicate a depth of -4,50 m NAP.
  - Mentioned depth of the top of the Wormer clay layers indicated in a letter from 5 January 1918. This would indicate a depth between -3,82 and -5,32 m NAP.
  - Logical thinking, following after the previous mentioned assumptions. Since the subsidence processes between 1918 and 2010 are assumed to be mostly creep and degradation of organic material, it makes sense that most the peat layer has caused most of the subsidence. This is because peat has a higher value of C_α and includes organic material. Therefore, a depth of -4,50 m NAP seems to be too high (as then most subsidence between 1918 and 2010 would originate from the layers below the peat layer).

- It is assumed that the upper soil layer indicated in the boorprofile from 1918 is the layer that was constructed in 1890. The soil type indicated in the boorprofile is 'teelaarde met zand', which is interpreted as an organic soil layer.

- Subsidence between 1890 and 1918 originates from a subsidence component of the already existing structure and a subsidence component of the newly applied soil layer in 1890. A ratio between these two components has been assumed. This is that 50% of the subsidence is related to processes regarding the constructed soil layer itself (shrinkage, compression by its own weight) and 50% is related to subsidence from the already existing structure (compression by loading, aerobic/anaerobic degradation of SOM).

  - Through this ratio, the initial thickness of the applied soil layer can be calculated.
  - The other subsidence is divided between the different soil layers:
    - ◇ It is assumed that 75% of the settlement originates from the peat layer
    - ◇ It is assumed that 25% of the settlement originates from the other soil layers

- All calculations/levels originating from the boorprofiles or other information from 1918 are corrected with 0,02 cm to account for the correction of the NAP level in 2005.

Project location 3

To calculate subsidence from different components, an estimation of the initial soil profile is constructed. This is done based on several sources of information:

- Soil profile of the crest of the dike in 1916, based on a boorprofile of the crest, shown in figure E.10.
- Soil profile of the crest of the dike in 2010, based on CPT and boorprofiles, shown in figure E.11.
- Geological profile description of the subsurface by Deltares

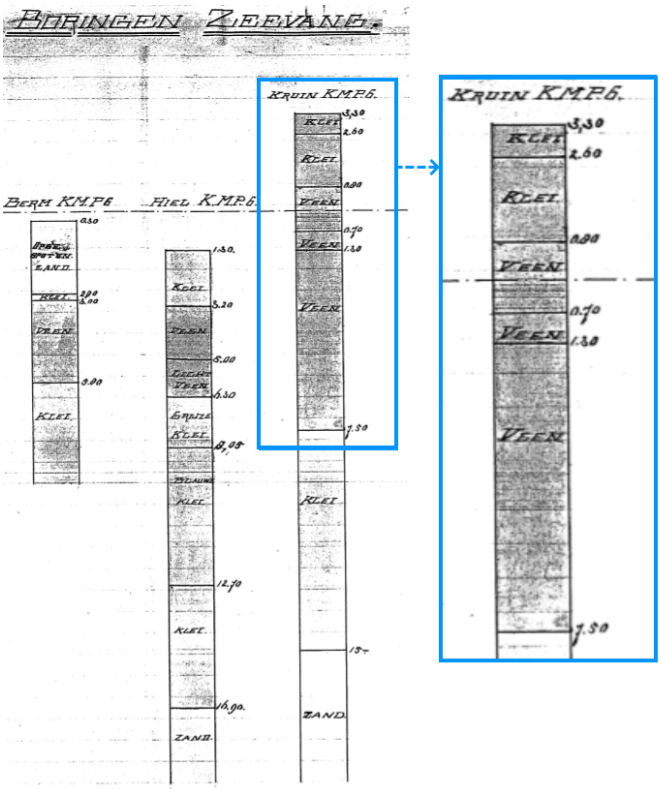

Figure E.10: Boorprofiles 1916 project location 3

An overview of the assumed soil profile over time is shown in figure E.12. Again with black lines indicate information based on site investigation or documents directly and green lines indicate the use of additional assumptions or calculations. The assumptions used are listed below:

- The upper limit of the Pleistocene sand layer as indicated in the soil profile from 2010 has not changed over time. In other words, it is expected that the level of this sand layer is the same in 1916 and 2010. The level is assumed to be around -17,00 m NAP, based on the geotechnical profile provided by Alliantie Markermeerdijken.
- The Calais sand layer has not changed in thickness over time. The clay and peat layers below the sand layer have changed in thickness, but this is negligible over the time period considered.
- The bottom of the Hollandveen peat layer shown in the boorprofile from 1916 is assumed to be unrealistic. The bottom of the layer is indicated at a deeper level in 1916 than the bottom of the peat layer in the profile from 2010. Therefore, another level of the boundary is assumed.
- Time, soil type and thickness of the last constructed soil layer to increase the height of the dike has to be assumed, no characteristics are available:

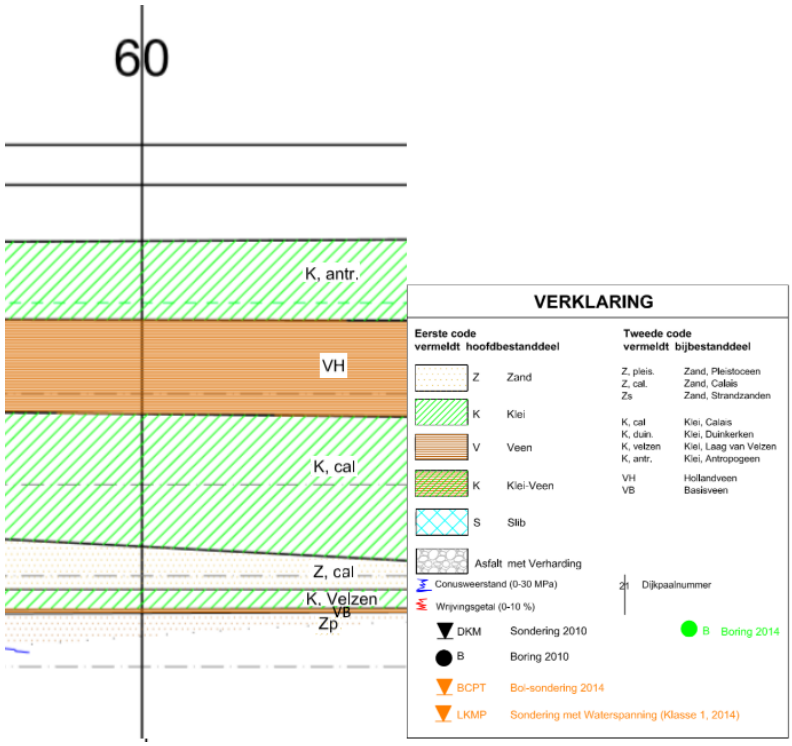

Figure E.11: Soil profile project location 3 based on site investigation 2010

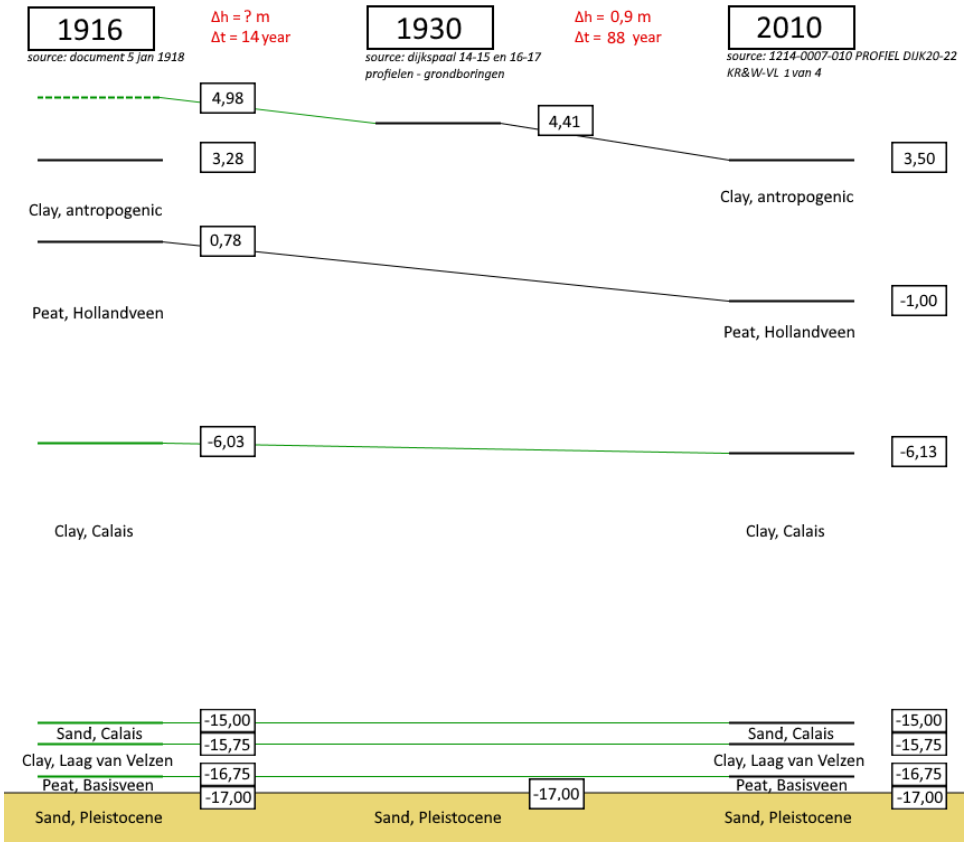

Figure E.12: Estimation soil profile over time location 3: dike 23, pole 60 (not to scale)

  - It is assumed that a similar material as for the other two locations is used for the construction of the 'new' soil layer. This is an organic soil type. This soil layer is included in the anthropogenic clay layer indicated in the soil profile from 2010.
  - It is assumed that the layer is constructed in 1917, one year after the boorprofiles. It is assumed that the boorprofiles were made as part of the site investigation before the construction.
  - It is estimated that the initial thickness of the new soil layer was approximately 1,70 meter, based on trial and error with the model.

- All calculations/levels originating from the boorprofiles or other information from 1918 are corrected with 0,02 cm to account for the correction of the NAP level in 2005.

Project location 4

Four boorprofiles located in and around the project area are used to construct an initial soil profile for this location. These come from the year 1994, which is used as starting point for the model calculation in this area. The boorprofiles only reached to a depth of approximately -3,4 m NAP and thus could only be used for the top of the soil profile. The other source used is the soil profile of the hinterland of the dike from Alliantie Markermeerdijken at pole 60. From this profile the depth of the sand layers and clay layers is used, as is it assumed that the influence of the water level lowerings over time on these layers is negligible. The soil profile used as input for the model is shown in figure E.13.

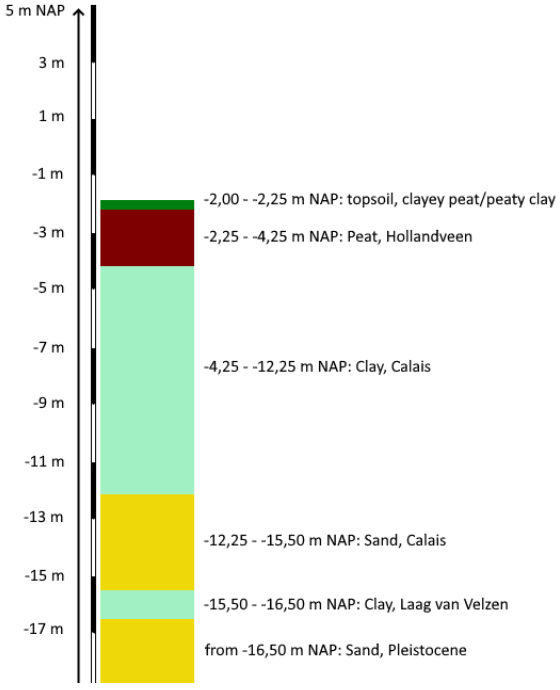

Figure E.13: Estimated initial soil profile representative for project location 4

E.5. Model parameters

In the tables below model parameters used as input are for the normal parameter scenarios are shown. These are the parameters related to the soil profile. Sources of these parameters are listed below the tables.

E.5.1. Project location 1

Table E.3: Soil parameters oxidation and shrinkage submodels, project location 1

Depth top layer [m NAP]	**Soil Type**	V_{ox} **[year^{-1}]**	V_{sh} **[year^{-1}]**		$\lambda_r^{(b)}$ **[-]**
			Koppejan estimate	**NEN-Bjerrum estimate**	
3,58	Clay, anthropogenic	0	0,17$^{(b)}$	0,27$^{(b)}$	0,66
2,48	Clay, anthropogenic	0	0	0	0,66
1,11	Peat, Hollandveen	0,015$^{(a)}$	0	0	0,09
-4,76	Clay, Calais	0	0	0	0,66
-9,10	Sand, Calais	0	0	0	1
-11,50	Clay, Calais	0	0	0	0,66
-12,75	Sand, Calais	0	0	0	1
-15,50	Clay, Laag van Velzen	0	0	0	0,66

(a) Value commonly stated in literature, based on study (Van der Meulen et al., 2007)
(b) Value based on results Fokker et al. (2019)

Table E.4: Soil parameters NEN-Bjerrum submodel, project location 1

Depth top layer [m NAP]	**Soil Type**	**RR**$^{(a)}$ **[-]**	**CR**$^{(a)}$ **[-]**	C_α $^{(a)}$ **[-]**	γ_{sat} $^{(a)}$ **[kN/m^3]**	γ_{unsat} **[kN/m^3]**	**cv**$^{(a)}$ **[m^2/s]**	**POP**$^{(a)}$ **[kPa]**
3,58	Clay, anthropogenic	0,0330	0,2210	0,011	14,3	13,3	1,70E-07	28,9
2,48	Clay, anthropogenic	0,0330	0,2210	0,011	14,3	13,3	1,70E-07	28,9
1,11	Peat, Hollandveen	0,0660	0,4170	0,024	10,4	5$^{(b)}$	1,30E-07	16,1
-4,76	Clay, Calais	0,0330	0,2210	0,011	14,3	13,3	1,00E-07	21,1
-9,10	Sand, Calais	0,0010	0,0040	0	20	18	0,04	10
-11,50	Clay, Calais	0,0330	0,2210	0,011	14,3	13,3	1,00E-07	21,1
-12,75	Sand, Calais	0,0010	0,0040	0	20	18	0,04	10
-15,50	Clay, Laag van Velzen	0,0330	0,2210	0,011	14,3	13,3	1,00E-07	21,1

(a) Values based on average parameters North, report Alliantie Markermeerdijken: *AMMD-003443 - Ontwerpbasis Zetting DO*
(b) Estimation based on Hsi et al. (2005) and laboratory study N3 samples

Table E.5: Soil parameters Koppejan submodel, project location 1

Depth top layer [m NAP]	**Soil Type**	**Cp'**$^{(b)}$ **[-]**	**Cs'**$^{(c)}$ **[-]**	**Cp**$^{(b)}$ **[-]**	**Cs**$^{(c)}$ **[-]**	γ_{sat} $^{(a)}$ **[kN/m^3]**	γ_{unsat} **[kN/m^3]**	**cv**$^{(a)}$ **[m^2/s]**	**POP**$^{(a)}$ **[kPa]**
3,58	Clay, anthropogenic	10,42	100	69,78	800	14,3	13,3	1,70E-07	28,90
2,48	Clay, anthropogenic	10,42	100	69,78	800	14,3	13,3	1,70E-07	28,90
1,11	Peat, Hollandveen	5,52	30	34,89	280	10,4	5$^{(d)}$	1,30E-07	16,1
-4,76	Clay, Calais	10,42	200	69,78	1600	14,3	13,3	1,00E-07	21,1
-9,10	Sand, Calais	575,65	1E09	2302,59	1E09	20	18	0,04	10
-11,50	Clay, Calais	10,42	200	69,78	1600	14,3	13,3	1,00E-07	21,1
-12,75	Sand, Calais	575,65	1E09	2302,59	1E09	20	18	0,04	10
-15,50	Clay, Laag van Velzen	10,42	200	69,78	1600	14,3	13,3	1,00E-07	21,1

(a) Values based on average parameters North, report Alliantie Markermeerdijken: *AMMD-003443 - Ontwerpbasis Zetting DO*
(b) Calculated based on NEN-Bjerrum parameter values:

$$C_p = \frac{\ln 10}{RR} \qquad C'_p = \frac{\ln 10}{CR} \tag{E.1}$$

(c) Based on Excel tool from Arcadis
(d) Estimation based on Hsi et al. (2005) and laboratory study N3 samples

E.5.2. Project location 2

Table E.6: Soil parameters oxidation and shrinkage submodels, project location 2

Depth top layer [m NAP]	**Soil Type**	V_{ox} **[year^{-1}]**	V_{sh} **[year^{-1}]**		$\lambda_r^{(b)}$ **[-]**
			Koppejan estimate	**NEN-Bjerrum estimate**	
3,58	Clay, anthropogenic	0	0,17$^{(b)}$	0,27$^{(b)}$	0,66
2,43	Clay, anthropogenic	0	0	0	0,66
1,13	Peat, Hollandveen	0,015$^{(a)}$	0	0	0,09
-2,30	Clay, Calais	0	0	0	0,66
-3,63	Peat, Hollandveen	0,015$^{(a)}$	0	0	0,09
-4,96	Clay, Calais	0	0	0	0,66
-9,25	Sand, Calais	0	0	0	1
-15,50	Clay, Laag van Velzen	0	0	0	0,66

(a) Value commonly stated in literature, based on study (Van der Meulen et al., 2007)
(b) Value based on results Fokker et al. (2019)

Table E.7: Soil parameters NEN-Bjerrum submodel, project location 2

Depth top layer [m NAP]	**Soil Type**	**RR**$^{(a)}$ **[-]**	**CR**$^{(a)}$ **[-]**	C_α $^{(a)}$ **[-]**	γ_{sat} $^{(a)}$ **[kN/m^3]**	γ_{unsat} **[kN/m^3]**	**cv**$^{(a)}$ **[m^2/s]**	**POP**$^{(a)}$ **[kPa]**
3,58	Clay, anthropogenic	0,0330	0,2210	0,011	14,3	13,3	1,70E-07	28,9
2,43	Clay, anthropogenic	0,0330	0,2210	0,011	14,3	13,3	1,70E-07	28,9
1,13	Peat, Hollandveen	0,0660	0,4170	0,024	10,4	5$^{(b)}$	1,30E-07	16,1
-2,30	Clay, Calais	0,0330	0,2210	0,011	14,3	13,3	1,00E-07	21,1
-3,63	Peat, Hollandveen	0,0660	0,4170	0,024	10,4	5$^{(b)}$	1,30E-07	16,1
-4,96	Clay, Calais	0,0330	0,2210	0,011	14,3	13,3	1,00E-07	21,1
-9,25	Sand, Calais	0,0010	0,0040	0	20	18	0,04	10
-15,50	Clay, Laag van Velzen	0,0330	0,2210	0,011	14,3	13,3	1,00E-07	21,1

(a) Values based on average parameters North, report Alliantie Markermeerdijken: *AMMD-003443 - Ontwerpbasis Zetting DO*

(b) Estimation based on Hsi et al. (2005) and laboratory study N3 samples

Table E.8: Soil parameters Koppejan submodel, project location 2

Depth top layer [m NAP]	**Soil Type**	**Cp'**$^{(b)}$ **[-]**	**Cs'**$^{(c)}$ **[-]**	**Cp**$^{(b)}$ **[-]**	**Cs**$^{(c)}$ **[-]**	γ_{sat} $^{(a)}$ **[kN/m^3]**	γ_{unsat} **[kN/m^3]**	**cv**$^{(a)}$ **[m^2/s]**	**POP**$^{(a)}$ **[kPa]**
3,58	Clay, anthropogenic	10,42	100	69,78	800	14,3	13,3	1,70E-07	28,90
2,43	Clay, anthropogenic	10,42	100	69,78	800	14,3	13,3	1,70E-07	28,90
1,13	Peat, Hollandveen	5,52	30	34,89	280	10,4	5$^{(d)}$	1,30E-07	16,1
-2,30	Clay, Calais	10,42	200	69,78	1600	14,3	13,3	1,00E-07	21,1
-3,63	Peat, Hollandveen	5,52	30	34,89	280	10,4	5$^{(d)}$	1,30E-07	16,1
-4,96	Clay, Calais	10,42	200	69,78	1600	14,3	13,3	1,00E-07	21,1
-9,25	Sand, Calais	575,65	1E09	2302,59	1E09	20	18	0,04	10
-15,50	Clay, Laag van Velzen	10,42	200	69,78	1600	14,3	13,3	1,00E-07	21,1

(a) Values based on average parameters North, report Alliantie Markermeerdijken: *AMMD-003443 - Ontwerpbasis Zetting DO*

(b) Calculated based on NEN-Bjerrum parameter values

(c) Based on Excel tool from Arcadis

(d) Estimation based on Hsi et al. (2005) and laboratory study N3 samples

E.5.3. Project location 3

Table E.9: Soil parameters oxidation and shrinkage submodels, project location 3

Depth top layer [m NAP]	**Soil Type**	V_{ox} **[year^{-1}]**	V_{sh} **[year^{-1}]**		$\lambda_r^{(b)}$ **[-]**
			Koppejan estimate	**NEN-Bjerrum estimate**	
4,98	Clay, anthropogenic	0	0,17$^{(b)}$	0,27$^{(b)}$	0,66
3,28	Clay, anthropogenic	0	0	0	0,66
0,78	Peat, Hollandveen	0,015$^{(a)}$	0	0	0,09
-6,03	Clay, Calais	0	0	0	0,66
-15,00	Sand, Calais	0	0	0	1
-15,75	Clay, Laag van Velzen	0	0	0	0,66
-16,75	Peat, Basisveen	0,015$^{(a)}$	0	0	0,09

(a) Value commonly stated in literature, based on study (Van der Meulen et al., 2007)
(b) Value based on results Fokker et al. (2019)

Table E.10: Soil parameters NEN-Bjerrum submodel, project location 3

Depth top layer [m NAP]	**Soil Type**	**RR**$^{(a)}$ **[-]**	**CR**$^{(a)}$ **[-]**	C_α $^{(a)}$ **[-]**	γ_{sat} $^{(a)}$ **[kN/m^3]**	γ_{unsat} **[kN/m^3]**	**cv**$^{(a)}$ **[m^2/s]**	**POP**$^{(a)}$ **[kPa]**
4,98	Clay, anthropogenic	0,0330	0,2210	0,011	14,3	13,3	1,70E-07	28,9
3,28	Clay, anthropogenic	0,0330	0,2210	0,011	14,3	13,3	1,70E-07	28,9
0,78	Peat, Hollandveen	0,0660	0,4170	0,024	10,4	5$^{(b)}$	1,30E-07	16,1
-6,03	Clay, Calais	0,0330	0,2210	0,011	14,3	13,3	1,00E-07	21,1
-15,00	Sand, Calais	0,0010	0,0040	0	20	18	0,04	10
-15,75	Clay, Laag van Velzen	0,0330	0,2210	0,011	14,3	13,3	1,00E-07	21,1
-16,75	Peat, Basisveen	0,0660	0,4170	0,024	10,4	5$^{(b)}$	1,30E-07	16,1

(a) Values based on average parameters North, report Alliantie Markermeerdijken: *AMMD-003443 - Ontwerpbasis Zetting DO*
(b) Estimation based on Hsi et al. (2005) and laboratory study N3 samples

Table E.11: Soil parameters Koppejan submodel, project location 3

Depth top layer [m NAP]	**Soil Type**	**Cp'**$^{(b)}$ **[-]**	**Cs'**$^{(c)}$ **[-]**	**Cp**$^{(b)}$ **[-]**	**Cs**$^{(c)}$ **[-]**	γ_{sat} $^{(a)}$ **[kN/m^3]**	γ_{unsat} **[kN/m^3]**	**cv**$^{(a)}$ **[m^2/s]**	**POP**$^{(a)}$ **[kPa]**
4,98	Clay, anthropogenic	10,42	100	69,78	800	14,3	13,3	1,70E-07	28,90
3,28	Clay, anthropogenic	10,42	100	69,78	800	14,3	13,3	1,70E-07	28,90
0,78	Peat, Hollandveen	5,52	30	34,89	280	10,4	5$^{(d)}$	1,30E-07	16,1
-6,03	Clay, Calais	10,42	200	69,78	1600	14,3	13,3	1,00E-07	21,1
-15,00	Sand, Calais	575,65	1E09	2302,59	1E09	20	18	0,04	10
-15,75	Clay, Laag van Velzen	10,42	200	69,78	1600	14,3	13,3	1,00E-07	21,1
-16,75	Peat, Basisveen	5,52	30	34,89	280	10,4	5$^{(d)}$	1,30E-07	16,1

(a) Values based on average parameters North, report Alliantie Markermeerdijken: *AMMD-003443 - Ontwerpbasis Zetting DO*
(b) Calculated based on NEN-Bjerrum parameter values
(c) Based on Excel tool from Arcadis
(d) Estimation based on Hsi et al. (2005) and laboratory study N3 samples

E.5.4. Project location 4

Table E.12: Soil parameters oxidation and shrinkage submodels, project location 4

Depth top layer [m NAP]	**Soil Type**	V_{ox} **[year-1]**	V_{sh} **[year-1]**	$\lambda_r^{(b)}$ **[-]**
-2,00	Topsoil	0	0	0,66
-2,25	Peat, Hollandveen	0,015$^{(a)}$	0	0,09
-4,25	Clay, Calais	0	0	0,66
-12,50	Sand, Calais	0	0	1
-15,50	Clay, Laag van Velzen	0	0	0,66

(a) Value commonly stated in literature, based on study (Van der Meulen et al., 2007)
(b) Value based on results Fokker et al. (2019)

Table E.13: Soil parameters NEN-Bjerrum submodel, project location 4

Depth top layer [m NAP]	**Soil Type**	**RR**$^{(a)}$ **[-]**	**CR**$^{(a)}$ **[-]**	C_α $^{(b)}$ **[-]**	γ_{sat} $^{(a)}$ **[kN/m^3]**	γ_{unsat} **[kN/m^3]**	**cv**$^{(a)}$ **[m^2/s]**	**POP**$^{(d)}$ **[kPa]**
-2,00	Topsoil	0,0380	0,2470	0,0091	13,5	12,5	9,3E-08	7,5
-2,25	Peat, Hollandveen	0,0790	0,4890	0,006	10,0	5$^{(c)}$	2,40E-07	7,5
-4,25	Clay, Calais	0,0350	0,2290	0,006	14,3	13,3	2,70E-07	7,5
-12,50	Sand, Calais	0,0010	0,0040	0	20	18	0,04	7,5
-15,50	Clay, Laag van Velzen	0,0350	0,2290	0,006	14,3	13,3	2,70E-07	7,5

(a) Values based on average parameters North, report Alliantie Markermeerdijken: *AMMD-003443 - Ontwerpbasis Zetting DO*
(b) Values based on findings Fokker et al. (2019)
(c) Estimation based on Hsi et al. (2005) and laboratory study N3 samples
(d) Same POP values used as for the Krimpenerwaard project locations

Table E.14: Soil parameters Koppejan submodel, project location 4

Depth top layer [m NAP]	**Soil Type**	**Cp'**$^{(b)}$ **[-]**	**Cs'**$^{(c)}$ **[-]**	**Cp**$^{(b)}$ **[-]**	**Cs**$^{(c)}$ **[-]**	γ_{sat} $^{(a)}$ **[kN/m^3]**	γ_{unsat} **[kN/m^3]**	**cv**$^{(a)}$ **[m^2/s]**	**POP**$^{(a)}$ **[kPa]**
-2,00	Topsoil	9,32	75	60,59	800	13,5	12,5	9,30E-08	7,5
-2,25	Peat, Hollandveen	4,71	30	29,15	800	10,0	5$^{(d)}$	2,40E-07	7,5
-4,25	Clay, Calais	10,05	200	65,79	280	14,3	13,3	2,70E-07	7,5
-12,50	Sand, Calais	575,65	1E09	2302,59	1600	20	18	0,04	7,5
-15,50	Clay, Calais	10,05	200	65,79	1E09	14,3	13,3	2,70E-07	7,5

(a) Values based on report Alliantie Markermeerdijken: *AMMD-003443 - Ontwerpbasis Zetting DO*
(b) Calculated based on NEN-Bjerrum parameter values
(c) Based on Excel tool from Arcadis
(d) Estimation based on Hsi et al. (2005) and laboratory study N3 samples

E.6. Water level and hydraulic head sand layers

A table with information about the water levels and hydraulic heads for the project locations is provided by Alliantie Markermeerdijken, table E.15:

Table E.15: Hydraulic conditions at the project locations, information provided by Alliantie Markermeerdijken

Project location	**Water level in crest [m NAP]**		**Hydraulic head sand layer [m NAP]**
	Daily	MHW	
1	0,85	1,00	-2,55
2	0,85	1,00	-2,55
3	1,35	1,50	-2,30

E.7. Model settings

Settings of the model used for the calculation of subsidence for all project location is shown in figure E.14.

```
start year location 1 and 2 = 1890
start year location 3 = 1917
time period evaluated location 1 and 2 = 130 years
time period evaluated location 3 = 103 years
time step (dt) = 1 year
days in a year = 365.25 days

bottom level evaluation project location 1 = -16.75 m NAP
bottom level evaluation project location 2 = -17.50 m NAP
bottom level evaluation project location 3 = -17.00 m NAP

number of evaluated layers within a soil layer = 7
number of evaluated layers within new constructed soil layer = 9
tau0 = 1 day
```

Figure E.14: Other input settings used in the model to come to the results presented in this section

E.8. Graphs results

In this appendix three types of graphs are presented for all scenarios calculated. The figures are ordered per type and location. The different scenarios are then indicated by the caption of each subfigure.

E.8.1. Project location 1

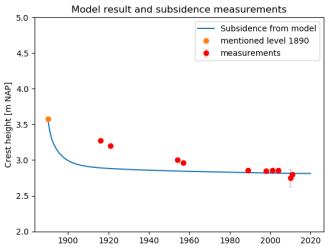

(a) Normal parameters Koppejan

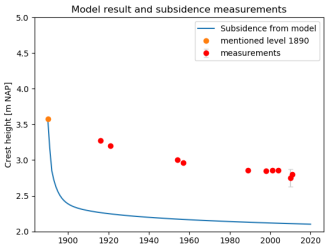

(b) Normal parameters NEN-Bjerrum

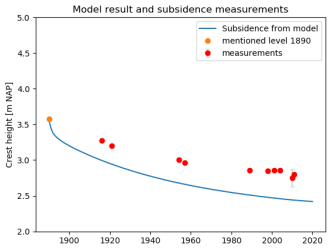

(c) Oxidation scenario

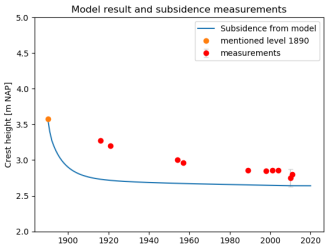

(d) Shrinkage organic clay scenario

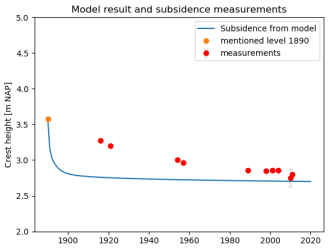

(e) Adjusted C_α scenario

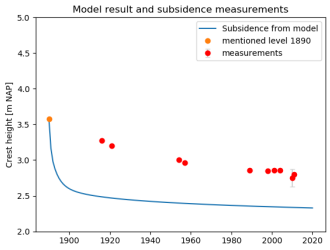

(f) Adjusted POP scenario

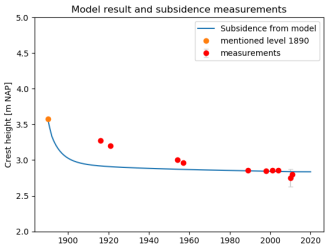

(g) Only creep from above water level scenario Koppejan

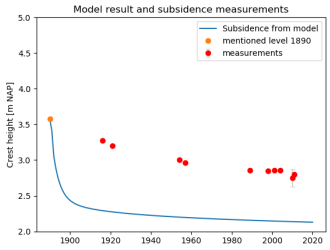

(h) Only creep from above water level scenario NEN-Bjerrum

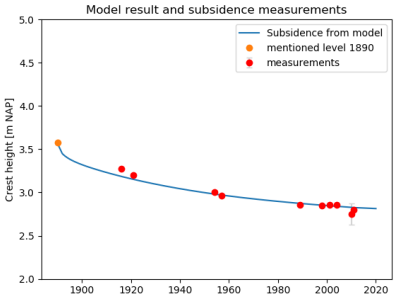

(i) Best fit parameters Koppejan loading model

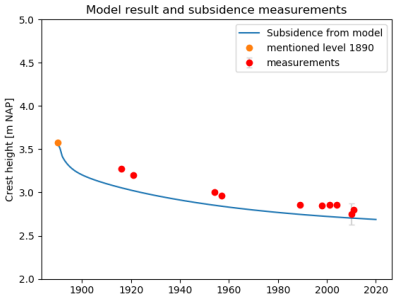

(j) Best fit parameters NEN-Bjerrum loading model

Figure E.15: Model results and measurements, project location 1

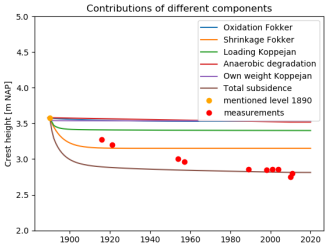

(a) Normal parameters koppejan

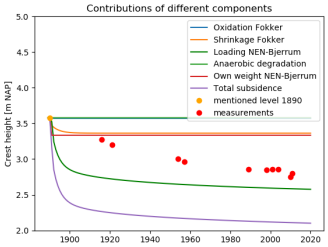

(b) Normal parameters NEN-Bjerrum

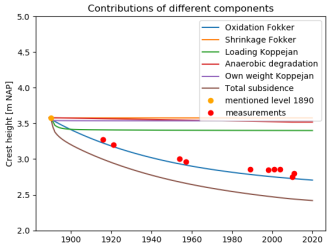

(c) Oxidation scenario

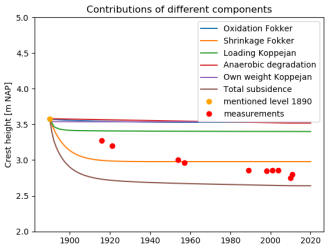

(d) Shrinkage organic clay scenario

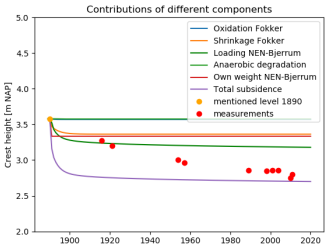

(e) Adjusted C_α scenario

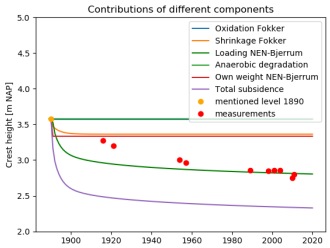

(f) Adjusted POP scenario

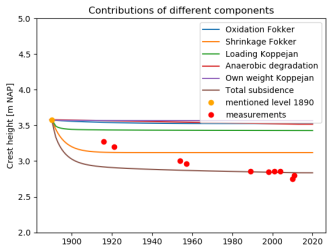

(g) Only creep from above water level scenario Koppejan

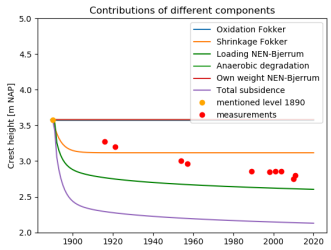

(h) Only creep from above water level scenario NEN-Bjerrum

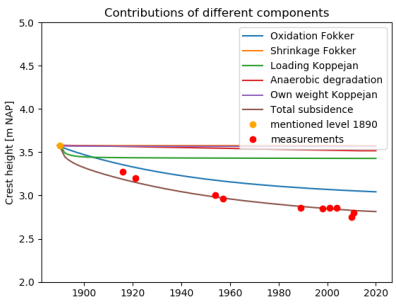

(i) Best fit parameters Koppejan loading model

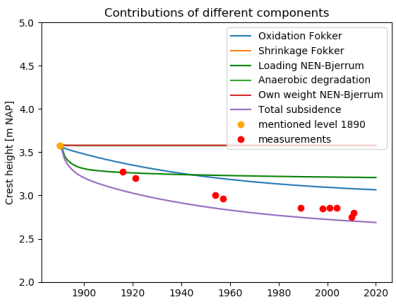

(j) Best fit parameters NEN-Bjerrum loading model

Figure E.16: Contributions of different components, project location 1

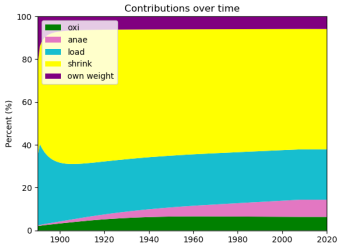

(a) Normal parameters koppejan

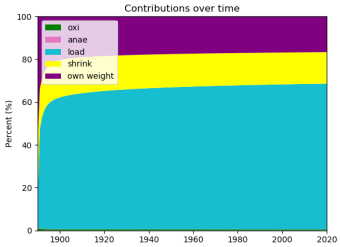

(b) Normal parameters NEN-Bjerrum

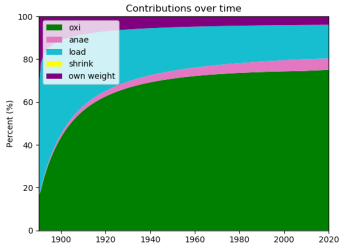

(c) Oxidation scenario

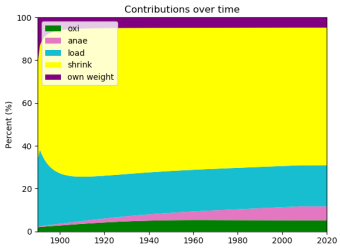

(d) Shrinkage organic clay scenario

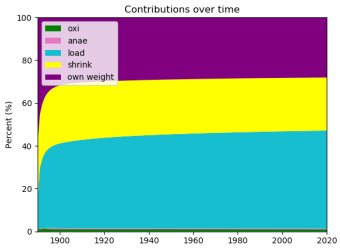

(e) Adjusted C_α scenario

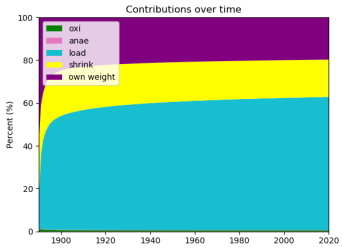

(f) Adjusted POP scenario

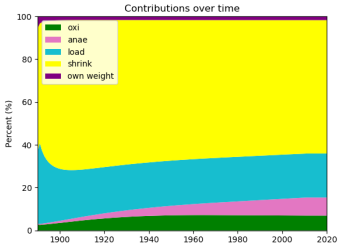

(g) Only creep from above water level scenario Koppejan

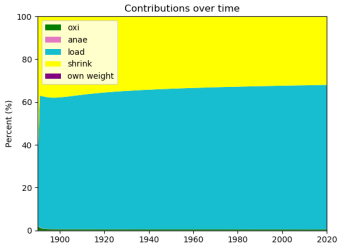

(h) Only creep from above water level scenario NEN-Bjerrum

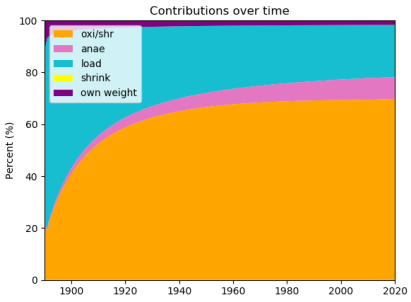

(i) Best fit parameters Koppejan loading model

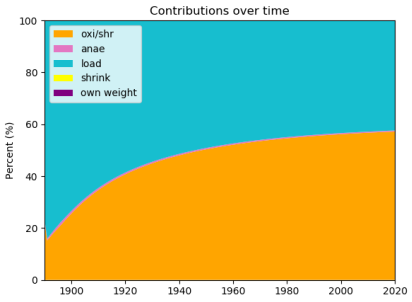

(j) Best fit parameters NEN-Bjerrum loading model

Figure E.17: Contributions of different components in percentages, project location 1

E.8.2. Project location 2

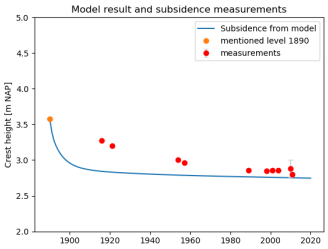

(a) Normal parameters koppejan

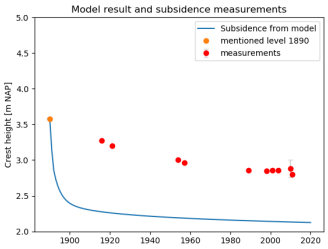

(b) Normal parameters NEN-Bjerrum

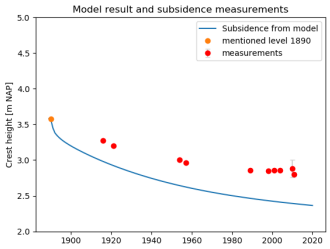

(c) Oxidation scenario

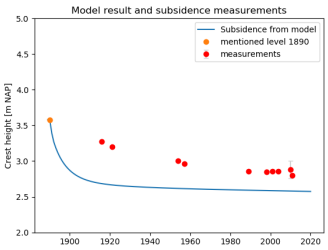

(d) Shrinkage organic clay scenario

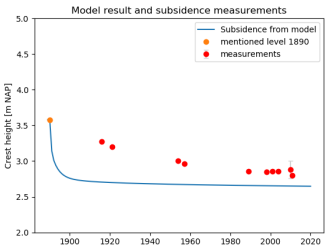

(e) Adjusted C_α scenario

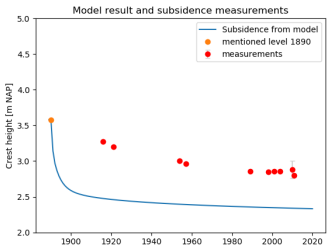

(f) Adjusted POP scenario

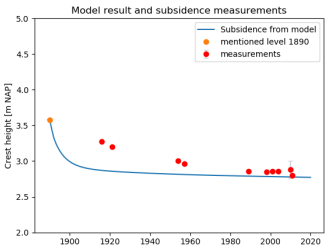

(g) Only creep from above water level scenario Koppejan

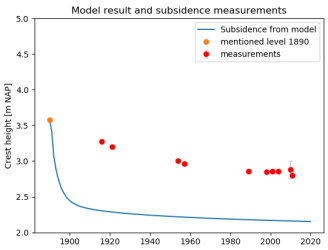

(h) Only creep from above water level scenario NEN-Bjerrum

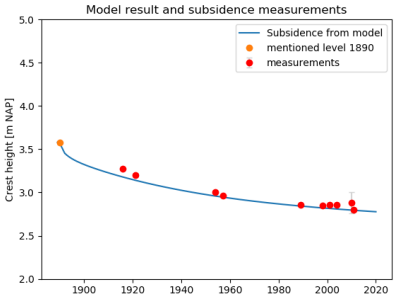

(i) Best fit parameters Koppejan loading model

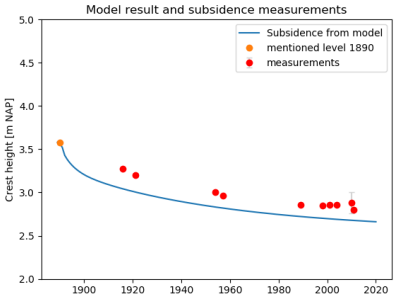

(j) Best fit parameters NEN-Bjerrum loading model

Figure E.18: Model results and measurements, project location 2

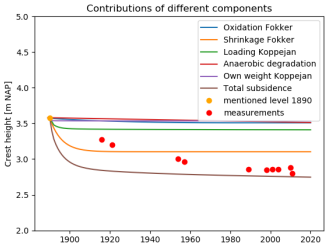

(a) Normal parameters koppejan

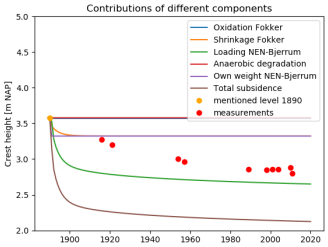

(b) Normal parameters NEN-Bjerrum

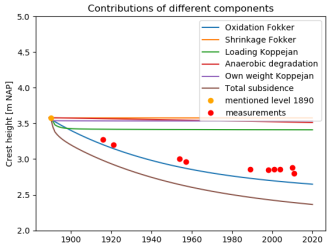

(c) Oxidation scenario

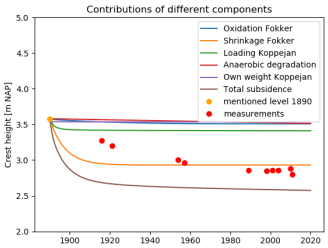

(d) Shrinkage organic clay scenario

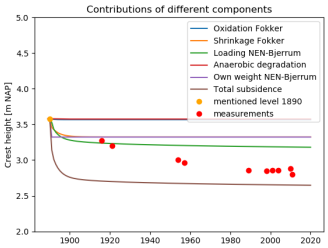

(e) Adjusted C_α scenario

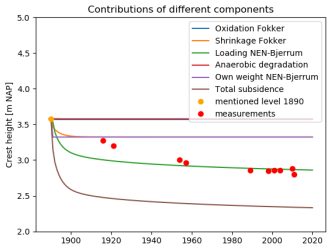

(f) Adjusted POP scenario

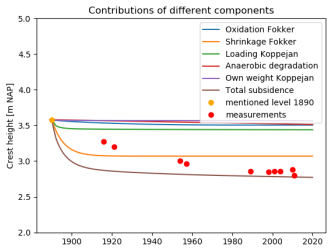

(g) Only creep from above water level scenario Koppejan

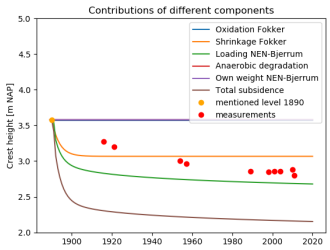

(h) Only creep from above water level scenario NEN-Bjerrum

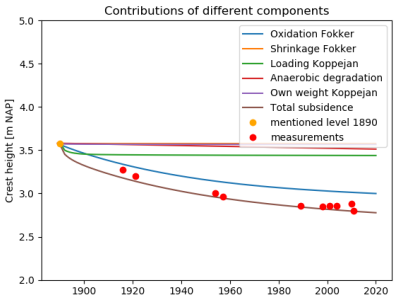

(i) Best fit parameters Koppejan loading model

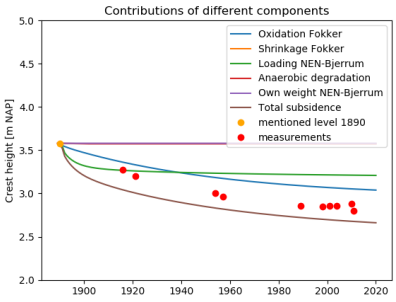

(j) Best fit parameters NEN-Bjerrum loading model

Figure E.19: Contributions of different components, project location 2

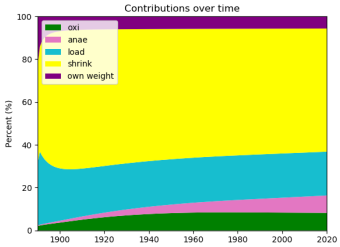

(a) Normal parameters koppejan

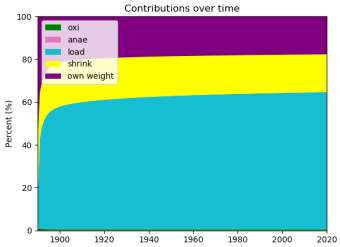

(b) Normal parameters NEN-Bjerrum

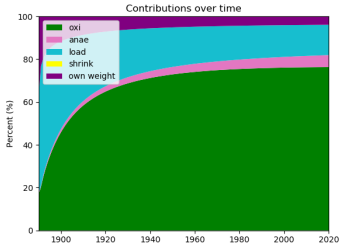

(c) Oxidation scenario

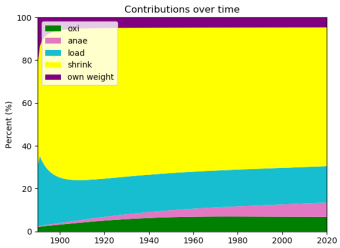

(d) Shrinkage organic clay scenario

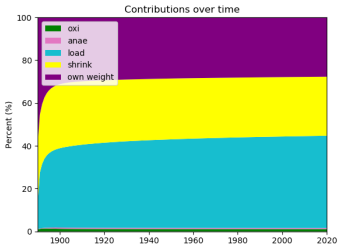

(e) Adjusted C_α scenario

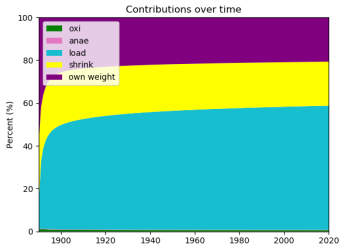

(f) Adjusted POP scenario

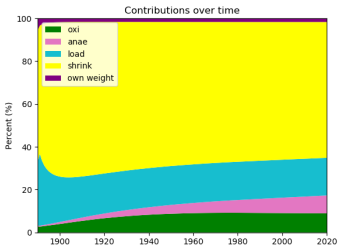

(g) Only creep from above water level scenario Koppejan

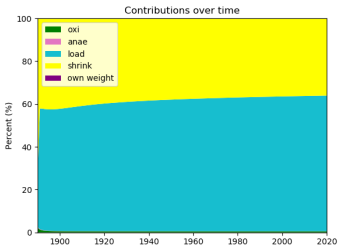

(h) Only creep from above water level scenario NEN-Bjerrum

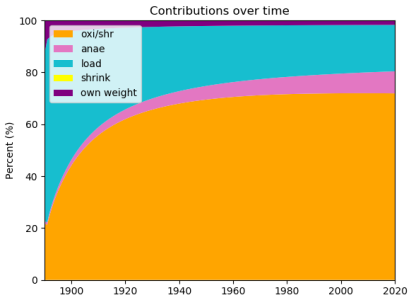

(i) Best fit parameters Koppejan loading model

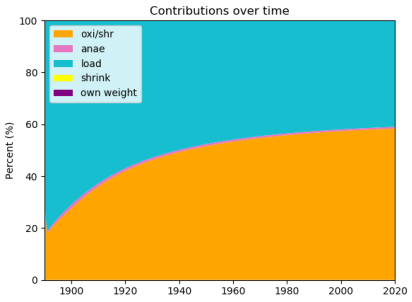

(j) Best fit parameters NEN-Bjerrum loading model

Figure E.20: Contributions of different components in percentages, project location 2

E.8.3. Project location 3

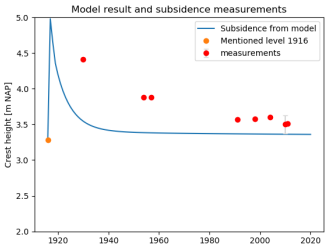

(a) Normal parameters koppejan

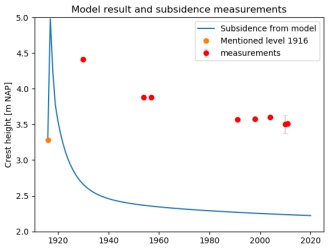

(b) Normal parameters NEN-Bjerrum

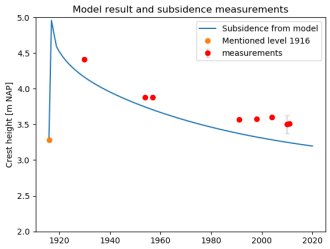

(c) Oxidation scenario

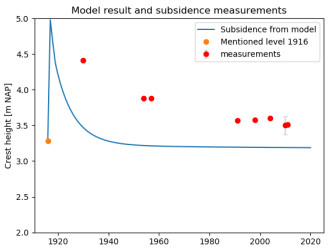

(d) Shrinkage organic clay scenario

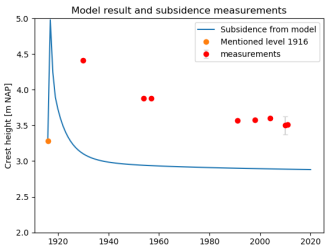

(e) Adjusted C_α scenario

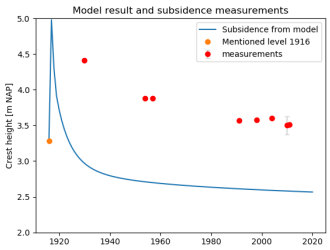

(f) Adjusted POP scenario

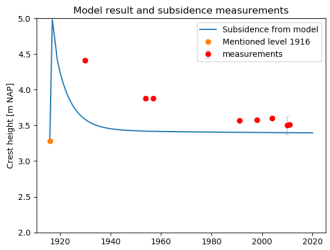

(g) Only creep from above water level scenario Koppejan

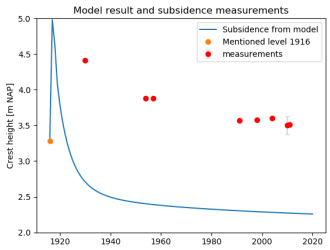

(h) Only creep from above water level scenario NEN-Bjerrum

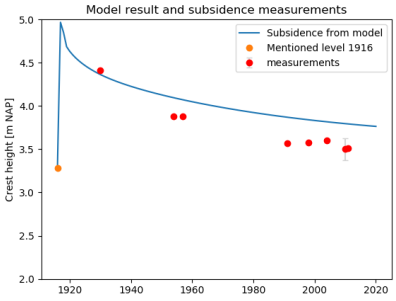

(i) Best fit parameters Koppejan loading model

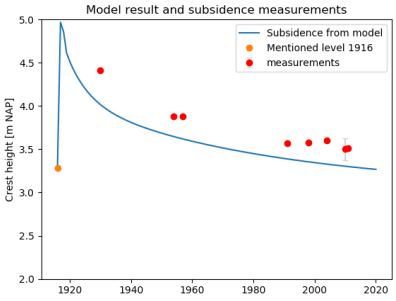

(j) Best fit parameters NEN-Bjerrum loading model

Figure E.21: Model results and measurements, project location 3

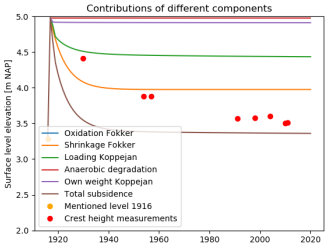

(a) Normal parameters koppejan

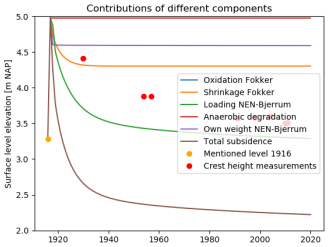

(b) Normal parameters NEN-Bjerrum

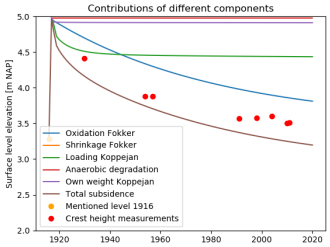

(c) Oxidation scenario

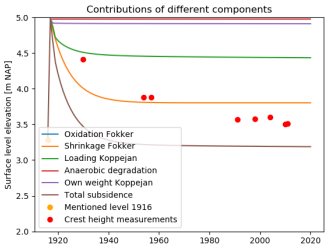

(d) Shrinkage organic clay scenario

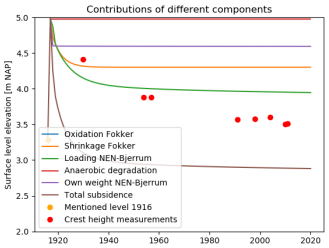

(e) Adjusted C_α scenario

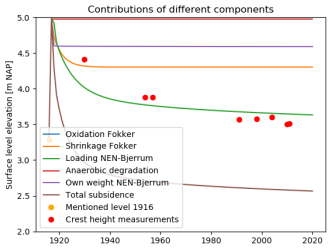

(f) Adjusted POP scenario

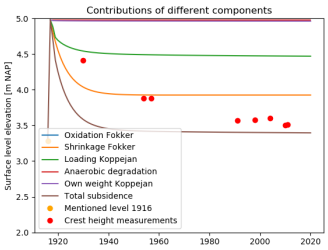

(g) Only creep from above water level scenario Koppejan

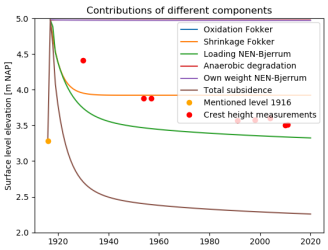

(h) Only creep from above water level scenario NEN-Bjerrum

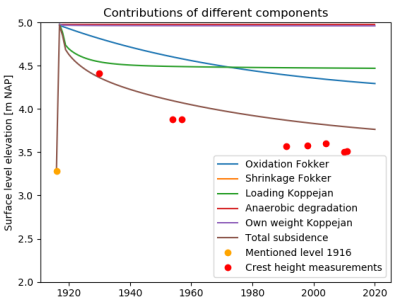

(i) Best fit parameters Koppejan loading model

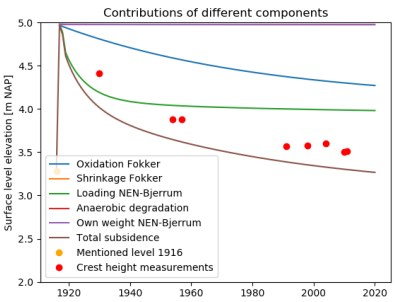

(j) Best fit parameters NEN-Bjerrum loading model

Figure E.22: Contributions of different components, project location 3

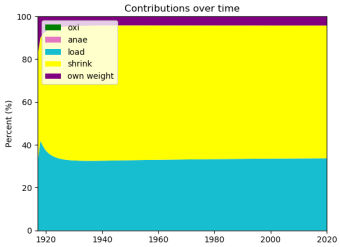

(a) Normal parameters koppejan

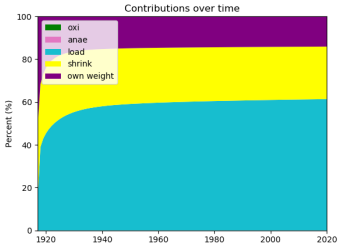

(b) Normal parameters NEN-Bjerrum

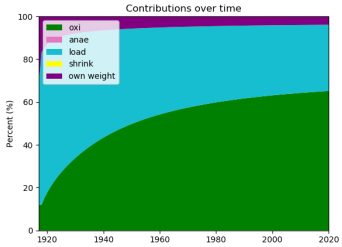

(c) Oxidation scenario

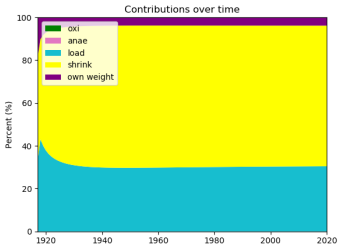

(d) Shrinkage organic clay scenario

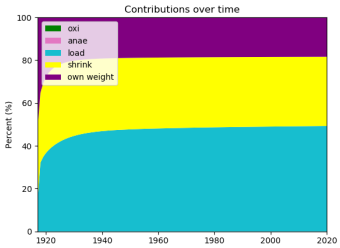

(e) Adjusted C_α scenario

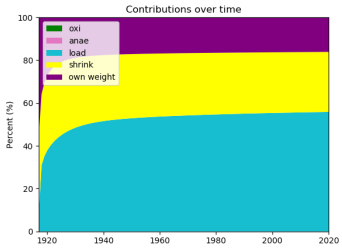

(f) Adjusted POP scenario

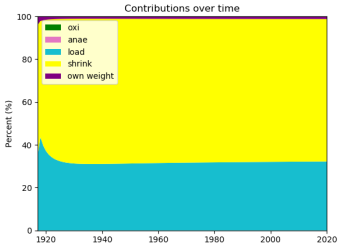

(g) Only creep from above water level scenario Koppejan

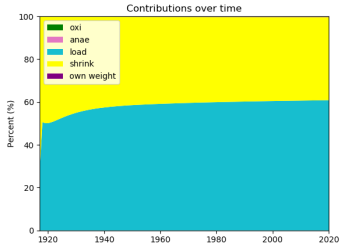

(h) Only creep from above water level scenario NEN-Bjerrum

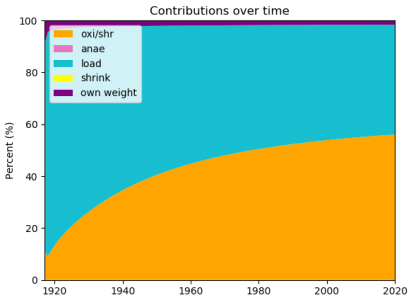

(i) Best fit parameters Koppejan loading model

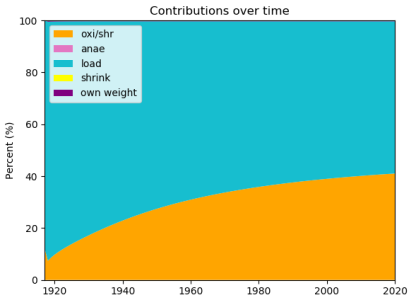

(j) Best fit parameters NEN-Bjerrum loading model

Figure E.23: Contributions of different components in percentages, project location 3